

FINAL REPORT ON THE DELINEATION OF FRESH, BRACKISH AND SALINE GROUNDWATER RESOURCES BASED ON INTERPRETATION OF GEOPHYSICAL LOGS

Prepared for:



Harris-Galveston Subsidence District



Fort Bend Subsidence District

Prepared by:



INTERA Incorporated



LBG-Guyton & Associates



Bureau of Economic Geology

December 2017

This page is intentionally left blank.

REPORT ON THE DELINEATION OF FRESH, BRACKISH AND SALINE GROUNDWATER RESOURCES BASED ON INTERPRETATION OF GEOPHYSICAL LOGS

Prepared By

Steve C. Young, Ph.D., P.G., P.E.

Van Kelley, P.G.

Neil Deeds, Ph.D., P.E.

Cody Hudson, P.E.

Deborah Piemonti

INTERA Incorporated

Thomas E. Ewing, Ph.D., P.G.

Consulting Geologist

Damayanti Banerji, Ph.D.

The University of Texas

Contributors

John Seifert, P.G.

Peter Lyman, E.I.T.

LBG-Guyton & Associates

December 2017

This page is intentionally left blank.



Final Report on the Delineation of Fresh, Brackish, and Saline Groundwater Resources Based on Interpretation of Geophysical Logs

GEOSCIENTIST AND ENGINEERING SEAL

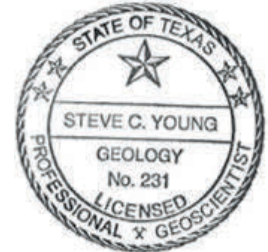
Steve Young was the Principal Investigator for this study. All work performed was under the direct supervision of Steven C. Young (P.G. 231). It is not to be used for construction, bidding or any other purposes not specifically sanctioned by the authors.

Steven C Young

Signature

12/18/2017

Date



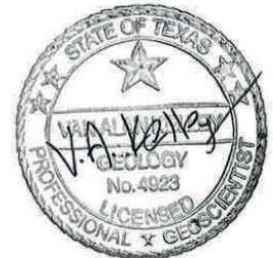
Van Kelley (P.G. 4923) was the Project Manager for this study. He has reviewed study results and participated in the documentation of the study.

Van Kelley

Signature

12/18/2017

Date



Neil Deeds was (P.E. 92741) ... Dr. Deeds was the technical lead for developing software to estimate Total Dissolved Solids concentrations from geophysical data and to map Total Dissolved Solids concentrations in three dimensions.

Neil Deeds

Signature

12/18/2017

Date



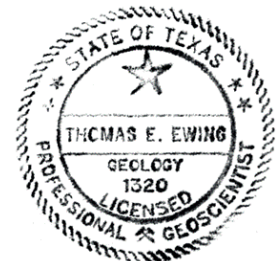
Tom Ewing (P.G. 1320) was responsible for interpreting geophysical logs along transects to delineate the stratigraphic boundaries, to identify sand beds, and to map the fault zones of the Gulf Coast Aquifer System.

Thomas Ewing

Signature

12/18/2017

Date





Final Report on the Delineation of Fresh, Brackish, and Saline Groundwater Resources Based on Interpretation of Geophysical Logs

This page is intentionally left blank.



TABLE OF CONTENTS

1.0	INTRODUCTION.....	1
1.1	Study Area	1
1.2	Study Technical Background and Approach	3
2.0	HYDROGEOLOGIC SETTING	11
2.1	Texas Gulf Coast	11
2.2	Stratigraphy	11
2.3	Geologic Faults	12
2.4	Salt Domes.....	12
3.0	AQUIFER LITHOLOGY AND STRUCTURE	19
3.1	Geophysical Logs	19
3.1.1	Types of Geophysical Logs	19
3.1.2	Raster and LAS Log Formats	20
3.1.3	Location of Geophysical Logs in the Study Area	20
3.2	Interpretation of Electric Logs.....	20
3.3	Vertical Profiles of Sand and Clay Sequences and Sand and Clay Thickness Maps.....	21
3.4	Stratigraphic Cross Sections	23
3.5	Porosity.....	23
4.0	WATER QUALITY	37
4.1	Water Quality	37
4.1.1	Salinity Classification by TDS Concentrations	37
4.2	Estimating TDS Concentrations from Geophysical Logs.....	37
4.2.1	Electrical Resistivity and Specific Conductance	38
4.2.2	Temperature Adjustments to Electrical Resistivity	39
4.2.3	Development of Methods to Estimate Salinity from Electrical Resistivity in the Study Area.....	40
4.3	Groundwater Salinity.....	41
4.3.1	Depth to the Base of Fresh Water	41
4.3.2	Depth to the Base of Slightly Saline Water.....	41
4.3.3	Depth to the Base of Moderately Saline Water.....	42
4.3.4	Depth to the Base of Very Saline Water	42
4.3.5	Comparison of the Depth to Base of Fresh and Slightly Saline Water to Texas Railroad Commission Data.....	43
4.3.6	Comparison of the Base of Fresh Water Zone with TDS Concentrations Measured in Water Wells	43
4.3.7	Brackish Groundwater Zone	44
4.4	Cross Sections Showing Stratigraphy, Lithology, and Water Quality	44
5.0	GROUNDWATER VOLUME BY SALINITY CLASS	67
5.1	Approach	67
5.1.1	Confined and Unconfined Aquifer	67
5.1.2	Hydraulic and Physical Properties for the Gulf Coast Aquifer System	68
5.1.3	Calculation of Groundwater Volumes by Salinity Classification	69
5.2	Calculated Groundwater Volumes	70



Final Report on the Delineation of Fresh, Brackish, and Saline Groundwater Resources Based on Interpretation of Geophysical Logs

6.0 STUDY SUMMARY 81

6.1 Aquifer Stratigraphy and Depositional Character 81

6.2 Aquifer Lithology 82

6.3 Aquifer Water Quality 83

6.4 Groundwater Volume by Salinity Class 84

7.0 REFERENCES 85

Appendix A: Geophysical Log Information Including Location, Placement on Cross Sections, Updated Picks for Stratigraphy and Picks for Base of Salinity Zone

Appendix B: Maps of Percent Sands, Total Sand Thickness, and Maximum Sand Interval for Geological Formations

Appendix C: Maps of the Geophysical Logs that are Used to Construct Dip Cross-Sections D-5, D-6, D-7, D-8, D-9, and D-10 and Strike Cross-Sections S-1, S-2, and S-3

Appendix D: Cross Sections Showing Sand and Clay Sequences, Stratigraphy, and Fault Zones

Appendix E: Location of Geophysical Logs Used to Estimate Porosity

Appendix F: Estimating TDS Concentrations from Geophysical Logs



LIST OF FIGURES

Figure 1-1	Boundary defining the study area	5
Figure 1-2	Regional water planning groups in the study area	6
Figure 1-3	Groundwater management areas, subsidence districts, and groundwater conservation districts in the study area.....	7
Figure 1-4	River basins in the study area	8
Figure 1-5	River authorities and conservation and reclamation district in the study area	9
Figure 2-1	Geologic and hydrogeologic units of the Gulf Coast Aquifer System (modified from Baker, 1979)	14
Figure 2-2	Map of the Texas Gulf Coast in the study area showing the surface geology and the outcrops of formations comprising the Gulf Coast Aquifer System, the Yegua-Jackson and Brazos Alluvium aquifers (geology from Texas Natural Resources Information System, 2007)	15
Figure 2-3	Map showing major growth fault zones and shallow salt domes in the onshore part of the Texas coastal zone (fault locations from Ewing, 1990)	16
Figure 2-4	Cross section of Barbers Hill salt dome in Chambers County showing the salt stock, cap rock mineralogical zones, and enclosing hydrostratigraphic intervals (modified from Hamlin and others, 1988).....	17
Figure 3-1	Example of a TIF raster image of a geophysical well log that uses the American Petroleum Institute format.....	25
Figure 3-2	Example of a LAS file that was produced from a TIF file	26
Figure 3-3	Location of the geophysical logs that were interpreted to develop TDS, lithology and stratigraphy and location of six cross-sections along dip and three cross sections along strike.....	27
Figure 3-4	Idealized spontaneous potential and resistivity curve showing the responses corresponding to alternating sand and clay strata that are saturated with groundwater which increases significantly in TDS concentrations with depth (modified from Driscoll [1986, p. 189])	28
Figure 3-5	Maps of log coverage, sand percentage, total sand thickness and maximum sand interval for the Chicot Aquifer. Log coverage is the percentage of the aquifer intersected by the portion of the geophysical log analyzed.....	29
Figure 3-6	Maps of log coverage, sand percentage, total sand thickness and maximum sand interval for the Evangeline Aquifer. Log coverage is the percentage of the aquifer intersected by the portion of the geophysical log analyzed.....	30
Figure 3-7	Maps of log coverage, sand percentage, total sand thickness and maximum sand interval for the Japser Aquifer. Log coverage is the percentage of the aquifer intersected by the portion of the geophysical log analyzed.....	31
Figure 3-8	Maps of log coverage, clay percentage, total clay thickness and maximum clay interval for the Chicot Aquifer. Log coverage is the percentage of the aquifer intersected by the portion of the geophysical log analyzed.....	32
Figure 3-9	Maps of log coverage, clay percentage, total clay thickness and maximum clay interval for the Evangeline Aquifer. Log coverage is the percentage of the aquifer intersected by the portion of the geophysical log analyzed.....	33



Final Report on the Delineation of Fresh, Brackish, and Saline Groundwater Resources Based on Interpretation of Geophysical Logs

Figure 3-10 Maps of log coverage, clay percentage, total clay thickness and maximum clay interval for the Japser Aquifer. Log coverage is the percentage of the aquifer intersected by the portion of the geophysical log analyzed..... 34

Figure 3-11 Locations of thirty-eight logs that were analyzed to determine porosity values..... 35

Figure 3-12 Measured porosity versus depth. Blue data is from the TWDB Gulf Coast Study (Young and others, 2016) and orange data is from this study. 36

Figure 4-1 Locations of 399 pairs consisting of a geophysical log(s) and a water well that were used to develop an R_o -TDS relationships for the Gulf Coast Aquifer System (from Young and others, 2016)..... 46

Figure 4-2 Depth to the base of the fresh water 47

Figure 4-3 Depth to the base of slightly saline water 48

Figure 4-4 Depth to base of moderately saline water 49

Figure 4-5 Depth to the base of very saline water..... 50

Figure 4-6 Estimated depth to base of fresh water, which is defined as a TDS concentration of 1,000 mg/L, based on 14,597 picks of depth to fresh water from a database maintained by the Groundwater Advisory Unit of the Railroad Commission of Texas.... 51

Figure 4-7 Estimated depth to useable quality water, which is defined as a TDS concentration of 3,000 mg/L, based on 7,017 picks of depth to fresh water from a database maintained by the Groundwater Advisory Unit of the Railroad Commission of Texas.... 52

Figure 4-8 Thickness of the brackish groundwater zone 53

Figure 4-9 Thickness of brackish groundwater in the Chicot Aquifer 54

Figure 4-10 Thickness of brackish groundwater in the Evangeline Aquifer..... 55

Figure 4-11 Thickness of brackish groundwater in the Jasper Aquifer 56

Figure 4-12 Profiles of calculated salinity zones for sand beds identified on geophysical logs aligned on Cross-Section D-5 shown in Figure 3-3. Markers represent the formation bottoms at each log location. The lines connecting the markers are for illustrative purposes only. Dashed line indicates crossing a log with no marker available in an active interval. 57

Figure 4-13 Profiles of calculated salinity zones for sand beds identified on geophysical logs aligned on Cross-Section D-6 shown in Figure 3-3.. Markers represent the formation bottoms at each log location. The lines connecting the markers are for illustrative purposes only. Dashed line indicates crossing a log with no marker available in an active interval. 58

Figure 4-14 Profiles of calculated salinity zones for sand beds identified on geophysical logs aligned on Cross-Section D-7 shown in Figure 3-3. Markers represent the formation bottoms at each log location. The lines connecting the markers are for illustrative purposes only. Dashed line indicates crossing a log with no marker available in an active interval. 59

Figure 4-15 Profiles of calculated salinity zones for sand beds identified on geophysical logs aligned on Cross-Section D-8 shown in Figure 3-3. Markers represent the formation bottoms at each log location. The lines connecting the markers are for illustrative purposes only. Dashed line indicates crossing a log with no marker available in an active interval. 60



Final Report on the Delineation of Fresh, Brackish, and Saline Groundwater Resources Based on Interpretation of Geophysical Logs

Figure 4-16 Profiles of calculated salinity zones for sand beds identified on geophysical logs aligned on Cross-Section D-9 shown in Figure 3-3. Markers represent the formation bottoms at each log location. The lines connecting the markers are for illustrative purposes only. Dashed line indicates crossing a log with no marker available in an active interval. 61

Figure 4-17 Profiles of calculated salinity zones for sand beds identified on geophysical logs aligned on Cross-Section D-10 shown in Figure 3-3. Markers represent the formation bottoms at each log location. The lines connecting the markers are for illustrative purposes only. Dashed line indicates crossing a log with no marker available in an active interval. 62

Figure 4-18 Profiles of calculated salinity zones for sand beds identified on geophysical logs aligned on Cross-Section S-1 shown in Figure 3-3. Markers represent the formation bottoms at each log location. The lines connecting the markers are for illustrative purposes only. Dashed line indicates crossing a log with no marker available in an active interval. 63

Figure 4-19 Profiles of calculated salinity zones for sand beds identified on geophysical logs aligned on Cross-Section S-2 shown in Figure 3-3. Markers represent the formation bottoms at each log location. The lines connecting the markers are for illustrative purposes only. Dashed line indicates crossing a log with no marker available in an active interval. 64

Figure 4-20 Profiles of calculated salinity zones for sand beds identified on geophysical logs aligned on Cross-Section S-3 shown in Figure 3-3. Markers represent the formation bottoms at each log location. The lines connecting the markers are for illustrative purposes only. Dashed line indicates crossing a log with no marker available in an active interval. 65

Figure 5-1 Schematic graph showing the difference between unconfined and confined aquifers (from Jigmond and Wade, 2013) 80

Figure 5-2 Schematic of aquifer transitioning from unconfined in outcrop region, where recharge from precipitation occurs, to confined conditions in the down dip regions of the aquifer (from http://www.geo.brown.edu/research/Hydrology/ge58_IntrodHydrology/ge58_index.htm)..... 80



LIST OF TABLES

Table 1-1	Regional water planning groups, subsidence districts, aquifer storage and recovery conservation district, and groundwater conservation districts in the study area.....	2
Table 1-2	River basins, river authorities, and conservation and reclamation district in the study area	2
Table 1-3	Total dissolved solids concentrations for fresh, slightly saline, moderately saline, very saline, and brine groundwater.....	3
Table 2-1	Salt domes located within 15,000 feet of land surface in the Texas Gulf Coast Aquifer System (data from Ewing, 1990).....	13
Table 3-1	Summary of the geophysical log types used for this study	19
Table 3-2	Aquifer sand and clay percentage for aquifers and formations	22
Table 4-1	Groundwater salinity classification based on the criteria established by Winslow and Kister (1956).....	37
Table 4-2	The recommended working range and maximum operating range for methods used for estimating TDS concentration from geophysical logs (from Estep, 1998)	38
Table 4-3	Electrical conductivity and electrical resistivity of sodium chloride (NaCl) and calcium carbonate (CaCO ₃) solutions at different concentrations (from Young and others, 2016).....	39
Table 5-1	Model layers that comprise the Gulf Coast Aquifer System in the Central Gulf Coast Groundwater Availability Model and model specific yield (Chowdhury and others, 2004)	69
Table 5-2	List of the different assumptions used to tabulate the volumes of groundwater associated with fresh, slightly saline, moderately saline, very saline, and brine	71
Table 5-3	Aquifer sand groundwater volume (in millions of acre-feet) by county and salinity class assuming a void fraction based upon specific yield	72
Table 5-4	Total aquifer groundwater volume (in millions of acre-feet) by county and salinity class assuming a void fraction based upon specific yield	73
Table 5-5	Aquifer sand groundwater volume (in millions of acre-feet) by Subsidence District and salinity class assuming a void fraction based upon specific yield.....	74
Table 5-6	Total aquifer groundwater volume (in millions of acre-feet) by Subsidence District and salinity class assuming a void fraction based upon specific yield.....	75
Table 5-7	Aquifer sand groundwater volume (in millions of acre-feet) by county and salinity class assuming a void fraction based upon porosity	76
Table 5-8	Total aquifer groundwater volume (in millions of acre-feet) by county and salinity class assuming a void fraction based upon porosity	77
Table 5-9	Aquifer sand groundwater volume (in millions of acre-feet) by Subsidence District and salinity class assuming a void fraction based upon porosity	78
Table 5-10	Total aquifer groundwater volume (in millions of acre-feet) by Subsidence District and salinity class assuming a void fraction based upon porosity	79
Table 6-1	Summary of the number and location of geophysical logs used to determine lithology, water quality and to update stratigraphic picks	82
Table 6-2	Estimated fresh and brackish groundwater in storage in sands (millions of acre-feet) in the Harris-Galveston and Fort Bend Subsidence Districts	84



ACROYNMS AND ABBREVIATIONS

°C	degrees Celsius
°F	degrees Fahrenheit
µmhos/cm	micromhos per centimeter
%	percent
API	American Petroleum Institute
BRACS	Brackish Resources Aquifers Characterization System
CGCGAM	Central Gulf Coast Groundwater Availability Model
FBSD	Fort Bend Subsidence District
GCD	Groundwater Conservation District
GMA	Groundwater Management Area
HAGM	Houston Area Groundwater Model
HGSD	Harris-Galveston Subsidence District
INTERA	INTERA Incorporated
mg/L	milligrams per liter
LAS	Log ASCII Standard
ohm-m	ohm-meter
SP	spontaneous potential
TERS	total estimated recoverable storage
TDS	total dissolved solids
TIF	tagged image file
TWDB	Texas Water Development Board



Final Report on the Delineation of Fresh, Brackish, and Saline Groundwater Resources Based on Interpretation of Geophysical Logs

This page is intentionally left blank.



1.0 INTRODUCTION

Recently there has been significant interest in Texas in brackish groundwater resources as a water supply alternative to fresh groundwater and surface water. The Texas Water Development Board (TWDB) defines brackish groundwater as groundwater having a total dissolved solids (TDS) concentration from 1,000 to 10,000 milligrams per liter (mg/L). Significant brackish groundwater resources exist in the Gulf Coast Aquifer System within the boundaries of the Harris-Galveston and Fort Bend Subsidence Districts and recently projects have been proposed and funded to produce brackish groundwater.

In 2015 both the Harris-Galveston and Fort Bend Subsidence Districts adopted Science and Research Plans to define the strategic direction for science and research conducted or supported by the Districts (Turco, 2015a; 2015b). In response to interest in brackish groundwater resource development within the Harris-Galveston and Fort Bend Subsidence Districts, their respective Science and Research Plans identified that research should be performed to:

- Develop a more vertically and horizontally resolute depiction of the hydrostratigraphy of the Harris-Galveston and Fort Bend Subsidence Districts and surrounding areas; and
- Determine the occurrence and hydrogeologic characteristics of the brackish resources within the Harris-Galveston and Fort Bend Subsidence Districts and surrounding areas.

This report documents the results of a study to address the objectives defined above. This study of brackish groundwater resources is a task within a larger scope of work being performed by INTERA for the Harris-Galveston (Contract HGSD-2016-001) and Fort Bend (Contract FBSD-2016-001) Subsidence Districts. The larger study uses data derived from the brackish groundwater characterization study documented herein to:

- Perform a risk assessment of the potential for subsidence that may result from development of brackish groundwater resources in the Jasper Aquifer within the Harris-Galveston and Fort Bend Subsidence Districts; and
- Provide guidance to the Harris-Galveston and Fort Bend Subsidence Districts regarding the types of activities and data that would be beneficial to the consideration of Jasper Aquifer brackish production permits.

The remainder of this section will introduce the study area, technical background, and approach.

1.1 Study Area

The study area is shown in **Figure 1-1**. The study area includes all of Brazoria, Fort Bend, Galveston and Harris counties. It also includes portions of Austin, Chambers, Liberty, Matagorda, Montgomery, Waller and Wharton counties and is approximately 8,244 square miles. The study area is located within three Regional Water Planning Groups (**Table 1-1, Figure 1-2**) and Groundwater Management Areas (GMAs) 14 and 15 (**Figure 1-3**). Contained in the study area are the Harris-Galveston and Fort Bend Subsidence Districts (project sponsors) and all or part of seven Groundwater Conservation Districts (GCDs) (Table 1-1, Figure 1-3). The study area includes portions of eight river basins and four River Authorities (**Table 1-2, Figure 1-4 and Figure 1-5**, respectively).



Final Report on the Delineation of Fresh, Brackish, and Saline Groundwater Resources Based on Interpretation of Geophysical Logs

Table 1-1

Regional water planning groups, subsidence districts, and groundwater conservation districts in the study area

Regional Water Planning Groups
Lower Colorado
Region G
Region H
Subsidence Districts
Fort Bend
Harris-Galveston
Groundwater Conservation Districts
Bluebonnet GCD
Brazoria County GCD
Coastal Bend GCD
Coastal Plains GCD
Colorado County GCD
Lone Star GCD
Lower Trinity GCD

Table 1-2

River basins, river authorities, and conservation and reclamation district in the study area

River Basins
Brazos River Basin
Brazos-Colorado Coastal Basin
Colorado River Basin
Neches-Trinity Coastal Basin
San Jacinto River Basin
San Jacinto-Brazos Coastal Basin
Trinity River Basin
Trinity-San Jacinto Coastal Basin
River Authorities
Brazos River Authority
Lower Colorado River Authority
San Jacinto River Authority
Trinity River Authority
Conservation and Reclamation District
Gulf Coast Water Authority

The aquifer underlying the study area is the Gulf Coast Aquifer System. The Gulf Coast Aquifer System is a TWDB-designated major aquifer in the state of Texas and underlies all or parts of 56 counties along the Texas Gulf Coast (George and others, 2011). It extends from the Louisiana-Texas border to the Mexico-United States border. The Gulf Coast Aquifer System is designated as a major aquifer because it provides large quantities of water in large areas of the state. The Gulf Coast Aquifer System is not a single aquifer, but rather consists of several aquifers and confining units; the Chicot, Evangeline, and Jasper aquifers and the Burkeville and Catahoula Confining System (Baker, 1979; Kasmarek, 2013).



1.2 Study Technical Background and Approach

The results presented in this report build on the recent work performed by the TWDB characterizing brackish groundwater resources in the Gulf Coast Aquifer System (Young and others, 2016). House Bill 30, passed by the 84th Texas Legislature, requires the TWDB to identify and designate brackish groundwater production zones in Texas aquifers no later than December 1st, 2022. Four aquifers were called out in the house bill to be studied and reported on no later than December 1st, 2016. The Gulf Coast Aquifer System was one of the aquifers to be reported on by December 1st, 2016. House Bill 30 excludes areas within the Harris-Galveston and Fort Bend Subsidence Districts from being identified or designated as local or regional brackish groundwater production zones by the TWDB.

This study uses a groundwater quality characterization methodology consistent with that used by the TWDB Gulf Coast Aquifer System House Bill 30 brackish production zone study and consistent with techniques applied by the United States Geological Survey. The study is based upon the interpretation of geophysical logs to determine aquifer stratigraphy, aquifer lithology and estimated water quality. The estimated water quality from geophysical logs is defined as TDS concentrations expressed in units of mg/L.

The TWDB (Meyer and Wise, 2012) classifies groundwater into five salinity classes by TDS concentration summarized in **Table 1-3**. Brackish water includes the slightly saline and moderately saline classifications.

Table 1-3 Total dissolved solids concentrations for fresh, slightly saline, moderately saline, very saline, and brine groundwater

Salinity Classification	Total Dissolved Solids Concentration Range (mg/L)
Fresh	Less than 1,000
Slightly Saline*	1,000 to 3,000
Moderately Saline*	3,000 to 10,000
Very Saline	10,000 to 35,000
Brine	>35,000

Note: mg/L=milligrams per liter

*Brackish water includes slightly saline and very saline water.

This study uses the Gulf Coast Aquifer System stratigraphic framework developed by the TWDB (Young and others, 2012). In the initial phase of the study, geophysical logs were assembled that provide adequate geographic coverage and include the Gulf Coast Aquifer System depth interval. Once adequate logs were collected, standard geophysical log interpretation methods discussed in this report were used to: estimate TDS concentrations using formation resistivity, to determine aquifer formation lithology, to estimate groundwater in storage by salinity classification and to perform stratigraphic interpretation of aquifer boundaries. A total of 438 geophysical logs were interpreted for the purposes described above.

Aquifer lithology was determined through the interpretation of 294 geophysical logs within the study area. Of the 294 logs analyzed for aquifer lithology, 169 are unique to this study to increase resolution within the Harris-Galveston and Fort Bend Subsidence Districts. Aquifer lithology was classified as either



Final Report on the Delineation of Fresh, Brackish, and Saline Groundwater Resources Based on Interpretation of Geophysical Logs

sand or clay. The lithology picks were made at the foot scale of vertical resolution. Maps were developed for sand percent, total sand thickness and maximum sand interval for the ten formations comprising the Gulf Coast Aquifer System and for the Chicot, Evangeline and Jasper aquifers. A similar set of maps for clay content were developed by formation and aquifer.

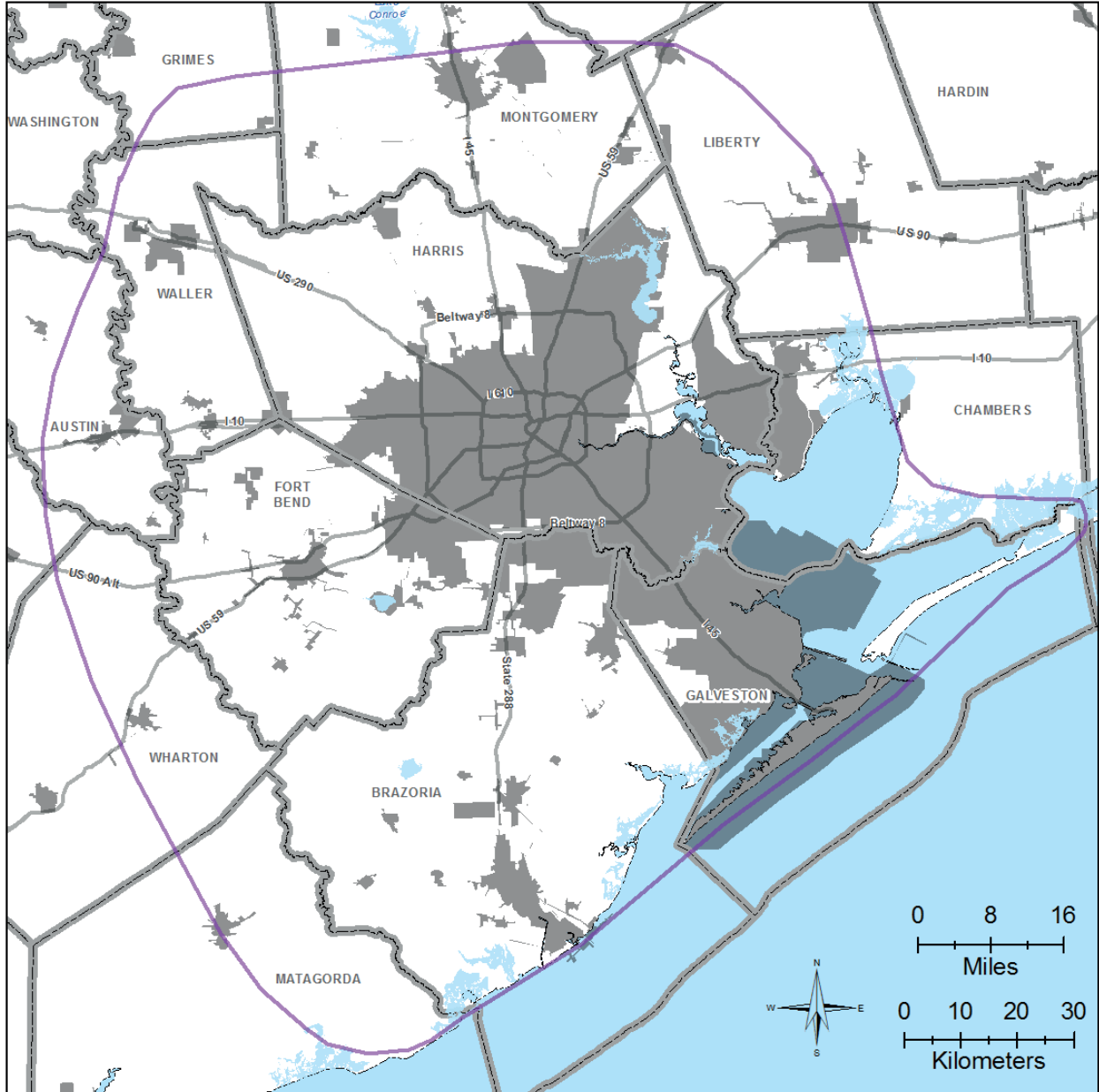
Aquifer water quality was classified by TDS concentration for a total of 299 geophysical logs in the study area. Water quality was only estimated for sand units of a thickness 10 feet or greater because of the limitations of the vertical averaging of a geophysical resistivity tool. The results of the geophysical analysis were checked against TDS measurements in 575 water wells and with similar geophysical analyses performed by the Groundwater Advisory Unit at the Texas Railroad Commission. Using the TDS concentration estimates and estimates of porosity, the volume of groundwater in storage was calculated by salinity water quality classification (fresh, slightly saline, moderately saline, very saline, and brine). The groundwater in storage volumes were calculated by aquifer and formation.

Using the water quality dataset, the depth to the top and bottom of each groundwater salinity classification were estimated. These boundaries were estimated using cross sections depicting aquifer lithology, TDS classification and formation. A total of fourteen cross sections were created to define the salinity classification boundaries. Nine of these cross sections are presented in the report. Five of the cross sections were working cross sections used to infill within the nine cross sections included in the report.

Nine stratigraphic cross sections were developed using 209 geophysical logs in the study area to characterize thick sand and clay sequences in context of aquifer location and water quality. In the process of developing these cross sections, stratigraphic picks were refined from Young and others (2012) if necessary. The nine stratigraphic cross sections provide additional information for the Harris-Galveston and Fort Bend Subsidence Districts to use when evaluating proposed brackish groundwater projects.



Final Report on the Delineation of Fresh, Brackish, and Saline Groundwater Resources Based on Interpretation of Geophysical Logs



Legend

- Study Area
- County Lines
- Major Highways
- Municipalities



Prepared for:



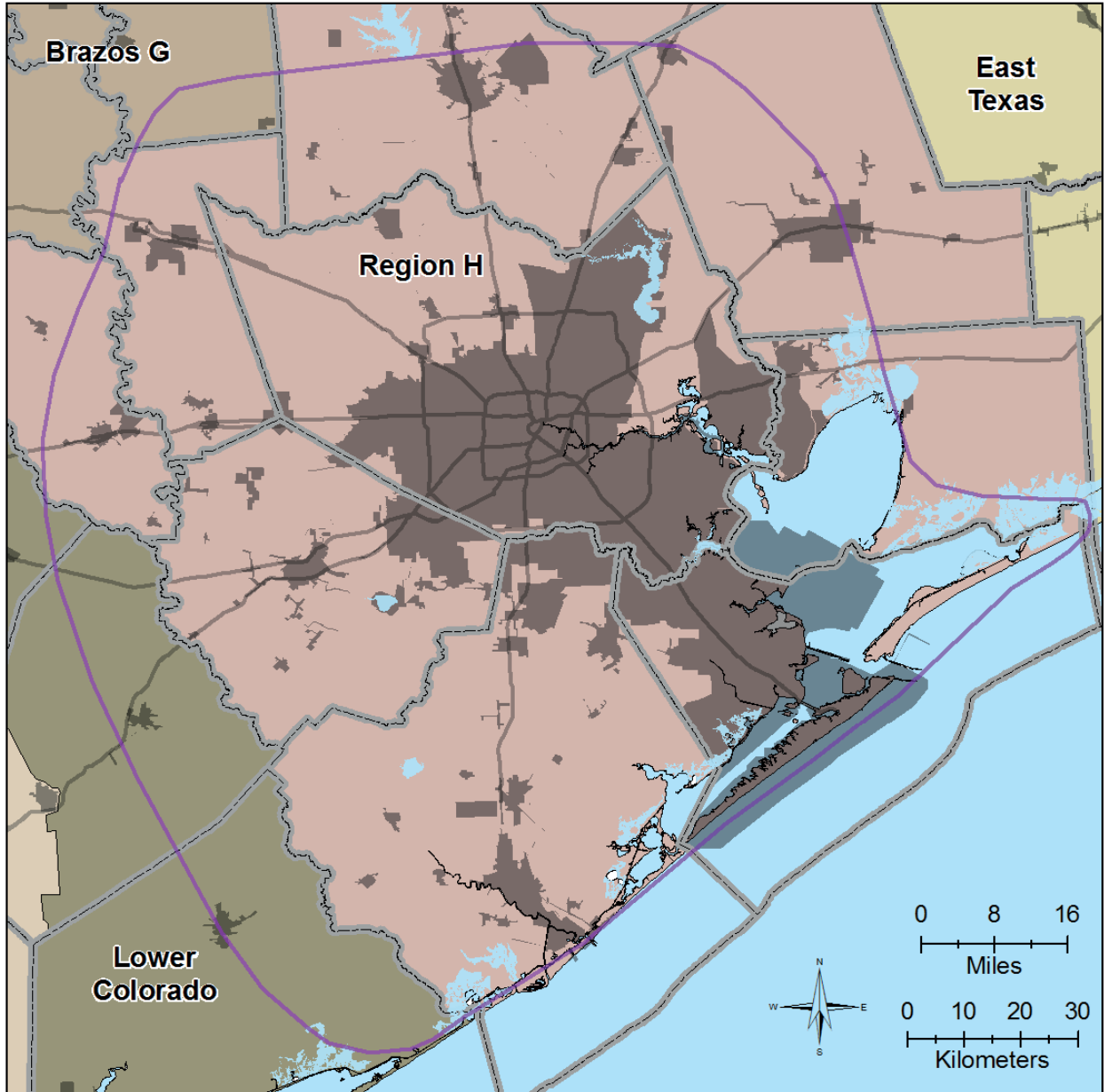
Prepared by:



Figure 1-1 Boundary defining the study area



Final Report on the Delineation of Fresh, Brackish, and Saline Groundwater Resources Based on Interpretation of Geophysical Logs



Legend

- Study Area
- County Lines
- Major Highways
- Municipalities

Regional Water Planning Groups

- Brazos G
- East Texas
- Lavaca
- Lower Colorado
- Region H

Prepared for:



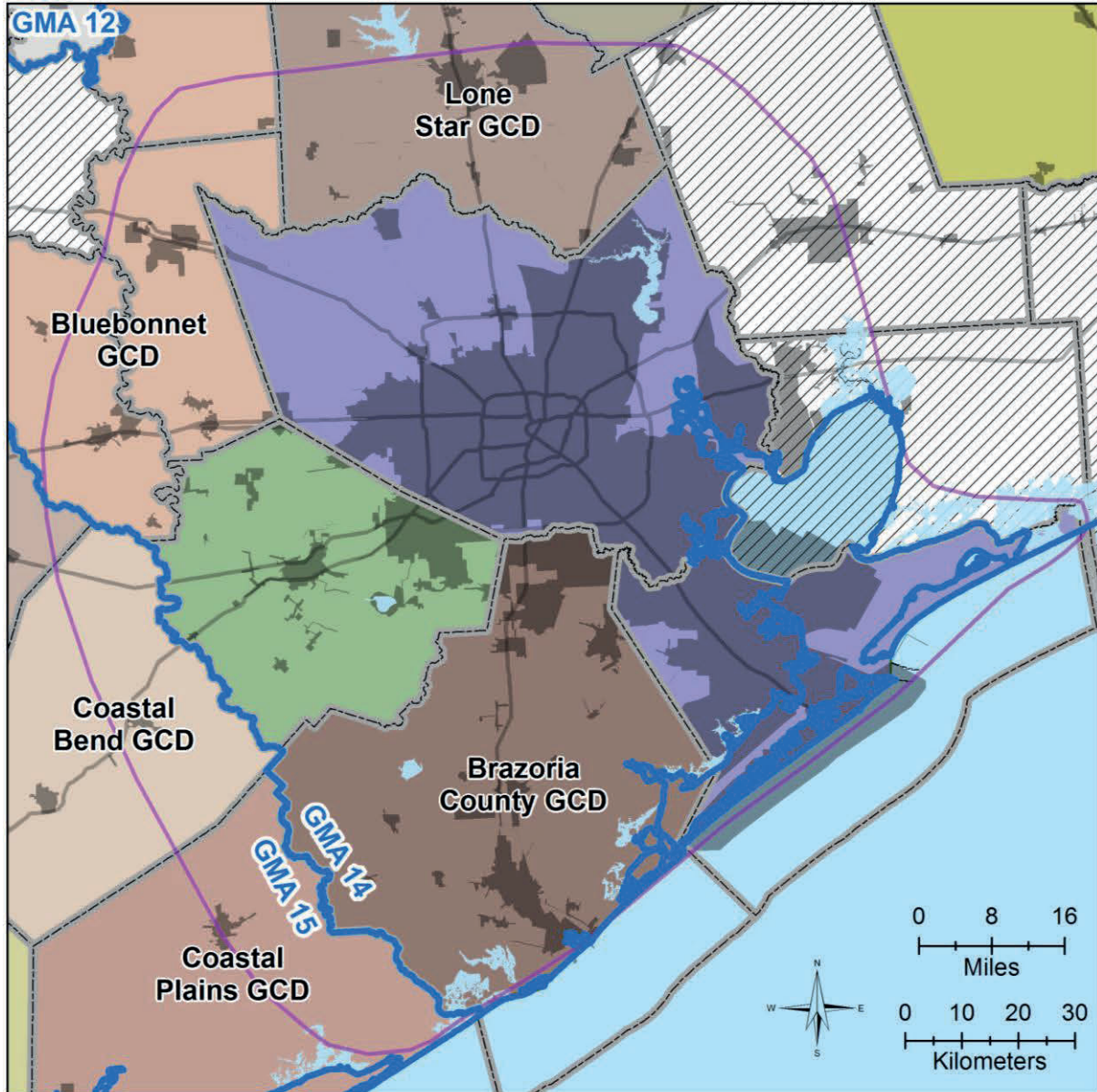
Prepared by:



Figure 1-2 Regional water planning groups in the study area



Final Report on the Delineation of Fresh, Brackish, and Saline Groundwater Resources Based on Interpretation of Geophysical Logs



Legend

- Study Area
- County Lines
- Major Highways
- Municipalities
- Groundwater Management Area (GMA) boundary
- Subsidence Districts**
- Fort Bend
- Harris-Galveston

Groundwater Conservation District (GCD)

- Bluebonnet GCD
- Brazoria County GCD
- Coastal Bend GCD
- Coastal Plains GCD
- Colorado County GCD
- Lone Star GCD
- Lower Trinity GCD
- No GCD

Prepared for:



Prepared by:

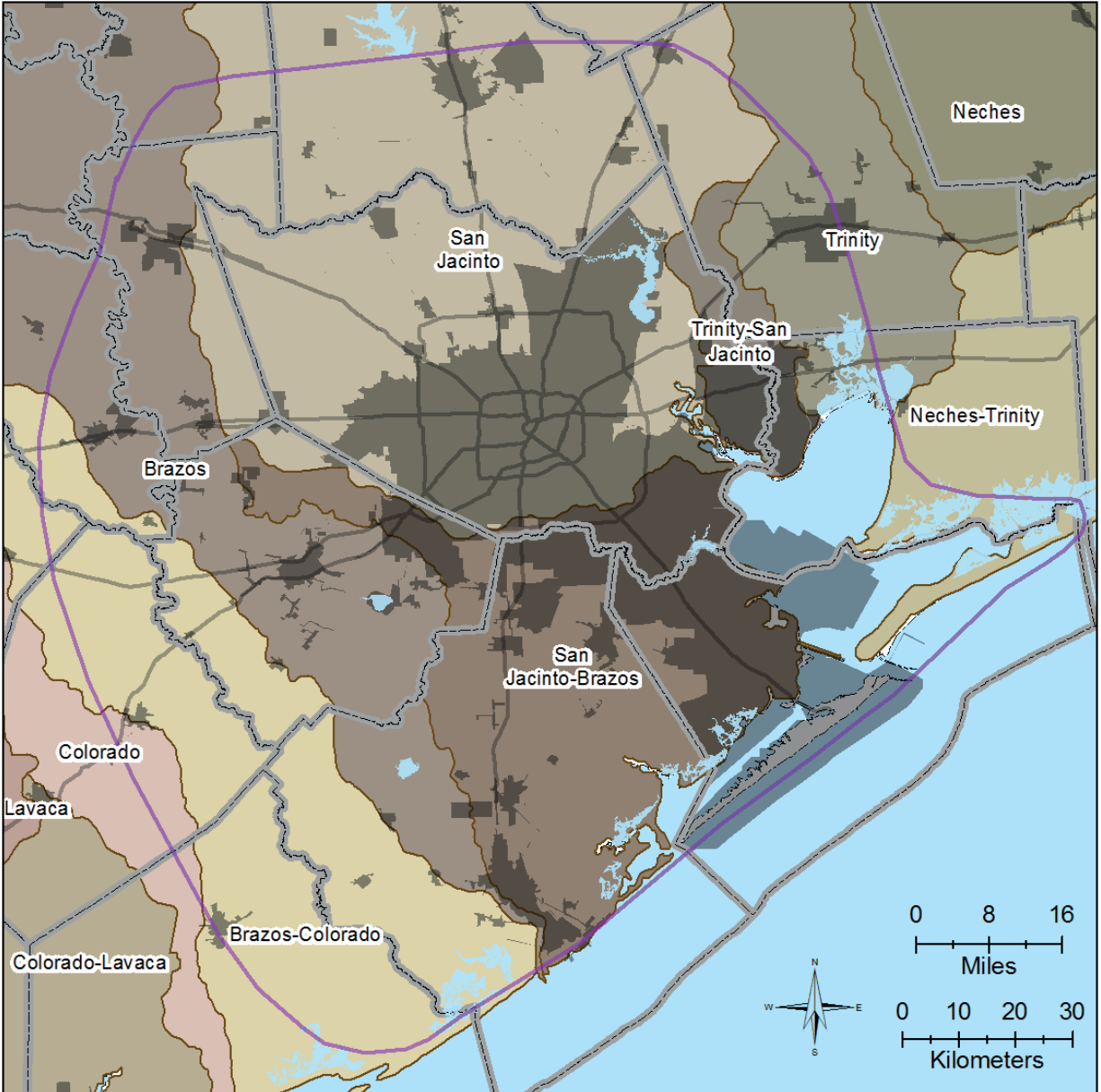


S:\AUS\HGSDM.M001.SUBSI\GIS\mxd_report\Arc10.2_Figure_1-3_Administrative_v1.mxd

Figure 1-3 Groundwater management areas, subsidence districts, and groundwater conservation districts in the study area



Final Report on the Delineation of Fresh, Brackish, and Saline Groundwater Resources Based on Interpretation of Geophysical Logs



Legend

- Study Area
- County Lines
- Major Highways
- Municipalities

River Basins

- | | |
|-----------------|---------------------|
| Brazos | Neches-Trinity |
| Brazos-Colorado | San Jacinto |
| Colorado | San Jacinto-Brazos |
| Colorado-Lavaca | Trinity |
| Lavaca | Trinity-San Jacinto |
| Neches | |

Prepared for:



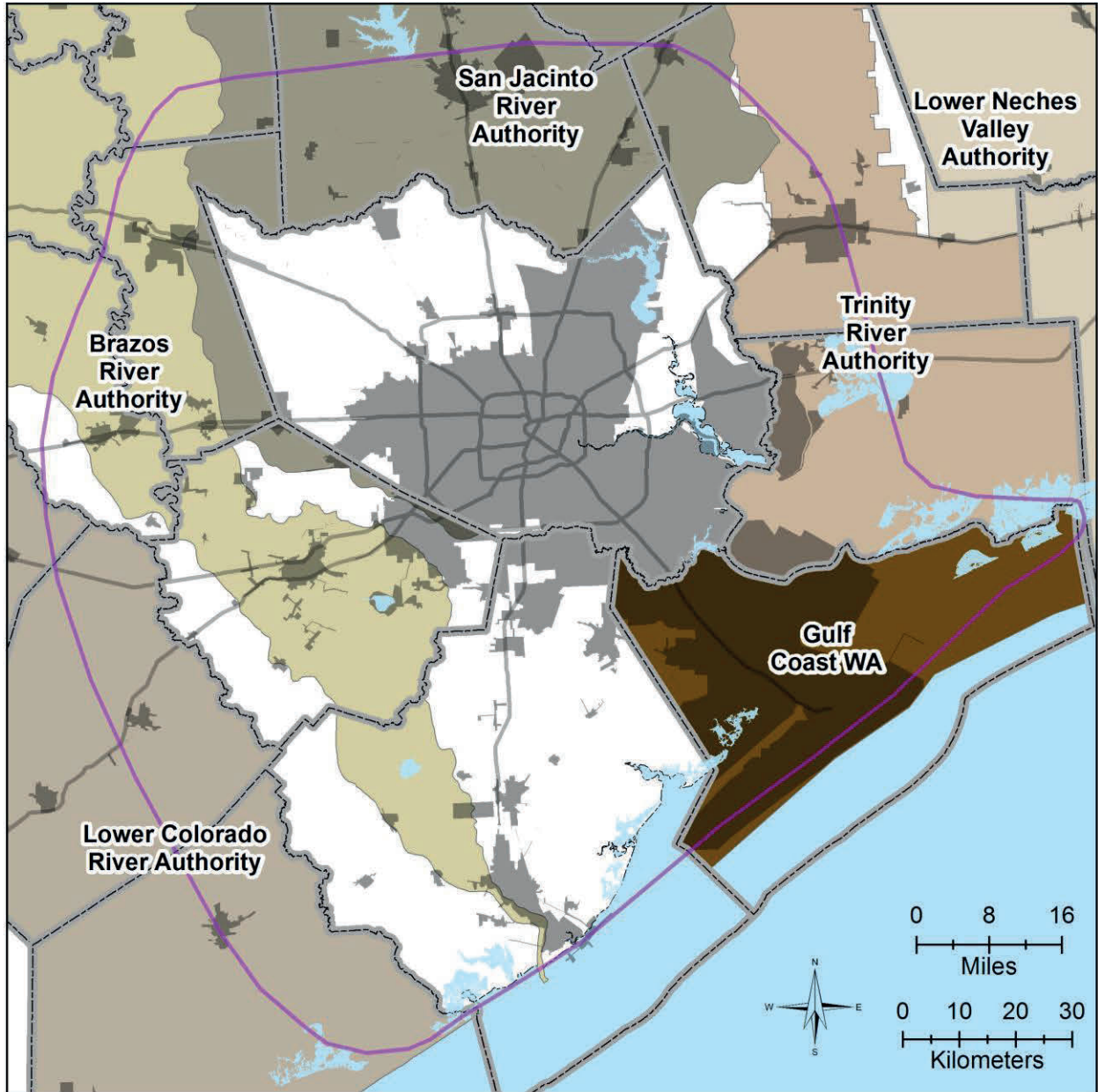
Prepared by:



Figure 1-4 River basins in the study area



Final Report on the Delineation of Fresh, Brackish, and Saline Groundwater Resources Based on Interpretation of Geophysical Logs



Legend

- Study Area
- County Lines
- Major Highways
- Municipalities

River Authorities

- Brazos River Authority
- Lower Colorado River Authority
- Lower Neches Valley Authority
- San Jacinto River Authority
- Trinity River Authority

Conservation and Reclamation District

- Gulf Coast Water Authority

Prepared for:



Prepared by:



Figure 1-5 River authorities and conservation and reclamation district in the study area



Final Report on the Delineation of Fresh, Brackish, and Saline Groundwater Resources Based on Interpretation of Geophysical Logs

This page intentionally left blank.



2.0 HYDROGEOLOGIC SETTING

2.1 Texas Gulf Coast

The Texas Gulf Coast is a part of the Gulf of Mexico, which is a small, semi-enclosed ocean basin surrounded by continental shelves and coastal plains (Bryant and others, 1991). The northwest portion of the Gulf of Mexico includes the major sand and sandstone aquifer systems that include the Texas Gulf Coast Aquifer System (Williamson and Grubb, 2001; Chowdhury and Turco, 2006). **Figure 2-1** provides a simplified stratigraphic and hydrogeologic chart of the Texas Gulf Coast Aquifer System. As shown in Figure 2-1, the Gulf Coast Aquifer System consists of five hydrogeologic units: (1) the Chicot Aquifer, (2) the Evangeline Aquifer, (3) the Burkeville Confining System, (4) the Jasper Aquifer, and (5) the Catahoula Confining System. (Baker, 1979; Kasmarek, 2013). Underlying the Catahoula Formation is the Yegua-Jackson Aquifer.

2.2 Stratigraphy

In the literature, there are considerable differences in the stratigraphic placement of the Catahoula Confining System and the Jasper Aquifer. This study uses the Gulf Coast Aquifer System stratigraphy developed recently by the TWDB (Young and others, 2010, 2012). TWDB based their stratigraphic correlation approach on the correlation and sequence stratigraphic concepts used by Gulf Basin Depositional Synthesis Project (Galloway, 1989; Galloway and others, 2000; Galloway 2005) and the Lower Colorado River Authority-San Antonio Water System Water Project (Knox and others, 2006; Young and Kelly, 2006; Young and others, 2009). The common approach among these studies is that chronostratigraphic correlations are used to identify clay-dominated flooding surfaces of the same age to represent the boundaries of depositional episodes that deposit the coarse sediments defining the aquifers.

The current TWDB Gulf Coast Aquifer System stratigraphy defines 10 geological units in the Gulf Coast Aquifer System. **Figure 2-2** shows the outcrops of the geological units in the Texas Gulf Coast Aquifer System, the Yegua-Jackson Aquifer, and the Brazos Alluvium Aquifer. The Chicot Aquifer includes, from shallowest to deepest, the Beaumont and Lissie formations of Pleistocene age and the Pliocene-age Willis Formation. The Evangeline Aquifer includes the Upper Goliad Formation of earliest Pliocene and late Miocene age, the Lower Goliad Formation of late Miocene age, and the upper unit of the Lagarto Formation (a member of the Fleming Group) of late and middle Miocene age. The Jasper Aquifer includes the Lower Lagarto unit of early Miocene age, the early Miocene Oakville sandstone member of the Fleming Group, and the portions of the Oligocene-age Catahoula Formation. The TWDB defines the base of the Jasper Aquifer as the lower of either the base of the Oakville Formation defined by the TWDB or the base of the Jasper Aquifer, defined by the Source Water Assessment Program (Strom and others, 2003).

The TWDB selected the Middle Lagarto Formation as the geologic unit that best represented the properties of a Burkeville Confining Unit for the entire Texas Gulf Coast Aquifer System. A review of Middle Lagarto Formation lithology, particularly in updip areas of the Gulf Coast Aquifer System and in northeast Texas, reveals that there are large areas where sands are prevalent.



2.3 Geologic Faults

Growth faults are one of the most prevalent fault types in the Gulf Coast Aquifer System. Growth faults are syndepositional normal faults that often form by gravitational creep or differential compaction during rapid sediment loading along an unstable shelf margin and upper slope (Winker and Edwards, 1983). Syndepositional means that sedimentation (deposition) is occurring at the same time as faulting. Growth faults are not isolated surfaces but instead are zones of sediment deformation that commonly enhance vertical flow and impede horizontal groundwater flow. It is believed that growth faults propagate upward through thin sedimentary cover as a series of minor en-echelon faults that constitute a single mapped fault (Crans and others, 1980; Durham, 1971; Roland and others, 1981).

Figure 2-3 shows the major faults mapped in the Gulf Coast Aquifer System by the Bureau of Economic Geology. As shown in **Figure 2-3**, the fault zones are generally parallel to the Gulf Coast Aquifer System basin margin and are grouped according to the shelf-margin positions of major Cenozoic depositional episodes. As expected, the age of the faults become progressively younger basinward. Maximum displacement (several thousand feet) on growth faults occurs in deep formations, such as the Wilcox and Frio, and decreases upward. In the Gulf Coast Aquifer System, maximum fault displacements are a few hundred feet, and surface expressions of active faults are generally only a few feet (Verbeek, 1979). Faults in the Gulf Coast Aquifer System have the potential to impact groundwater flow in several ways. As discussed by Young and others (2014), faults can hinder horizontal flow by offsetting sand units and restricting the continuity of sands across the fault zone. Faults can also enhance vertical flow by causing localized breaches in confining units.

2.4 Salt Domes

Salt domes have the potential to affect the salinity of groundwater as a result of dissolution and introduction of sodium chloride salt into the groundwater system. **Figure 2-3** also shows the location of 34 salt domes in the study area within 15,000 feet of ground surface. **Table 2-1** provides the names, depths, and aquifers in which the salt domes terminate.

Wesselman (1971, 1972) and Hamlin and others (1988) have used geophysical logs to identify high-salinity plumes within otherwise fresh water sands near several Gulf Coast Aquifer System salt domes. Shallow salt domes have the greatest potential to affect groundwater quality. There are 21 shallow salt domes in the study area within the Gulf Coast Aquifer System that range in depth from 0 to 1,500 feet (**Figure 2-3**, **Table 2-1**).

Salt domes typically include three elements: salt stock, cap rock, and surrounding uplifted sediments. The core of a salt dome forms a vertically elongate, cylindrical stock, consisting of 90 to 99 percent (%) crystalline rock salt (halite). Salt-dome crests are generally one to three miles in diameter. Cap rock composed of sulfate and carbonate minerals commonly overlies the crest of the salt stock and drapes down the uppermost flanks (**Figure 2-4**). Cap rock formation results from salt dissolution. Anhydrite (calcium sulfate), the main impurity in the salt stock, forms a residual accumulation at the dome crest after the salt has dissolved. Several researchers have documented the dissolution of salt domes by groundwater and the resulting increase in the salinity of nearby groundwater (Seni and Jackson, 1984; Bruno and Hanor, 2003; Wesselman, 1971 and 1972; and Hamlin and others, 1988).



Final Report on the Delineation of Fresh, Brackish, and Saline Groundwater Resources Based on Interpretation of Geophysical Logs

Table 2-1

Salt domes located within 15,000 feet of land surface in the Texas Gulf Coast Aquifer System (data from Ewing, 1990)

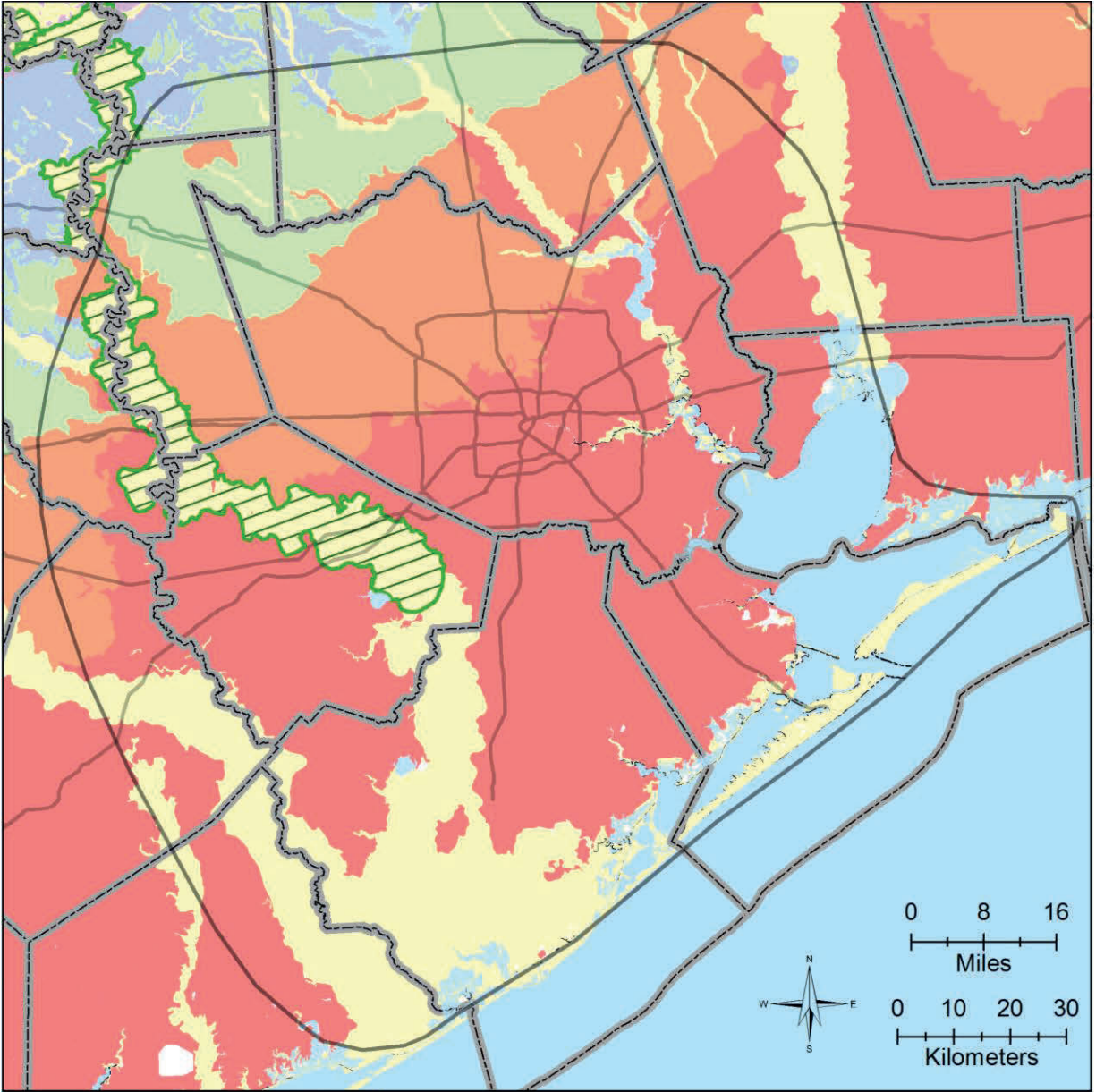
Salt Dome Name	Land Surface (ft, msl)	Depth (ft) to Cap	Depth (ft) to Salt	Aquifer at Dome Top	Salt Dome Name	Land Surface (ft, msl)	Depth (ft) to Cap	Depth (ft) to Salt	Aquifer at Dome Top
Allen	5	760	1,380	Chicot	Manvel	55	11,400	11,400	Deep
Barbers Hill	75	350	1,000	Chicot	Mykawa	50	7,100	7,100	Deep
Big Creek	80	450	600	Chicot	Nash	55	620	950	Chicot
Blue Ridge	85	143	230	Chicot	North Dayton	85	580	800	Chicot
Boling	75	380	975	Chicot	Orchard	110	285	369	Chicot
Bryan Mound	10	680	1,067	Chicot	Pierce Junction	60	730	950	Chicot
Cedar Point	0	10,300	10,300	Deep	Raccoon Bend	150	11,000	11,000	Deep
Clemens	13	600	1,400	Chicot	Red Fish Reef	0	15,200	15,200	Deep
Damon Mound	110	0	530	Chicot	San Felipe	120	3,160	4,200	Deep
Danbury	20	5,000	5,000	Jasper	South Houston	35	4,406	4,406	Jasper
Esperson	55	6,000	6,000	Deep	South Liberty	20	320	480	Chicot
Hawkinsville	10	95	600	Chicot	Stratton Ridge	10	850	1,308	Chicot
High island	20	150	1,100	Chicot	Sugarland	65	3,450	4,280	Jasper
Hockley	170	76	1,000	Chicot	Thompson	55	9,315	9,315	Deep
Hoskins Mound	20	574	1,070	Chicot	Webster	30	10,500	10,500	Deep
Humble	75	700	1,200	Chicot	West Columbia	30	740	790	Chicot
Long Point	75	550	930	Chicot	<i>Note: ft=feet; msl=mean sea level</i>				
Lost Lake	5	3,275	5,430	Evangeline					



Final Report on the Delineation of Fresh, Brackish, and Saline Groundwater Resources Based on Interpretation of Geophysical Logs

ERA	Epoch		Est. Age (M.Y)	Geologic Unit	Hydrogeologic Unit
Cenozoic	Pleistocene		0.7	Beaumont	CHICOT AQUIFER
			1.6	Lissie	
			3.8	Willis	
	Pliocene		11.2	Upper Goliad	EVANGELINE AQUIFER
			14.5	Lower Goliad	
	Miocene	Late	17.8	Upper Lagarto	BURKEVILLE
				Middle Lagarto	
		Early		Lower Lagarto	JASPER AQUIFER
	Oligocene		24.2	Oakville	CATAHOULA
			32	Frio	
			34	Vicksburg	

Figure 2-1 Geologic and hydrogeologic units of the Gulf Coast Aquifer System (modified from Baker, 1979)



**Texas Water Development Board
Geologic Atlas of Texas
Surface Geology**

Legend

- Study Area
- County Lines
- Major Highways
- Brazos River Alluvium Aquifer

Surface geology

- Alluvial, coastal, and other recent deposits
- Beaumont Formation
- Lissie Formation
- Willis Formation
- Oakville Formation
- Catahoula Formation

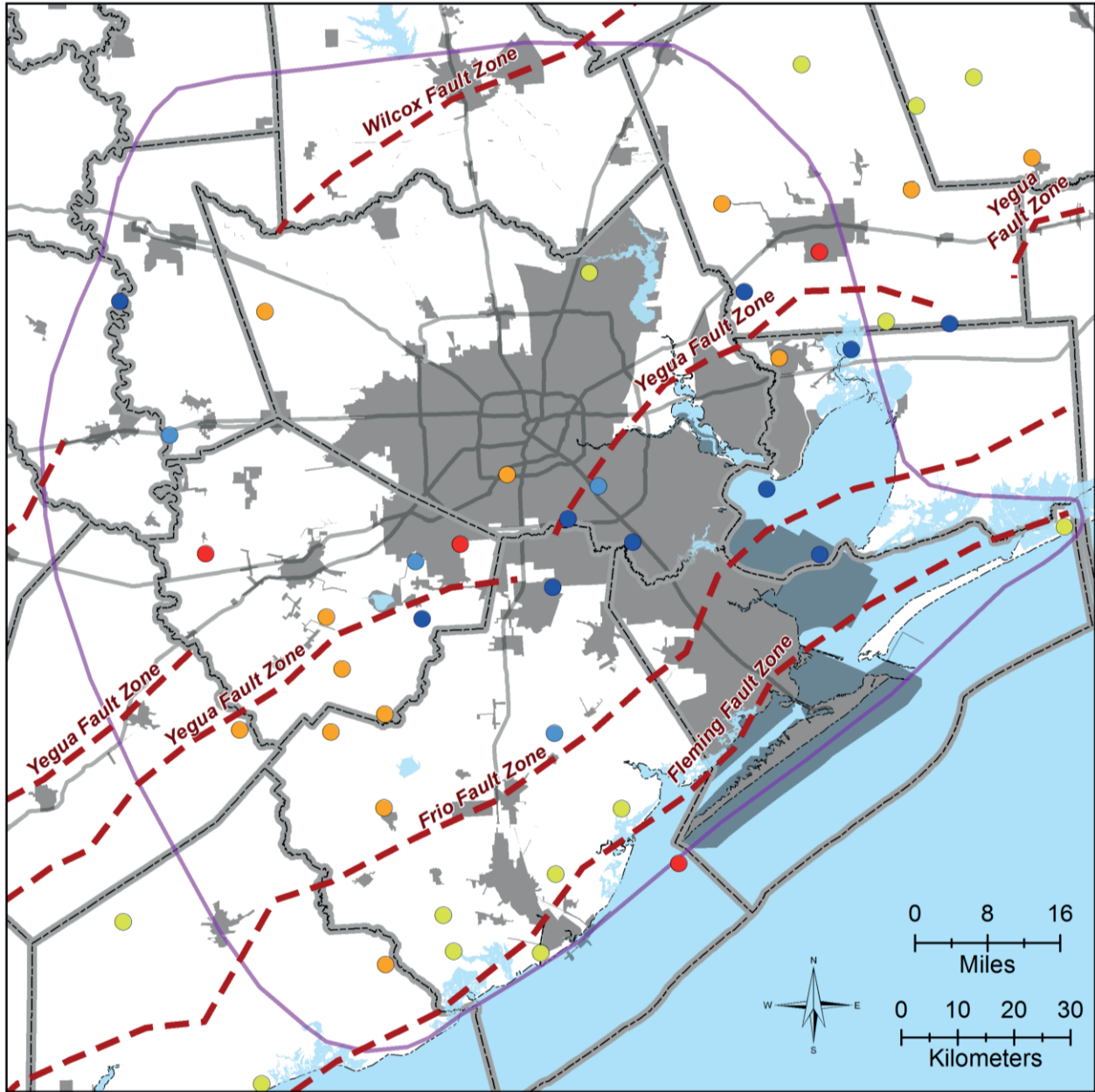
Prepared for:



Prepared by:



Figure 2-2 Map of the Texas Gulf Coast in the study area showing the surface geology and the outcrops of formations comprising the Gulf Coast Aquifer System, the Yegua-Jackson and Brazos Alluvium aquifers (geology from Texas Natural Resources Information System, 2007)



Legend

- Study Area
- County Lines
- Major Highways
- Municipalities
- Major Growth Fault Zone

Depth to Top of Salt Dome (feet)

- < 500
- 500 to 1000
- 1000 to 2000
- 2000 to 3000
- 3000 to 5000
- > 5000

Prepared for:



Prepared by:



Figure 2-3 Map showing major growth fault zones and shallow salt domes in the onshore part of the Texas coastal zone (fault locations from Ewing, 1990)



Final Report on the Delineation of Fresh, Brackish, and Saline Groundwater Resources Based on Interpretation of Geophysical Logs

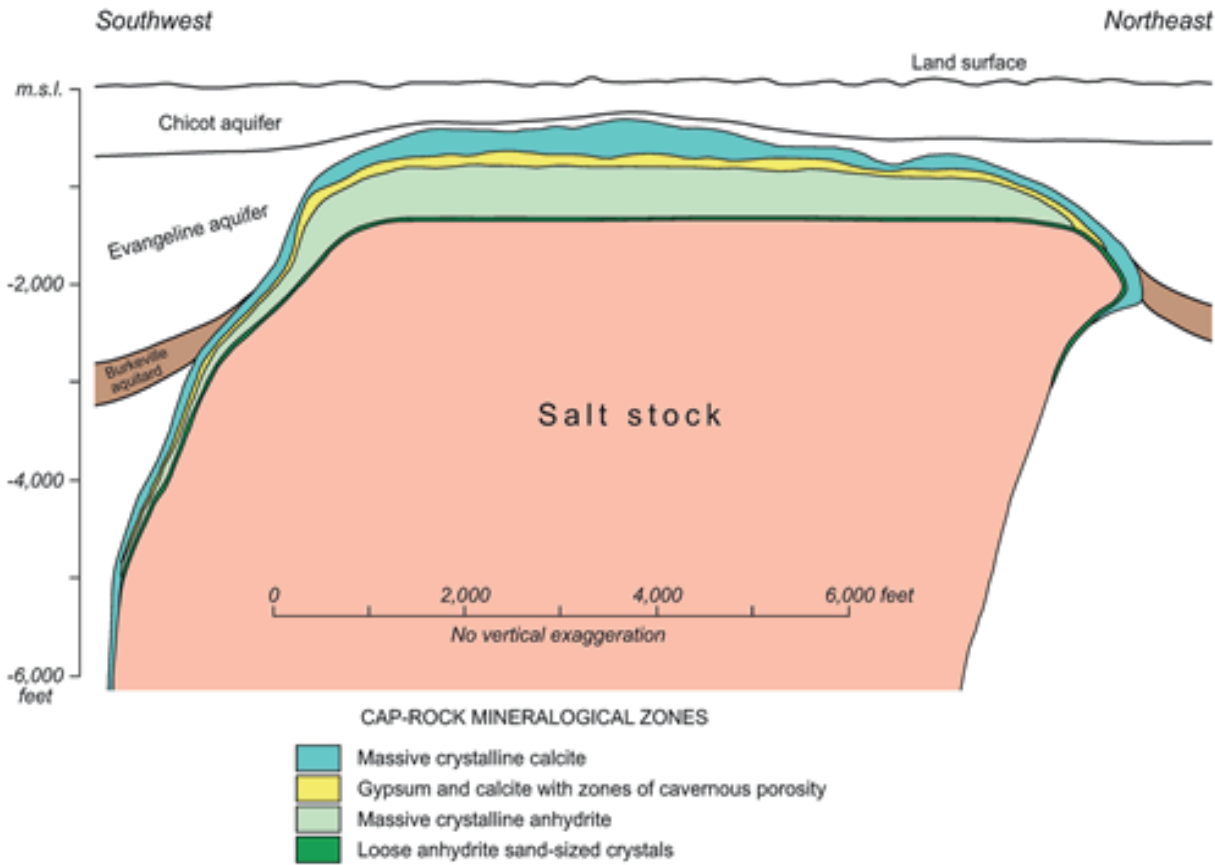


Figure 2-4 Cross section of Barbers Hill salt dome in Chambers County showing the salt stock, cap rock mineralogical zones, and enclosing hydrostratigraphic intervals (modified from Hamlin and others, 1988)



Final Report on the Delineation of Fresh, Brackish, and Saline Groundwater Resources Based on Interpretation of Geophysical Logs

This page is intentionally left blank.



3.0 AQUIFER LITHOLOGY AND STRUCTURE

The study relies on the geologic framework developed for the Gulf Coast Aquifer System by the TWDB (Young and others, 2010, 2012, 2013, 2016). This framework was developed at a regional scale that consists of the analysis of geophysical logs to define vertical profiles of sands and clays and top and bottom surfaces of geological formations. As part of this study, we have refined the TWDB’s regional analyses by doubling the number of analyzed logs in the study area. Nine cross sections have been developed to review stratigraphic boundaries and lithology in the study area. In some cross sections, stratigraphic picks from TWDB were augmented by the new well control.

3.1 Geophysical Logs

Borehole geophysics is the science of recording and analyzing physical and electrical property measurements made in wells or boreholes. Probes are lowered into the borehole to collect continuous or point data that are graphically displayed as a geophysical log. Multiple logs typically are collected to take advantage of their synergistic nature. Much more can be learned by the analysis of a suite of logs as a group than by the analysis of the same logs individually.

3.1.1 Types of Geophysical Logs

The different logging probes are not named according to a consistent system: Some are named based on the parameter measured, others according to the principle by which the measurement is made, and still others based on the geometry of the probe or the trade name. **Table 3-1** summarizes basic information on the geophysical logs used for this study.

Table 3-1 Summary of the geophysical log types used for this study

Log type	Specific log	Borehole Conditions	Information
Nuclear	Gamma-ray Gamma-gamma (density) Neutron-neutron (porosity)	Open and cased holes with or without fluid Open holes with fluid	Lithology, density, porosity, calibration of surface geophysics
Electrical	Spontaneous Potential Resistivity Focused Resistivity	Open or screened holes with fluid	Lithology, salinity of groundwater, calibration of surface geophysics, location of PVC screens
Electromagnetic	Induction Nuclear magnetic resonance	Open and PVC cased holes with or without fluid	Lithology, salinity of groundwater
Acoustical	Sonic	Open holes with fluids	Lithology (porosity)



3.1.2 Raster and LAS Log Formats

The most common format for geophysical files for purchase or exchange is a Tagged Image File (TIF). A TIF is an efficient file format for storing high quality raster graphics. The primary advantage of a TIF format is that it is well suited for capturing highly detailed images for print. **Figure 3-1** is an example of a TIF raster image of a geophysical log.

To process the information in a TIF file, the images of geophysical curves need to be digitized and stored as numeric information. Log ASCII Standard (LAS) is a standard file-format common in the oil-and-gas and water well industries to store digital well log information. A LAS file is a structured ASCII file containing log curve data and header information. **Figure 3-2** is an example of a LAS file.

3.1.3 Location of Geophysical Logs in the Study Area

Table A-1 in **Appendix A** provides the API, spatial coordinates and other descriptors for the 438 logs used in the study. The logs were used to identify sand units, check and update stratigraphy, estimate porosity, estimate TDS concentrations in groundwater, and delineate surfaces of salinity zones. **Figure 3-3** shows the location of 294 logs that were used to identify sand units in the study area and 172 logs used to delineate the Texas Gulf Coast stratigraphy on-shore. An additional 37 logs are located off-shore and have stratigraphic surfaces based on paleo markers. Among the project deliverables are TIF files for all on-shore wells and both TIF files and LAS files for the 294 logs analyzed for sand and clay sequences. Prior to this study, there were 125 logs analyzed and digitized in the study area for sand and clay sequences as part of previous TWDB studies (e.g., Young and others, 2016) which included 125 digitized logs. This study has increased the number of digitized logs in the study areas from 125 logs to 294 logs, which is about double the number of logs previously utilized in other regional studies.

3.2 Interpretation of Electric Logs

Most of the geophysical logs used in this study are electric logs. Electric logs are comprised of a spontaneous potential (SP) curve on the left side of the log tract and a resistivity curve(s) on the right side of the log tract. **Figure 3-4** was created to illustrate the basic concepts associated with interpreting electric logs. Figure 3-4 shows formation resistivity and SP signatures for a hypothetical borehole with idealized lithologic layers of clay and idealized layers of fresh and brackish groundwater.

In conventional resistivity logging, an electric current is induced between two electrodes, and the resulting electric potential (voltage) is measured between two other electrodes. The resistivity logging measures an apparent electrical resistance in and within the vicinity of the borehole and represents a composite measurement of the resistivity of the geological formation and of groundwater in the formation. The unit of resistivity (reciprocal of conductivity) measurement is the ohm-meter (ohm-m). Dry formations have very high resistivities because they are poor conductors of electricity. Saturation of a deposit reduces its resistivity because water is an electrical conductor. Fresh water deposits composed of sands and gravel tend to have high resistivities. The resistivity of a formation will vary inversely with the TDS concentrations in its pore water. One reason that clays tend to have low apparent resistivities is because their interstitial waters are often highly mineralized. In contrast, sands and gravels saturated with fresh water tend to have high apparent resistivities because their surfaces are relatively inert and tend to release few minerals into solution.

In practice, a resistivity “spike” to the right measuring an increase in resistivity is indicative of a sand. Conversely, a resistivity “spike” to the left measuring a decrease in resistivity is indicative of a clay. The magnitude of a “spike” in the resistivity value is a function of the ionic makeup of the water filling the pores.



Final Report on the Delineation of Fresh, Brackish, and Saline Groundwater Resources Based on Interpretation of Geophysical Logs

That is, the fresher and more interconnected (permeable) a sand/gravel unit is, the higher the magnitude of the resistivity “spikes.” As the water quality in the sand/gravel formation degrades and the TDS concentration increases, the pore fluid within the unit becomes more conductive, and the relative amplitude of “spikes” associated with changes in lithology become increasingly less pronounced. This sensitivity is shown in Figure 3-4. In Figure 3-4, the spikes in the resistivity log associated with clays and sands log are easily interpreted for fresh groundwater but are not so easily defined for brackish groundwater.

At the point at which resistivity “spikes” become unreliable for identifying lithology changes, the SP log is used to identify changes in lithology. An SP log records the measurement of a naturally occurring voltage (or “potential”) caused when conductive drilling fluids contact the geologic formations. Where fresh water is used to create the drilling mud, spikes in the SP log can be used to mark changes in the lithology in aquifers containing brackish groundwater. As shown in Figure 3-4, at shallow depths where there may be little difference in the concentration of ions between the drilling fluids and the aquifer, the analysis of the SP log may be difficult because of the similarity of the salinity of the drilling fluid relative to the formation fluid. However, at deeper depths where the formation waters are more mineralized than the drilling fluids, the leftward deflections (more negative values) in the SP logs are useful for identifying sand and clays.

3.3 Vertical Profiles of Sand and Clay Sequences and Sand and Clay Thickness Maps

For the logs marked in **Figure 3-3**, the study provides a continuous profile of sand and clay picks. The identification of individual sands is important to study for two reasons. First, our methodology for characterizing the quality of groundwater is only applicable to sands and cannot be applied to clay. Second, sand and clay sequences along cross sections provide useful information for identifying possible production areas and confinement zones. The two most important lithologic categories for estimation of hydraulic properties from lithology are sands and clays. Sand intervals are important because their interconnections, thicknesses, and the continuity are the primary factors that determine the average horizontal hydraulic conductivity and transmissivity of a deposit. The clay intervals are important because their thicknesses can be used for regional models to estimate the average vertical hydraulic conductivity of a formation and the clay thickness data are direct inputs to compaction calculations in subsidence studies.

The 294 geophysical logs used to characterize the sand and clay distribution in the study area can be categorized into two groups. One group consists of the 125 logs that were analyzed as part of the TWDB study of brackish groundwater in the Texas Gulf Coast Aquifer System (Young and others, 2016). Existing sand and clay picks for these 125 logs were not changed except where additional picks were made on the log to extend coverage deeper into the Jasper Aquifer. The additional 169 logs obtained for this study were assembled from the following sources:

- Bureau of Economic Geology Geophysical Log Facility
- Company/private log collection
- Texas Commission on Environmental Quality files on public water supply wells
- Railroad Commission of Texas Collection of “Q” logs
- Texas Water Development Board Groundwater Database, Brackish Resources Aquifers Characterization System (BRACS) Database

The same guidelines were applied for delineating sands and clay sequences for both groups of logs. As a general rule, sand and clay beds were delineated at a minimum resolution of 1 foot.

The vertical sand and clay profiles were collectively analyzed to generate sand maps of aquifers and geological formations underlying the study area. **Figure 3-5**, **Figure 3-6**, and **Figure 3-7** show sand maps generated for the



Final Report on the Delineation of Fresh, Brackish, and Saline Groundwater Resources Based on Interpretation of Geophysical Logs

Chicot Aquifer, the Evangeline Aquifer, and the Jasper Aquifer, respectively. Each of the figures consists of four panels. The upper left panel shows the location of the logs that were used to develop the sand maps. Each log location is color-coded to show the percent of the aquifer thickness for which the log has data. Percentages less than 100% indicate that either the log data begin below the top of the aquifer and/or the log data terminate above the bottom of the aquifer. Values from these locations were interpolated in ArcGIS® using a kriging algorithm to produce the maps shown in the other three panels. The upper right panel is a map of sand percentage, and the lower left panel is a map of total sand thickness. The lower right panel is a map of the maximum sand interval.

Figure 3-5 through Figure 3-7 show that the net sand thicknesses associated with the aquifers thicken toward the coast as the aquifer itself thickens. The figures also indicate that the aquifers' ranking from highest to lowest sand percentages is the Chicot Aquifer, the Evangeline Aquifer, and the Jasper Aquifer, which are characterized by average sand percentages of 68, 46, and 40% in the study area, respectively. Sand percentages provide a good proxy for transmissivity. After accounting for the effect of the depth of burial and different depositional environments on the permeability of aquifer deposits, the transmissivity of each aquifer should be positively correlated with increases in sand percentages, total sand thickness, and maximum sand interval.

Figure 3-8 through **Figure 3-10** show clay maps generated for the Chicot Aquifer, the Evangeline Aquifer, and the Jasper Aquifer, respectively, similar in nature to the sand maps above. From a review of these figures, one can see that the clay percentage of the Chicot Aquifer is significantly lower than both the Evangeline and the Jasper aquifers. The average clay percent for the Chicot, Evangeline and Jasper aquifers are 32, 54 and 60%, respectively. One can also see an increase in the total clay thickness as one moves towards the gulf, which also correlates to aquifer depth of burial. The clay percent and the thickness of clay in each aquifer is very important when one considers the compaction potential of that aquifer.

Appendix B provides similar sand and clay maps for the geological formations that comprise the Texas Gulf Coast Aquifer System. **Figure B-1** through **Figure B-9** show sand maps for the Beaumont, Lissie, Willis, Upper Goliad, Lower Goliad, Upper Lagarto, Middle Lagarto, Lower Lagarto, and Oakville formations. **Figure B-10** through **Figure B-18** show clay maps for each formation above. **Table 3-2** lists the average sand and clay percentages for the formations and aquifers that comprise the Texas Gulf Coast Aquifer System.

Table 3-2 Aquifer sand and clay percentage for aquifers and formations

Aquifer /Unit	Average Sand / Clay Percentage	Formation	Average Sand / Clay Percentage
Chicot	68 / 32	Beaumont	67 / 33
		Lissie	70 / 30
		Willis	69 / 31
Evangeline	46 / 54	Upper Goliad	61 / 39
		Lower Goliad	48 / 52
		Upper Lagarto	45 / 55
Burkeville	42 / 58	Middle Lagarto	42 / 58
Jasper	40 / 60	Lower Lagarto	41 / 59
		Oakville	46 / 54



3.4 Stratigraphic Cross Sections

To augment the sand and clay maps discussed above, nine stratigraphic cross sections were developed to provide a basis to improve the understanding of the distribution of major sand and clay rich sequences in relation to aquifer stratigraphy and groundwater salinity boundaries. Each cross section is annotated with the following:

- Aquifer stratigraphy,
- Thick marine shale wedges,
- Thick sand sequences or fairways consisting of productive sands,
- Possible confining units consisting of mudstone or shales,
- Base of water salinity zones,
- Location of geo-pressured areas and probable fault zones.

Gulf Coast Aquifer formations were studied for the occurrence of significant sand and clay sequences using six dip cross sections (D-5, D-6, D-7, D-8, D-9, and D-10) and three strike cross sections (S-1, S-2, and S-3) shown in Figure 3-3. The analysis included adding and replacing logs to provide a more complete cross section through the Gulf Coast Aquifer System as compared to earlier work by Young and others (2012). The nine cross sections use the TWDB structure as their basis for defining formation boundaries. Because additional logs were made available with this study, the TWDB structure (Young and others, 2012) was reviewed and in some cases modified on these sections. Any edits on these sections were performed by Dr. Thomas Ewing, who also served in the same technical role for the TWDB North Gulf Coast Aquifer stratigraphy study. The TWDB methodology for developing structure is based upon chronostratigraphic correlations documented in several studies of Texas Gulf Coast Aquifer System (Knox and others, 2006, 2007; Young and Kelley, 2006; Young and others, 2010, 2012, 2016).

Appendix C contains maps of the geophysical logs used to construct dip stratigraphic Cross-Sections D-5, D-6, D-7, D-8, D-9, and D-10 and strike Cross-Sections S-1, S-2, and S-3. **Appendix D** contains the cross sections and describes the approaches used to map surfaces: marine shale wedges, major sand sequences (or fairways), clay-rich confining zones and fault zones. **Figure D-1** through **Figure D-5** show the along cross sections along dip (Sections D-5, D-6, D-7, D-8, D-9, and D-10). **Figure D-6** through **Figure D-9** show the cross sections along strike (S-1, S-2, and S-3). **Table A-3** in Appendix A lists the formation aquifer boundary elevations from new logs assembled for this study and consistent with Appendix D cross sections.

3.5 Porosity

Porosity is the volume of the void space of a geologic material divided by the total volume of the material and is a key variable required to estimate TDS concentrations from geophysical logs and to estimate groundwater in storage. **Figure 3-11** shows the location of 38 geophysical logs where porosity was determined from the analysis of neutron and density logs. The porosity information was collected as part of this study and another study (Young and others, 2016) to evaluate how the porosity varies spatially and with depth. Young and others (2016) used neutron and density logs to obtain porosity values from log locations P-1 through P-34, which are shown in Figure 3-11. This study added neutron and density logs from log locations P-35 through P-38 to obtain porosity values. **Appendix E** provides the location and API numbers for the 12 logs in the study area and for the two logs within 3 miles of the study area.

Figure 3-12 shows porosity plotted as a function of depth. The data points represent an average porosity value calculated from a neutron-porosity log and a density-porosity log over a sand interval. The neutron log measures



Final Report on the Delineation of Fresh, Brackish, and Saline Groundwater Resources Based on Interpretation of Geophysical Logs

porosity by estimating the amount of water in the sand, and the density log measures porosity by estimating the density of the sand. The sand interval is determined by interpretation of other geophysical logs such as a resistivity log and/ or a gamma log.

In Figure 3-12, blue data points are from Young and others (2016), and orange data points are from this study. The selection criterion for the blue data was a difference of 5% or less between the porosity values measured by the neutron-porosity and the density-porosity logs. A 5% difference translated to an uncertainty of about 5% so that a measurement of 30% porosity is $\pm 1.5\%$. To acquire the 294 porosity measurements, 34 logs were selected out of 300 reviewed porosity logs. Such a large review of logs was conducted so that a low measurement error would help to identify whether a depth-trend with porosity was an appropriate premise for analysis.

To augment the TWDB study, this study calculated 99 porosity estimates from neutron-porosity and density-porosity logs in the study area for individual sands at borehole log locations P-35 through P-38. However, many of the porosity estimates are much less reliable than those used for the TWDB study. We used the criterion of 5% to filter the new measurements and were only left with 42 new porosity estimates. The addition of the new data did not make an appreciable change to the overall depth trends observed from the TWDB data set. Figure 3-12 includes the measurements from locations P-35 to P-38.

The line in Figure 3-12 represents a regression fit to 336 data points, composed of 294 blue data points and 42 orange data points. The regression is expressed as **Equation 3-1**. **Equation 3-2** is the regression developed by Young and others (2016). Both equations indicate that the average porosity is about 37% near ground surface and decreases by 1% for every 1,000 feet of increase in depth of burial. Because of the high degree of scatter about the regression line, the R-square of the regression is less than 0.25. However, there is a notable difference in the porosity values associated with depths less than 1,000 feet and with depths greater than 5,000 feet, so the premise of porosity decreasing with depth will be accepted for this study.

$$\Phi = 36.5 - 0.001 * d \quad \text{(Equation 3-1)}$$

$$\Phi = 36.6 - 0.001 * d \quad \text{(Equation 3-2)}$$

where

Φ = porosity as a percentage of total volume

d = depth (feet)

Two studies that support the presumption that porosity varies as a function of depth in the Texas Gulf Coast Aquifer System are Wallace and others (1972) and Loucks and others (1984). Both studies also indicate that a decrease in porosity occurs with depth at a similar rate represented by Equations 3-1 and 3-2. Wallace and others (1972) report a decrease in porosity of approximately 0.95% every 1,000 feet in the Gulf Coast Aquifer in Texas. Loucks and others (1984) report a range of 1.3 to 2.1% decrease in porosity for every 1,000 feet of depth for the southern, central, and northern portions of the Catahoula Formation.



Final Report on the Delineation of Fresh, Brackish, and Saline Groundwater Resources Based on Interpretation of Geophysical Logs

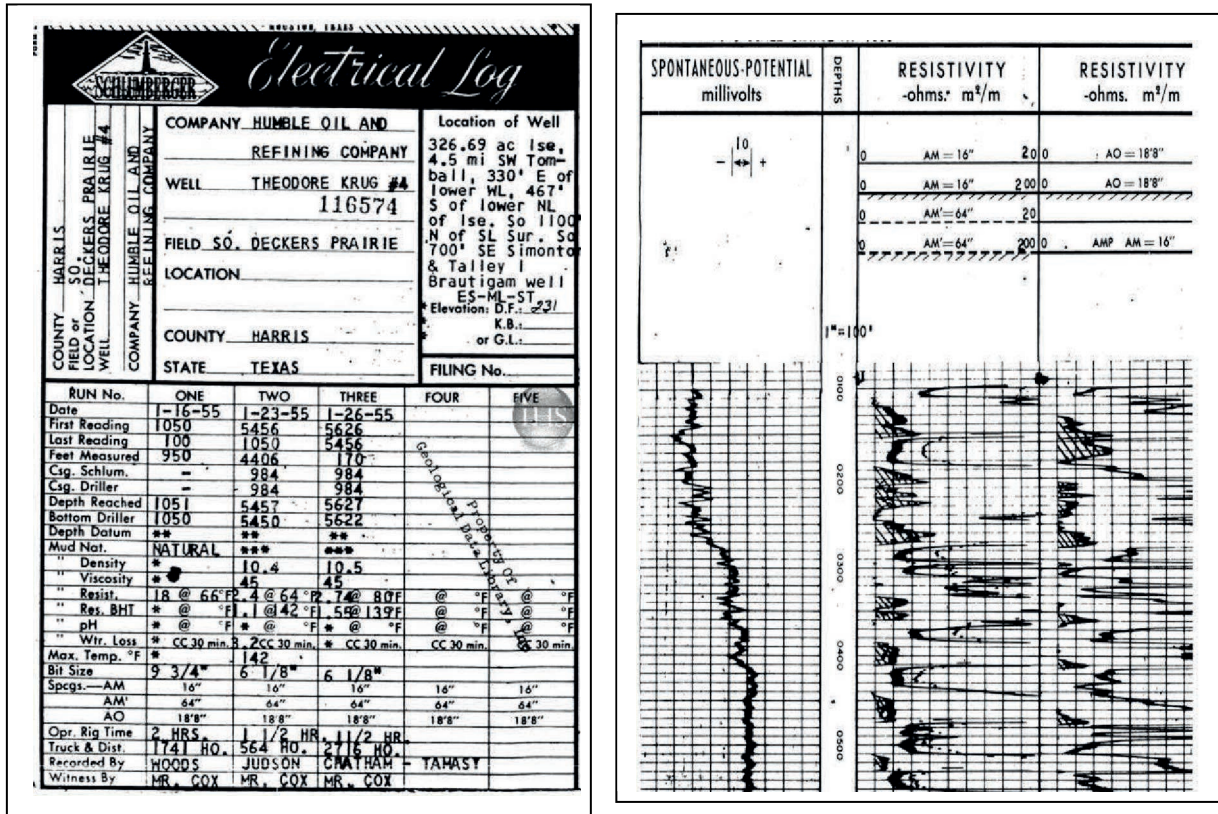


Figure 3-1 Example of a TIF raster image of a geophysical well log that uses the American Petroleum Institute format



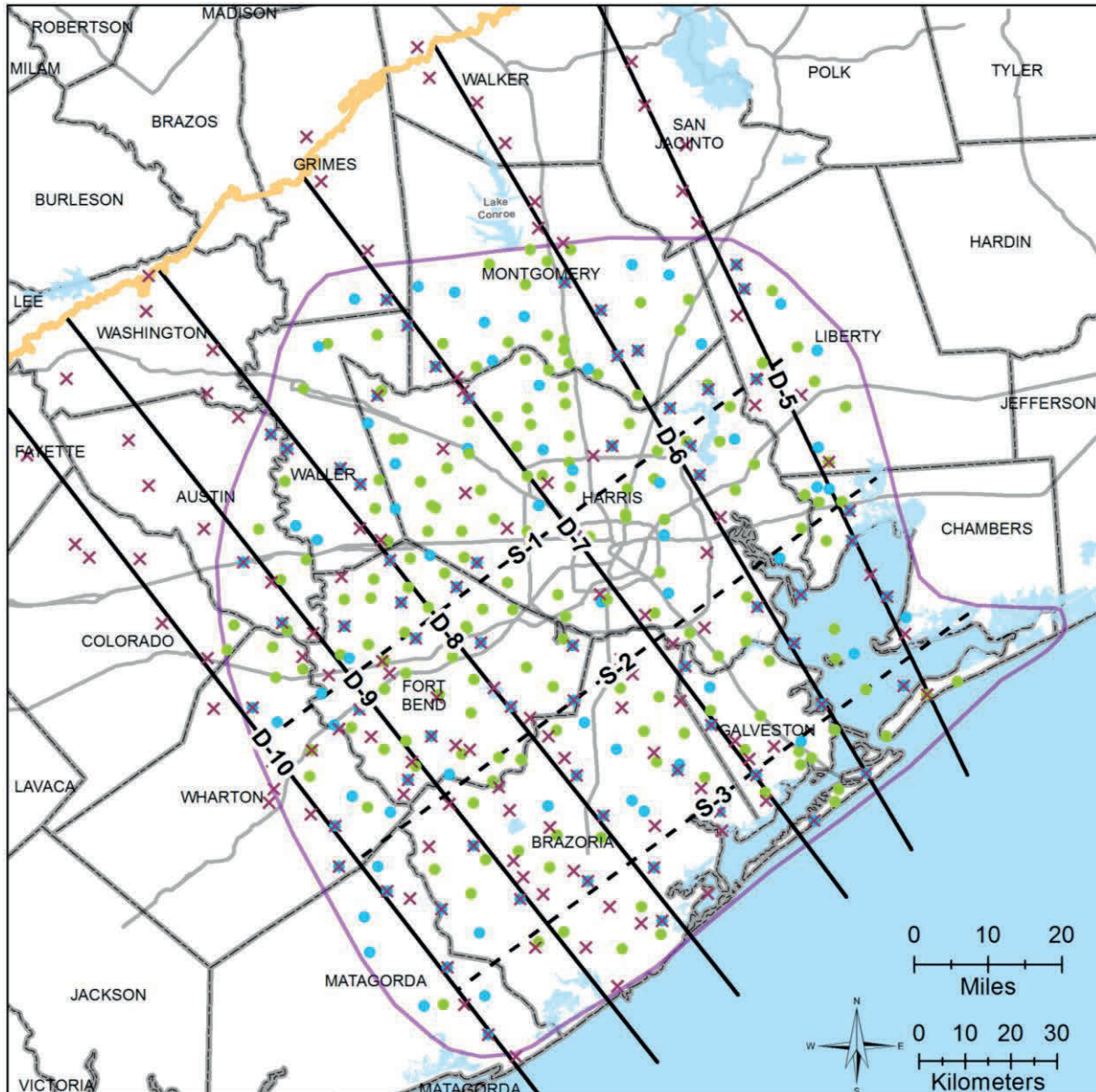
Final Report on the Delineation of Fresh, Brackish, and Saline Groundwater Resources Based on Interpretation of Geophysical Logs

```

# WellGreen Tech Inc. Digitizing Services
# www.wellgreentech.com
# email: sales@wellgreentech.com
#
~Version Information Block
VERS. 2.00: CWLS LOG ASCII STANDARD - VERSION 2.000000
WRAP. NO: One Line Per Depth Step
#
~Well Information Block
#MNM UNIT Data Information
#-----
STRT FT 40.0000: START DEPTH
STOP FT 2010.0000: STOP DEPTH
STEP FT 0.5000: STEP
NULL. -999.2500: NULL VALUE
COMP. SUN EXPLORATION & PROD. CO.: COMPANY
WELL. SANTOS MONTOYA #1: WELL
-----
FLD. OILTON: FIELD
LOC. : LOCATION
CNTY. WEBB: COUNTY
STAT. TEXAS: STATE
CTRY. USA: COUNTRY
SRVC. SCHLUMBERGER: SERVICE COMPANY
DATE. 01/24/1984: DATE
API. 42479338120000: API NUMBER
UWI. 42479338120000: UWI NUMBER
TVD. NO: TVD flag
WSTA. LOC: Well status
#
~Curve Information Block
#MNM UNIT API CODE Curve Description
#-----
DEPT FT : Depth in Feet
SP_MV 01 010 01 01: Spontaneous Potential
RES_SHAL.OHMM 10 220 01 01: Spherically Focused Laterolog
RES_DEEP.OHMM 05 120 46 01: Deep Induction
#
~Parameter Information Block
#MNM UNIT Value Description
#-----
RUN. ONE: Run Number
PDAT. UNK: Permanent Datum
EPD FT 0.0000: Elevation Of Perm. Datum
WSTA. LOC:
E. FT 0.0000: E (Stretch Coefficient Of The Cable)
TD FT 2000.0000: Total Depth
LMF KELLY BUSHING: Logging measured from Kelly Bushing
EKB FT 870.0: Elevation Kelly Bushing
GL FT 859.0: Ground Level
DF FT 869.0: Drill Floor
CSGL FT 53.0: Casing Bottom Logger
CSGD FT 53.0: Casing Bottom Driller
MUD. GEL-DRISPAC: Mud Type
MUDD LB/USG 9.7: Mud Weight/Density
MUDV CP 41.0: Mud Viscosity
PH 9.5: Mud ph
FL ml/30min 7.0: Mud Fluid Loss Rate
MUDS TANK: Mud Source
Rm OHMM 2.98: Mud Resistivity
RmT DEGF 70.0: Mud Temperature
Rmf OHMM 2.59: Mud Filtrate Resistivity
RmT DEGF 74.0: Mud Filtrate Temperature
Rmc OHMM 4.2: Mud Cake Resistivity
RmC DEGF 75.0: Mud Cake Temperature
RMB OHMM 2.1: Mud Resistivity Bottom Hole
BHT DEGF 102.0: Bottom Hole Temperature
#
~Other Information Block
<DescLogPlotStart> NEURALOG PLOT DEFINITION
PLOTDEFVERSION: 3
LASFILE: E:\nds\projects\Intera - Feb 23\las\42479338120000.las
DEPTHSCALE: 240.000000
RESOLUTION: 400
DEPTHLABELFREQ: 100.000000
HEAVYGRIDFREQ: 100.000000
MEDIUMGRIDFREQ: 50.000000
LIGHTGRIDFREQ: 10.000000
#
# TRACK 1
#
STARTTRACK:
LEFTX: 0.500000 inch
RIGHTX: 3.000000 inch
SCALETYPE: Linear
NUMCHARTDIVISIONS: 10
CURVE: SP -80.000000 20.000000 (0,0.255) Solid 2 N
ENDTRACK:
#
# TRACK 2
#
STARTTRACK:
LEFTX: 3.500000 inch
RIGHTX: 8.500000 inch
SCALETYPE: Log
NUMCYCLES: 4
STARTCYCLE: 2
CURVE: RES_SHAL 0.200000 2000.000000 (0,131,131) Solid 2 N
CURVE: RES_DEEP 0.200000 2000.000000 (255,0.255) Dot 2 N
ENDTRACK:
~A DEPTH SP RES_SHAL RES_DEEP
40.000 -999.250 0.324 -999.250
40.500 -999.250 0.322 -999.250
41.000 -999.250 0.321 -999.250
41.500 -999.250 0.318 -999.250
42.000 -999.250 0.315 -999.250
42.500 -999.250 0.316 -999.250
43.000 -999.250 0.317 -999.250
43.500 -999.250 0.318 1888.541
44.000 -999.250 0.318 1074.619
44.500 -999.250 0.319 606.204
45.000 -999.250 0.322 604.297
45.500 -999.250 0.322 1640.593
46.000 -999.250 0.320 1963.692

```

Figure 3-2 Example of a LAS file that was produced from a TIF file



Geophysical Well Log Locations.

Legend

- Study Area
- Major Highway
- County Line

- Cross Section Dip Line
- Cross Section Strike Line
- Catahoula Updip Extent

- Logs with Updated Stratigraphic Picks
- Logs with Sand Picks in the Study Area**
 - TWDB Study (Young et al., 2016)
 - This Study



Map Location

Prepared for:



Prepared by:



Figure 3-3 Location of the geophysical logs that were interpreted to develop TDS, lithology and stratigraphy and location of six cross sections along dip and three cross sections along strike

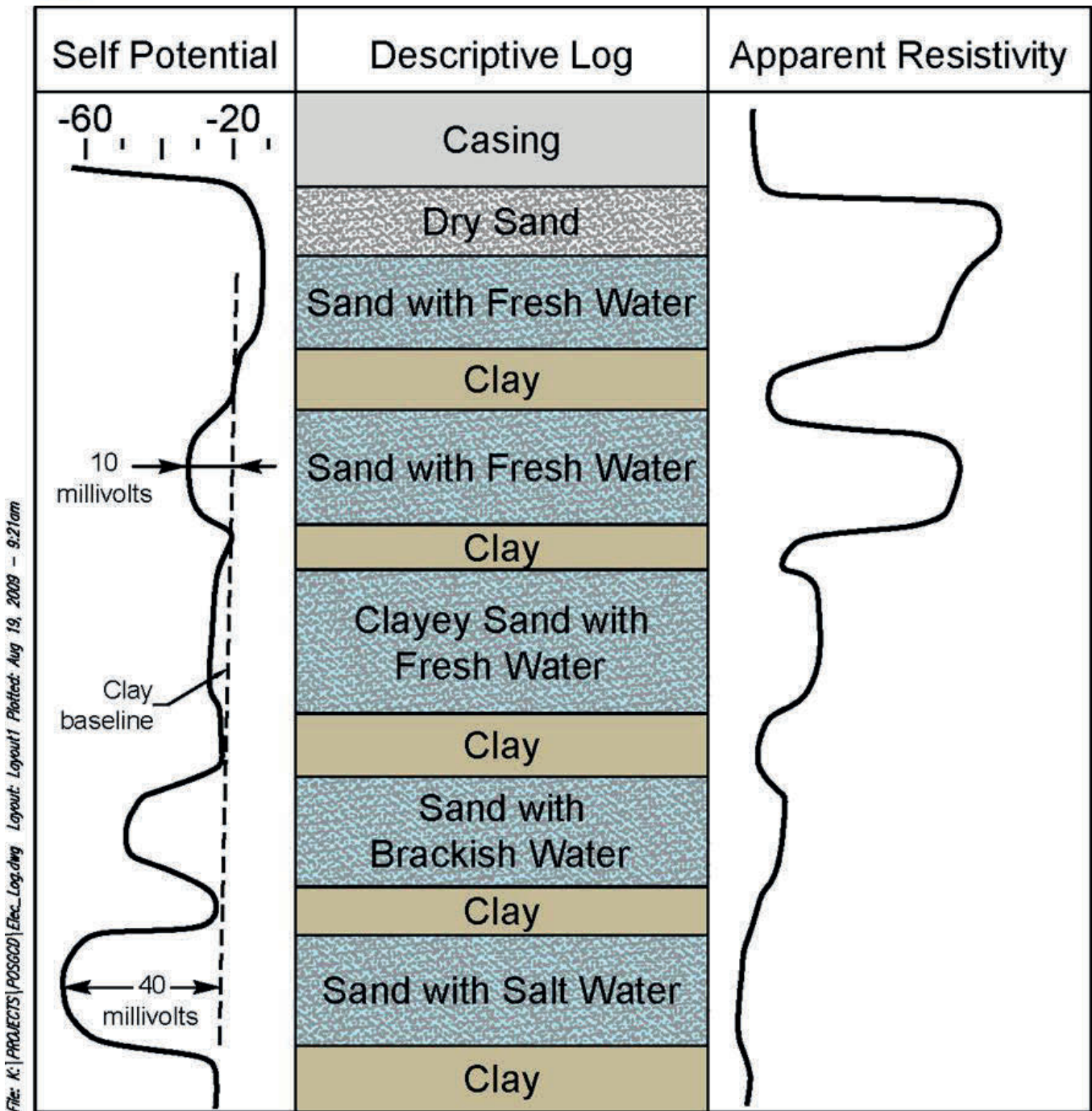


Figure 3-4 Idealized spontaneous potential and resistivity curve showing the responses corresponding to alternating sand and clay strata that are saturated with groundwater which increases significantly in TDS concentrations with depth (modified from Driscoll [1986, p. 189])

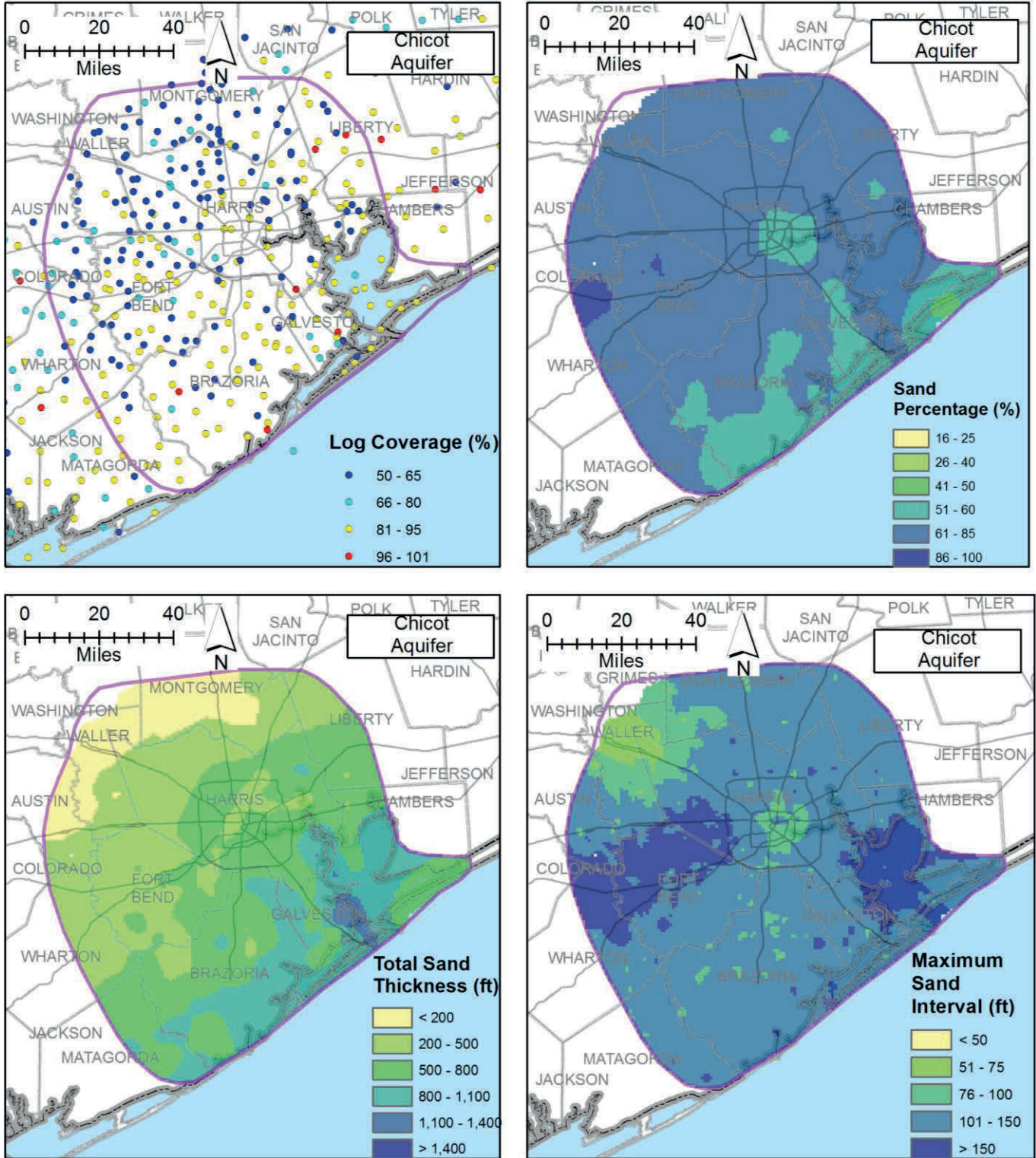


Figure 3-5 Maps of log coverage, sand percentage, total sand thickness and maximum sand interval for the Chicot Aquifer. Log coverage is the percentage of the aquifer intersected by the portion of the geophysical log analyzed.

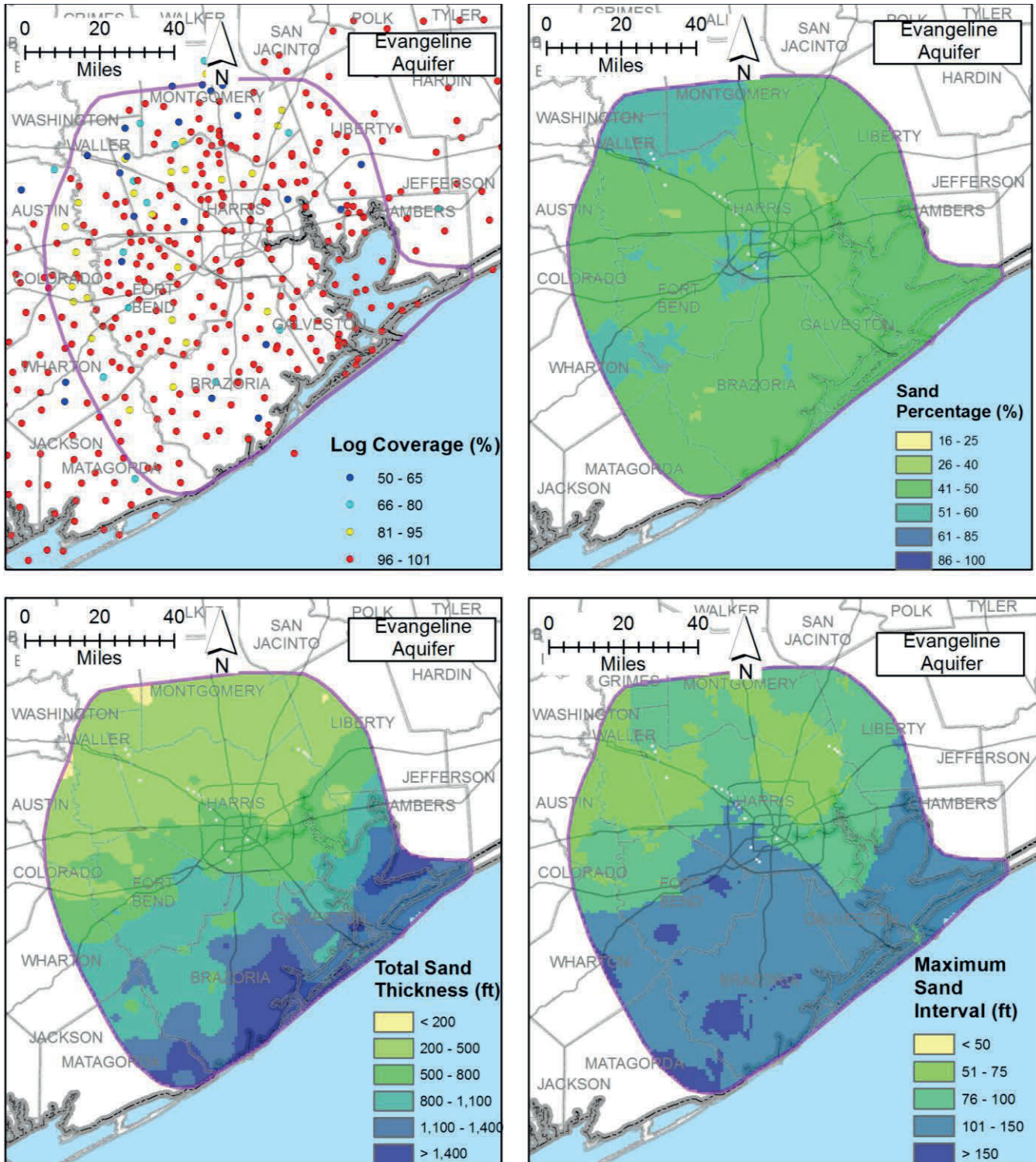


Figure 3-6 Maps of log coverage, sand percentage, total sand thickness and maximum sand interval for the Evangeline Aquifer. Log coverage is the percentage of the aquifer intersected by the portion of the geophysical log analyzed.



Final Report on the Delineation of Fresh, Brackish, and Saline Groundwater Resources Based on Interpretation of Geophysical Logs

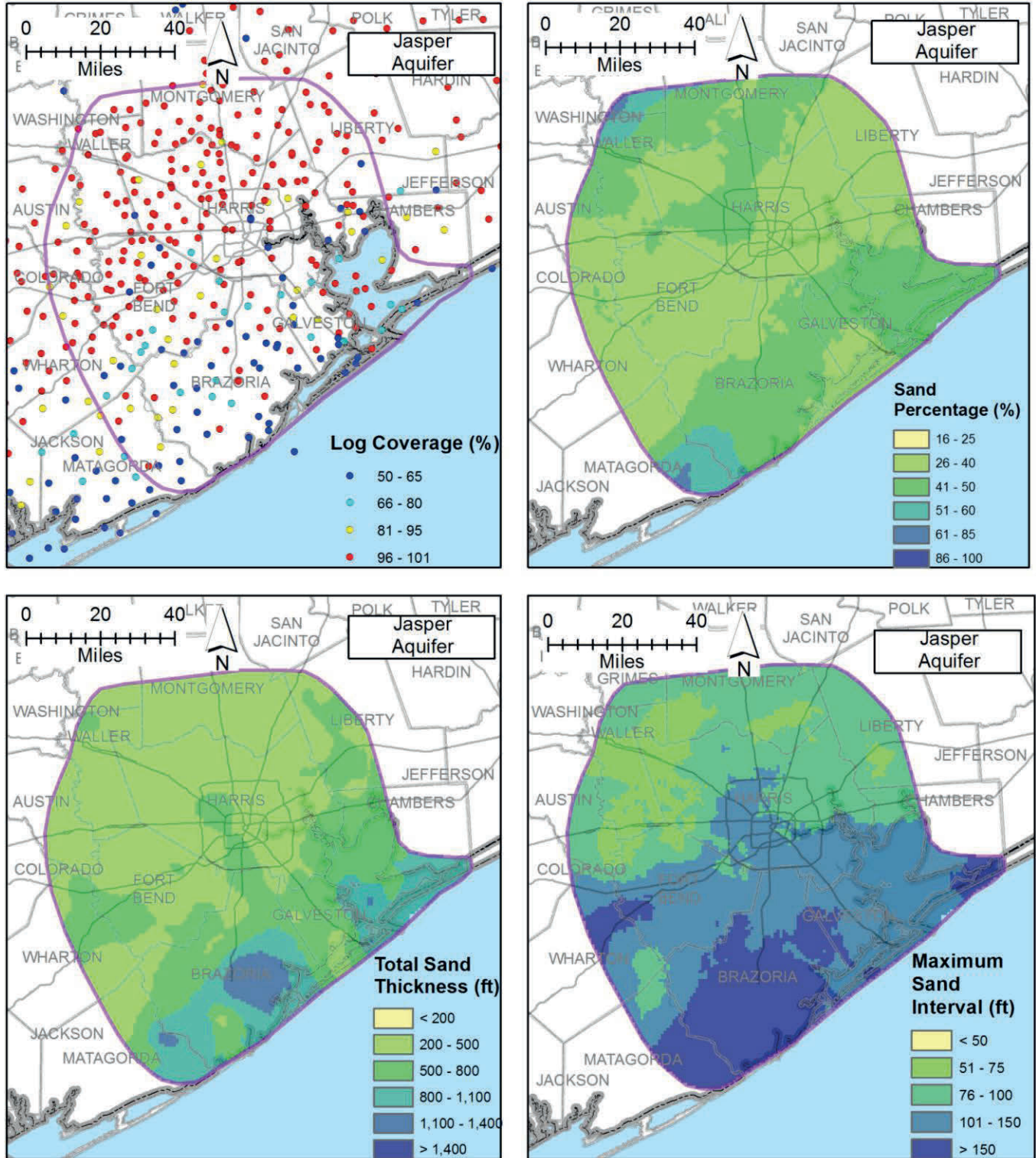


Figure 3-7 Maps of log coverage, sand percentage, total sand thickness and maximum sand interval for the Jasper Aquifer. Log coverage is the percentage of the aquifer intersected by the portion of the geophysical log analyzed.



Final Report on the Delineation of Fresh, Brackish, and Saline Groundwater Resources Based on Interpretation of Geophysical Logs

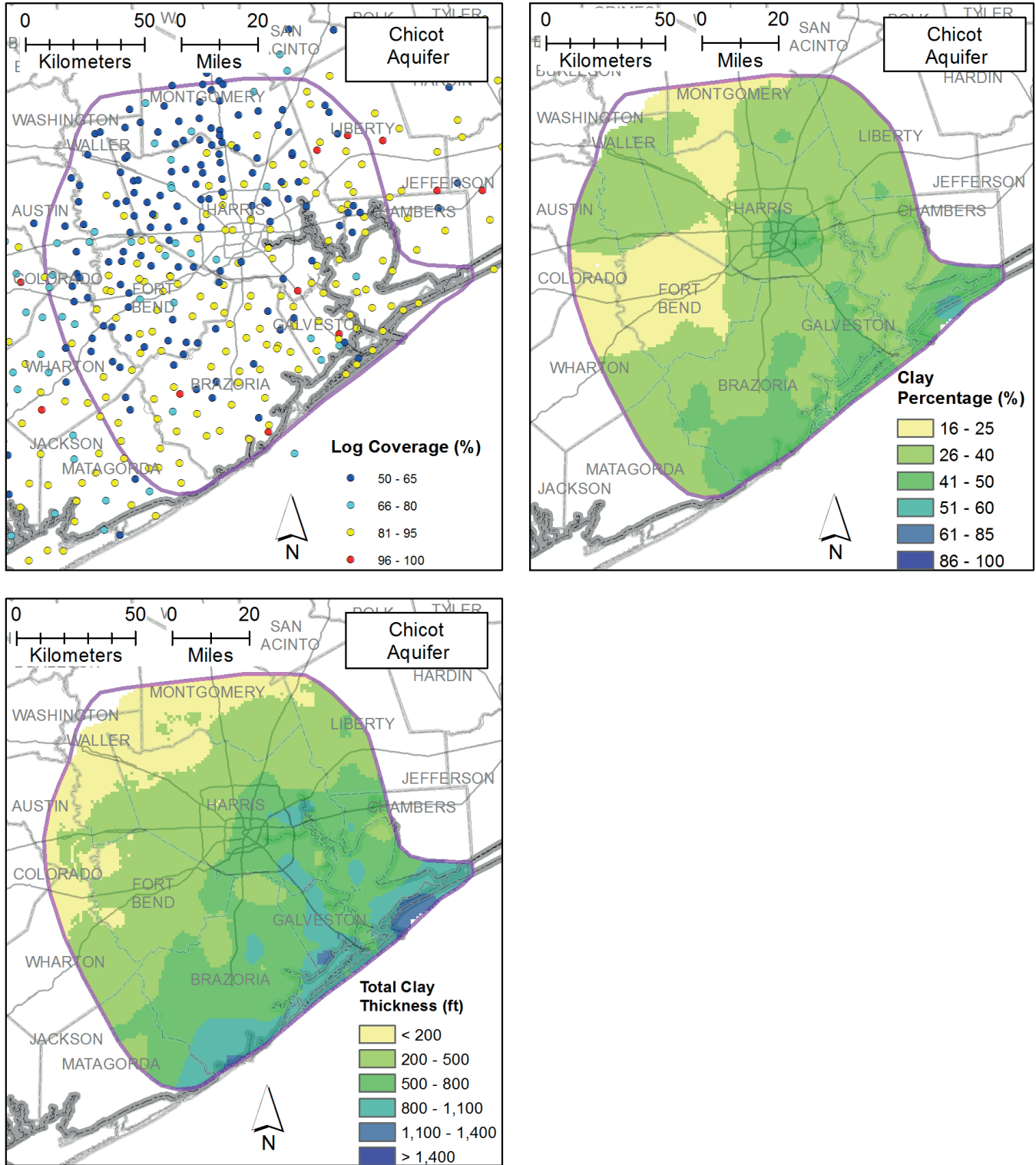


Figure 3-8 Maps of log coverage, clay percentage, total clay thickness and maximum clay interval for the Chicot Aquifer. Log coverage is the percentage of the aquifer intersected by the portion of the geophysical log analyzed.

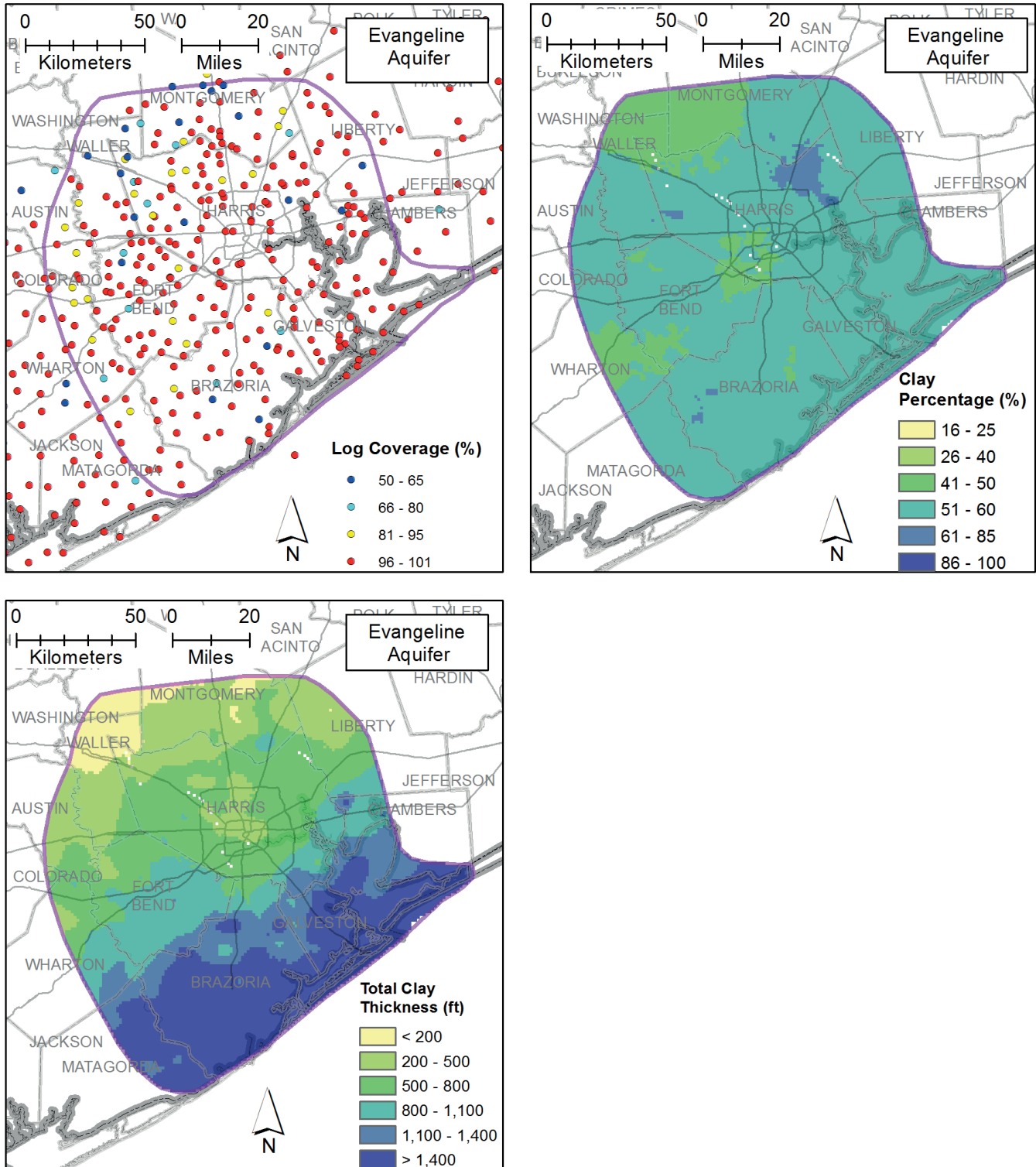


Figure 3-9 Maps of log coverage, clay percentage, total clay thickness and maximum clay interval for the Evangeline Aquifer. Log coverage is the percentage of the aquifer intersected by the portion of the geophysical log analyzed.

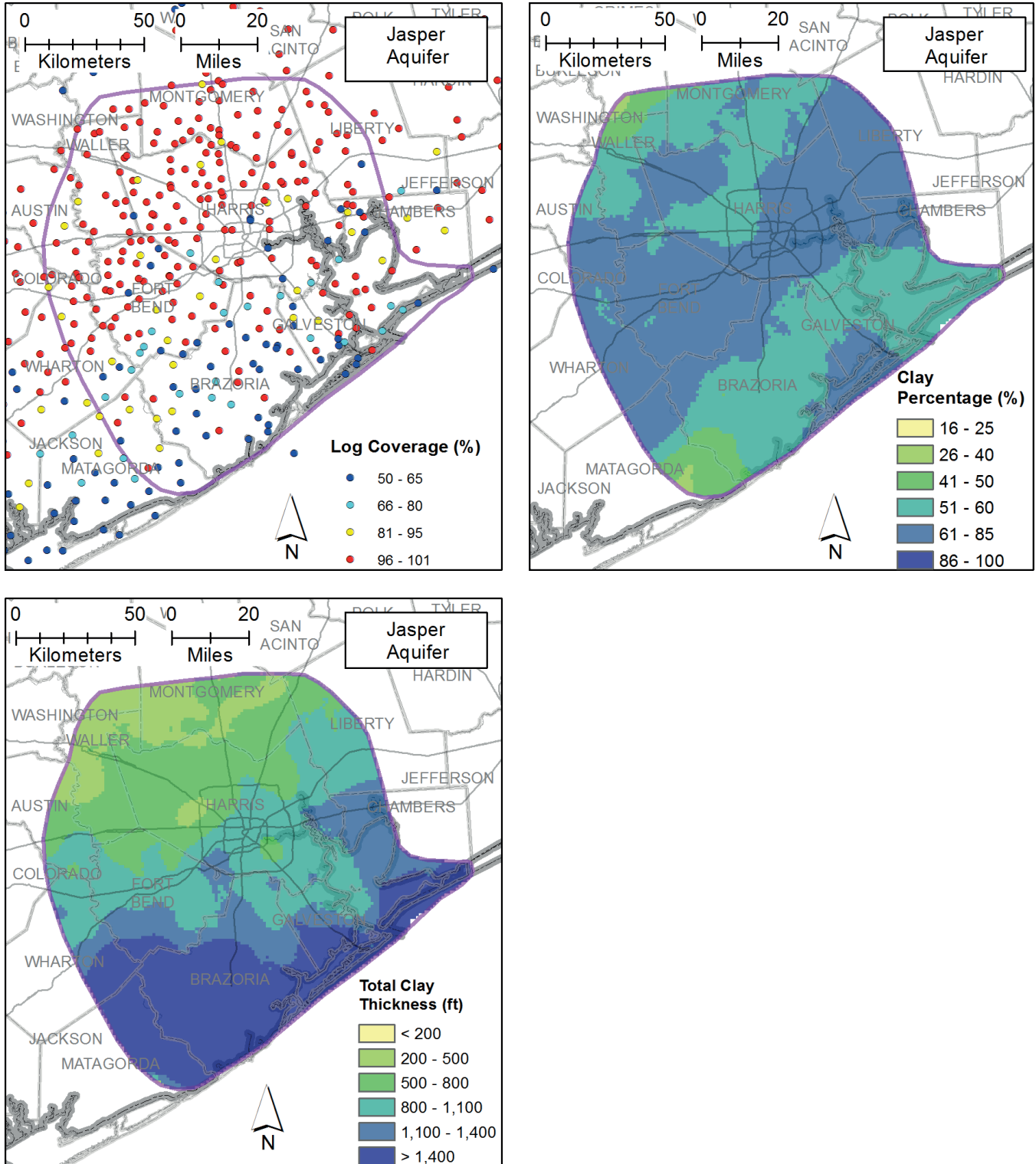
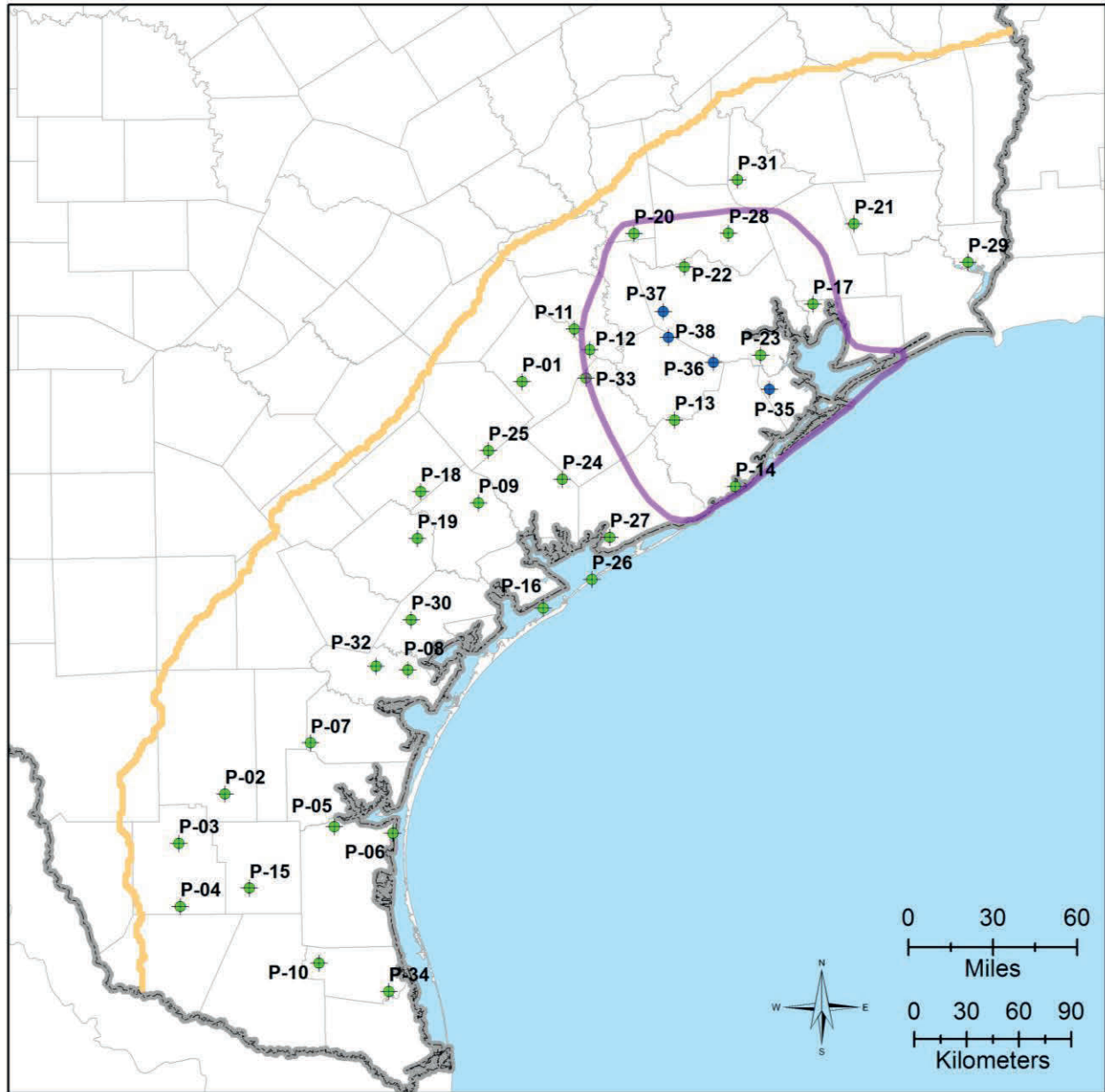


Figure 3-10 Maps of log coverage, clay percentage, total clay thickness and maximum clay interval for the Jasper Aquifer. Log coverage is the percentage of the aquifer intersected by the portion of the geophysical log analyzed.



Porosity Log Locations

Legend

- Study Area
- Catahoula Updip Extent

Porosity Log Source

- TWDB Study (Young et al., 2016)
- This Study



Map Location

Prepared for:



Prepared by:



Figure 3-11 Locations of thirty-eight logs that were analyzed to determine porosity values

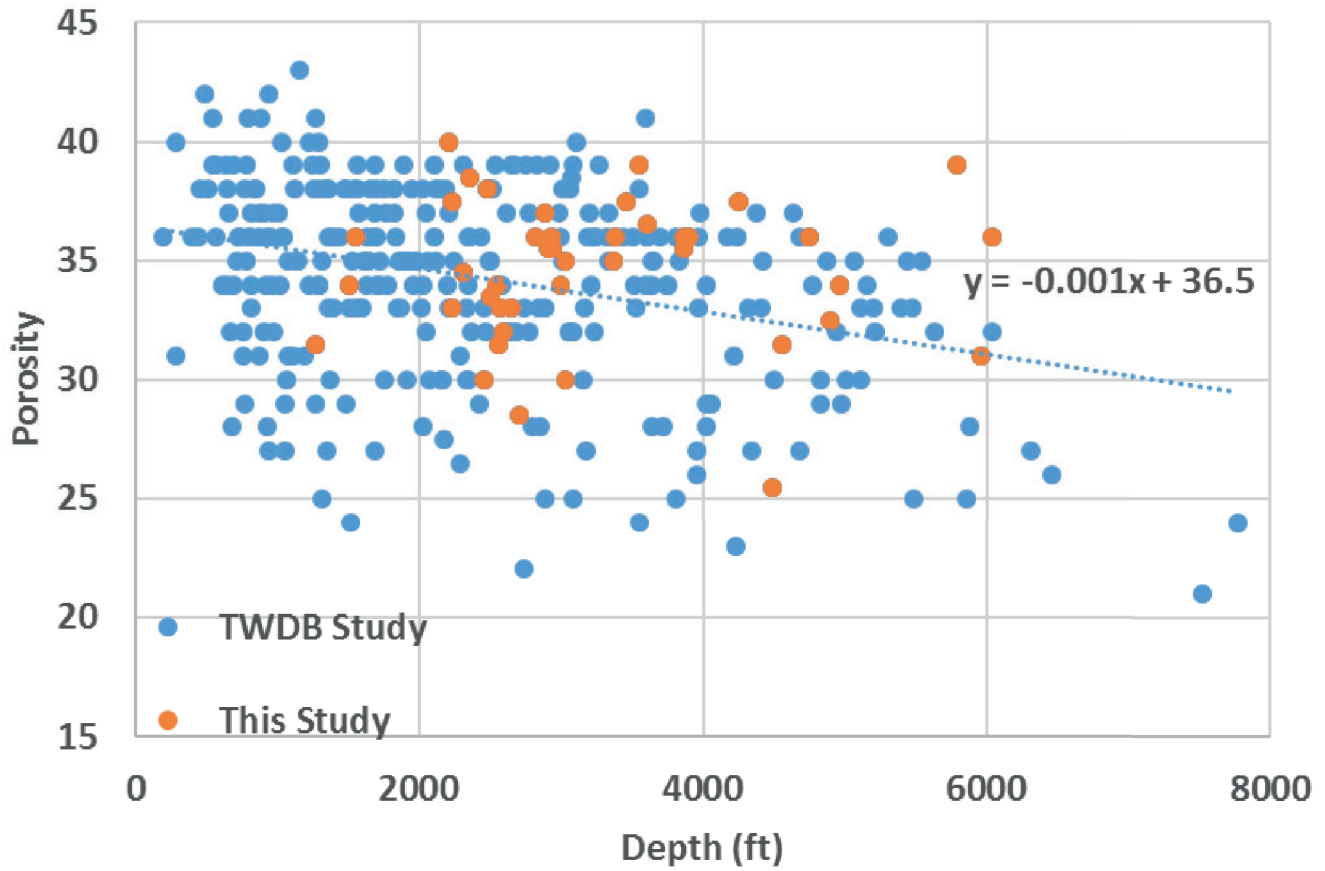


Figure 3-12 Measured porosity versus depth. Blue data is from the TWDB Gulf Coast Study (Young and others, 2016) and orange data is from this study.



4.0 WATER QUALITY

This section describes the process and methods for estimating TDS from electrical resistivity geophysical logs and spatially interpolating the TDS estimates at wells to estimate the depth to base of fresh, slightly saline, moderately saline, and very saline water. This section also presents thickness maps of the brackish groundwater zone in the study area and nine cross sections are presented depicting aquifer TDS (by salinity classification), lithology and formation boundaries.

4.1 Water Quality

A measure of the overall quality of groundwater is salinity. A common measurement of groundwater salinity is the concentration of TDS, typically reported in units of mg/L. The primary sources of groundwater to the Gulf Coast Aquifer System consist of relatively fresher meteoric water derived from precipitation recharging the aquifers since their deposition. As groundwater moves through the subsurface, it becomes mineralized, and its salinity increases as the groundwater interacts with the aquifer materials. Among the sources of groundwater salinity in the Texas Gulf Coast Aquifer System are saline connate water trapped in the sediments at the time of deposition, dissolution of salt domes, the upwelling of brine from geothermal zones along growth faults, natural deposits of evaporate minerals, salt water intrusion, sea salt spray, and oil and gas development (Young and others, 2013).

4.1.1 Salinity Classification by TDS Concentrations

For this study, groundwater water quality is classified using the criteria presented in **Table 4-1**. The first four criteria were developed by the United States Geological Survey (Winslow and Kister, 1956). The TDS value defining a brine salinity zone (greater than 35,000 mg/L) is consistent with TWBD BRACS study for the Texas Gulf Coast Aquifer (Young and others, 2016). For a complete description of the various groundwater quality classification schemes based upon TDS concentration the reader is referred to USGS Professional Paper 1833 (Stanton and others, 2017).

Table 4-1 Groundwater salinity classification based on the criteria established by Winslow and Kister (1956)

Salinity Classification	TDS Concentration Range
Fresh	Less than 1,000 mg/L
Slightly Saline*	1,000 to 3,000 mg/L
Moderately Saline*	3,000 to 10,000 mg/L
Very Saline	10,000 to 35,000 mg/L
Brine	>35,000 mg/L

*Brackish water includes slightly saline and very saline water.

4.2 Estimating TDS Concentrations from Geophysical Logs

Estep (1998) is an important reference for geophysical log analysis used by several Texas state agencies managing groundwater resources. **Table 4-2** shows the six primary methods described by Estep (1998) to estimate TDS concentrations from geophysical logs, as well as the range of TDS concentrations for their application. Young and others (2016) reviewed the six methods and identified the Mean R_o (formation



resistivity) Method and the R_{wa} (apparent water resistivity) Minimum Method as the best methods for use in the Texas Gulf Coast Aquifer System to identify and delineate groundwater salinity.

Table 4-2 The recommended working range and maximum operating range for methods used for estimating TDS concentration from geophysical logs (from Estep, 1998)

Analysis Method	Recommended Working TDS (mg/L) Range	Requires Fresh Water Correction	Maximum Operating TDS (mg/L) Range
R_w from SP	3,000 to 100,000	100 to 3,000	NA
Modified Alger-Harrison	3,000 to 100,000	100 to 3,000	NA
Estep	100 to 3,000	NA	3,000 to 10,000
Mean R_o	100 to 100,000	NA	NA
Guyod	1,000 to 3,000	NA	3,000 to 10,000
R_{wa} Minimum	3,000 to 100,000	1,000 to 3,000	NA

Note: SP=spontaneous potential; R_w =resistivity of the formation water; R_o =resistivity of formation; R_{wa} = apparent water resistivity; NA=not applicable

As shown in Table 4-2, only the Mean R_o Method has a recommended working range that spans the entire TDS concentration range from fresh water to brine. This method has been successfully used by investigators of Texas aquifers (Fogg and Blanchard, 1986; Hamlin and others, 1988; Estep, 1998; Hamlin and Luciana de la Rocha, 2015; Ayers and Lewis, 1985; Fogg, 1980; Fogg and Kreitler, 1982; Meyer, 2012; Young and others, 2016; Hamlin and others, 2016). The Mean R_o Method uses an empirically-derived correlation between measured resistivity in a formation and the TDS concentration of groundwater in that formation. Because of the limited range of measured groundwater TDS concentrations in the Gulf Coast Aquifer System, the Mean R_o Method developed by Young and others (2016) could not be developed to predict TDS concentrations greater than 5,000 mg/L. For TDS concentrations values above 5,000 mg/L in the Gulf Coast Aquifer System, Young and others (2016) developed and applied the R_{wa} Minimum Method. The R_{wa} Minimum Method relies on a theoretical relationship that predicts TDS concentration using porosity and formation resistivity. In the Gulf Coast Aquifer System, Meyer (2012) and Young and Lupton (2014) have successfully used the R_{wa} Minimum Method. For a complete discussion on these two resistivity methods and their application in this study please see **Appendix F**.

4.2.1 Electrical Resistivity and Specific Conductance

Electrical resistivity is a measurement of water’s opposition to the flow of an electrical current over distance. As described in Section 3.2, formation resistivity is a composite measurement of the resistivity of the geological formation and of groundwater in the formation. The standard international unit of electrical resistivity is the ohm-meter (ohm-m). Both the Mean R_o Method and the R_{wa} Minimum Method use formation resistivity to estimate TDS concentrations.

Equation 4-1 calculates electrical resistivity from specific conductance, and **Equation 4-2** provides the reverse. These equations are from Estep (1998, pg 9-2). **Table 4-3** provides the relationship between electrical conductivity, resistivity and concentrations of sodium chloride and calcium carbonate in solution. This relationship shows the correlation of groundwater salinity to resistivity and conductivity which is the basis for groundwater salinity estimation using geophysical resistivity logs.



Final Report on the Delineation of Fresh, Brackish, and Saline Groundwater Resources Based on Interpretation of Geophysical Logs

$$R_{w25^{\circ}C} = 10,000/SC_{w25^{\circ}C} \quad \text{(Equation 4-1)}$$

$$SC_{w25^{\circ}C} = \frac{10,000}{R_{w25^{\circ}C}} \quad \text{(Equation 4-2)}$$

where

$SC_{w25^{\circ}C}$ = specific conductance (micromhos per centimeter [$\mu\text{mhos/cm}$] at 25 degrees Celsius ($^{\circ}\text{C}$) or 77 degrees Fahrenheit [$^{\circ}\text{F}$])

$R_{w25^{\circ}C}$ = water resistivity (ohm-m at 25 $^{\circ}\text{C}$ or 77 $^{\circ}\text{F}$)

Table 4-3 Electrical conductivity and electrical resistivity of sodium chloride (NaCl) and calcium carbonate (CaCO_3) solutions at different concentrations (from Young and others, 2016)

Dissolved Solids (ppm)		Conductivity ($\mu\text{mhos/cm}$)	Resistivity (ohm-m)
CaCO_3	NaCl		
1,700	2,000	3,860	2.6
1,275	1,500	2,930	3.4
850	1,000	1,990	5
425	500	1,020	9.9
85	100	210	48
42.5	50	105	95
8.5	10	21.4	470
1.7	2	4.35	2,300
0.85	1	2.21	4,500

4.2.2 Temperature Adjustments to Electrical Resistivity

The electrical resistivity of water changes with temperature because elevating temperature increases the kinetic energy of ions and decreases water viscosity, which increases ionic movement. Temperature adjustments to electrical conductivity are non-linear. Among the first equations to account for non-linear changes in resistivity with temperature is the Arp equation (Arps, 1953), which can be found in most logging manuals, such as Schlumberger (2009). For this study, the Arp equation is used to correct electric resistivity for temperature.

Equation 4-3 and **Equation 4-4** provide the corrections for temperature measured in Fahrenheit and Celsius, respectively.

For Fahrenheit
$$R_w^2 = R_w^1 \frac{(T_1 + 6.77)}{(T_2 + 6.77)} \quad \text{(Equation 4-3)}$$

For Celsius
$$R_w^2 = R_w^1 \frac{(T_1 + 21.5)}{(T_2 + 21.5)} \quad \text{(Equation 4-4)}$$

where

R_w^2 = resistivity at temperature T2

R_w^1 = resistivity at temperature T1

T1 = temperature T1

T2 = temperature T2



Temperature adjustments to the measured formation resistivity are necessary because temperature in the subsurface varies with depth. The relationship between depth and temperature is typically called the geothermal gradient. Young and others (2016) account for the spatial variability in the geothermal gradient by interpolation between a map of average air temperature at ground surface and a map of average temperature at a depth of 11,500 feet. For the study area, this application produces geothermal gradients that range from 18 to 12.5°F per 1,000 feet of depth. For this study, we used the same procedure and data explained by Young and others (2016) to adjust all formation resistivities obtained from geophysical logs to a standard temperature of 77°C.

4.2.3 Development of Methods to Estimate Salinity from Electrical Resistivity in the Study Area

The methods selected for estimating TDS concentrations from electrical resistivity data are the same methods used by Young and others (2016) for the Texas Gulf Coast Aquifer System. The development and application of these methods have been accepted by the TWDB BRACs personnel and have been demonstrated to produce reasonable and defensible results. The purpose of this section is to explain the underlying assumptions and data associated with both the Mean R_o Method and the R_{wa} Minimum Method.

4.2.3.1 Mean R_o Method

The Mean R_o method involves correlating deep formation resistivity (long normal or deep induction) of sand with a TDS concentration of groundwater samples from the same zone. Deep resistivity is assumed to be approximately equal to true formation resistivity (R_t), where water saturation is 100% (no hydrocarbons) (Jones and Buford, 1951; Turcan, 1962; Alger, 1966). Bed thickness also affects deep resistivity. For beds thinner than about twice the electrode spacing, the deep resistivity does not equal true formation resistivity (Jones and Buford, 1951). Therefore, only sand layers more than 10 feet thick were used in developing and applying the correlations and calculations.

The correlation between deep formation resistivity and TDS concentration requires that a geophysical log be paired to a water well with a measured TDS concentration. Young and others (2016) censored the data so that the horizontal distance between a paired geophysical log and the water well was less than one mile. This study uses the same approach used in Young and others (2016) to associate sands measured by a geophysical log with the well screen where a water sample was measured for TDS. This process accounts for the dip angle of the formation intersected by the well screen and for the differences in the length of the well screen and the sand bed thicknesses in the formation.

The results of numerous pairings of TDS concentrations and formation resistivities are tabulated for a specific aquifer and plotted to create R_o -TDS graph. Young and others (2016) developed R_o -TDS graphs for the Chicot, Evangeline, and Jasper aquifers from 762 pairs consisting of a geophysical log and a water well measurement of TDS. These 762 well-log pairs were generated by using 399 unique water wells and multiple logs pairings to the same water well. **Figure 4-1** shows the water-well locations and the number of pairings associated with each water well used by Young and others (2016). A statistical analysis presented in **Appendix F** shows that additional TDS and resistivity data from this study did not change the R_o -TDS relationship derived in Young and others (2016) for the Chicot and Evangeline aquifers. A lack of additional new data in the Jasper Aquifer and Catahoula Formation prevented comparison of the R_o -TDS relationship to the TWDB relationship. Because the previously derived R_o -TDS relationship in Young and others (2016) is consistent with the TDS and resistivity data collected as part of this study, it is used in this study. The relationship between TDS and formation resistivity for a TDS of less than 5,000 mg/L is presented in **Table F-5**.



4.2.3.2 R_{wa} Minimum Method

The development of the R_{wa} Minimum Method follows the formulas provided by Estepp (1988) and Meyer and others (2014). The R_{wa} Minimum Method incorporates depth-dependent porosity in the estimation of TDS for concentrations equal to or above 5,000 mg/L. The details for the approach are presented in Appendix F. A summary of the relationship between resistivity, porosity, and the estimated TDS is presented in **Table F-7** for TDS values between 10,000 and 35,000 mg/L.

4.3 Groundwater Salinity

With the TDS concentrations estimated for all sands equal to or greater than 10 feet in length, a dataset is created from which groundwater salinity boundaries can be developed. By estimating a salinity boundary top and bottom, one can define a salinity zone for each salinity groundwater class. The salinity boundaries were developed by interpolation of manual picks for the base of salinity classifications defined in Table 4-1. The manual picks were made by visual inspection on geophysical logs arranged along fourteen cross sections. Nine of the cross sections are presented in Section 4.4. Maps were generated to represent the base of the of fresh, slightly saline, moderately saline, and very saline groundwater by interpolating the manually-selected salinity picks on the geophysical logs using the topo-to-raster tool, an interpolation method provided in ArcGIS®.

4.3.1 Depth to the Base of Fresh Water

Figure 4-2 shows the base of fresh water constructed by interpolating manually-selected picks of the base of fresh water made on 228 geophysical logs in the study area. The figure shows contours of depth from ground surface. The orientation of most of the contours is along geologic strike and parallel to the shoreline. In the middle of the study area, the base of fresh water is the deepest and is typically at a depth between 1,500 and 2,200 feet. Down-dip of the deepest part of the base of fresh water zone, the base becomes increasingly shallower toward the shoreline. Near the shoreline, the depth to the base of fresh water varies between depths of 0 to 500 feet.

In developing the depth to base of fresh water, logs close enough to salt domes to observe local abrupt changes in groundwater salinity were omitted. Initial attempts to develop surfaces using these logs led to large over-projections of the zone of influence associated with salt domes. We did not attempt to map locations where slightly saline or moderately saline groundwater appears to exist above fresh water. Possible causes for such inversions of water quality could be salt/ocean spray along the coast and pollution sources such as oil and gas open brine pits, which have been outlawed since 1964.

After the base of the fresh water was created, we compared it to measured TDS concentrations from 575 water wells that are located in the study area and have well screen information. This comparison led to the development of the three areas marked by the green polygons in Figure 4-2. At these three areas, the measured TDS concentrations suggest that the predicted base of fresh water in Figure 4-2 may be predicted to be too shallow by a few hundred feet. This analysis will be discussed further in Section 4.3.6.

4.3.2 Depth to the Base of Slightly Saline Water

Figure 4-3 shows the base of slightly saline water constructed by interpolating manual picks of the base of slightly saline water made on 220 geophysical logs in the study area. The figure shows contours that mimic the general pattern in the base of fresh water map but are up to about 500 feet deeper. In the up dip and most northeast region of the study area, the depth to base of slightly saline water is typically near 2,000 feet below



ground surface. The deepest part of the base of slightly saline water occurs in the same general location as does the deepest part of the fresh water with the depth values in the range between 2,500 and 3,100 feet. Unlike the fresh water map (see Figure 4-2), however, there is a much steeper change in the depth contours toward the coast. In the vicinity of the Yegua fault zone (see Figure 2-3), the base of the slightly saline zone becomes shallower by 1,500 feet across a distance of approximately 10 to 15 miles. This rate of change is significantly higher than any other region and suggests that the fault zone may be part of the cause for the large changes in the contoured depths. Down gradient and on the southeast sided of the Frio fault zone, the depth to the base of slightly saline groundwater remains fairly uniform at depths between 1,000 and 1,500 feet.

4.3.3 Depth to the Base of Moderately Saline Water

Figure 4-4 shows the depth to the base of moderately saline water constructed by interpolating manual picks of the base of slightly saline water made on 198 geophysical logs in the study area. Figure 4-4 shows contours that mimic the general pattern in the base of slightly saline water with the exception that the elevation change in the vicinity of the Frio fault zone is more pronounced. In the up dip and most northeastern region of the study area, the depth to base of moderately saline water is typically near 2,700 feet below ground surface. The deepest area of the base of moderately saline water occurs in the same general location as is the deepest part of the slightly saline water, with depths ranging between 3,000 and 4,000 feet. Within about 20 miles of the coast, the depth is relatively uniform, remaining between 1,000 and 1,500 feet.

In the vicinity of the Yegua fault zone, the depth changes from 3,000 to 2,000 feet across a distance of approximately 5 to 10 miles. Two possible causes for such relatively abrupt changes in TDS concentrations are discussed in the literature. One mechanism is that the faults restrict horizontal groundwater flow toward the coast and thereby prevent mixing of the more saline coastal groundwater with the less saline inland groundwater. Kreitler and others (1977) suggest that this mechanism is active near the boundary of Harris and Galveston counties, which is in vicinity of the Frio fault zone. Another mechanism is that the fault zone is acting as a conduit for vertical fluid migration of brines from a deep geopressed groundwater zone into the Gulf Coast Aquifer System. Field data and results from several studies such as Bourgeois (1997) and Lindsay (2009) support that this mechanism is active and plausible in the study area.

4.3.4 Depth to the Base of Very Saline Water

Figure 4-5 shows the depth to the base of the very saline water constructed by interpolating manual picks of the base of very saline water made on 87 geophysical logs in the study area. The lower number of picks for this salinity classification boundary depth is a result of the fact that the bottom of the very saline zone is below the Jasper Aquifer for much of the up-dip region of the study area. For approximately one-third of the study area, the base of the very saline zone is coincident with the bottom of the Jasper Aquifer. Included in Figure 4-5 is the down dip extent of where the base of the Jasper Aquifer is above the base of the very saline water. Along the coastline, the depth to the base of the very saline water typically ranges between 1,500 to 2,000 feet.

In the vicinity of the Yegua fault zone, significant changes in the depth contours again occur, and these changes vary across the study area. In the southwest portion of the study area (Wharton, Matagorda, Fort Bend and Brazoria counties), the depth contours change from 4,000 to 2,000 feet across a distance of approximately 10 miles. In the northeast portion of the study area (Chambers, Liberty, Galveston, and Harris counties), the depth contours change from 2,500 to 4,000 feet across a distance of approximately 10 miles. In the central portion of the study area (Fort Bend, Galveston, and Harris counties), depth contours change from 3,000 to 4,000 feet across a distance of approximately 10 miles. These large depth changes over about a 10-mile distance provide



additional evidence that geologic faults are an important factor that affects groundwater salinity in the study area.

4.3.5 Comparison of the Depth to Base of Fresh and Slightly Saline Water to Texas Railroad Commission Data

Figure 4-6 shows the depth to fresh water based on interpretation of geophysical logs and other data made by the Groundwater Advisory Unit of the Railroad Commission of Texas and its program predecessor agencies. The map was recreated from an analysis of 14,597 picks to the depth of fresh water. Out of these 14,597 picks, 10,411 of the picks are located within the study area. To help smooth the data, we divided the picks into 5-mile by 5-mile grid blocks and calculated the average depth to fresh water.

The pattern and depths to base of fresh water in **Figure 4-6** shows good agreement with the base of fresh water in **Figure 4-2**. The differences in depth across the entire study area typically ranges within a few hundred feet. For both figures, the deep region of the base of fresh water occurs in the middle of the study area at depths between 1,500 and 2,000 feet, and the depth to base of fresh water is typically 500 feet or less near the shoreline. Also, there is a large change in depth from about 750 to 1,500 feet across a distance of about 10 miles in the vicinity of the Yegua fault zone.

Figure 4-7 shows the depth to water with a TDS concentration less than 3,000 mg/L based on interpretation of geophysical logs and other data made by the Groundwater Advisory Unit of the Railroad Commission of Texas and its program predecessor agencies. The map was recreated from an analysis of approximately 7,017. Out of these 7,017 picks, 5,090 of the picks are located within the study area. To help smooth the data, we divided the picks into 5-mile by 5-mile grid blocks and calculated the average depth to slightly saline water.

Comparison of the base of the useable (slightly saline) groundwater in **Figure 4-7** shows good agreement with the base of slightly saline groundwater shown in **Figure 4-3**. The Railroad Commission defines useable quality water in the Gulf Coast Aquifer System as groundwater with a TDS concentration of 3,000 mg/L or less. The pattern and values of the base of slightly saline water in **Figure 4-7** and **4-3** are similar and in good agreement with each other. Across most of the study area, the difference in the two estimates of depth to base of slightly saline water is less than 600 feet. For both figures, the deep region of the base of slightly saline water typically occurs in the middle of the study area at depths between 2,500 and 3,500 feet. Within 20 miles of the shoreline, the depths are between 500 and 1,500 feet. Also, **Figure 4-7** and **Figure 4-3** show a depth from about 750 to about 2,500 feet occurs across a distance of about 10 miles in the vicinity of the Yegua fault zone.

4.3.6 Comparison of the Base of Fresh Water Zone with TDS Concentrations Measured in Water Wells

In the study area, there are 575 water wells with water sample TDS concentrations and well screen information. The measured TDS concentration values range from 57 to 4,058 mg/L. **Table F-1** provides a summary of the TDS concentrations. This well water quality data was used to check the base elevations of the salinity boundaries shown in **Figure 4-2** through **Figure 4-5**. The checking process involved comparing the measured TDS concentrations in the water well to the thickness of the salinity zones intersected by the well screens. This comparison process was considered approximate because many of the longer well screens intersected more than one salinity zone. Nonetheless, we were able to use the well information to provide a useful check on whether the observed TDS data supported the placement of the salinity zones (see **Table F-1**). At 85% of the wells, the well screen was totally located in a single salinity zone, and the measured TDS concentration was contained in the range of TDS values represented by the single salinity zone. Because 543 of the 575 wells had



Final Report on the Delineation of Fresh, Brackish, and Saline Groundwater Resources Based on Interpretation of Geophysical Logs

TDS concentrations less than 1,000 mg/L, most of our checks were aimed at checking the base of the fresh water zone shown in Figure 4-2.

The three polygons shown in Figure 4-2 represent areas where there may be potential bias in the estimated base of freshwater groundwater surface. In these areas, actual well water quality data suggested that the base of fresh groundwater could be up to 300 feet deeper. Some of this uncertainty is caused by the large screens typical of the area. For example, for the 18 wells contained in the middle polygon located in Harris County, the average distance from the top to the bottom of the well screen length is 900 feet, and all of the 18 well screens intersect both the fresh and the slightly-salinity zones.

4.3.7 Brackish Groundwater Zone

Figure 4-8 shows the thickness of the brackish groundwater zone within all aquifers in the study. For this study, brackish groundwater is characterized by having a TDS concentration from 1,000 mg/L to 10,000 mg/L consistent with the TWDB practice. The thickness of a brackish groundwater zone was calculated by subtracting the base elevations of the fresh water zone in Figure 4-2 from the base elevation of the moderately saline groundwater zone in Figure 4-4. Near the shoreline, the brackish groundwater zone is about 1,000 feet thick. Sixty miles inland from the shoreline, the thickness of the brackish zone is less than 600 feet and it continues to thin as it approaches the southern boundaries of Fort Bend and Harris counties. Across most of Fort Bend County and in the central portion of Harris County, the thickness of brackish groundwater zone averages about 1,600 feet thick and is usually between 1,400 and 1,800 feet thick. In the northern portion of Waller County and the southern portion of Montgomery County, the thickness of the brackish zone is typically less than 600 feet thick.

Figure 4-9 shows the thickness of the brackish groundwater zone in the Chicot Aquifer. The greatest zone thickness occurs near the shoreline. Within about 20 miles of the shoreline, the brackish zone thickness averages about 750 to 1,000 feet. Up dip of 20 miles, the brackish zone noticeably thins and pinches out at a distance of about 50 miles from the shoreline.

Figure 4-10 shows the thickness of the brackish groundwater zone in the Evangeline Aquifer. There is no brackish groundwater within about 30 miles of the shoreline and very little brackish groundwater in Montgomery County and the northern region of Waller County. The thickest region of the brackish groundwater zone occurs in the southern region Fort Bend and Harris counties, where there is an approximately 10-mile wide area of the Evangeline Aquifer where the thickness of the brackish groundwater zone averages about 1,300 feet thick. Across a large portion of northern Fort Bend and Harris counties, the thickness of the brackish groundwater zone is less than 500 feet.

Figure 4-11 shows the thickness of the brackish groundwater zone in the Jasper Aquifer. Brackish groundwater occurs in the Jasper Aquifer in the up-dip region of the study area. Across most of Fort Bend and Harris counties the thickness averages between 750 and 1,200 feet with the thickest zones occurring in Fort Bend County.

4.4 Cross Sections Showing Stratigraphy, Lithology, and Water Quality

Figure 4-12 through **Figure 4-20** show the calculated salinity for sand beds identified on geophysical logs associated with the nine cross sections shown in Figure 3-3. The layout for each cross section consists of geophysical logs plotted along a transect either oriented along dip (perpendicular to the shoreline) or along strike (parallel to the shoreline). Appendix A lists the locations of each of the geophysical logs associated with the nine cross sections. Appendix C provides a map of the geographic location of each log used by cross section



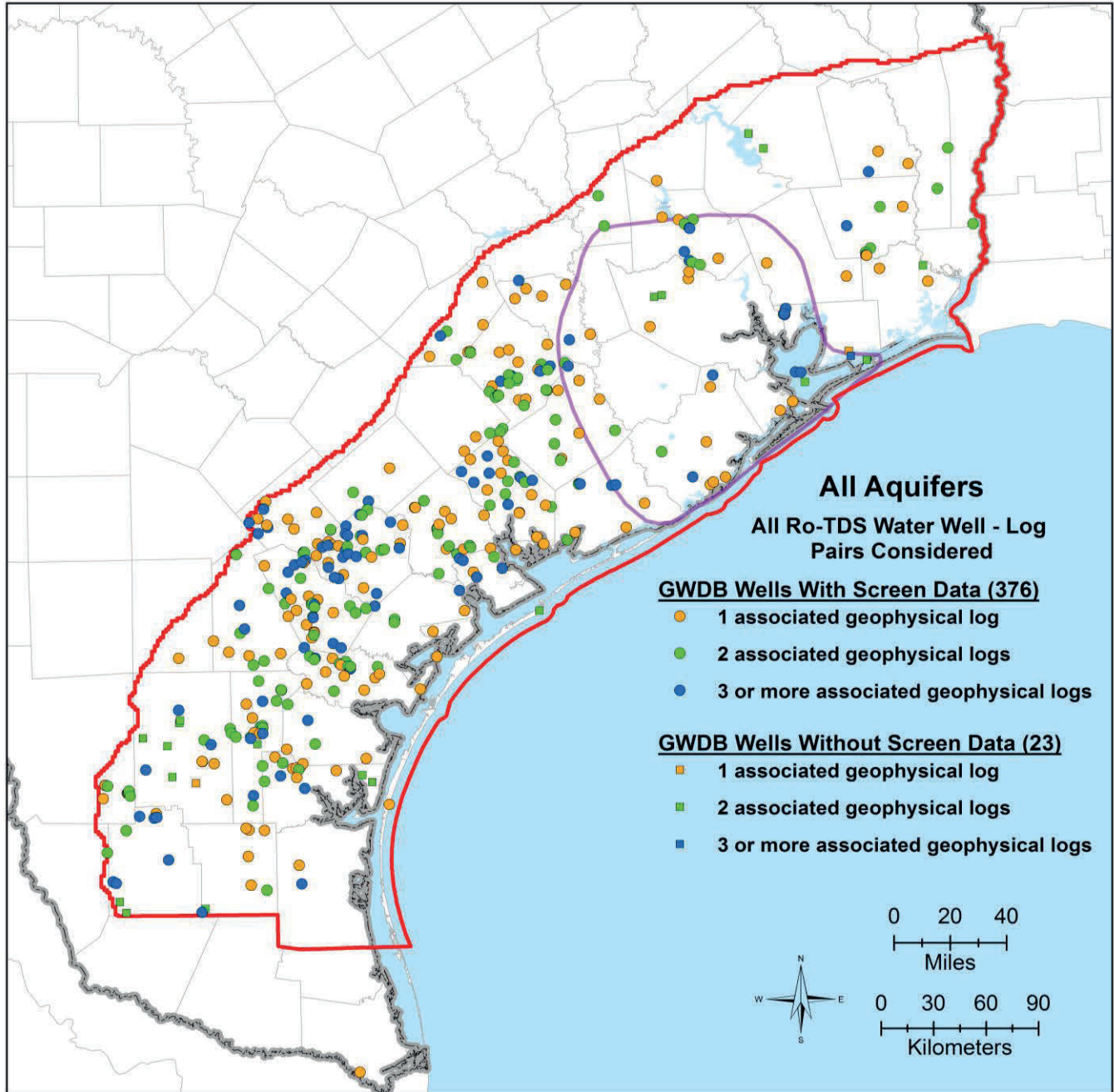
Final Report on the Delineation of Fresh, Brackish, and Saline Groundwater Resources Based on Interpretation of Geophysical Logs

number. Above the top of each log, the log's American Petroleum Institute (API) number is provided. For the six dip sections, the distance listed below the API number is measured from the up-dip extent of the Catahoula Formation outcrop. For the three strike sections, the distance listed below the API number is measured perpendicular to Cross-Section D-10. For each log, the SP is plotted on the left-hand side and the deep resistivity curve is plotted on the right-hand side. Where sands have been identified on the geophysical log, the interval between the deep resistivity and the SP curve is colored to indicate the salinity of the groundwater. The salinity zones are listed in the legend that exists in the upper right corner of every plot. Intervals between the sand beds are colored black and represent clays. The formation elevations are included on the cross section and are based on the formation surfaces developed as part of a TWDB-funded project to update the stratigraphy of the Texas Gulf Coast Aquifer System (Young and others, 2012). The elevation markers are connected to illustrate the location of each formation and thus the stratigraphy for the cross section.

General Discussions and Observations

Listed below are general observations relevant to the cross sections.

- The color-coding of the geophysical logs provides a graphical method for assessing the general groundwater trends in the subsurface. As should be expected, the patterns and layering of salinity values are more consistent along strike than along dip.
- Near the coastline in Brazoria and Galveston counties, all fresh water appears to be contained in the Chicot Aquifer.
- As shown in cross-sections D-7, D-8, and S-1, there are regions in the up-dip areas of Harris and Fort Bend counties where abundant slightly saline water and occasional fresh water occurs through the Middle Lagarto Formation.
- The significant effects that salt domes can have on groundwater quality is shown in Cross-Section D-9 at log 4215731732. The location of this log is approximately one mile from a salt dome and the depth to the base of the slightly saline salinity zone is at a depth of approximately 200 feet.
- At some log locations, there is an alternating behavior in the salinity zones that can occur over relatively short vertical distances. Where alternating behavior does occur, and thick sands are adjacent to thin sands, the thin sand will tend to indicate a higher TDS concentration zone than indicated by the thicker sand. This difference is attributed to the different properties, such as porosity, and clay content, between the two sand beds. In this situation, we have presumed that the more reliable estimate of water quality is associated with the thicker sand bed.
- Along the coastline, there is evidence of occasional inversion of the water quality where slightly saline water overlies fresh water. One occurrence of such an inversion is shown in Cross-Section S-3 in Figure 4-20 where the four logs located in the eastern region of the transect show a more than 100 feet thick zone of slightly saline groundwater above an approximate 100-foot thick zone of fresh water.
- Localized and isolated spikes in the resistivity values that cause apparent anomalous shifts in salinity occasionally occur. Because of their isolated nature, we are uncertain on whether the cause for the relatively high resistivity is the groundwater quality or changes in lithology types or the presence of gas or hydrocarbons. We know that, in several formations, small amounts of limestone are present, and could be contributing to the spike in resistivity values sometimes observed. Among the sources of the limestone are old oyster reefs. Also, at depth, there is evidence to suggest gases, such as methane and hydrogen sulfide, may be affecting the formation resistivity. Examples of these spikes occur at logs 4229105450 and 4207132442 in Cross-Section D-5 and logs 4201500683 and 403902865 in Cross-Section D-9.



Legend

- Gulf Coast Aquifer
- Study Area
- County Lines



Prepared for:



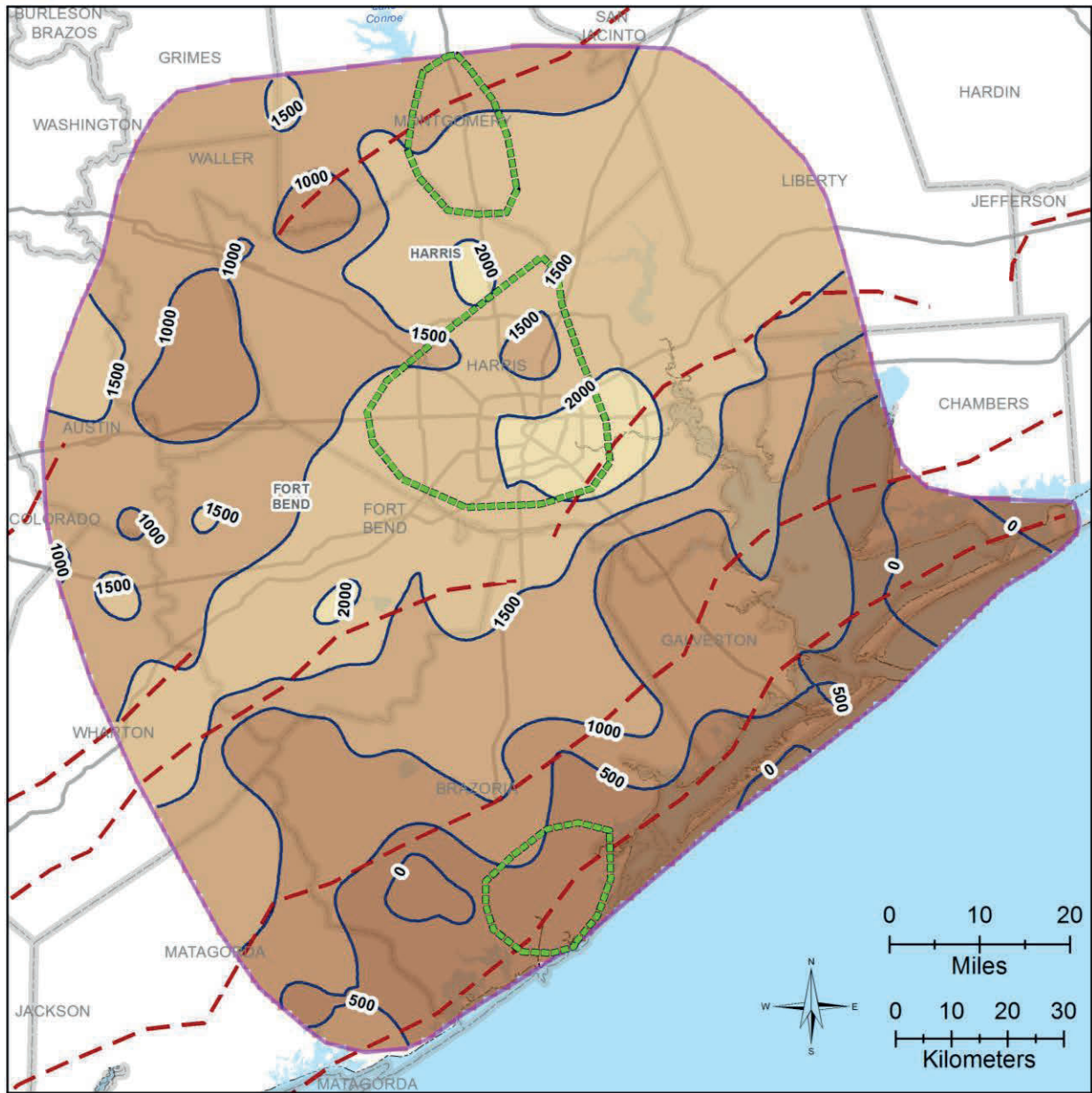
Prepared by:



Figure 4-1 Locations of 399 pairs consisting of a geophysical log(s) and a water well that were used to develop an R_o -TDS relationships for the Gulf Coast Aquifer System (from Young and others, 2016)



Final Report on the Delineation of Fresh, Brackish, and Saline Groundwater Resources Based on Interpretation of Geophysical Logs



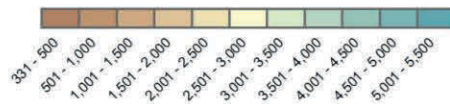
Depth to Base of Groundwater with Total Dissolved Solids < 1,000 mg/L

Legend

- Study Area
- Fault Zones
- County
- Major Highway

- Area where TDS measurements in wells indicate depths may be too high

Depth to Base (feet)



Map Location

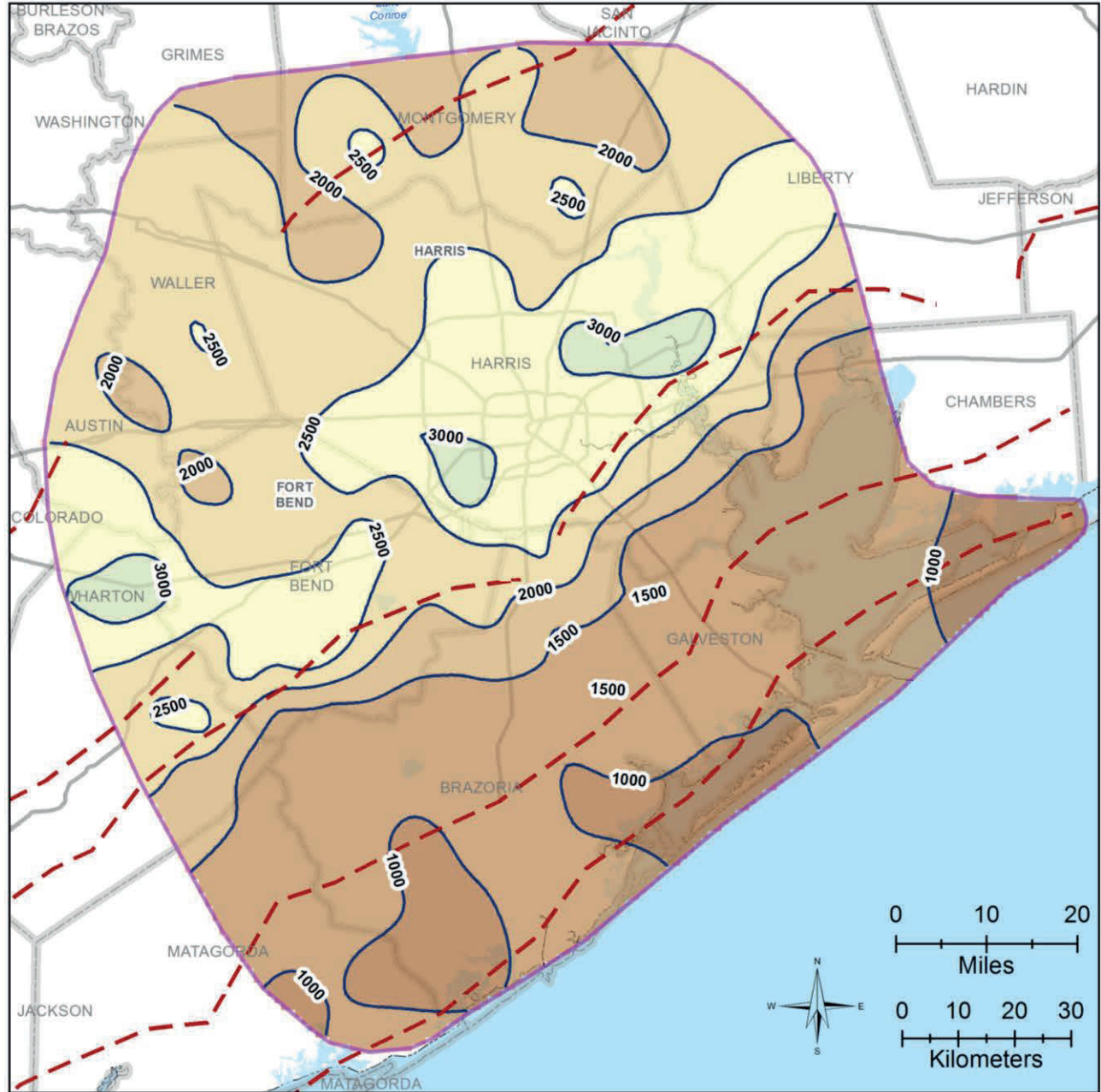
Prepared for:



Prepared by:



Figure 4-2 Depth to the base of the fresh water

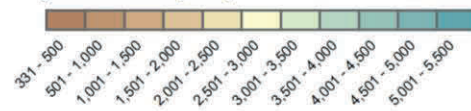


Depth to Base of Groundwater with Total Dissolved Solids < 3,000 mg/L

Legend

- Study Area
- Fault Zones
- County
- Major Highway

Depth to Base (feet)



Map Location

Prepared for:



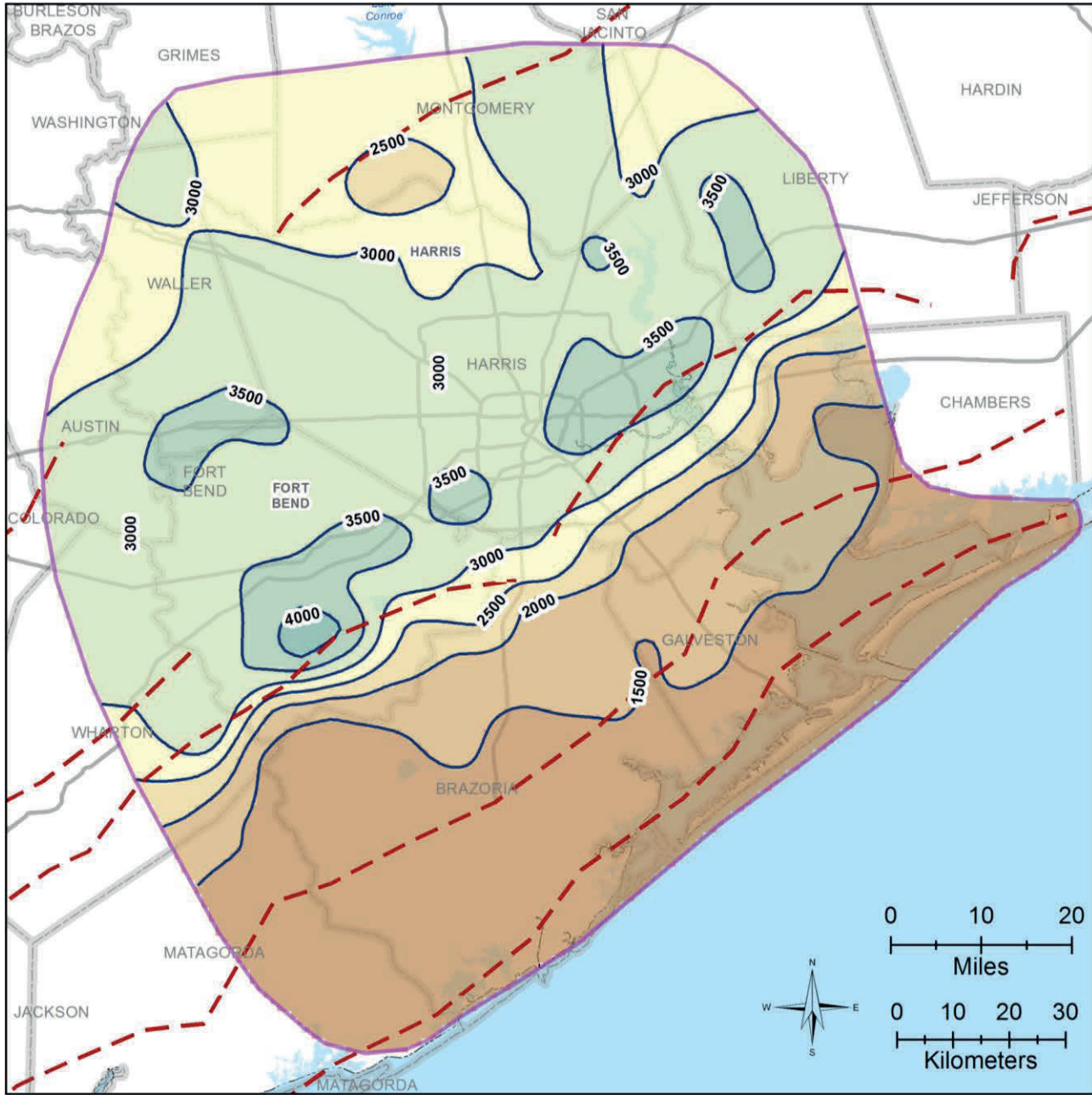
Prepared by:



Figure 4-3 Depth to the base of slightly saline water



Final Report on the Delineation of Fresh, Brackish, and Saline Groundwater Resources Based on Interpretation of Geophysical Logs

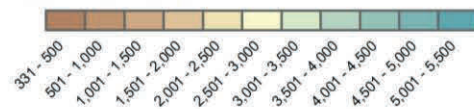


Depth to Base of Groundwater with Total Dissolved Solids < 10,000 mg/L

Legend

- Study Area
- Fault Zones
- County
- Major Highway

Depth to Base (feet)



Map Location

Prepared for:



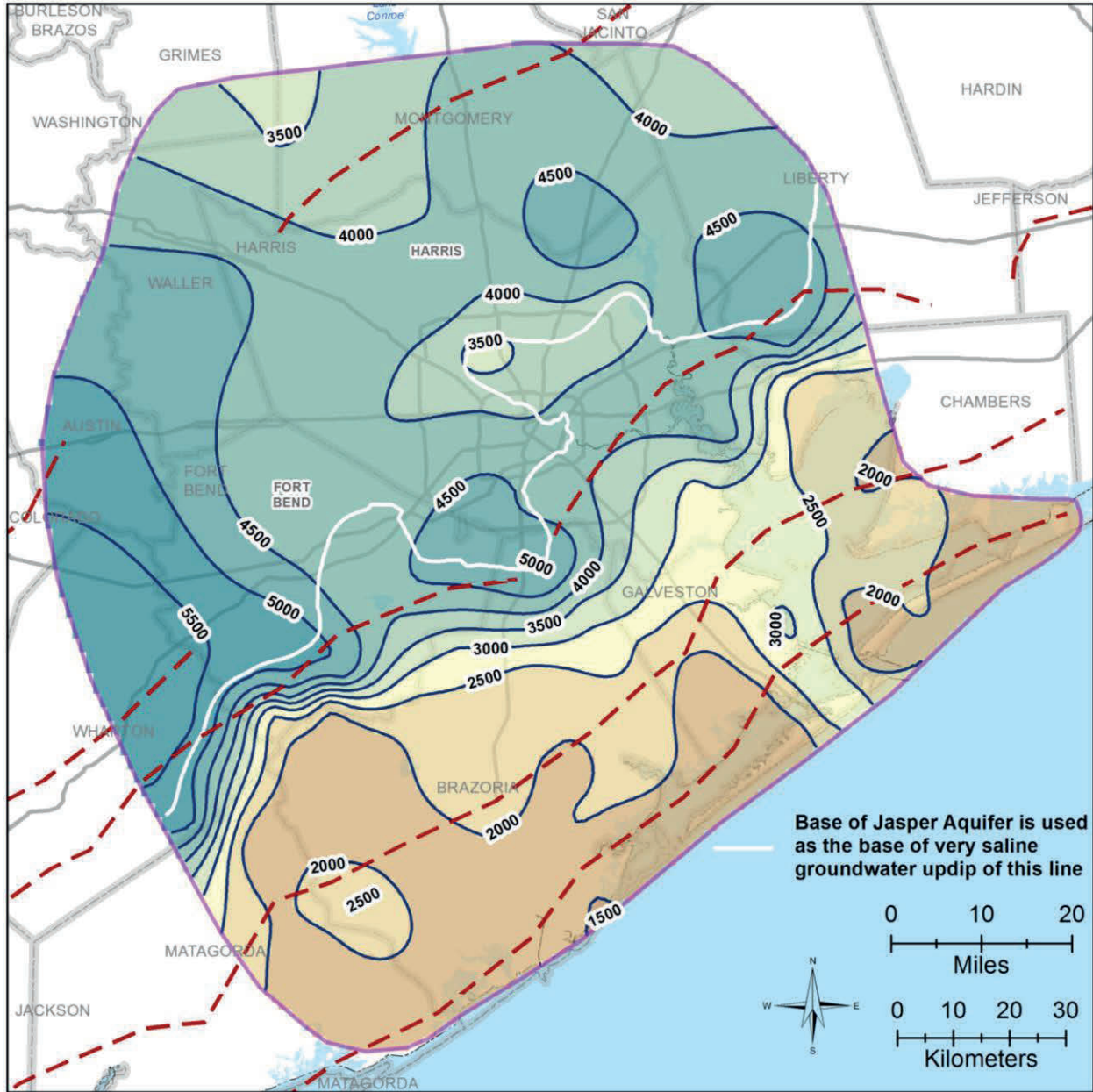
Prepared by:



Figure 4-4 Depth to base of moderately saline water



Final Report on the Delineation of Fresh, Brackish, and Saline Groundwater Resources Based on Interpretation of Geophysical Logs

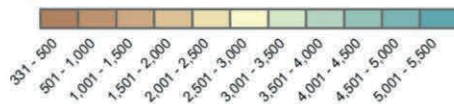


Depth to Base of Groundwater with Total Dissolved Solids < 35,000 mg/L

Legend

- Study Area
- Fault Zones
- County
- Major Highway

Depth to Base (feet)



Map Location

Prepared for:



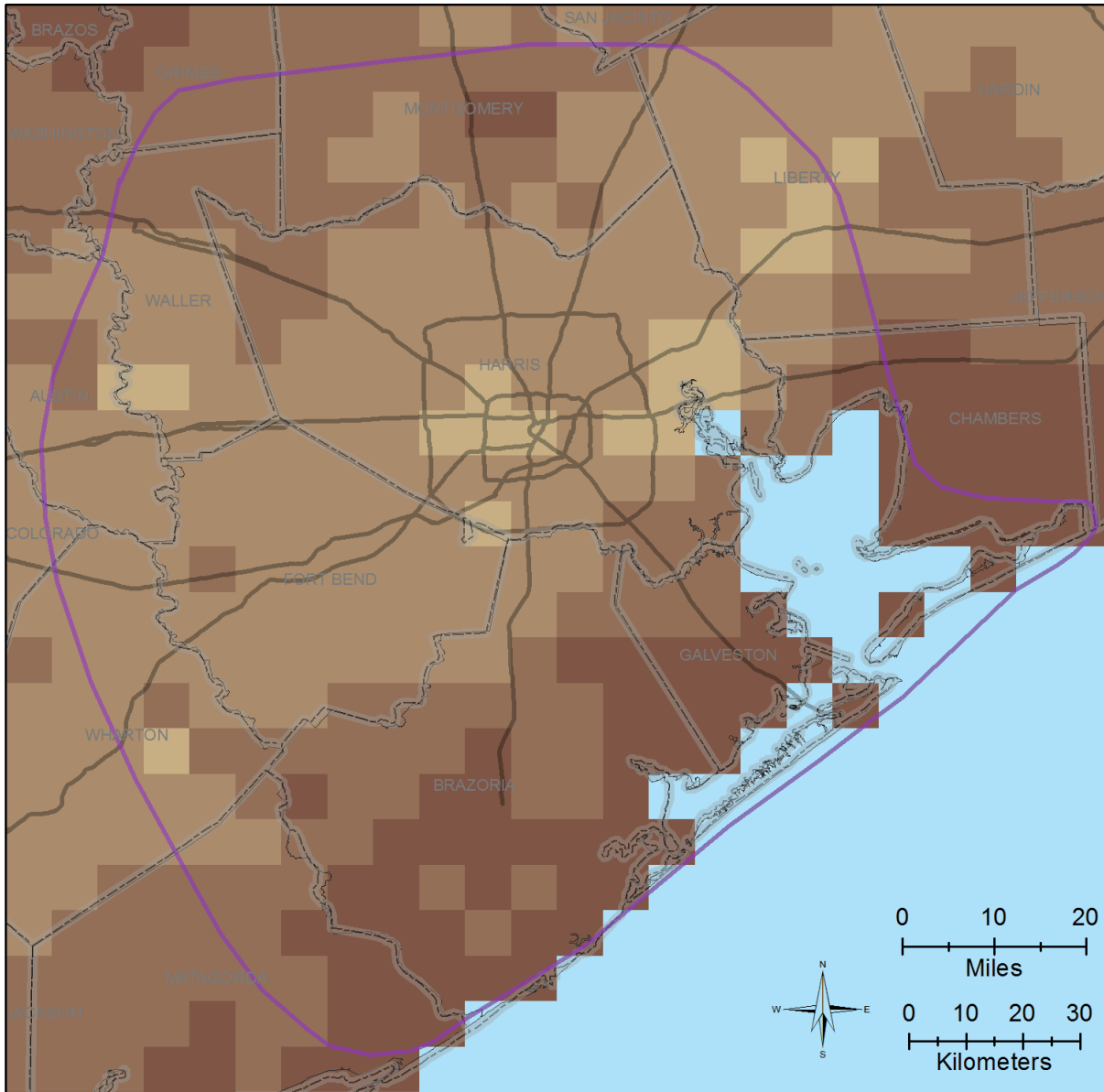
Prepared by:



Figure 4-5 Depth to the base of very saline water



Final Report on the Delineation of Fresh, Brackish, and Saline Groundwater Resources Based on Interpretation of Geophysical Logs



**Depth to Base of Fresh Groundwater
(Railroad Commission of Texas)**

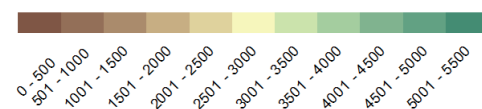
Legend

Study Area

County

Major Highway

Depth (feet)



Block represents the average value of the Groundwater Advisory Unit picks for depth to base of fresh water over a 25 square-mile area



Map Location

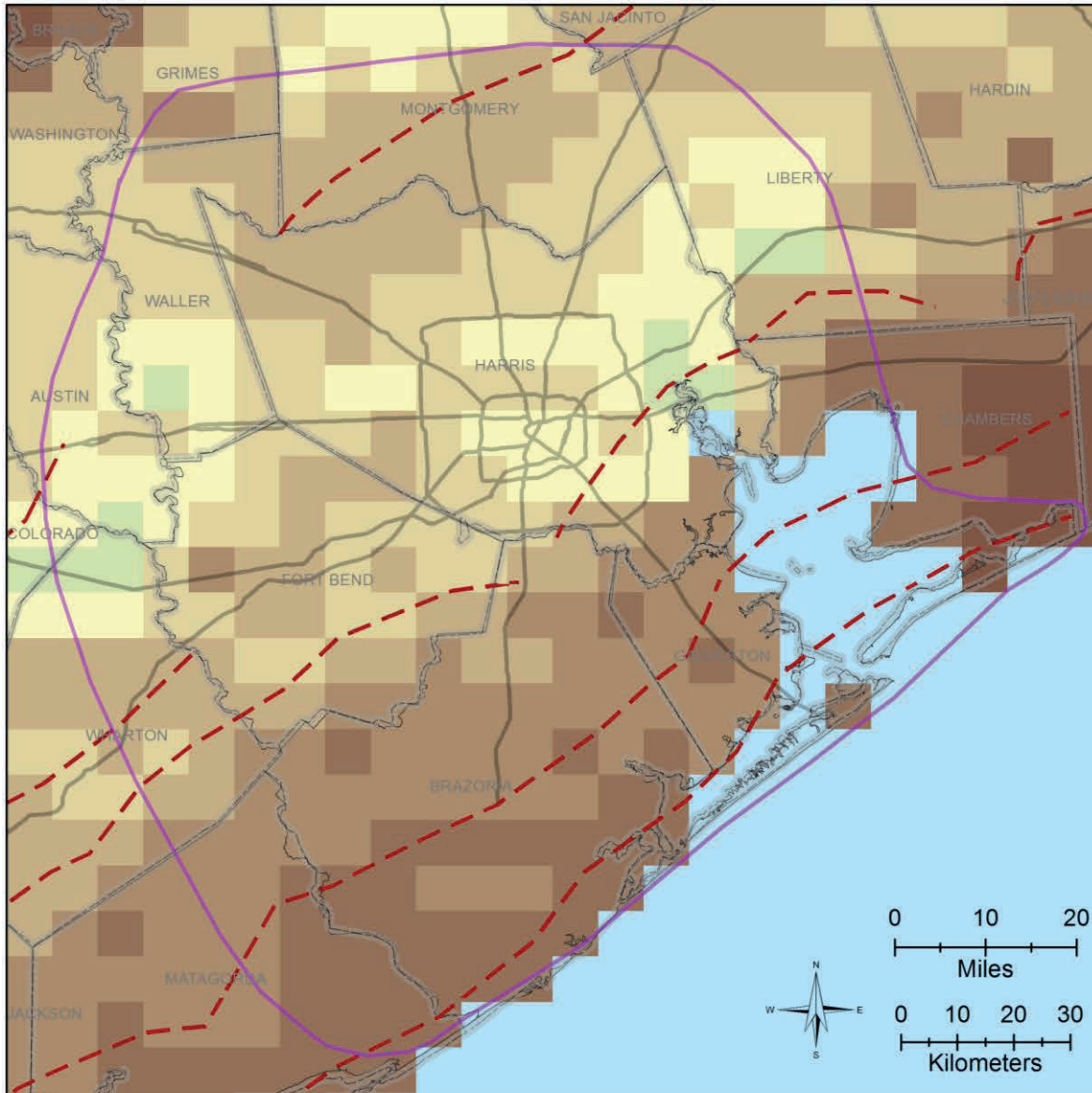
Prepared for:



Prepared by:



Figure 4-6 Estimated depth to base of fresh water, which is defined as a TDS concentration of 1,000 mg/L, based on 14,597 picks of depth to fresh water from a database maintained by the Groundwater Advisory Unit of the Railroad Commission of Texas



**Depth to Base of Usable Quality Groundwater
(Railroad Commission of Texas)**

Legend

- Study Area
- Fault Zones
- County
- Major Highway

Depth (feet)



Block represents the average value of the Groundwater Advisory Unit picks for depth to base of usable water over a 25 square-mile area



Map Location

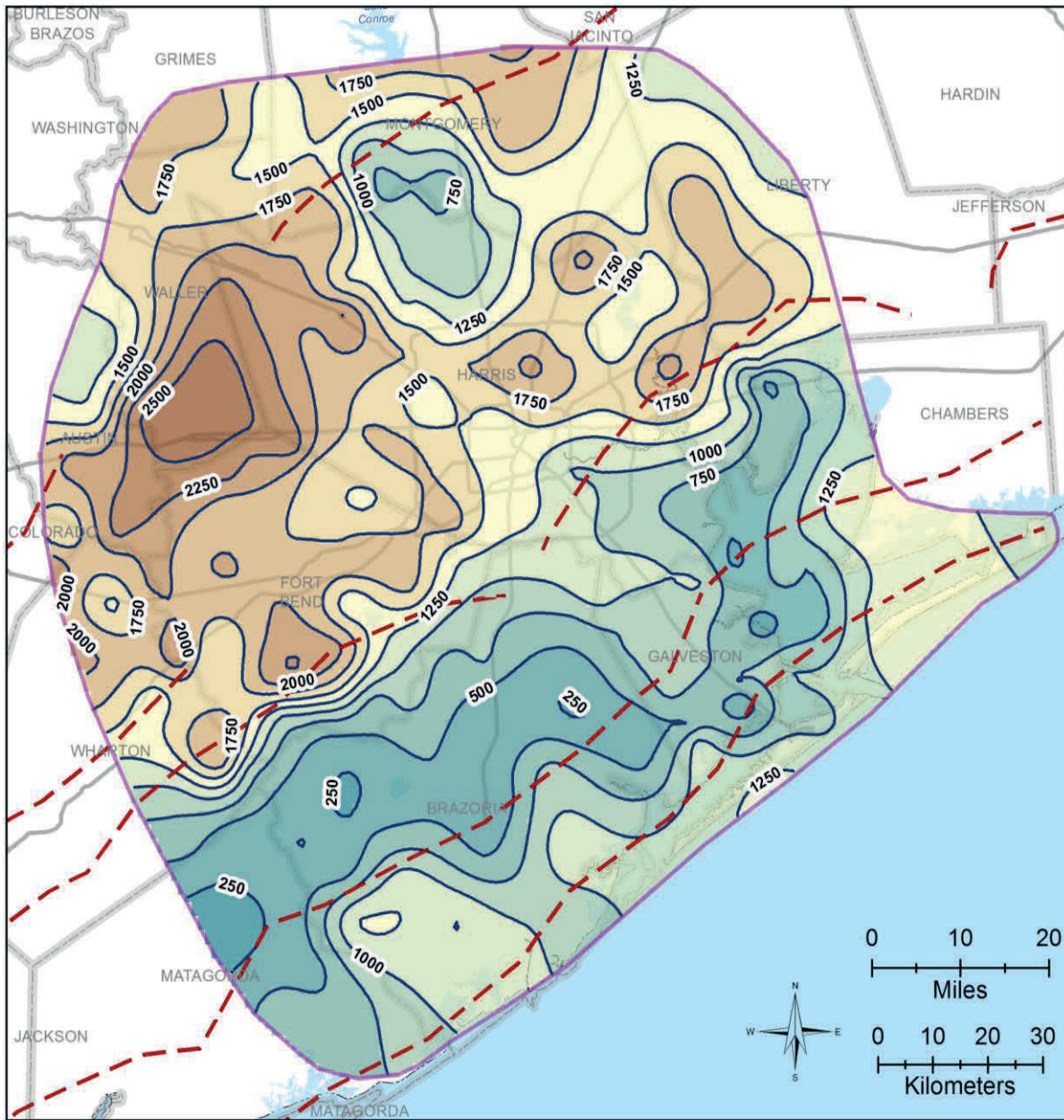
Prepared for:



Prepared by:



Figure 4-7 Estimated depth to useable quality water, which is defined as a TDS concentration of 3,000 mg/L, based on 7,017 picks of depth to fresh water from a database maintained by the Groundwater Advisory Unit of the Railroad Commission of Texas



**Thickness of Brackish Zone
(Total Dissolved Solids 1,000 - 10,000 mg/L)**

Legend

- Study Area
- Fault Zones
- County
- Major Highway

Thickness (feet)

	< 250		1500 - 1750
	250 - 500		1750 - 2000
	500 - 750		2000 - 2250
	750 - 1000		2250 - 2500
	1000 - 1250		> 2500
	1250 - 1500		



Map Location

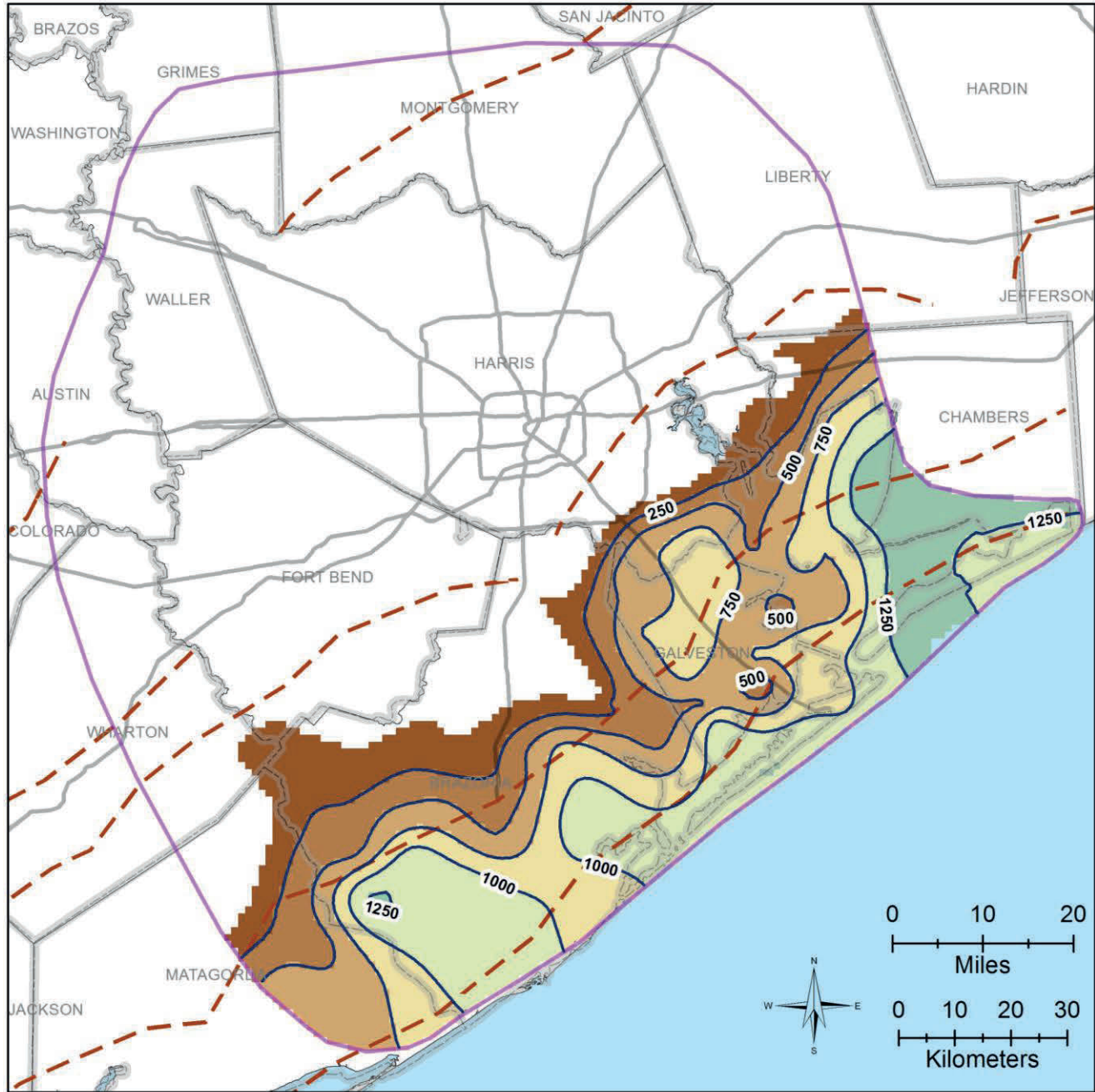
Prepared for:



Prepared by:



Figure 4-8 Thickness of the brackish groundwater zone

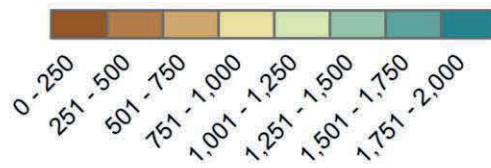


Thickness of Chicot Brackish Zone

Legend

- Study Area
- Fault Zones
- County
- Major Highway

Thickness (feet)



Map Location

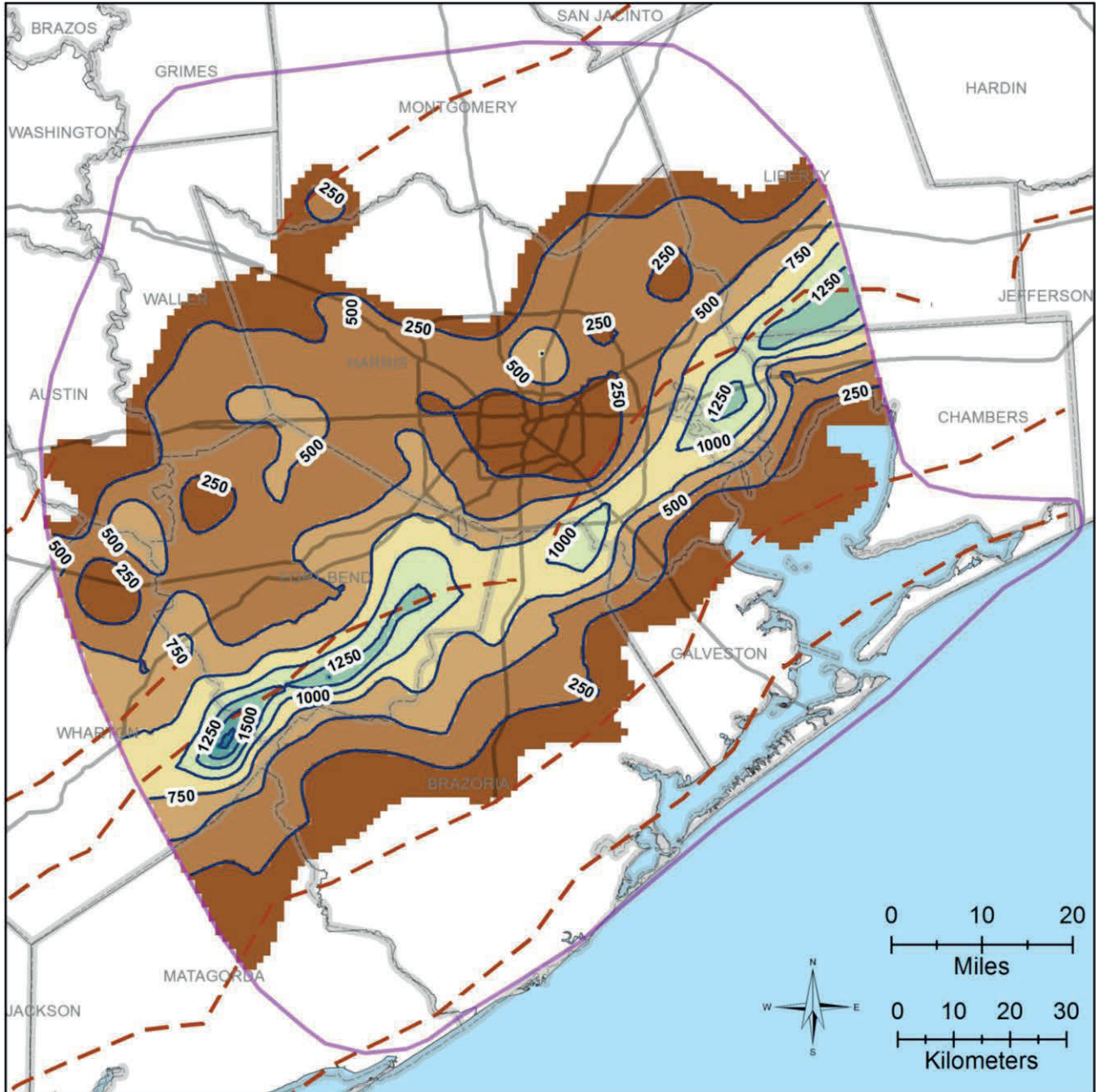
Prepared for:



Prepared by:



Figure 4-9 Thickness of brackish groundwater in the Chicot Aquifer

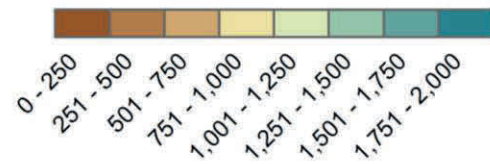


Thickness of Evangeline Brackish Zone

Legend

- Study Area
- Fault Zones
- County
- Major Highway

Thickness (feet)



Map Location

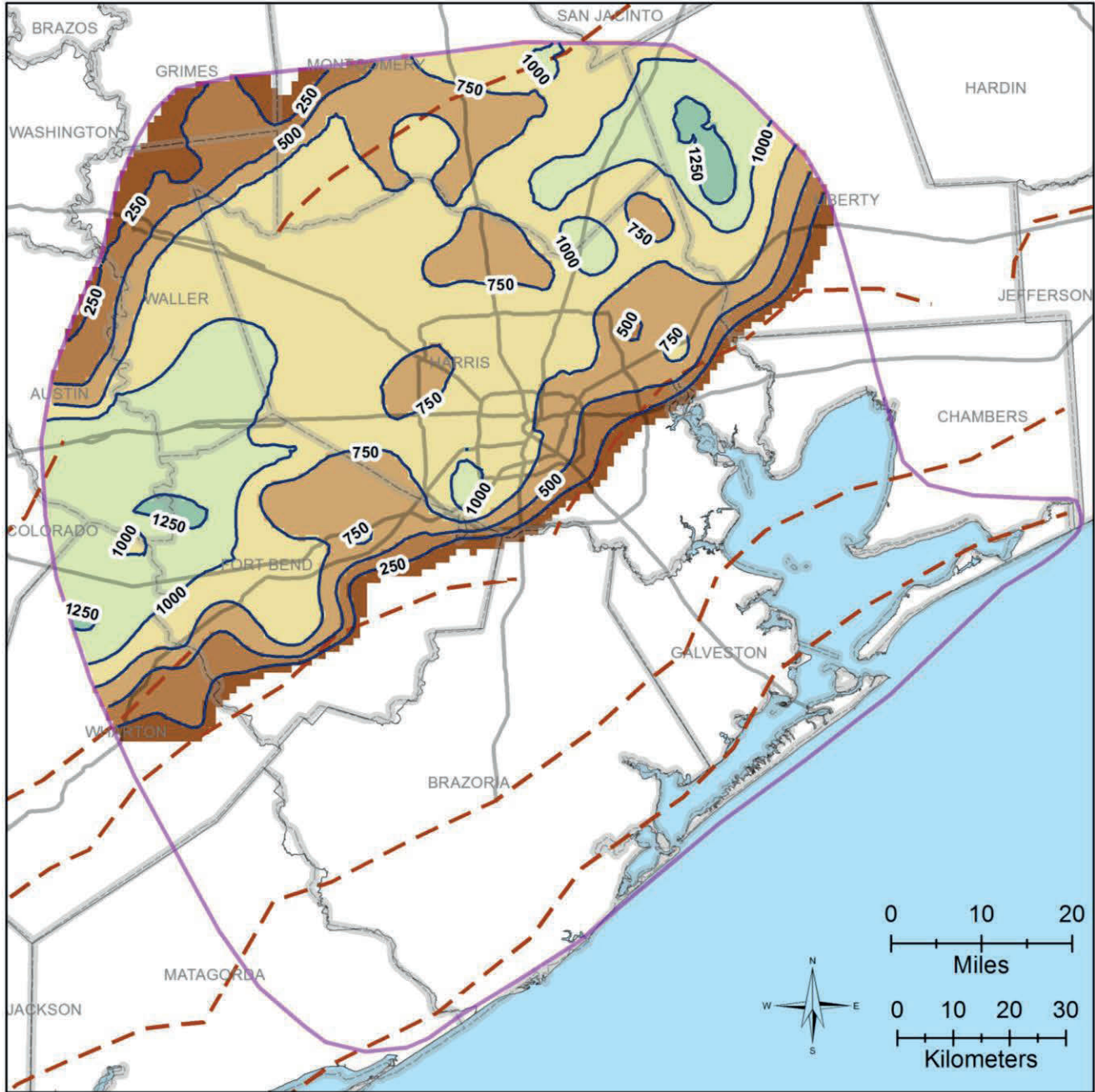
Prepared for:



Prepared by:



Figure 4-10 Thickness of brackish groundwater in the Evangeline Aquifer



Thickness of Jasper Brackish Zone

Legend

- Study Area
- Fault Zones
- County
- Major Highway

Thickness (feet)



Map Location

Prepared for:



Prepared by:



Figure 4-11 Thickness of brackish groundwater in the Jasper Aquifer

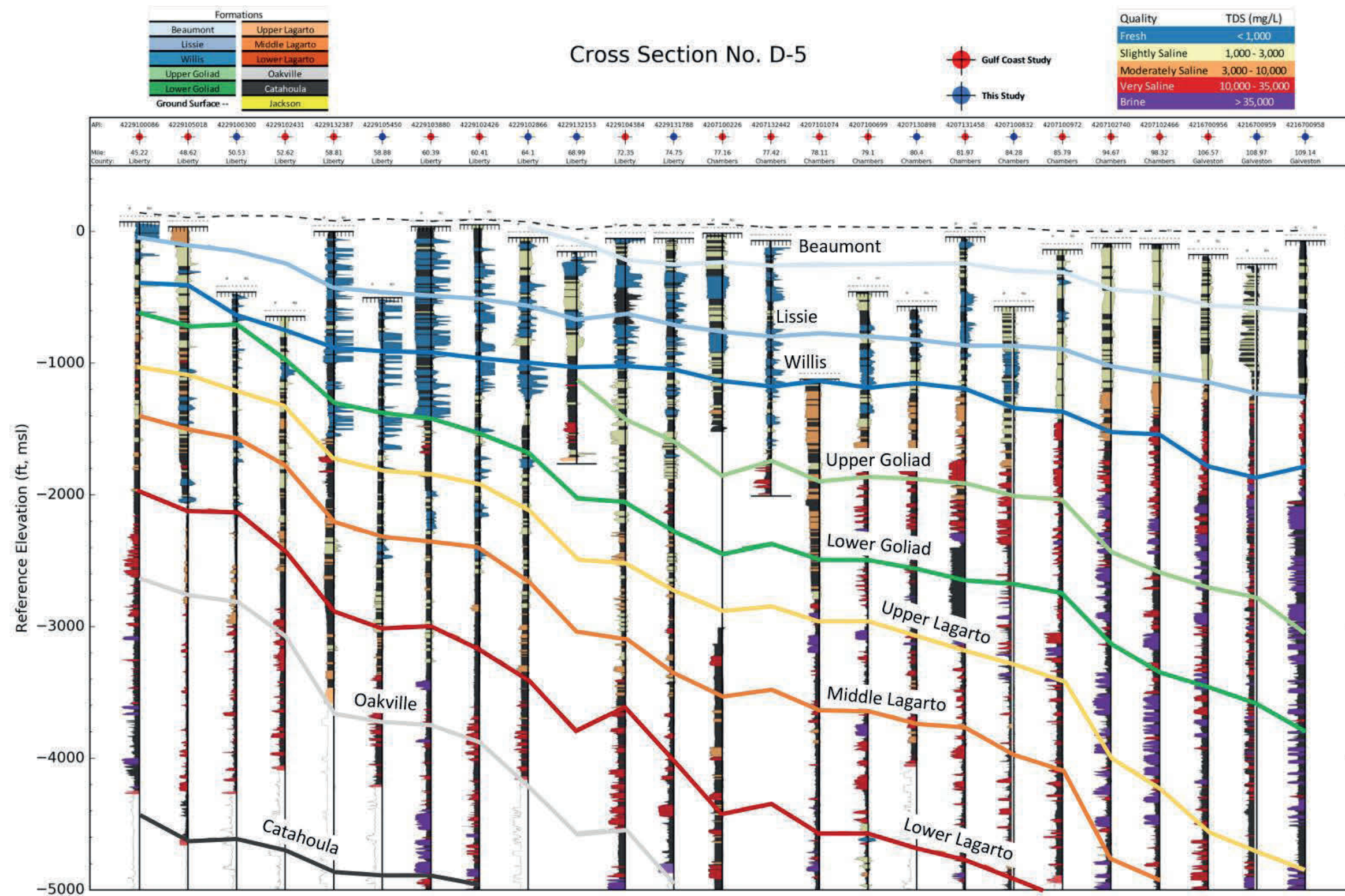


Figure 4-12 Profiles of calculated salinity zones for sand beds identified on geophysical logs aligned on Cross-Section D-5 shown in Figure 3-3. Markers represent the formation bottoms at each log location. The lines connecting the markers are for illustrative purposes only. Dashed line indicates crossing a log with no marker available in an active interval.

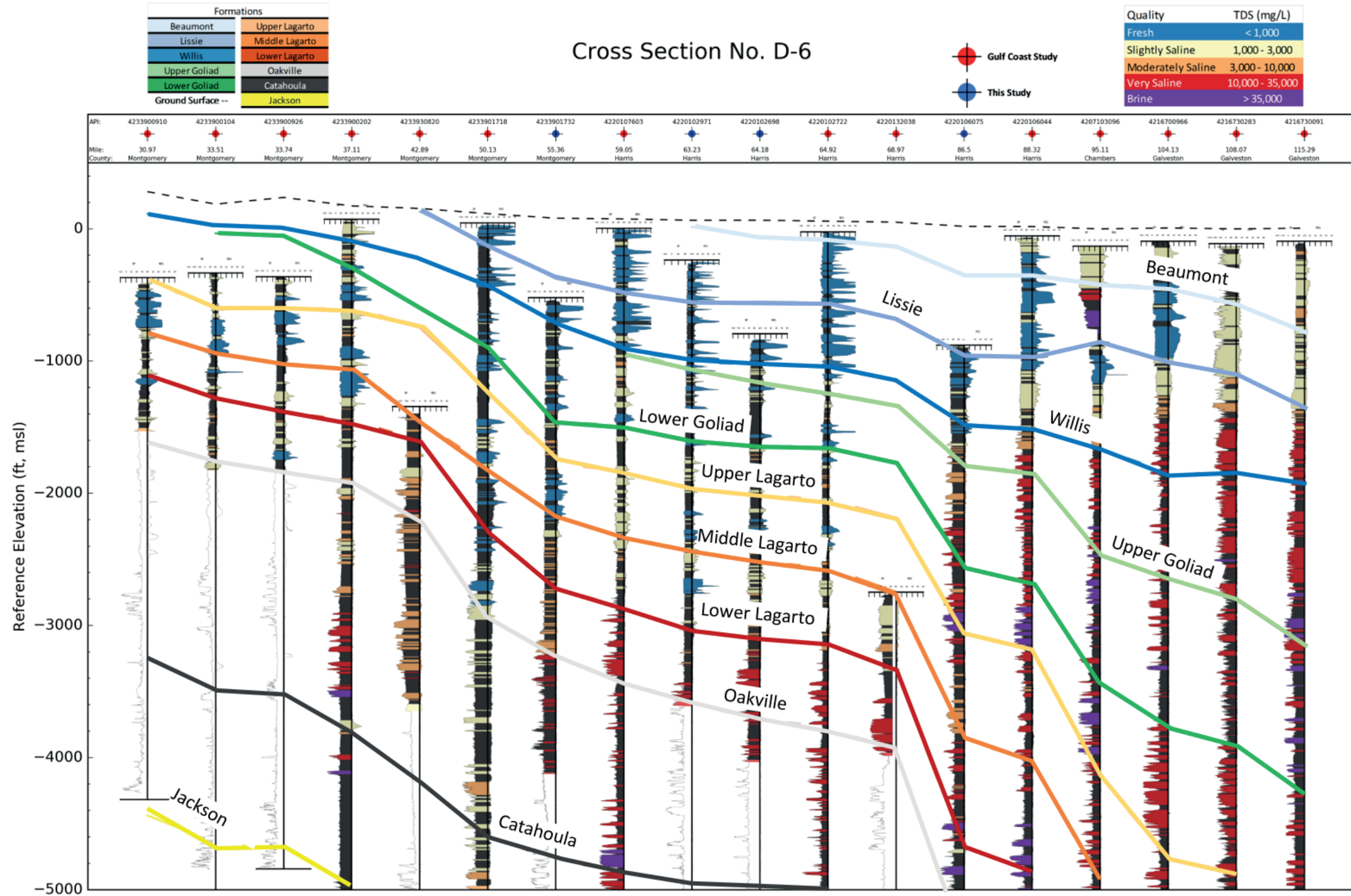


Figure 4-13 Profiles of calculated salinity zones for sand beds identified on geophysical logs aligned on Cross-Section D-6 shown in Figure 3-3.. Markers represent the formation bottoms at each log location. The lines connecting the markers are for illustrative purposes only. Dashed line indicates crossing a log with no marker available in an active interval.

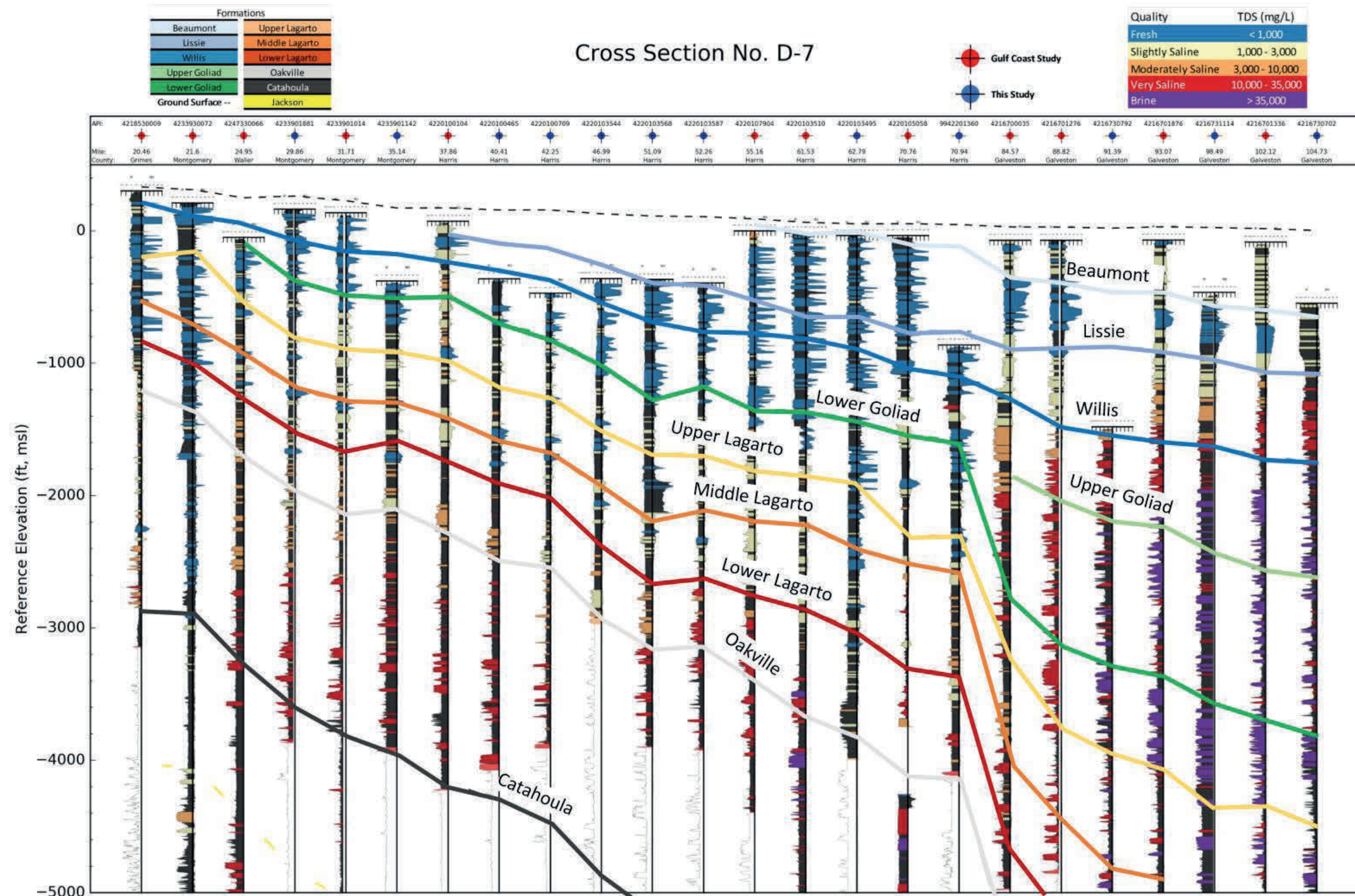


Figure 4-14 Profiles of calculated salinity zones for sand beds identified on geophysical logs aligned on Cross-Section D-7 shown in Figure 3-3. Markers represent the formation bottoms at each log location. The lines connecting the markers are for illustrative purposes only. Dashed line indicates crossing a log with no marker available in an active interval.

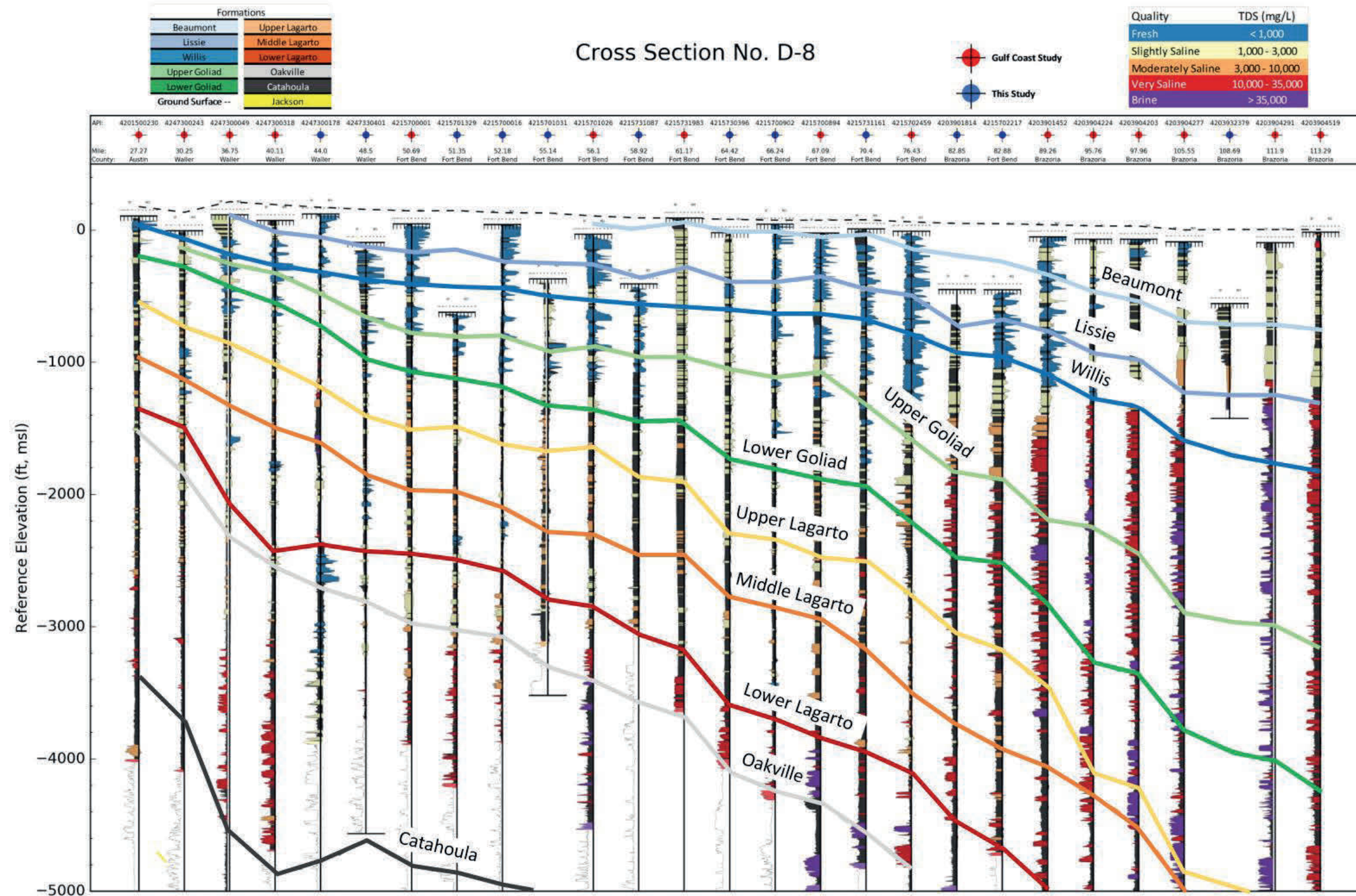


Figure 4-15 Profiles of calculated salinity zones for sand beds identified on geophysical logs aligned on Cross-Section D-8 shown in Figure 3-3. Markers represent the formation bottoms at each log location. The lines connecting the markers are for illustrative purposes only. Dashed line indicates crossing a log with no marker available in an active interval.

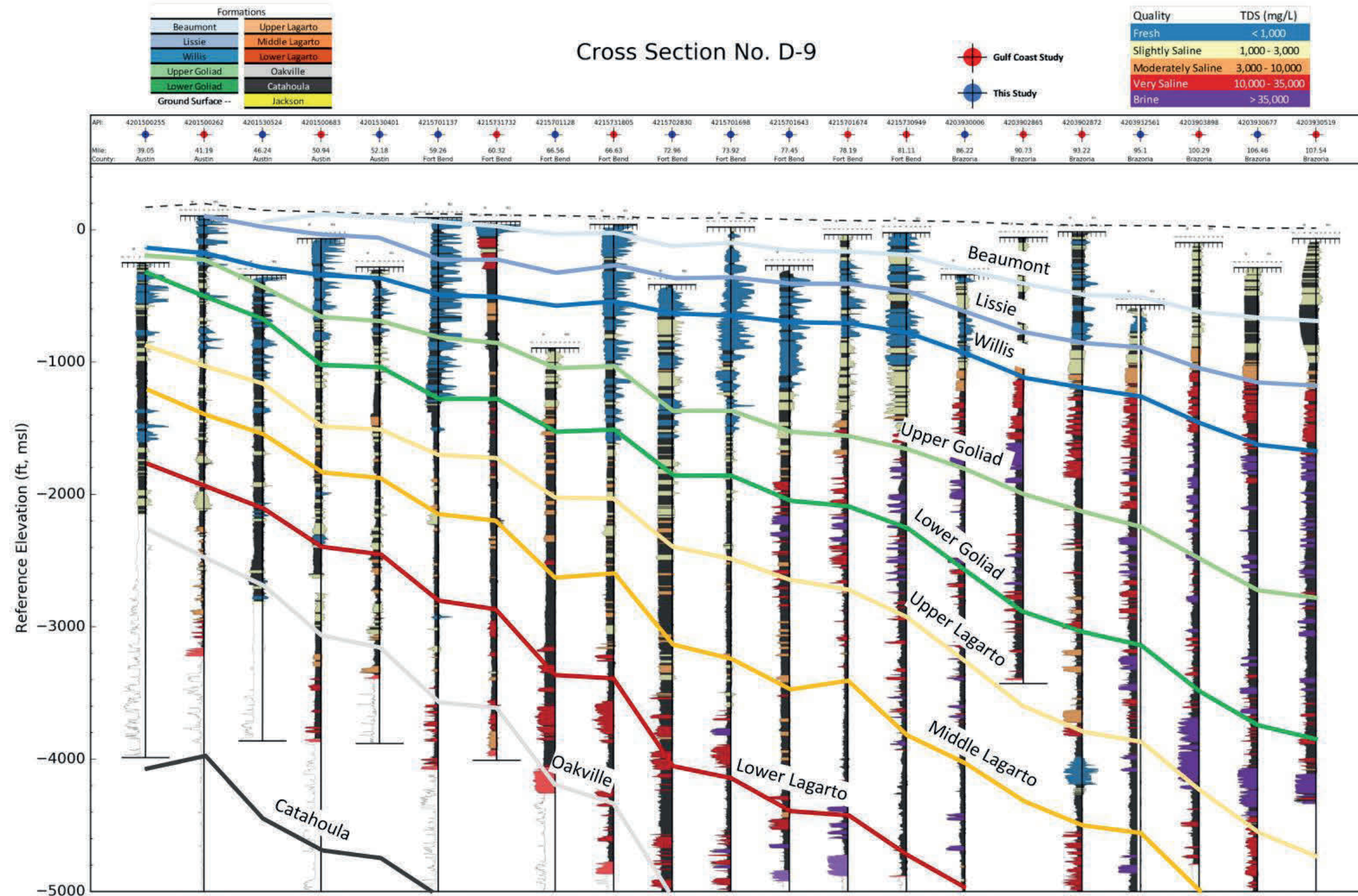


Figure 4-16 Profiles of calculated salinity zones for sand beds identified on geophysical logs aligned on Cross-Section D-9 shown in Figure 3-3. Markers represent the formation bottoms at each log location. The lines connecting the markers are for illustrative purposes only. Dashed line indicates crossing a log with no marker available in an active interval.

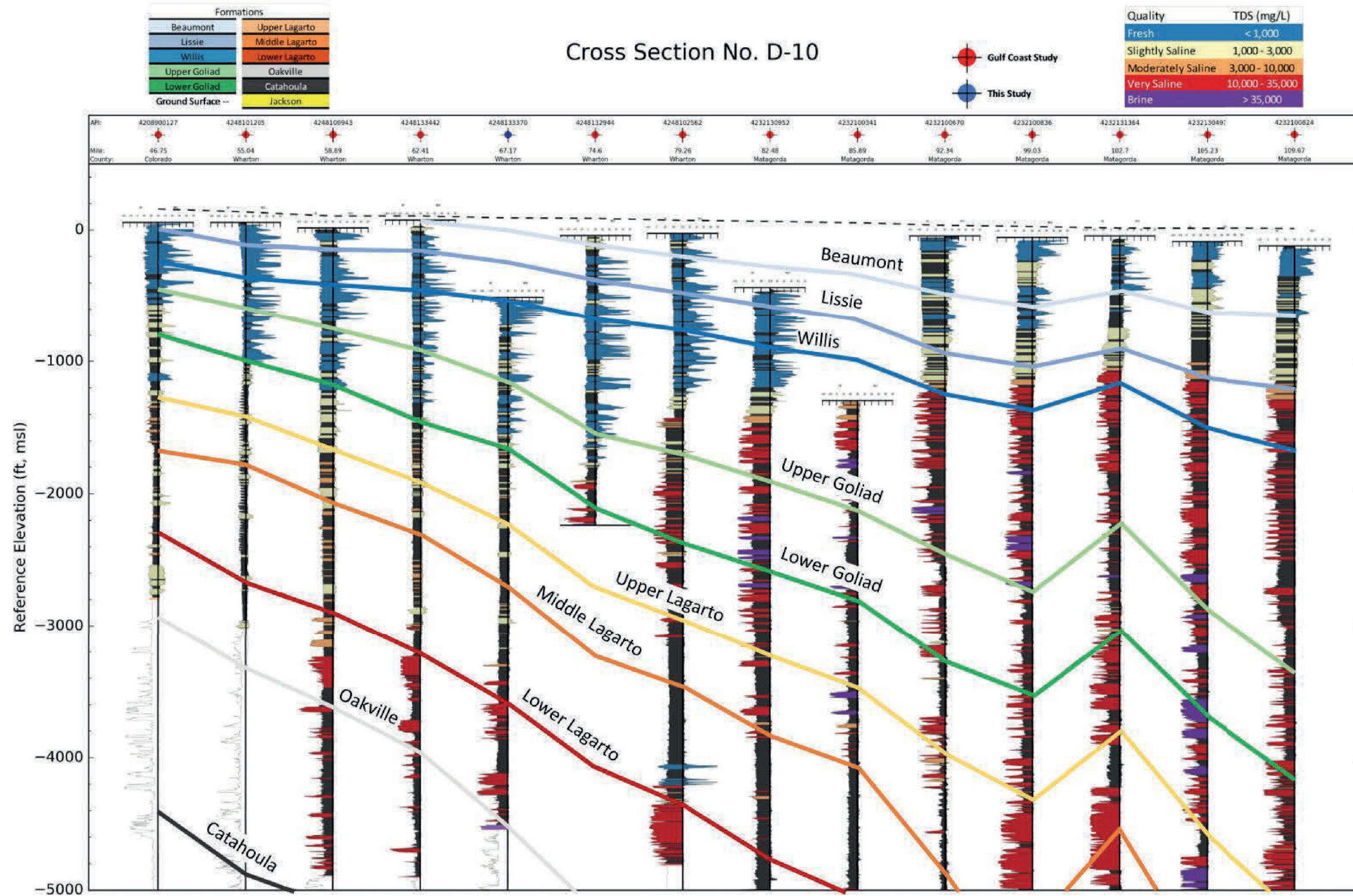


Figure 4-17 Profiles of calculated salinity zones for sand beds identified on geophysical logs aligned on Cross-Section D-10 shown in Figure 3-3. Markers represent the formation bottoms at each log location. The lines connecting the markers are for illustrative purposes only. Dashed line indicates crossing a log with no marker available in an active interval.

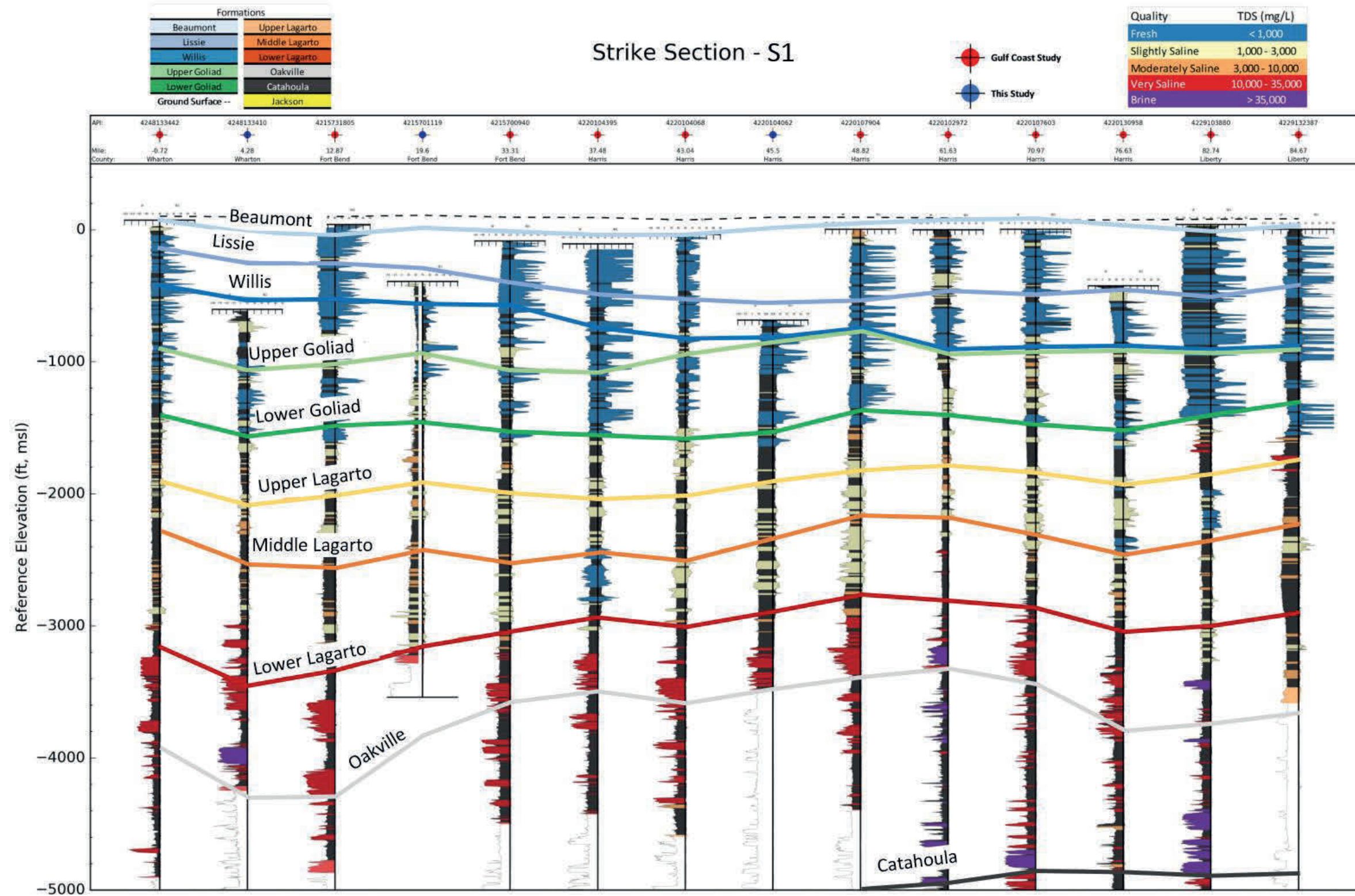


Figure 4-18 Profiles of calculated salinity zones for sand beds identified on geophysical logs aligned on Cross-Section S-1 shown in Figure 3-3. Markers represent the formation bottoms at each log location. The lines connecting the markers are for illustrative purposes only. Dashed line indicates crossing a log with no marker available in an active interval.

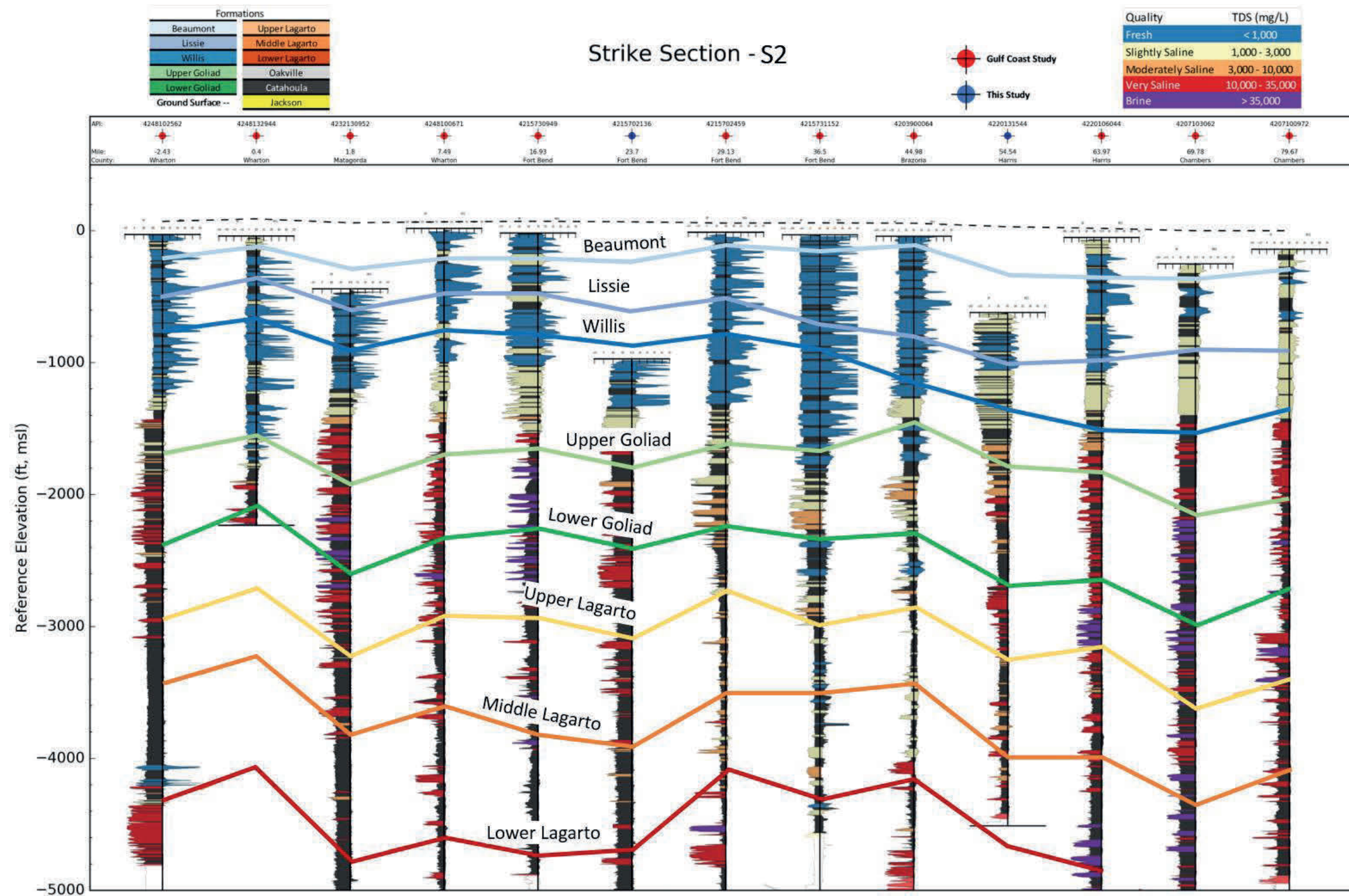


Figure 4-19 Profiles of calculated salinity zones for sand beds identified on geophysical logs aligned on Cross-Section S-2 shown in Figure 3-3. Markers represent the formation bottoms at each log location. The lines connecting the markers are for illustrative purposes only. Dashed line indicates crossing a log with no marker available in an active interval.

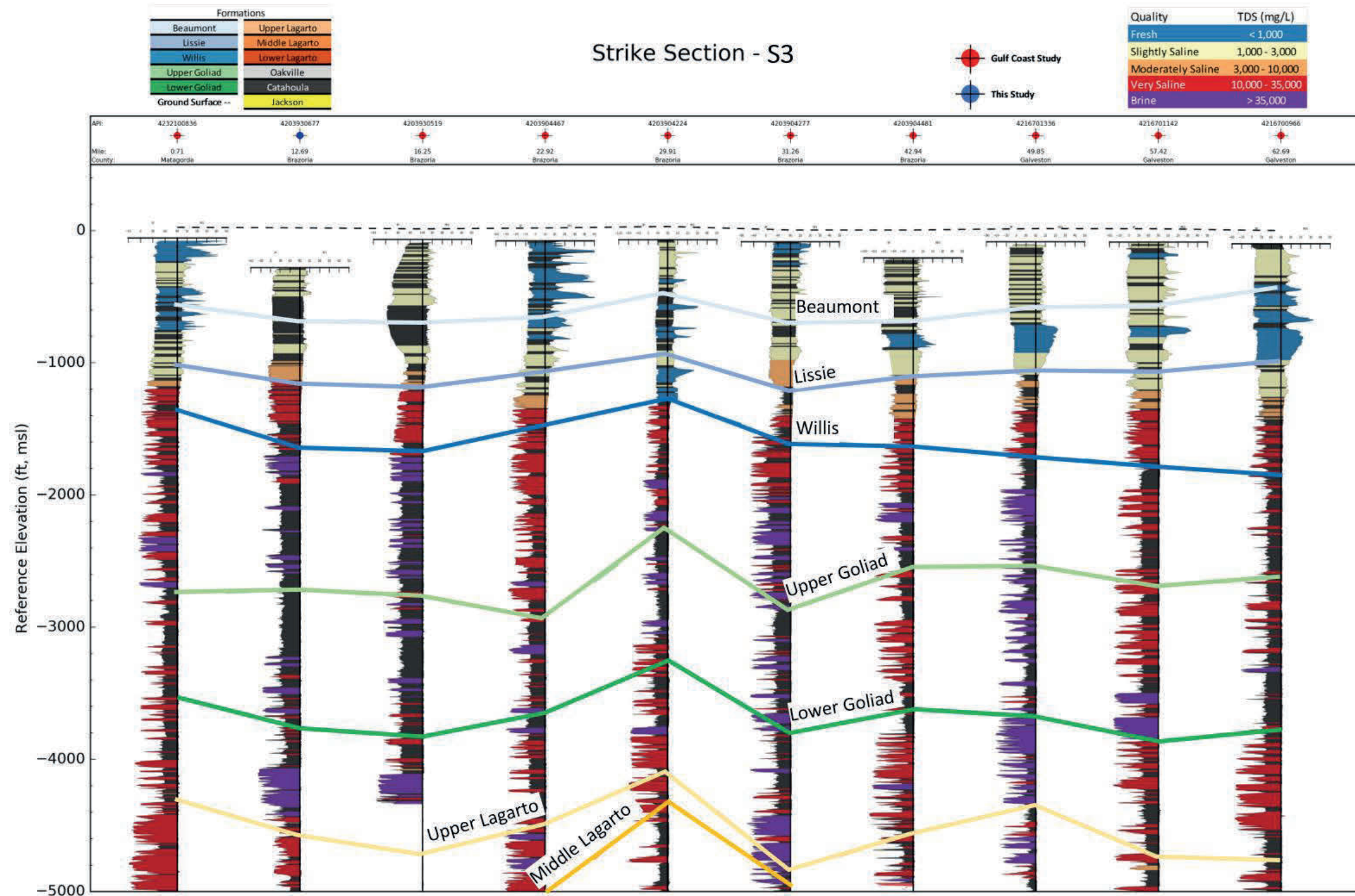


Figure 4-20 Profiles of calculated salinity zones for sand beds identified on geophysical logs aligned on Cross-Section S-3 shown in Figure 3-3. Markers represent the formation bottoms at each log location. The lines connecting the markers are for illustrative purposes only. Dashed line indicates crossing a log with no marker available in an active interval.



This page is intentionally left blank.



5.0 GROUNDWATER VOLUME BY SALINITY CLASS

This section presents estimates of groundwater volumes in storage in the formations of the Gulf Coast Aquifer System by salinity class. The groundwater storage volumes are calculated by formation, by county and by subsidence district for each salinity class.

5.1 Approach

The approach used is consistent with the approach used by the TWDB (Young and others, 2016) with the exception that data density is greatly improved providing better estimates. As part of this study, we performed the same type of calculation as presented in Young and others (2016) to partition the groundwater into the five groundwater salinity classes listed in Table 4-1.

The approach used is consistent with methods used to estimate Total Estimated Recoverable Storage (TERS) for aquifers in Groundwater Management Area 15 (Wade and Anaya, 2014). For both the TWDB House Bill 30 methodology and the TERS methodology, the groundwater volume calculation method is dependent on whether the aquifer is confined or unconfined; both conditions apply to portions of aquifers in the Gulf Coast Aquifer System. Before describing the equations used to calculate the groundwater volumes, a general discussion of confined and unconfined aquifers is presented to introduce the terminology for the volume calculations.

5.1.1 Confined and Unconfined Aquifer

Figure 5-1 provides a schematic of a confined and unconfined aquifer. Like most dipping aquifers in the Texas coastal plain aquifers, the Gulf Coast Aquifer System includes both unconfined and confined regions. **Figure 5-2** shows a schematic of a dipping aquifer that is unconfined up dip and is confined down dip, similar in concept to the Gulf Coast Aquifer System.

For an unconfined aquifer, the total storage is equal to the volume of groundwater removed by pumping that makes the water level fall to the base of the aquifer. For a confined aquifer, the total storage contains two parts. The first part is groundwater released from the aquifer when the water level falls from above the top of the aquifer to the top of the aquifer. For the confined aquifer case, the reduction of water level (hydraulic pressure) in the aquifer by pumping causes expansion of groundwater and deformation of aquifer solids. The aquifer is still fully saturated to this point. After the water level falls below the top of the aquifer the aquifer is considered to behave as an unconfined aquifer and the calculation of groundwater storage is the same as for an unconfined aquifer described above. Given the same aquifer area and water level decline, the amount of water released in the second part is much greater than the first part. The difference is quantified by two parameters: storativity, which is related to the confined aquifer, and specific yield, which is related to the unconfined aquifer. Storativity values typically range from 10^{-5} to 10^{-3} for most confined aquifers, while specific yield values typically range from 0.01 to 0.3 for most unconfined aquifers. The equations for calculating the total groundwater volume are presented below:

For unconfined aquifers:

$$\text{Total Volume} = V_{\text{drainable}} = \text{Area} * S_y * (\text{Water Level} - \text{Bottom}) \quad (\text{Equation 5-1a})$$

$$\text{Total Volume} = V_{\text{in place}} = \text{Area} * \theta * (\text{Water Level} - \text{Bottom}) \quad (\text{Equation 5-1b})$$



For confined aquifers:

$$\text{Total Volume} = V_{\text{confined}} + V_{\text{drainable}} \quad (\text{Equation 5-1c})$$

- Volume for confined part

$$V_{\text{confined}} = \text{Area} * [S * (\text{Water Level-Top})] \quad (\text{Equation 5-2})$$

or

$$V_{\text{confined}} = \text{Area} * [S_s * (\text{Top-Bottom}) * (\text{Water level-Top})] \quad (\text{Equation 5-3})$$

- Volume for unconfined part

$$V_{\text{drainable}} = \text{Area} * [S_y * (\text{Top-Bottom})] \quad (\text{Equation 5-4a})$$

$$V_{\text{in place}} = \text{Area} * [\theta * (\text{Top-Bottom})] \quad (\text{Equation 5-4b})$$

where

- $V_{\text{drainable}}$ = storage volume due to water draining from the formation (acre-feet)
- V_{confined} = storage volume due to elastic properties of the aquifer and water (acre-feet)
- $V_{\text{in place}}$ = storage volume due to void spaces in the aquifer occupied by water (acre-feet)
- Area = area of aquifer (acre)
- Water Level = groundwater elevation (feet above mean sea level)
- Top = elevation of aquifer top (feet above mean sea level)
- Bottom = elevation of aquifer bottom (feet above mean sea level)
- S_y = specific yield (unitless)
- S_s = specific storage (1/feet)
- S = storativity or storage coefficient (unitless)
- θ = porosity (unitless)

In the above equations, two options are provided to calculate the volume in the unconfined aquifer. Equations 5-1a and 5-4a use specific yield, whereas Equations 5-1b and 5-4b use total porosity. Wade and Anaya (2014) use Equations 5-1a and 5-4a to calculate TERS. The use of specific yield in Equations 5-1a and 5-4a implies that the unconfined aquifer has not fully drained because specific yield is less than the porosity of an unconfined aquifer. The selection of specific yield or porosity is dependent on the purpose of the calculation. Neither calculation provides an estimate of available groundwater in the confined portions of the aquifer. Rather, they are two different estimates of groundwater in place or in storage. One could never physically, economically, nor because of environmental issues such as subsidence develop even a specific yield based volume estimate from a deeply confined aquifer.

5.1.2 Hydraulic and Physical Properties for the Gulf Coast Aquifer System

The equations for calculating groundwater volumes described above require specification of aquifer properties such as aquifer structure, thickness, water level, specific storage, and specific yield. These are described below.

Structure and Thickness – **Table 5-1** lists the formations that represent the hydrogeologic units of the Gulf Coast Aquifer System. The aquifer top elevation, bottom elevation, and model layer thickness for each model layer required for the calculations were obtained from Young and others (2012, 2016). Each model grid cell is one mile by one mile.

Specific Storage and Water Level – The water levels used to calculate the aquifer volumes and the specific storage values used to calculate the confined water volumes are extracted from the Houston Area Groundwater



Model (HAGM) (Kasmarek, 2013). The water levels used for the calculations are based on the values simulated for the last year of the calibration period. This corresponds to the end of 2009 for the HAGM. The water level and specific storage values are assigned to each of the grid cells representing the formation that comprise the aquifers shown in Table 5-1. Because the HAGM is a fully confined aquifer model (i.e., layers are non-convertible), the model does not have specific yield values as model parameter inputs. Specific yield values were obtained from the Central Gulf Coast Groundwater Availability Model (CGCGAM) (Chowdhury and others, 2004) because it simulates unconfined aquifer conditions. The specific yield values vary between 0.005 for the Burkeville Confining Unit and 0.05 for the Chicot Aquifer as listed in Table 5-1. The specific storage values for the Catahoula Formation are assigned values based on the Jasper Aquifer. The same specific storage values are assumed for the sand layers and the clays in the same grid cell consistent with Young and others (2016). Water level elevations for the Catahoula Formation are set to 75 feet below ground surface elevation.

The porosity values assigned to each grid cell is calculated as a function of depth using Equation 3-1. This function generates a porosity values of 0.36 near ground surface with a decrease of 0.01 for every 1,000 feet of depth. An assumption in the groundwater volume calculations is that the same porosity values are assigned to sand layers and the clay layers in the same grid cell.

Table 5-1 Model layers that comprise the Gulf Coast Aquifer System in the Central Gulf Coast Groundwater Availability Model and model specific yield (Chowdhury and others, 2004)

Model Layer	Aquifer or Formation	Hydrogeologic Unit (Baker, 1979)	Specific Yield
1	Beaumont	Chicot Aquifer	0.05
2	Lissie		0.05
3	Willis		0.05
4	Upper Goliad	Evangeline Aquifer	0.01
5	Lower Goliad		0.01
6	Upper Lagarto		0.01
7	Middle Lagarto	Burkeville Confining Unit	0.005
8	Lower Lagarto	Jasper Aquifer	0.05
9	Oakville		0.05
10	Catahoula	Catahoula	0.05

5.1.3 Calculation of Groundwater Volumes by Salinity Classification

The process for calculating groundwater volumes is based on the same process and equations used by Young and others (2016). The primary difference between the calculated volumes in this study with those from Young and others (2016) is the greater density of geophysical logs used to define the spatial variability of salinity and sands within each formation.

Groundwater volumes for each of the ten formations comprising the Gulf Coast Aquifer System were performed independently from each other. All the formation calculations were performed using the same grid, which divided the study area into square blocks that measured 0.5 mile along a side. The process of calculating groundwater volumes is summarized by the six steps described below.



Final Report on the Delineation of Fresh, Brackish, and Saline Groundwater Resources Based on Interpretation of Geophysical Logs

Step 1. Assign sand layers to aquifer units. Intersect the surfaces for the ten formation layers onto every geophysical log within the study area and partition vertical intervals of each geophysical log to specific formations. Calculate the percent sand for each formation at the location of the geophysical log.

Step 2. Generate sand percentages for each grid cell. Use kriging to interpolate the point measurements of percent sand at the location of the geophysical logs to create a continuous sand percentage map for each formation. Then calculate the percent sand for each formation at each grid block location.

Step 3. Determine groundwater water classification categories for each grid cell. Create maps for each model layer that allocate the percentage of sands are associated with the fresh, slightly saline, moderately saline, very saline, and brine water quality (see Table 4-1). The summation of these water quality percentages for each formation will equal 100%. Develop a continuous map of the percentage of sand assigned to a water quality category by kriging the point measurements at each geophysical log location. Summarize the total percentage of sands assigned to the different water qualities for every grid block and check make sure the percentages equal 100%. If the values are different than 100%, then normalize each of the individual percentage so that they equal 100%.

Step 4. Calculate the Confined and Unconfined Groundwater for every Grid Cell. For every grid cell, calculate the confined groundwater in the sand layers using Equation 6-3 and the unconfined groundwater in the sand layers using Equations 5-4a or 5-4b.

Step 5. Add up the groundwater volumes in each grid cell. Add up the groundwater volumes for both the confined and unconfined groundwater volumes in each grid cell. For the unconfined aquifers, use either the specific yield assigned to the grid cell reported in **Table 5-2**, or use a porosity value calculated from the porosity versus depth relationship in Equation 3-1. Partition the sand volumes into the different salinity classes based on the percentages generated in Step 3.

5.2 Calculated Groundwater Volumes

Groundwater volumes were calculated for Brazoria, Fort Bend, Galveston, and Harris counties using the methodology described above. A total of nine tables were created to provide the calculated volumes per geological formation and per salinity class. The geologic formations included in each table include the Beaumont, Lissie, and Willis formations, which comprise the Chicot Aquifer; the Upper Goliad, the Lower Goliad, and the Upper Lagarto formations, which comprise the Evangeline Aquifer; the Middle Lagarto Formation, which represents a confining unit between the Evangeline and Jasper aquifers; the Lower Lagarto and Oakville formations, which comprise the Jasper Aquifer, and the Catahoula Formation. The salinity classes include fresh water, slightly saline water, moderately saline water, very saline water, and brine. Table 5-2 describes three of the criteria used to summarize the calculated volumes and correlates these to **Table 5-3** through **Table 5-10**.



Table 5-2

List of the different assumptions used to tabulate the volumes of groundwater associated with fresh, slightly saline, moderately saline, very saline, and brine

Table Number	Voids		Subsurface Deposit		Geography	
	Specific Yield	Porosity	Only Sands	Sands and Clays	County	Subsidence District
Table 5-3	X		X		X	
Table 5-4	X			X	X	
Table 5-5	X		X			X
Table 5-6	X			X		X
Table 5-7		X	X		X	
Table 5-8		X		X	X	
Table 5-9		X	X			X
Table 5-10		X		X		X

Tables 5-3 through 5-6 provide the volumes of fresh, slightly saline, moderately saline, very saline, and brine groundwater using specific yield as the void volume once the water level falls below the top of the formation. Tables 5-3 and 5-4 provide estimates of groundwater volume by salinity class for Brazoria, Fort Bend, Galveston and Harris counties for the aquifer volume only determined to be composed of sand and for the total aquifer volume (sand and clay), respectively. Tables 5-5 and 5-6 provide the same information organized by subsidence district.

Tables 5-7 through 5-10 provide the volumes of fresh, slightly saline, moderately saline, very saline, and brine groundwater using porosity as the void volume once the water level falls below the top of the formation. Tables 5-7 and 5-8 provide estimates of groundwater volume by salinity class for Brazoria, Fort Bend, Galveston and Harris counties for the aquifer volume only determined to be composed of sand and for the total aquifer volume (sand and clay), respectively. Tables 5-9 and 5-10 provide the same information organized by subsidence district.

All groundwater volume estimates provided in Tables 5-3 through 5-10 are estimates of groundwater in place. As one can see through inspection of these tables, even for estimates based upon groundwater just in sand portions of the aquifers, these estimates are very large. These volume estimates do not reflect the amount of groundwater that could be produced from each of these aquifers. They do not consider physical aquifer limitations inherent in development using groundwater wells, economics or environmental impacts such as subsidence. These groundwater volume estimates do provide an understanding of how brackish and saline groundwater resources are distributed within the study area. Combined with the lithologic data derived in this study, the Harris-Galveston and Fort Bend Subsidence Districts can use the data to develop a regulatory framework for brackish and saline groundwater.



Final Report on the Delineation of Fresh, Brackish, and Saline Groundwater Resources Based on Interpretation of Geophysical Logs

Table 5-3 Aquifer sand groundwater volume (in millions of acre-feet) by county and salinity class assuming a void fraction based upon specific yield

Formation	Fresh Water	Slightly Saline Water	Moderately Saline Water	Very Saline Water	Brine Water	Total
Brazoria County						
Beaumont	4.85	8.05	0.09	0.04	-	13.02
Lissie	5.07	6.31	1.90	0.16	-	13.44
Willis	3.72	2.58	2.13	3.73	0.58	12.73
Upper Goliad	0.26	0.44	0.37	2.73	1.42	5.22
Lower Goliad	0.07	0.15	0.10	1.85	1.27	3.44
Upper Lagarto	0.04	0.13	0.09	1.68	1.61	3.56
Middle Lagarto	0.23	0.07	0.15	4.83	4.36	9.63
Lower Lagarto	0.36	1.09	0.71	12.39	10.04	24.59
Oakville	0.88	0.37	0.41	28.66	16.16	46.49
Catahoula						
Total	15.47	19.17	5.94	56.09	35.45	132.12
Fort Bend County						
Beaumont	0.68	0.29	-	-	-	0.96
Lissie	5.68	1.03	0.36	0.18	-	7.25
Willis	5.49	1.30	0.42	0.17	-	7.38
Upper Goliad	1.14	0.66	0.14	0.07	0.00	2.01
Lower Goliad	0.55	0.63	0.19	0.15	0.02	1.54
Upper Lagarto	0.08	0.38	0.31	0.20	0.04	1.01
Middle Lagarto	0.01	0.28	0.51	0.24	0.01	1.05
Lower Lagarto	0.26	1.94	2.37	1.66	0.15	6.38
Oakville	0.15	0.98	1.41	6.45	1.47	10.45
Catahoula	0.01	0.75	3.00	6.87	0.31	10.94
Total	14.04	8.22	8.71	15.99	2.01	48.97
Galveston County						
Beaumont	0.72	3.48	0.29	0.00	-	4.49
Lissie	1.54	2.17	0.38	0.09	0.03	4.21
Willis	0.23	1.46	1.53	2.42	0.07	5.71
Upper Goliad	0.001	0.01	0.06	0.68	0.54	1.29
Lower Goliad	0.000	0.002	0.01	0.65	0.56	1.22
Upper Lagarto	0.000	0.001	0.002	0.48	0.63	1.11
Middle Lagarto	0.000	0.001	0.03	0.42	0.33	0.77
Lower Lagarto	0.01	0.03	0.05	2.23	3.12	5.45
Oakville	-	0.06	0.20	2.99	3.89	7.14
Catahoula						
Total	2.49	7.22	2.55	9.97	9.16	31.38
Harris County						
Beaumont	0.83	0.90	0.18	-	-	1.91
Lissie	13.66	1.99	0.37	0.05	0.03	16.10
Willis	12.21	2.72	0.34	0.03	-	15.30
Upper Goliad	0.42	0.17	0.14	0.06	0.00	0.78
Lower Goliad	1.80	0.72	0.20	0.25	0.03	3.00
Upper Lagarto	0.67	0.86	0.21	0.18	0.13	2.05
Middle Lagarto	0.32	0.67	0.24	0.20	0.02	1.44
Lower Lagarto	1.51	5.74	2.38	1.51	0.47	11.61
Oakville	0.40	2.45	3.54	5.30	2.12	13.80
Catahoula	0.09	0.60	7.92	14.25	2.15	25.02
Total	31.90	16.82	15.51	21.84	4.95	91.02



Final Report on the Delineation of Fresh, Brackish, and Saline Groundwater Resources Based on Interpretation of Geophysical Logs

Table 5-4 Total aquifer groundwater volume (in millions of acre-feet) by county and salinity class assuming a void fraction based upon specific yield

Formation	Fresh Water	Slightly Saline Water	Moderately Saline Water	Very Saline Water	Brine Water	Total
Brazoria County						
Beaumont	8.14	14.49	0.16	0.08	-	22.87
Lissie	7.99	10.71	3.36	0.29	-	22.35
Willis	5.21	3.77	3.32	6.25	1.14	19.68
Upper Goliad	0.44	0.75	0.63	5.45	3.02	10.29
Lower Goliad	0.16	0.32	0.26	4.94	3.50	9.18
Upper Lagarto	0.10	0.31	0.25	4.04	3.49	8.19
Middle Lagarto	1.03	0.28	0.61	12.94	9.08	23.93
Lower Lagarto	0.96	3.02	2.69	40.78	29.64	77.10
Oakville	2.16	0.90	1.16	65.71	35.93	105.87
Catahoula						
Total	26.19	34.55	12.44	140.48	85.80	299.47
Fort Bend County						
Beaumont	0.86	0.39	-	-	-	1.26
Lissie	7.49	1.37	0.46	0.22	-	9.54
Willis	7.05	1.73	0.60	0.26	-	9.64
Upper Goliad	1.76	1.00	0.23	0.11	0.00	3.10
Lower Goliad	1.13	1.27	0.41	0.37	0.06	3.23
Upper Lagarto	0.22	1.23	1.00	0.60	0.12	3.17
Middle Lagarto	0.03	1.09	2.10	1.07	0.06	4.35
Lower Lagarto	0.85	7.03	8.98	6.42	0.79	24.06
Oakville	0.41	2.51	3.47	15.12	3.87	25.38
Catahoula	0.02	1.49	5.03	13.10	0.84	20.48
Total	19.82	19.11	22.27	37.27	5.74	104.22
Galveston County						
Beaumont	1.20	5.80	0.47	0.01	-	7.48
Lissie	2.61	3.90	0.73	0.20	0.05	7.50
Willis	0.35	2.28	2.44	4.33	0.14	9.55
Upper Goliad	0.002	0.01	0.11	1.52	1.15	2.79
Lower Goliad	0.000	0.004	0.03	1.75	1.49	3.27
Upper Lagarto	0.000	0.003	0.004	1.09	1.38	2.47
Middle Lagarto	0.000	0.001	0.09	1.26	0.95	2.29
Lower Lagarto	0.03	0.09	0.14	5.52	7.71	13.49
Oakville	-	0.50	0.95	7.89	9.21	18.55
Catahoula						
Total	4.19	12.60	4.97	23.57	22.07	67.40
Harris County						
Beaumont	1.25	1.31	0.24	-	-	2.80
Lissie	20.28	3.16	0.60	0.09	0.04	24.18
Willis	18.49	4.47	0.61	0.06	-	23.63
Upper Goliad	0.76	0.34	0.28	0.14	0.001	1.52
Lower Goliad	3.51	1.49	0.45	0.62	0.09	6.17
Upper Lagarto	1.71	2.37	0.59	0.45	0.28	5.40
Middle Lagarto	0.84	1.93	0.75	0.60	0.06	4.18
Lower Lagarto	4.21	16.32	7.23	4.47	1.39	33.60
Oakville	1.00	6.38	8.94	14.16	4.82	35.30
Catahoula	0.26	1.66	17.24	35.64	4.27	59.06
Total	52.30	39.44	36.93	56.22	10.95	195.84



Final Report on the Delineation of Fresh, Brackish, and Saline Groundwater Resources Based on Interpretation of Geophysical Logs

Table 5-5 Aquifer sand groundwater volume (in millions of acre-feet) by Subsidence District and salinity class assuming a void fraction based upon specific yield

Formation	Fresh Water	Slightly Saline Water	Moderately Saline Water	Very Saline Water	Brine Water	Total
Harris-Galveston Subsidence District						
Beaumont	1.55	4.38	0.46	0.00	-	6.40
Lissie	15.20	4.16	0.75	0.15	0.06	20.31
Willis	12.43	4.18	1.87	2.45	0.07	21.00
Upper Goliad	0.42	0.18	0.19	0.75	0.54	2.07
Lower Goliad	1.80	0.72	0.21	0.90	0.59	4.22
Upper Lagarto	0.67	0.86	0.21	0.67	0.76	3.16
Middle Lagarto	0.32	0.67	0.27	0.62	0.35	2.22
Lower Lagarto	1.52	5.77	2.43	3.75	3.59	17.06
Oakville	0.40	2.52	3.74	8.28	6.00	20.94
Catahoula	0.09	0.60	7.92	14.25	2.15	25.02
Total	34.39	24.04	18.06	31.81	14.11	122.41
Fort Bend Subsidence District						
Beaumont	0.68	0.29	-	-	-	0.96
Lissie	5.68	1.03	0.36	0.18	-	7.25
Willis	5.49	1.30	0.42	0.17	-	7.38
Upper Goliad	1.14	0.66	0.14	0.07	0.00	2.01
Lower Goliad	0.55	0.63	0.19	0.15	0.02	1.54
Upper Lagarto	0.08	0.38	0.31	0.20	0.04	1.01
Middle Lagarto	0.01	0.28	0.51	0.24	0.01	1.05
Lower Lagarto	0.26	1.94	2.37	1.66	0.15	6.38
Oakville	0.15	0.98	1.41	6.45	1.47	10.45
Catahoula	0.01	0.75	3.00	6.87	0.31	10.94
Total	14.04	8.22	8.71	15.99	2.01	48.97



Final Report on the Delineation of Fresh, Brackish, and Saline Groundwater Resources Based on Interpretation of Geophysical Logs

Table 5-6 Total aquifer groundwater volume (in millions of acre-feet) by Subsidence District and salinity class assuming a void fraction based upon specific yield

Formation	Fresh Water	Slightly Saline Water	Moderately Saline Water	Very Saline Water	Brine Water	Total
Harris-Galveston Subsidence District						
Beaumont	2.44	7.11	0.71	0.01	-	10.28
Lissie	22.88	7.06	1.34	0.29	0.10	31.68
Willis	18.85	6.75	3.05	4.39	0.14	33.18
Upper Goliad	0.76	0.35	0.39	1.66	1.15	4.31
Lower Goliad	3.51	1.49	0.48	2.38	1.58	9.44
Upper Lagarto	1.71	2.38	0.60	1.54	1.66	7.88
Middle Lagarto	0.84	1.94	0.84	1.85	1.01	6.47
Lower Lagarto	4.23	16.41	7.37	9.99	9.10	47.09
Oakville	1.00	6.88	9.89	22.05	14.03	53.85
Catahoula	0.26	1.66	17.24	35.64	4.27	59.06
Total	56.49	52.04	41.90	79.79	33.02	263.24
Fort Bend Subsidence District						
Beaumont	0.86	0.39	-	-	-	1.26
Lissie	7.49	1.37	0.46	0.22	-	9.54
Willis	7.05	1.73	0.60	0.26	-	9.64
Upper Goliad	1.76	1.00	0.23	0.11	0.00	3.10
Lower Goliad	1.13	1.27	0.41	0.37	0.06	3.23
Upper Lagarto	0.22	1.23	1.00	0.60	0.12	3.17
Middle Lagarto	0.03	1.09	2.10	1.07	0.06	4.35
Lower Lagarto	0.85	7.03	8.98	6.42	0.79	24.06
Oakville	0.41	2.51	3.47	15.12	3.87	25.38
Catahoula	0.02	1.49	5.03	13.10	0.84	20.48
Total	19.82	19.11	22.27	37.27	5.74	104.22



Final Report on the Delineation of Fresh, Brackish, and Saline Groundwater Resources Based on Interpretation of Geophysical Logs

Table 5-7 Aquifer sand groundwater volume (in millions of acre-feet) by county and salinity class assuming a void fraction based upon porosity

Formation	Fresh Water	Slightly Saline Water	Moderately Saline Water	Very Saline Water	Brine Water	Total
Brazoria County						
Beaumont	35.24	58.47	0.63	0.30	-	94.63
Lissie	36.32	45.05	13.54	1.16	-	96.07
Willis	26.22	18.04	14.93	26.16	4.05	89.41
Upper Goliad	8.94	15.24	12.64	92.67	47.58	177.07
Lower Goliad	2.45	4.96	3.35	60.08	41.00	111.85
Upper Lagarto	1.30	4.24	2.94	52.32	49.68	110.48
Middle Lagarto	2.38	1.78	3.14	47.96	36.55	91.81
Lower Lagarto	2.03	6.56	3.60	58.23	43.00	113.42
Oakville	3.60	1.86	1.81	119.26	69.42	195.94
Catahoula						
Total	118.48	156.20	56.57	458.13	291.29	1080.68
Fort Bend County						
Beaumont	4.94	2.08	-	-	-	7.03
Lissie	40.92	7.45	2.58	1.26	-	52.21
Willis	31.90	7.31	2.02	0.79	-	42.02
Upper Goliad	40.14	22.99	4.90	2.29	0.06	70.37
Lower Goliad	18.77	21.43	6.44	5.00	0.83	52.47
Upper Lagarto	2.66	12.67	10.28	6.61	1.39	33.61
Middle Lagarto	0.40	9.45	16.36	4.88	0.15	31.25
Lower Lagarto	1.64	11.92	14.80	9.08	0.72	38.17
Oakville	0.81	6.32	8.74	35.61	7.23	58.71
Catahoula	0.05	4.34	18.49	40.67	1.86	65.42
Total	142.23	105.97	84.61	106.21	12.24	451.26
Galveston County						
Beaumont	5.23	25.31	2.07	0.03	-	32.64
Lissie	10.93	15.44	2.72	0.67	0.21	29.97
Willis	1.58	10.06	10.65	16.87	0.52	39.68
Upper Goliad	0.03	0.22	1.98	23.09	18.09	43.41
Lower Goliad	0.004	0.05	0.36	20.93	18.11	39.45
Upper Lagarto	0.002	0.04	0.05	14.96	19.56	34.61
Middle Lagarto	0.004	0.02	1.05	14.45	10.87	26.40
Lower Lagarto	0.05	0.19	0.33	13.54	18.86	32.97
Oakville	-	0.36	1.13	17.30	22.77	41.56
Catahoula						
Total	17.82	51.69	20.35	121.85	108.98	320.69
Harris County						
Beaumont	6.08	6.55	1.30	-	-	13.93
Lissie	98.12	14.10	2.65	0.37	0.19	115.43
Willis	76.62	17.01	2.14	0.20	-	95.97
Upper Goliad	14.44	5.80	4.63	2.16	0.02	27.05
Lower Goliad	62.44	24.90	6.63	8.36	1.12	103.44
Upper Lagarto	22.58	29.14	7.00	5.98	4.12	68.81
Middle Lagarto	16.71	34.73	11.75	8.39	0.86	72.44
Lower Lagarto	10.17	38.49	15.88	9.79	3.00	77.33
Oakville	2.62	16.20	23.41	34.53	13.28	90.04
Catahoula	0.59	3.86	51.05	91.20	13.69	160.40
Total	310.38	190.77	126.43	160.98	36.28	824.83



Final Report on the Delineation of Fresh, Brackish, and Saline Groundwater Resources Based on Interpretation of Geophysical Logs

Table 5-8 Total aquifer groundwater volume (in millions of acre-feet) by county and salinity class assuming a void fraction based upon porosity

Formation	Fresh Water	Slightly Saline Water	Moderately Saline Water	Very Saline Water	Brine Water	Total
Brazoria County						
Beaumont	59.21	105.25	1.16	0.57	-	166.20
Lissie	57.27	76.50	23.93	2.03	-	159.73
Willis	36.69	26.42	23.31	43.75	7.97	138.13
Upper Goliad	15.16	26.01	21.70	184.52	101.44	348.82
Lower Goliad	5.40	10.80	8.60	160.41	112.78	298.00
Upper Lagarto	3.27	9.78	8.01	126.01	107.57	254.64
Middle Lagarto	10.41	7.34	12.68	138.28	79.16	247.87
Lower Lagarto	5.35	17.80	13.12	191.01	123.34	350.63
Oakville	8.86	4.65	5.11	270.63	153.74	442.99
Catahoula						
Total	201.62	284.54	117.63	1117.21	686.00	2407.01
Fort Bend County						
Beaumont	6.31	2.87	-	-	-	9.17
Lissie	53.97	9.94	3.27	1.54	-	68.72
Willis	40.85	9.70	2.88	1.22	-	54.64
Upper Goliad	61.73	35.19	7.93	3.76	0.09	108.69
Lower Goliad	38.77	43.29	13.89	12.21	2.14	110.30
Upper Lagarto	7.56	40.94	33.19	19.64	3.80	105.12
Middle Lagarto	1.33	33.16	61.74	20.67	0.69	117.58
Lower Lagarto	5.34	43.31	55.82	34.93	3.67	143.06
Oakville	2.27	16.12	21.32	83.06	18.82	141.61
Catahoula	0.11	8.53	30.88	77.78	5.17	122.47
Total	218.23	243.04	230.91	254.80	34.38	981.37
Galveston County						
Beaumont	8.71	42.16	3.43	0.05	-	54.36
Lissie	18.56	27.78	5.21	1.44	0.37	53.37
Willis	2.46	15.76	17.01	30.21	1.00	66.44
Upper Goliad	0.05	0.39	3.80	51.19	38.53	93.96
Lower Goliad	0.01	0.13	0.96	56.80	48.21	106.12
Upper Lagarto	0.005	0.09	0.11	33.77	42.93	76.89
Middle Lagarto	0.01	0.05	3.37	43.37	31.81	78.61
Lower Lagarto	0.15	0.55	0.85	33.45	46.58	81.57
Oakville	-	2.81	5.38	45.66	53.87	107.71
Catahoula						
Total	29.96	89.72	40.13	295.93	263.30	719.03
Harris County						
Beaumont	9.10	9.56	1.75	-	-	20.41
Lissie	145.46	22.31	4.33	0.65	0.31	173.06
Willis	116.34	27.94	3.82	0.35	-	148.46
Upper Goliad	26.52	11.69	9.44	4.89	0.04	52.56
Lower Goliad	121.69	51.28	15.30	20.79	2.96	212.02
Upper Lagarto	57.52	80.19	19.94	14.69	8.86	181.22
Middle Lagarto	44.04	100.23	36.04	25.26	2.48	208.05
Lower Lagarto	28.33	109.33	48.19	28.95	8.85	223.64
Oakville	6.55	42.13	59.05	92.25	30.37	230.35
Catahoula	1.63	10.75	111.25	228.39	27.19	379.21
Total	557.17	465.40	309.11	416.24	81.05	1828.98



Final Report on the Delineation of Fresh, Brackish, and Saline Groundwater Resources Based on Interpretation of Geophysical Logs

Table 5-9 Aquifer sand groundwater volume (in millions of acre-feet) by Subsidence District and salinity class assuming a void fraction based upon porosity

Formation	Fresh Water	Slightly Saline Water	Moderately Saline Water	Very Saline Water	Brine Water	Total
Fort Bend Subsidence District						
Beaumont	4.94	2.08	-	-	-	7.03
Lissie	40.92	7.45	2.58	1.26	-	52.21
Willis	31.90	7.31	2.02	0.79	-	42.02
Upper Goliad	40.14	22.99	4.90	2.29	0.06	70.37
Lower Goliad	18.77	21.43	6.44	5.00	0.83	52.47
Upper Lagarto	2.66	12.67	10.28	6.61	1.39	33.61
Middle Lagarto	0.40	9.45	16.36	4.88	0.15	31.25
Lower Lagarto	1.64	11.92	14.80	9.08	0.72	38.17
Oakville	0.81	6.32	8.74	35.61	7.23	58.71
Catahoula	0.05	4.34	18.49	40.67	1.86	65.42
Total	142.23	105.97	84.61	106.21	12.24	451.26
Harris-Galveston Subsidence District						
Beaumont	11.31	31.85	3.37	0.03	-	46.56
Lissie	109.05	29.53	5.37	1.03	0.41	145.40
Willis	78.20	27.07	12.79	17.07	0.52	135.65
Upper Goliad	14.47	6.02	6.62	25.25	18.11	70.46
Lower Goliad	62.45	24.95	6.98	29.29	19.23	142.90
Upper Lagarto	22.58	29.18	7.05	20.94	23.68	103.42
Middle Lagarto	16.72	34.75	12.80	22.84	11.73	98.84
Lower Lagarto	10.22	38.68	16.21	23.34	21.85	110.30
Oakville	2.62	16.56	24.54	51.83	36.04	131.60
Catahoula	0.59	3.86	51.05	91.20	13.69	160.40
Total	328.20	242.46	146.78	282.83	145.26	1145.53



Final Report on the Delineation of Fresh, Brackish, and Saline Groundwater Resources Based on Interpretation of Geophysical Logs

Table 5-10 Total aquifer groundwater volume (in millions of acre-feet) by Subsidence District and salinity class assuming a void fraction based upon porosity

Formation	Fresh Water	Slightly Saline Water	Moderately Saline Water	Very Saline Water	Brine Water	Total
Fort Bend Subsidence District						
Beaumont	6.31	2.87	-	-	-	9.17
Lissie	53.97	9.94	3.27	1.54	-	68.72
Willis	40.85	9.70	2.88	1.22	-	54.64
Upper Goliad	61.73	35.19	7.93	3.76	0.09	108.69
Lower Goliad	38.77	43.29	13.89	12.21	2.14	110.30
Upper Lagarto	7.56	40.94	33.19	19.64	3.80	105.12
Middle Lagarto	1.33	33.16	61.74	20.67	0.69	117.58
Lower Lagarto	5.34	43.31	55.82	34.93	3.67	143.06
Oakville	2.27	16.12	21.32	83.06	18.82	141.61
Catahoula	0.11	8.53	30.88	77.78	5.17	122.47
Total	218.23	243.04	230.91	254.80	34.38	981.37
Harris-Galveston Subsidence District						
Beaumont	17.82	51.72	5.18	0.05	-	74.77
Lissie	164.01	50.09	9.55	2.09	0.68	226.43
Willis	118.80	43.70	20.84	30.56	1.00	214.89
Upper Goliad	26.57	12.08	13.24	56.08	38.57	146.53
Lower Goliad	121.70	51.42	16.26	77.59	51.17	318.14
Upper Lagarto	57.53	80.28	20.06	48.46	51.79	258.11
Middle Lagarto	44.05	100.27	39.41	68.64	34.29	286.66
Lower Lagarto	28.48	109.87	49.04	62.40	55.42	305.21
Oakville	6.55	44.93	64.43	137.91	84.24	338.06
Catahoula	1.63	10.75	111.25	228.39	27.19	379.21
Total	587.13	555.12	349.24	712.17	344.35	2548.01

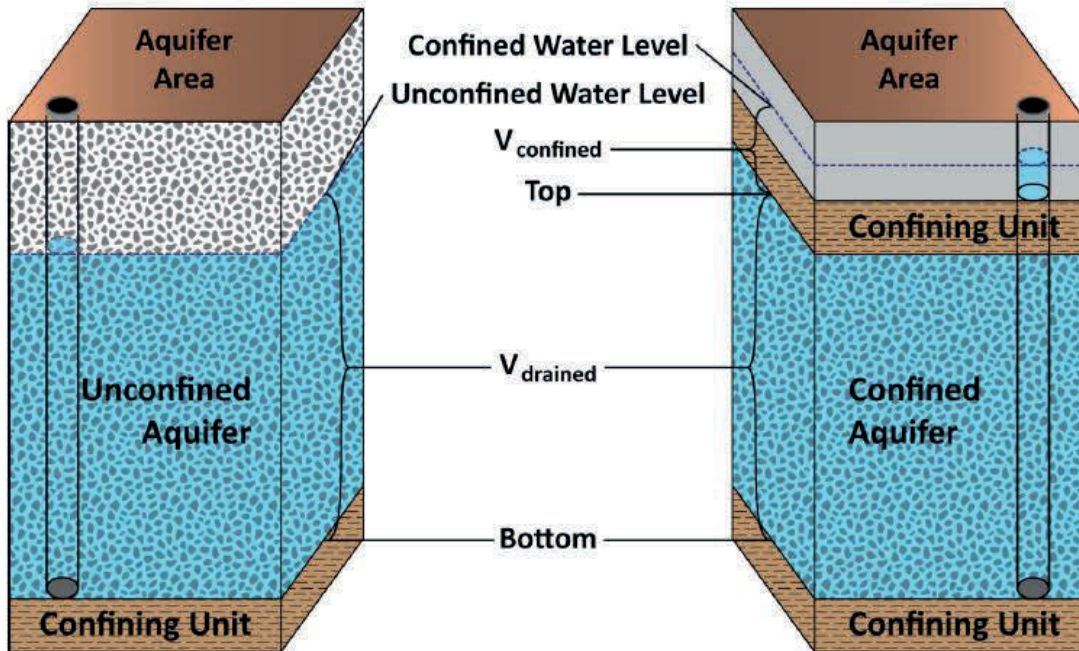


Figure 5-1 Schematic graph showing the difference between unconfined and confined aquifers (from Jigmond and Wade, 2013)

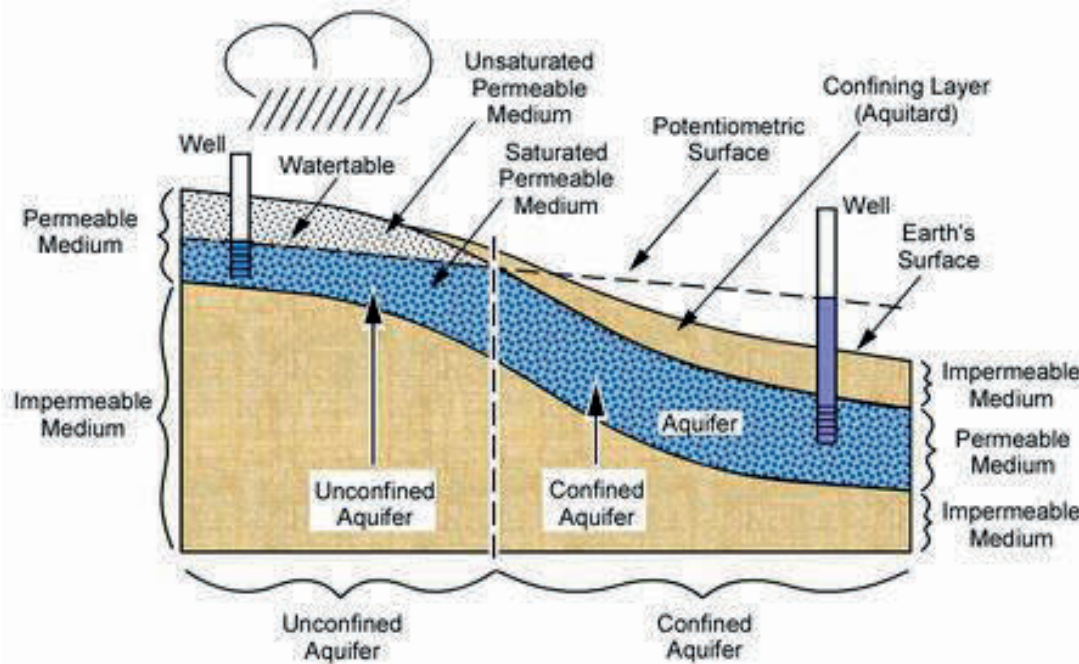


Figure 5-2 Schematic of aquifer transitioning from unconfined in outcrop region, where recharge from precipitation occurs, to confined conditions in the down dip regions of the aquifer (from http://www.geo.brown.edu/research/Hydrology/ge58_IntrodHydrology/ge58_index.htm)



6.0 STUDY SUMMARY

This report documents both the lithology and groundwater quality within the Gulf Coast Aquifer System within the Harris-Galveston and Fort Bend Subsidence Districts at a high resolution based on the analysis of geophysical logs. This study provides the framework dataset and understanding for the further study of brackish and saline groundwater resources within the Districts and provides the key lithologic and TDS data to perform a risk assessment for brackish groundwater production in the Jasper Aquifer. In addition, because of the detailed lithologic model that has been developed, this study provides the framework for future subsidence studies, including further subsidence model development and application and study of the subsidence potential for aquifer storage and recovery.

This study builds upon and uses methods consistent with those most recently applied in the TWDB Gulf Coast Aquifer System Brackish Production Zone Study performed in response to House Bill 30 (Young and others, 2016). Hundreds of geophysical logs were collected and used to interpret aquifer lithology, stratigraphy and water quality (TDS). **Table 6-1** provides a summary of the number of geophysical logs used to estimate lithology and water quality, and to update stratigraphy within the study area and within Brazoria, Fort Bend, Galveston and Harris counties (four counties completely within the study area). Because of log control and the vertical interval available for each log, the number of logs used to characterize water salinity is different for each salinity class with the maximum number for fresh groundwater classification and a minimum for the very saline groundwater classification.

The data derived from the analysis of the geophysical logs are presented in several ways to better interpret and delineate both aquifer stratigraphy, lithology and water quality, expressed as TDS, within the Gulf Coast Aquifer System. A summary of the information developed is provided below.

6.1 Aquifer Stratigraphy and Depositional Character

Nine stratigraphic cross sections were developed to improve the understanding of aquifer stratigraphy and depositional character within the study area. Six dip-oriented cross sections (D-5 through D-10) and three strike-oriented cross sections (S-1 through S-3) were developed in the study area. Each stratigraphic section includes water quality classification boundaries, aquifer formations, aquifer lithology and interpretation of the nature of sandstone and marine shale and mudstone sequences. Each cross section is annotated to show the following:

- Aquifer stratigraphy;
- Thick correlated marine shale wedges;
- Thick correlated sand sequences “fairways” consisting of productive sands;
- Potential confining units consisting of mudstones;
- Base of water salinity zones;
- Location of geo-pressured areas and probable fault zones.

The stratigraphy of the formations comprising the Gulf Coast Aquifer System was based upon the framework of Young and others (2012). In addition, this study added an additional 209 geophysical logs that were used to make local adjustments in the stratigraphy of the Gulf Coast Aquifer System in the study area. These stratigraphic picks are documented in Appendix A (Table A.3) and are shown on the cross sections presented in Appendix D.

The stratigraphic cross sections provide a basis from which to understand the distribution of major sand and clay rich sequences in relation to aquifer stratigraphy and water quality boundaries. They offer valuable information



Final Report on the Delineation of Fresh, Brackish, and Saline Groundwater Resources Based on Interpretation of Geophysical Logs

to be used by the Harris-Galveston and Fort Bend Subsidence Districts in their review of potential brackish groundwater permit applications.

Table 6-1 Summary of the number and location of geophysical logs used to determine lithology, water quality and to update stratigraphic picks

	Study Area*	County			
		Brazoria	Fort Bend	Galveston	Harris
Digitized Logs with Sand Picks	294	37	48	24	77
TWDB Study (Young and others, 2016)	125	17	16	9	24
This Study	169	20	32	15	53
Logs with Water Quality Picks	299	38	48	24	81
Fresh Water	228	24	36	16	68
Slight Saline	220	27	31	23	66
Moderately Saline	198	29	32	24	52
Very Saline	87	21	9	21	11
Logs with Updated Stratigraphy Picks	209	33	25	12	24
Beaumont	115	31	18	12	12
Lissie	159	33	25	12	21
Willis	187	33	25	12	22
Upper Goliad	161	33	25	12	16
Lower Goliad	176	33	25	12	22
Upper Lagarto	163	33	23	12	20
Middle Lagarto	173	33	25	12	24
Lower Lagarto	126	29	24	11	22
Oakville	161	27	25	10	24
Catahoula	129	13	22	2	24

*Study Area does not apply to the Updated Stratigraphy Picks

6.2 Aquifer Lithology

Aquifer lithology was analyzed for all digital logs collected for this study. The lithologic character of the formations comprising the Gulf Coast Aquifer System were presented and discussed by using maps as well as cross sections. Maps were developed for sand and clay percent, total sand and total clay thickness and maximum sand and maximum clay interval thickness for the formations comprising the Gulf Coast Aquifer System and for the Chicot, Evangeline and Jasper aquifers.



Final Report on the Delineation of Fresh, Brackish, and Saline Groundwater Resources Based on Interpretation of Geophysical Logs

The average sand percent for the Chicot, Evangeline and Jasper aquifers in the study area are 68, 46 and 40%, respectively. By comparison, the Burkeville Confining Unit has an average sand percent of 42% in the study area. The sand content of an aquifer correlates to aquifer transmissivity or productivity of the aquifer. The average clay percent for the Chicot, Evangeline and Jasper aquifers in the study area are 32, 54 and 60%, respectively. By comparison, the Burkeville Confining Unit has an average clay percent of 58% in the study area. The clay content of an aquifer is of direct importance to the compaction potential of an aquifer with the highest clay content having the highest potential for compaction. The clay data collected and presented in this report is an essential input to the Jasper Aquifer subsidence risk assessment.

The lithology of the aquifers and formations was also represented in the same nine cross sections described above in separate figures presented in Section 4 of this report. The formation boundaries used to calculate lithology statistics and to estimate groundwater in storage (shown on the cross sections in Section 4) are based on the TWDB formation boundaries within the Gulf Coast Aquifer System (Young and others, 2012).

6.3 Aquifer Water Quality

Groundwater TDS in mg/L was determined for 299 geophysical logs in the study area. The TDS was estimated for sand beds 10 feet or greater. For each TDS estimate for a sand unit, it was assigned a salinity classification consistent with Table 4-1. For the nine cross sections described above and five more working cross sections not included in the report, geophysical signature, calculated salinity classification for sand beds and aquifer stratigraphic boundaries were defined. The color-coding of the geophysical logs by salinity class provides a graphical method for assessing the general groundwater quality trends in the subsurface. As should be expected, the patterns and layering of the different salinity zones are more consistent along strike than along dip. The salinity zone cross sections effectively illustrate the thickening of the freshwater (less than 1,000 mg/L TDS) between the up-dip outcrop areas and the coastline. Impacts of salt domes and faults also can be observed in the water quality cross sections.

Maps were developed to represent the depth to the base of fresh, slightly saline, moderately saline, and very saline groundwater by interpolating the manually-selected salinity picks on the geophysical logs on the fourteen cross sections developed. Experience has shown that salinity boundaries must be manually developed through inspection of cross sections because of the vertical variability of TDS observed. The depth to base of salinity class maps are considered representative of regional to sub-regional trends at the scale of a few miles to tens of miles. The base of fresh water is the deepest in the middle of the study area in a zone that parallels aquifer strike. The fresh-water boundary can reach depths of over 2,000 feet in the deepest portions. The fresh water boundary becomes shallower as you approach the coastline with depths varying from 0 to 500 feet. Fault zones appear to influence the depth to the slightly, moderately and very saline boundaries in a trend that strengthens as the salinity increases which generally correlates with depth. At a local scale, salt domes have a significant impact on groundwater quality.

Thickness of brackish groundwater zone (greater than 1,000 mg/L and less than 10,000 mg/L TDS) maps were developed for the Chicot, Evangeline and Jasper aquifers. For the Chicot Aquifer, the brackish zone is thickest near the coastline with an average thickness of 1,000 feet. The Chicot Aquifer brackish zone pinches out approximately 50 miles from the coastline. The thickest regions of the Evangeline Aquifer brackish zone are in southern Fort Bend and Harris counties, with an average thickness of 1,300 feet. Brackish groundwater occurs in most of the Jasper Aquifer across most of Harris and Fort Bend counties, with the thickest brackish zone in Fort Bend County averaging 1,200 feet thick.



6.4 Groundwater Volume by Salinity Class

Using methods consistent with the Gulf Coast Aquifer House Bill 30 Study documented in Young and others (2016) and consistent with methods used to estimate aquifer storage by the TWDB (Wade and others, 2014), estimates of groundwater volumes have been developed for the five salinity classes defined in Table 4-1. Groundwater volumes were calculated by formation for Brazoria, Fort Bend, Galveston, and Harris counties. Volumes were estimated for the entire aquifer volume and for only the sand portions of the aquifers. Both specific yield and aquifer porosity determined in this study were used as the aquifer void volume. INTERA believes using porosity provides the best estimate of groundwater in storage as compared to specific yield. However, estimates of groundwater in storage have been reported using both porosity and specific yield to be consistent with the TWDB House Bill 30 study for the region.

Table 6-2 provides an estimate of fresh and brackish groundwater volume estimated to be in sands in the Harris-Galveston and Fort Bend Subsidence Districts. It is estimated that there is 18 and 34% more brackish groundwater than fresh groundwater in storage in Harris-Galveston and Fort Bend Subsidence Districts, respectively.

Table 6-2 Estimated fresh and brackish groundwater in storage in sands (millions of acre-feet) in the Harris-Galveston and Fort Bend Subsidence Districts

Subsidence District	Fresh Water	Brackish Water
Million Acre-Feet of Groundwater in Storage in Sands		
Harris-Galveston	328.2	389.24
Fort Bend	142.23	190.58

Groundwater volumes estimated in this study do not reflect the amount of groundwater that could be produced from each of these aquifers. Volume calculations do not consider physical aquifer limitations inherent in well hydraulics, economics or environmental impacts such as subsidence. These groundwater volume estimates do provide an understanding of how brackish and saline groundwater resources are distributed within the aquifers and formations within the study area.

Combined with the lithologic data derived in this study, the Harris-Galveston and Fort Bend Subsidence Districts can use the data developed in this study to improve their understanding of brackish and saline groundwater resources and to estimate the potential impacts of development with regards to subsidence. This study is foundational to support future studies of the aquifers in the Districts and to support future decision-making and regulatory plan updates.



7.0 REFERENCES

- Alger, R.P. 1966. Interpretation of electric logs in fresh water wells in unconsolidated formations, paper CC, *in* 7th Annual Symposium Transactions: Society of Professional Well Log Analysts, 25 p.
- Arps, J.J. 1953. "The effect of temperature on the density and electrical resistivity of sodium chloride solutions," *Petroleum Transactions, AIME*, 1953.
- Ayers, W.B., and A. Lewis. 1985. *The Wilcox Group and Carrizo Sand (Palogene) in East Central Texas: Depositional Systems and Deep-Basin Lignite*: The University of Texas at Austin, Bureau of Economic Geology.
- Baker, E.T., Jr. 1979. Stratigraphic and hydrogeologic framework of part of the coastal plain of Texas: Texas Department of Water Resources Report 236, 43 p.
- Bourgeois, F.M. 1997. *Elemental and Stable Isotope Study to Determine the Source of Salt-Water Contamination in the Chicot Aquifer of the Gulf Coast Aquifer System*: University of Houston, Houston, Texas, Master's Thesis, 313 p.
- Bruno, R.S., and J.S. Hanor. 2003. Large-scale fluid migration driven by salt dissolution, Bay Marchand dome, offshore Louisiana. *Gulf Coast of Geological Societies Transactions*, v. 53, p. 97-107.
- Bryant, W.R., J. Lugo, C. Cordova, and A. Salvador. 1991. Physiography and bathymetry: *in* Salvador, A., ed., *The geology of North America: the Gulf of Mexico basin*, vol. J: Boulder, Colorado, Geological Society of America, p. 13–30.
- Chowdhury, A., S. Wade, R.E. Mace, and C. Ridgeway. 2004. *Groundwater Availability of the Central Gulf Coast Aquifer System: Numerical Simulations through 1999*: Texas Water Development Board, unpublished report.
- Chowdhury, A.H., and M.J. Turco. 2006. *Geology of the Gulf Coast Aquifer System, Texas*, *in* R.E. Mace and others, eds., *Aquifers of the Gulf Coast of Texas*: Texas Water Development Board Report 365, p. 23–50.
- Crans, W., G. Mandl, and J. Haremboure. 1980. On the theory of growth faulting—A geochemical delta model based on gravity sliding: *Journal of Petroleum Geology*, 2, p. 265–307.
- Driscoll, F.G. 1986. *Groundwater and Wells*: St. Paul, MN, Johnson Filtration Systems, Inc., 1079 p.
- Durham C.O., Jr. 1971. *A study of the Scotlandville-Denham Springs faults and their effect on school sites*. East Baton Rouge Parish, Louisiana: Etco Engineers and Associates Report.
- Estep, J. 1998. *Evaluation of ground-water quality using geophysical logs*: Texas Natural Resource Conservation Commission, unpublished Report, 516 p.
- Ewing, T.E. 1990. *Tectonic map of Texas*: University of Texas at Austin, Bureau of Economic Geology, scale 1:750,000, 4 sheets.
- Fogg, G.E. 1980. *Geochemistry of ground water in the Wilcox aquifer*, *in* Kreitler, C.W., Agagu, O.K., Basciano, J.M., Collins, E.W., Dix, O., Dutton, S.P., Fogg, G.E., Giles, A.B., Guevara, E.H., Harris, D.W., Hobday, D.K., McGowen, M.K., Pass, D. and Wood, D.H., 1979, *Geology and Geohydrology of the East Texas Basin A Report on the Progress of Nuclear Waste Isolation Feasibility Studies*: The University of Texas at Austin, Bureau of Economic Geology (1979), *Geologic Circular No. 80-12*, p. 73-78.
- Fogg, G.E., and C.W. Kreitler. 1982. *Ground-water hydraulics and hydrochemical facies in Eocene aquifers of the East Texas Basin*. The University of Texas at Austin, Bureau of Economic Geology, *Report of Investigations No. 127*, 75 p.



Final Report on the Delineation of Fresh, Brackish, and Saline Groundwater Resources Based on Interpretation of Geophysical Logs

- Fogg, G.E., and P.E. Blanchard. 1986. Empirical relations between Wilcox groundwater quality and electric log resistivity, Sabine Uplift area, *in* Kaiser, W.R. ed., *Geology and Groundwater hydrology of deep-basin lignite in the Wilcox Group of East Texas*: The University of Texas at Austin, Bureau of Economic Geology, Special Report No. 10, p. 115-118.
- Galloway, W.E. 2005. Gulf of Mexico Basin depositional record of Cenozoic North American drainage basin evolution: *International Association Sedimentologists Special Publication 35*, p. 409–423
- Galloway, W.E., 1989, Genetic stratigraphic sequences in basin analysis II: application to northeast Gulf of Mexico Cenozoic basin: *American Association of Petroleum Geologists Bulletin*, v. 73, p. 143–154.
- Galloway, W.E., P.E. Ganey-Curry, X. Li, and R.T. Buffler. 2000. Cenozoic depositional history of the Gulf of Mexico basin: *American Association of Petroleum Geologists Bulletin*, V. 84, p. 1743–1774.
- George, P.G., R.E. Mace, and R. Petrossian. 2011. *Aquifers of Texas*: Texas Water Development Board, Report 380.
- Hamlin and L. de la Rocha. 2015. Using electric logs to estimate groundwater salinity and map brackish groundwater resources in the Carrizo-Wilcox Aquifer in South Texas: *GCAGS Journal v.4 (2015)*, p. 109-131.
- Hamlin, H.S., D.A. Smith, and M.S. Akhter. 1988. Hydrogeology of Barbers Hill salt dome, Texas coastal plain: The University of Texas at Austin, Bureau of Economic Geology, Report of Investigations No. 176, 41 p.
- Hamlin, S., B.R. Scanlon, R. Reedy, S. Young, and M. Jigmond, M. 2016. Fresh, Brackish, and Saline Groundwater Resources in the Carrizo-Wilcox Aquifer in Groundwater Management Area 13 -- Location, Quantification, Producibility, and Impacts, draft report to the Texas Water Development Board, TWDB, Austin, Texas
- Jones, P.H., and T.B. Buford. 1951. Electric logging applied to ground-water exploration: *Geophysics*, V. 16, no. 1, p. 115–139.
- Kasmarek, M.C. 2013. Hydrogeology and Simulation of Groundwater Flow and Land-Surface Subsidence in the Northern Part of the Gulf Coast Aquifer System, Texas, 1891—2009. Prepared in cooperation with the Harris-Galveston Subsidence District, the Fort Bend Subsidence District, and the Lone Star Groundwater Conservation District: U.S. Department of the Interior, U.S. Geological Survey Scientific Investigations Report 2012-5154, Version 1.1, December 2013.
- Knox P.R., V.A. Kelley, A. Vreugdenhil, N. Deeds, and S. Seni. 2007. Structure of the Yegua-Jackson Aquifer of the Texas Gulf Coastal Plain: Texas Water Development Board.
- Knox, P.R., S.C. Young, W.E. Galloway, E.T. Baker Jr., and T. Budge. 2006. A stratigraphic approach to Chicot and Evangeline Aquifer boundaries, Central Texas Gulf Coast, *Gulf Coast Association of Geological Societies: Transactions Volume*.
- Kreitler, C.W., E. Guevera, G. Granata, and D. McKalips. 1977. Hydrogeology of Gulf Coast aquifers, Houston-Galveston area, Texas: *Gulf Coast Association of Geological Societies Transactions*, vol. 27, p. 72–89.
- Lindsay, S.V. 2009. Sources of saline water in the Chicot and Evangeline aquifers of Brazoria, Fort Bend, and Wharton counties using multielement hydrochemical analyses: Master's thesis, University of Houston, 107 p.
- Loucks, R.G., M.M. Dodge, and W.E. Galloway. 1984. Regional controls on diagenesis and reservoir quality in lower Tertiary sandstones along the Texas Gulf Coast, *in* *Clastic Diagenesis*, eds McDonald, D.A., and Surdam, R.C.: *American Association of Petroleum Geologists Memoir 37*.
- Meyer, J., A. Croskrey, M. Wise, and S. Kalaswad. 2014. Brackish Groundwater in the Gulf Coast Aquifer, Lower Rio Grande Valley, Texas. Texas Water Development Board, Austin, TX, Report 383.



Final Report on the Delineation of Fresh, Brackish, and Saline
Groundwater Resources Based on Interpretation of Geophysical Logs

- Meyer, J.E. 2012. Geologic characterization of and data collection in the Corpus Christi Aquifer Storage and Recovery Conservation District and surrounding counties: Texas Water Development Board, Austin, TX, Open File Report 12-01.
- Meyer, J.E. and M.R. Wise, 2012. Pecos Valley Aquifer, West Texas: Structure and Brackish Groundwater, Texas Water Development Board, Austin, TX, Report 382.
- Roland, H.L., T.F. Hill, C.O. Autin, P. Durham Jr., and C.G. Smith. 1981. The Baton Rouge and Denham Springs-Scotlandville faults: A report prepared for the Louisiana Department of Natural Resources by the Louisiana Geological Survey and Durham Geological Associates Consultants, Baton Rouge.
- Schlumberger. 2009. Log interpretation Charts, Schlumberger, Houston, Texas.
- Seni, S.J., and M.P.A. Jackson. 1984. Sedimentary record of Cretaceous and Tertiary salt movement, East Texas basin-Times, rates, and volume of salt flow and their implications for nuclear waste isolation and petroleum exploration: The University of Texas at Austin, Bureau of Economic Geology Report of Investigations No. 139, 89 p.
- Stanton, J.S., D.W. Anning, C.J. Brown, R.B. Moore, V.L. McGuire, S.L. Qi, A.C. Harris, K.F. Dennehy, P.B. McMahon, J.R. Degnan, and J.K. Bohlke. 2017. Brackish groundwater in the United States: U.S. Geological Survey Professional Paper 1833, 185p., <https://doi.org/10.3133/pp1833>
- Strom E.W., N.A. Houston, and C.A. Garcia. 2003. "Selected hydrogeologic datasets for the Jasper aquifer, Texas," USGS Open-File Report 03-299, 1 CD-ROM.
- Texas Natural Resources Information System. 2007. Data search/download, Geologic Atlas of Texas, <https://tnris.org/data-catalog/entry/geologic-atlas-of-texas>)
- Turcan, A.N., Jr. 1962. Estimating water quality from electrical logs: U.S. Geological Survey Professional Paper 450-C, p. 135-136.
- Turco, M., 2015a. Science and Research Plan; Fort Bend Subsidence District, Richmond, TX
- Turco, M., 2015b. Science and Research Plan; Harris-Galveston Subsidence District, Harris-Galveston Subsidence District, Houston, TX.
- Verbeek, E.R. 1979. Surface faults in the Gulf Coastal Plain between Victoria and Beaumont, Texas: *Tectonophysics*, v. 52, p. 373–375.
- Wade, S., and R. Anaya. 2014. GAM task 13-038: Total estimated recoverable storage for aquifers in Groundwater Management Area 15, Texas Water Development Board.
- Wade, S., D. Thorkildsen, and R. Anaya. 2014. GAM task 13-037: Total estimated recoverable storage for aquifers in Groundwater Management Area 14.
- Wallace, R.H., T. F. Kraemeer, R.E. Taylor, and J.B. Wesselman. 1972. Assessment of geopressed-geothermal resources in the Northern Gulf of Mexico Basin,
- Wesselman, J.B. 1971. Ground-water resources of Chambers and Jefferson counties, Texas. Texas Water Development Board, Report 133.
- Wesselman, J.B. 1972. Ground-water resources of Fort Bend County, Texas. Texas Water Development Board, Report 155.
- Williamson, A.K., and H.F. Grubb. 2001. Groundwater flow in the Gulf Coast Aquifer Systems, South-Central United States, Regional Aquifer System Analyses – Gulf Coast Plains: U.S. Geological Survey Professional Paper 1416-F.



Final Report on the Delineation of Fresh, Brackish, and Saline
Groundwater Resources Based on Interpretation of Geophysical Logs

- Winker, C.D., and M.B. Edwards. 1983. Unstable progradational clastic shelf margins, *in* Stanley, D.J., and Moore, G.T., eds, *The shelfbreak; Critical interface on continental margins*: SEPM Special Publication 33, p. 139-157.
- Winslow, A.G., and L.R. Kister. 1956. Saline-water resources of Texas: U.S. Geological Survey Water-Supply Paper 1365, 105 p.
- Young, S. C. and V. Kelley, editors. 2006. A site conceptual model to support the development of a detailed groundwater model for Colorado, Wharton, and Matagorda counties, prepared for the Lower Colorado River Authority, Austin, TX.
- Young, S., T. Budge, P. Knox, R. Kalbouss, E. Baker, S. Hamlin, B. Galloway, and N. Deeds. 2010. Final hydrostratigraphy of the Gulf Coast Aquifer System from the Brazos River to the Rio Grande, (Final Report): Texas Water Development Board, 203p.
- Young, S., T. Ewing, S. Hamlin, E. Baker, and D. Lupton. 2012. Final Report updating the hydrogeologic framework for the Northern Portion of the Gulf Coast Aquifer System. Prepared for the Texas Water Development Board, June 2012. Young and others (2013).
- Young, S.C., and D. Lupton. 2014. Gulf Coast Aquifer System groundwater study for the City of Corpus Christi: Phase 1. Prepared for the City of Corpus Christi, Corpus Christi, TX. April 2014.
- Young, S.C., J. Pinkard, R. Bassett, A. and Chowdhury. 2013. Hydrogeochemical Evaluation of the Texas Gulf Coast Aquifer System and Implications for Developing Groundwater Availability Models, prepared for the Texas Water Development Board, unnumbered report.
- Young, S.C., M. Jigmond, N. Deeds, J. Blainey, T. Ewing, and D. Banerj. 2016. FINAL REPORT: Identification of Potential Brackish Groundwater Production Areas – Gulf Coast Aquifer System. TWDB Contract Number 1600011947, prepared for the Texas Water Development Board.
- Young, S.C., V. Kelley, T. Budge, N. Deeds, and P. Knox. 2009. Development of the LCRB Groundwater Flow Model for the Chicot and Evangeline aquifers in Colorado, Wharton, and Matagorda counties: LSWP Report Prepared by the URS Corporation, prepared for the Lower Colorado River Authority, Austin, TX.

Appendix A

Geophysical Log Information Including Location, Placement on Cross Sections, Updated Picks for Stratigraphy, and Picks for Base of Salinity Zone

This page is intentionally left blank.

LIST OF TABLES

Table A-1	List of geophysical logs including spatial coordinates, land surface elevation, and placement in cross sections aligned along geologic dip or geologic strike.	A-1
Table A-2	List of geophysical logs with manually picked elevations for base of fresh water, slightly saline, moderately saline, very saline, and brine salinity zones	A-13
Table A-3	List of geophysical logs with formation picks that update the stratigraphic surfaces developed by Young and others (2012)	A-21

Appendix A: Geophysical Log Information Including location, Placement on Cross Sections, updated Picks for Stratigraphy and Picks for Base of Salinity Zone

This page is intentionally left blank.

Appendix A: Geophysical Log Information Including location, Placement on Cross Sections, updated Picks for Stratigraphy and Picks for Base of Salinity Zone

Table A-1

List of geophysical logs including spatial coordinates, land surface elevation, and placement in cross sections aligned along geologic dip or geologic strike.

API	Lat (NAD 83)	Long (NAD 83)	County	Study Area	Sand Picks	Strat. Update	Dip Cross Section				Strike Cross Section			
							Fig. D-1 to D-6		Fig. 4.12 - 4.17		Fig. D-7 to D-9		Fig. 4.18 - 4.20	
							Sec.	Pos.	Sec.	Pos.	Sec.	Pos.	Sec.	Pos.
4201500017	30.00772	-96.45109	Austin	No	No	Yes	9	2	--	--	--	--	--	--
4201500230	30.01004	-96.12960	Austin	Yes	Yes	Yes	8	6	8	1	--	--	--	--
4201500255	29.82370	-96.16398	Austin	Yes	Yes	No	--	--	9	1	--	--	--	--
4201500262	29.76085	-96.20192	Austin	Yes	Yes	Yes	9	5	9	2	--	--	--	--
4201500530	29.76093	-96.05938	Austin	Yes	Yes	No	--	--	--	--	--	--	--	--
4201500663	29.82873	-96.28792	Austin	No	No	Yes	9	4	--	--	--	--	--	--
4201500683	29.63866	-96.11890	Austin	Yes	Yes	Yes	9	7	9	4	--	--	--	--
4201530138	30.04654	-96.20137	Austin	No	Yes	Yes	8	5	--	--	--	--	--	--
4201530401	29.62376	-96.10735	Austin	Yes	Yes	No	--	--	9	5	--	--	--	--
4201530524	29.72345	-96.11853	Austin	Yes	Yes	No	--	--	9	3	--	--	--	--
4201530539	29.91720	-96.41002	Austin	No	No	Yes	9	3	--	--	--	--	--	--
4201530601	29.71906	-96.13945	Austin	Yes	No	Yes	9	6	--	--	--	--	--	--
4201530738	29.61677	-96.0498	Austin	Yes	No	Yes	--	--	--	--	--	--	--	--
4203900015	29.54209	-95.3599	Brazoria	Yes	No	Yes	--	--	--	--	--	--	--	--
4203900064	29.52766	-95.34807	Brazoria	Yes	Yes	No	--	--	--	--	--	--	2	9
4203900847	29.45450	-95.23097	Brazoria	Yes	No	Yes	7	16	--	--	--	--	--	--
4203900965	29.32989	-95.23858	Brazoria	Yes	Yes	No	--	--	--	--	--	--	--	--
4203900984	29.31907	-95.24332	Brazoria	Yes	Yes	Yes	--	--	--	--	--	--	--	--
4203901023	29.30276	-95.18275	Brazoria	Yes	Yes	No	--	--	--	--	--	--	--	--
4203901032	29.28198	-95.1928	Brazoria	Yes	No	Yes	--	--	--	--	--	--	--	--
4203901186	29.39741	-95.31406	Brazoria	Yes	Yes	No	--	--	--	--	--	--	--	--
4203901203	29.44629	-95.362	Brazoria	Yes	No	Yes	--	--	--	--	--	--	--	--
4203901326	29.48489	-95.36393	Brazoria	Yes	Yes	No	--	--	--	--	--	--	--	--
4203901420	29.36516	-95.37812	Brazoria	Yes	Yes	No	--	--	--	--	--	--	--	--
4203901452	29.31662	-95.47059	Brazoria	Yes	Yes	Yes	8	21	8	22	--	--	--	--
4203901526	29.35534	-95.2949	Brazoria	Yes	No	Yes	--	--	--	--	--	--	--	--
4203901711	29.26269	-95.34805	Brazoria	Yes	Yes	No	--	--	--	--	--	--	--	--
4203901814	29.40642	-95.51047	Brazoria	Yes	Yes	No	--	--	8	20	--	--	--	--
4203901815	29.39604	-95.52990	Brazoria	Yes	No	Yes	8	19	--	--	--	--	--	--
4203901910	29.25873	-95.53747	Brazoria	Yes	Yes	No	--	--	--	--	--	--	--	--
4203901916	29.25355	-95.624	Brazoria	Yes	No	Yes	--	--	--	--	--	--	--	--
4203902715	29.27034	-95.7585	Brazoria	Yes	No	Yes	--	--	--	--	--	--	--	--
4203902752	29.18820	-95.80816	Brazoria	Yes	No	Yes	9	15	--	--	--	--	--	--

Appendix A: Geophysical Log Information Including location, Placement on Cross Sections, updated Picks for Stratigraphy and Picks for Base of Salinity Zone

API	Lat (NAD 83)	Long (NAD 83)	County	Study Area	Sand Picks	Strat. Update	Dip Cross Section				Strike Cross Section			
							Fig. D-1 to D-6		Fig. 4.12 - 4.17		Fig. D-7 to D-9		Fig. 4.18 - 4.20	
							Sec.	Pos.	Sec.	Pos.	Sec.	Pos.	Sec.	Pos.
4203902772	29.14260	-95.79624	Brazoria	Yes	Yes	No	--	--	--	--	--	--	--	--
4203902865	29.18654	-95.70782	Brazoria	Yes	Yes	Yes	9	16	9	16	--	--	--	--
4203902872	29.15849	-95.68163	Brazoria	Yes	Yes	No	--	--	9	17	--	--	--	--
4203903754	29.15400	-95.61922	Brazoria	Yes	No	Yes	9	17	--	--	--	--	--	--
4203903798	29.20112	-95.51932	Brazoria	Yes	Yes	No	--	--	--	--	--	--	--	--
4203903864	29.13739	-95.53869	Brazoria	Yes	Yes	No	--	--	--	--	--	--	--	--
4203903878	29.12067	-95.59974	Brazoria	Yes	No	Yes	9	18	--	--	--	--	--	--
4203903888	29.08639	-95.55666	Brazoria	Yes	No	Yes	--	--	--	--	3	3	--	--
4203903898	29.07845	-95.60827	Brazoria	Yes	Yes	Yes	9	19	9	19	--	--	--	--
4203903927	29.09236	-95.71755	Brazoria	Yes	Yes	No	--	--	--	--	--	--	--	--
4203904069	29.01443	-95.70175	Brazoria	Yes	Yes	No	--	--	--	--	--	--	--	--
4203904181	29.12952	-95.48519	Brazoria	Yes	No	Yes	--	--	--	--	3	4	--	--
4203904203	29.19267	-95.42010	Brazoria	Yes	Yes	No	--	--	8	24	--	--	--	--
4203904224	29.23591	-95.41423	Brazoria	Yes	Yes	Yes	8	22	8	23	3	5	3	5
4203904263	29.24091	-95.32256	Brazoria	Yes	Yes	No	--	--	--	--	--	--	--	--
4203904271	29.21130	-95.29939	Brazoria	Yes	No	Yes	--	--	--	--	3	6	--	--
4203904277	29.12977	-95.30537	Brazoria	Yes	Yes	Yes	8	23	8	25	--	--	3	6
4203904291	29.02418	-95.29214	Brazoria	Yes	Yes	Yes	8	24	8	27	--	--	--	--
4203904402	29.05632	-95.4085	Brazoria	Yes	No	Yes	--	--	--	--	--	--	--	--
4203904467	29.10806	-95.45512	Brazoria	Yes	Yes	Yes	--	--	--	--	--	--	3	4
4203904481	29.23450	-95.15266	Brazoria	Yes	Yes	Yes	--	--	--	--	3	7	3	7
4203904518	29.07314	-95.1876	Brazoria	Yes	No	Yes	--	--	--	--	--	--	--	--
4203904519	28.99697	-95.29577	Brazoria	Yes	Yes	No	--	--	8	28	--	--	--	--
4203904811	28.89873	-95.39835	Brazoria	Yes	No	Yes	9	22	--	--	--	--	--	--
4203904823	29.35170	-95.49596	Brazoria	Yes	No	Yes	8	20	--	--	--	--	--	--
4203930006	29.27032	-95.70345	Brazoria	Yes	Yes	No	--	--	9	15	--	--	--	--
4203930024	29.33660	-95.28892	Brazoria	Yes	Yes	No	--	--	--	--	--	--	--	--
4203930263	28.97223	-95.38366	Brazoria	Yes	Yes	No	--	--	--	--	--	--	--	--
4203930346	29.51098	-95.33542	Brazoria	Yes	No	Yes	--	--	--	--	2	6	--	--
4203930350	28.98131	-95.57832	Brazoria	Yes	No	Yes	9	20	--	--	3	2	--	--
4203930506	29.19641	-95.1502	Brazoria	Yes	No	Yes	--	--	--	--	--	--	--	--
4203930519	29.00958	-95.51241	Brazoria	Yes	Yes	No	--	--	9	21	--	--	3	3
4203930677	28.99216	-95.57003	Brazoria	Yes	Yes	No	--	--	9	20	--	--	3	2
4203931761	29.21719	-95.5354	Brazoria	Yes	No	Yes	--	--	--	--	--	--	--	--
4203932063	29.39083	-95.22450	Brazoria	Yes	Yes	No	--	--	--	--	--	--	--	--

Appendix A: Geophysical Log Information Including location, Placement on Cross Sections, updated Picks for Stratigraphy and Picks for Base of Salinity Zone

API	Lat (NAD 83)	Long (NAD 83)	County	Study Area	Sand Picks	Strat. Update	Dip Cross Section				Strike Cross Section			
							Fig. D-1 to D-6		Fig. 4.12 - 4.17		Fig. D-7 to D-9		Fig. 4.18 - 4.20	
							Sec.	Pos.	Sec.	Pos.	Sec.	Pos.	Sec.	Pos.
4203932110	28.97731	-95.46539	Brazoria	Yes	No	Yes	9	21	--	--	--	--	--	--
4203932152	29.42036	-95.44757	Brazoria	Yes	Yes	No	--	--	--	--	--	--	--	--
4203932225	29.02055	-95.3388	Brazoria	Yes	No	Yes	--	--	--	--	--	--	--	--
4203932309	29.46407	-95.27716	Brazoria	Yes	Yes	No	--	--	--	--	--	--	--	--
4203932379	29.05327	-95.33680	Brazoria	Yes	Yes	No	--	--	8	26	--	--	--	--
4203932561	29.17237	-95.60713	Brazoria	Yes	Yes	No	--	--	9	18	--	--	--	--
4207100226	29.86306	-94.90034	Chambers	Yes	Yes	No	--	--	5	13	--	--	--	--
4207100699	29.83352	-94.89755	Chambers	Yes	Yes	No	--	--	5	16	--	--	--	--
4207100832	29.75639	-94.88572	Chambers	Yes	Yes	No	--	--	5	19	--	--	--	--
4207100972	29.75410	-94.82718	Chambers	Yes	Yes	Yes	5	15	5	20	2	11	2	13
4207101074	29.85802	-94.87344	Chambers	Yes	Yes	No	--	--	5	15	--	--	--	--
4207102432	29.56666	-94.71876	Chambers	Yes	No	Yes	5	18	--	--	--	--	--	--
4207102466	29.59869	-94.71389	Chambers	Yes	Yes	No	--	--	5	22	--	--	--	--
4207102696	29.68543	-94.78972	Chambers	Yes	No	Yes	5	16	--	--	--	--	--	--
4207102740	29.64089	-94.75510	Chambers	Yes	Yes	Yes	5	17	5	21	--	--	--	--
4207102853	29.58255	-94.87603	Chambers	Yes	Yes	No	--	--	--	--	--	--	--	--
4207102880	29.53176	-94.83537	Chambers	Yes	Yes	No	--	--	--	--	--	--	--	--
4207102975	29.52433	-94.87682	Chambers	Yes	Yes	No	--	--	--	--	--	--	--	--
4207103062	29.65318	-94.94776	Chambers	Yes	Yes	Yes	--	--	--	--	2	10	2	12
4207103096	29.55808	-94.96872	Chambers	Yes	Yes	Yes	6	17	6	18	--	--	--	--
4207130898	29.83206	-94.84599	Chambers	Yes	Yes	No	--	--	5	17	--	--	--	--
4207131458	29.81320	-94.82988	Chambers	Yes	Yes	Yes	5	14	5	18	--	--	--	--
4207132442	29.84842	-94.92916	Chambers	Yes	Yes	No	--	--	5	14	--	--	--	--
4208900057	29.77984	-96.54943	Colorado	No	Yes	Yes	10	4	--	--	--	--	--	--
4208900090	29.77349	-96.43538	Colorado	No	Yes	Yes	10	5	--	--	--	--	--	--
4208900110	29.63676	-96.22707	Colorado	Yes	Yes	No	--	--	--	--	--	--	--	--
4208900127	29.58919	-96.24502	Colorado	Yes	Yes	No	--	--	10	1	--	--	--	--
4208900270	29.57402	-96.28985	Colorado	No	No	Yes	10	7	--	--	--	--	--	--
4208931246	29.64540	-96.38917	Colorado	No	Yes	Yes	10	6	--	--	--	--	--	--
4208931531	29.80661	-96.57926	Colorado	No	Yes	Yes	10	3	--	--	--	--	--	--
4214931329	29.98421	-96.68224	Fayette	No	No	Yes	10	2	--	--	--	--	--	--
4214932088	30.07481	-96.84888	Fayette	No	No	Yes	10	1	--	--	--	--	--	--
4215700001	29.75413	-95.87074	Fort Bend	Yes	Yes	Yes	8	12	8	7	--	--	--	--
4215700016	29.75654	-95.82512	Fort Bend	Yes	Yes	No	--	--	8	9	--	--	--	--
4215700030	29.76072	-95.78042	Fort Bend	Yes	Yes	No	--	--	--	--	--	--	--	--

Appendix A: Geophysical Log Information Including location, Placement on Cross Sections, updated Picks for Stratigraphy and Picks for Base of Salinity Zone

API	Lat (NAD 83)	Long (NAD 83)	County	Study Area	Sand Picks	Strat. Update	Dip Cross Section				Strike Cross Section			
							Fig. D-1 to D-6		Fig. 4.12 - 4.17		Fig. D-7 to D-9		Fig. 4.18 - 4.20	
							Sec.	Pos.	Sec.	Pos.	Sec.	Pos.	Sec.	Pos.
4215700781	29.53282	-95.57280	Fort Bend	Yes	Yes	No	--	--	--	--	--	--	--	--
4215700893	29.64777	-95.59879	Fort Bend	Yes	Yes	No	--	--	--	--	--	--	--	--
4215700894	29.58563	-95.67306	Fort Bend	Yes	Yes	Yes	8	15	8	17	--	--	--	--
4215700902	29.55937	-95.73802	Fort Bend	Yes	Yes	No	--	--	8	16	--	--	--	--
4215700919	29.65109	-95.66632	Fort Bend	Yes	Yes	No	--	--	--	--	--	--	--	--
4215700940	29.69697	-95.72363	Fort Bend	Yes	Yes	Yes	--	--	--	--	1	7	1	5
4215701026	29.67017	-95.84968	Fort Bend	Yes	Yes	Yes	8	13	8	11	--	--	--	--
4215701031	29.69888	-95.83201	Fort Bend	Yes	Yes	No	--	--	8	10	--	--	--	--
4215701074	29.61114	-95.84268	Fort Bend	Yes	Yes	No	--	--	--	--	--	--	--	--
4215701104	29.53039	-95.84398	Fort Bend	Yes	Yes	No	--	--	--	--	--	--	--	--
4215701119	29.55760	-95.89086	Fort Bend	Yes	Yes	No	--	--	--	--	--	--	1	4
4215701128	29.50144	-95.89421	Fort Bend	Yes	Yes	No	--	--	9	8	--	--	--	--
4215701137	29.57139	-95.99014	Fort Bend	Yes	Yes	No	--	--	9	6	--	--	--	--
4215701300	29.59016	-95.92637	Fort Bend	Yes	Yes	No	--	--	--	--	--	--	--	--
4215701329	29.71781	-95.90895	Fort Bend	Yes	Yes	No	--	--	8	8	--	--	--	--
4215701350	29.72526	-95.9823	Fort Bend	Yes	No	Yes	--	--	--	--	--	--	--	--
4215701374	29.43381	-96.00990	Fort Bend	Yes	Yes	No	--	--	--	--	--	--	--	--
4215701392	29.40824	-95.92830	Fort Bend	Yes	No	Yes	9	11	--	--	--	--	--	--
4215701396	29.42846	-95.97101	Fort Bend	Yes	Yes	No	--	--	--	--	--	--	--	--
4215701643	29.34681	-95.83019	Fort Bend	Yes	Yes	No	--	--	9	12	--	--	--	--
4215701674	29.32147	-95.84903	Fort Bend	Yes	Yes	Yes	9	13	9	13	--	--	--	--
4215701698	29.39774	-95.84973	Fort Bend	Yes	Yes	No	--	--	9	11	--	--	--	--
4215701729	29.40504	-95.79294	Fort Bend	Yes	Yes	Yes	--	--	--	--	--	--	--	--
4215701752	29.48134	-95.7776	Fort Bend	Yes	No	Yes	--	--	--	--	--	--	--	--
4215701965	29.44748	-95.70168	Fort Bend	Yes	Yes	No	--	--	--	--	--	--	--	--
4215701974	29.49601	-95.64746	Fort Bend	Yes	No	Yes	8	16	--	--	--	--	--	--
4215702129	29.36717	-95.72522	Fort Bend	Yes	Yes	No	--	--	--	--	--	--	--	--
4215702136	29.35776	-95.64327	Fort Bend	Yes	Yes	No	--	--	--	--	--	--	2	6
4215702199	29.30018	-95.6462	Fort Bend	Yes	No	Yes	--	--	--	--	--	--	--	--
4215702217	29.35251	-95.59361	Fort Bend	Yes	Yes	No	--	--	8	21	--	--	--	--
4215702320	29.43400	-95.56987	Fort Bend	Yes	No	Yes	8	18	--	--	--	--	--	--
4215702459	29.45705	-95.61153	Fort Bend	Yes	Yes	Yes	8	17	8	19	2	4	2	7
4215702773	29.49275	-95.51455	Fort Bend	Yes	Yes	No	--	--	--	--	--	--	--	--
4215702819	29.53159	-95.8811	Fort Bend	Yes	No	Yes	--	--	--	--	--	--	--	--
4215702830	29.38279	-95.89987	Fort Bend	Yes	Yes	No	--	--	9	10	--	--	--	--

Appendix A: Geophysical Log Information Including location, Placement on Cross Sections, updated Picks for Stratigraphy and Picks for Base of Salinity Zone

API	Lat (NAD 83)	Long (NAD 83)	County	Study Area	Sand Picks	Strat. Update	Dip Cross Section				Strike Cross Section			
							Fig. D-1 to D-6		Fig. 4.12 - 4.17		Fig. D-7 to D-9		Fig. 4.18 - 4.20	
							Sec.	Pos.	Sec.	Pos.	Sec.	Pos.	Sec.	Pos.
4215702848	29.31141	-95.65810	Fort Bend	Yes	Yes	No	--	--	--	--	--	--	--	--
4215730122	29.35599	-95.83893	Fort Bend	Yes	No	Yes	9	12	--	--	--	--	--	--
4215730311	29.67987	-95.97702	Fort Bend	Yes	Yes	No	--	--	--	--	--	--	--	--
4215730373	29.48631	-95.77068	Fort Bend	Yes	Yes	No	--	--	--	--	--	--	--	--
4215730386	29.61766	-95.70489	Fort Bend	Yes	Yes	No	--	--	--	--	--	--	--	--
4215730396	29.61462	-95.70276	Fort Bend	Yes	Yes	No	--	--	8	15	--	--	--	--
4215730949	29.32824	-95.75624	Fort Bend	Yes	Yes	No	--	--	9	14	--	--	2	5
4215730976	29.37546	-95.70779	Fort Bend	Yes	No	Yes	--	--	--	--	2	3	--	--
4215730998	29.68074	-95.91694	Fort Bend	Yes	Yes	No	--	--	--	--	--	--	--	--
4215731087	29.65869	-95.78842	Fort Bend	Yes	Yes	No	--	--	8	12	--	--	--	--
4215731108	29.55683	-95.89671	Fort Bend	Yes	No	Yes	--	--	--	--	1	5	--	--
4215731152	29.46506	-95.46982	Fort Bend	Yes	Yes	Yes	--	--	--	--	2	5	2	8
4215731161	29.51379	-95.69240	Fort Bend	Yes	Yes	No	--	--	8	18	--	--	--	--
4215731388	29.3852	-95.7387	Fort Bend	Yes	No	Yes	--	--	--	--	--	--	--	--
4215731513	29.57228	-95.46688	Fort Bend	Yes	Yes	Yes	--	--	--	--	--	--	--	--
4215731695	29.62787	-95.97879	Fort Bend	Yes	Yes	Yes	--	--	--	--	--	--	--	--
4215731732	29.56483	-95.97063	Fort Bend	Yes	Yes	No	--	--	9	7	--	--	--	--
4215731752	29.53261	-96.01878	Fort Bend	Yes	No	Yes	9	9	--	--	--	--	--	--
4215731805	29.46308	-95.95219	Fort Bend	Yes	Yes	Yes	9	10	9	9	1	4	1	3
4215731815	29.29276	-95.85951	Fort Bend	Yes	No	Yes	9	14	--	--	2	2	--	--
4215731983	29.59861	-95.81901	Fort Bend	Yes	Yes	Yes	8	14	8	13	1	6	--	--
4215732782	29.58525	-95.48677	Fort Bend	Yes	Yes	No	--	--	--	--	--	--	--	--
4216700035	29.52209	-95.21560	Galveston	Yes	Yes	Yes	7	15	7	19	--	--	--	--
4216700056	29.52552	-95.02596	Galveston	Yes	Yes	No	--	--	--	--	--	--	--	--
4216700956	29.46414	-94.72671	Galveston	Yes	Yes	Yes	5	19	5	23	--	--	--	--
4216700958	29.46813	-94.60553	Galveston	Yes	Yes	No	--	--	5	25	--	--	--	--
4216700959	29.44504	-94.67590	Galveston	Yes	Yes	Yes	5	20	5	24	3	11	--	--
4216700961	29.46041	-94.81207	Galveston	Yes	Yes	No	--	--	--	--	--	--	--	--
4216700966	29.43604	-94.91272	Galveston	Yes	Yes	Yes	6	18	6	19	3	10	3	10
4216701072	29.26650	-94.88302	Galveston	Yes	Yes	No	--	--	--	--	--	--	--	--
4216701075	29.33070	-94.94054	Galveston	Yes	Yes	No	--	--	--	--	--	--	--	--
4216701080	29.31860	-94.96662	Galveston	Yes	Yes	No	--	--	--	--	--	--	--	--
4216701132	29.34500	-94.96830	Galveston	Yes	Yes	No	--	--	--	--	--	--	--	--
4216701142	29.36454	-94.96317	Galveston	Yes	Yes	No	--	--	--	--	--	--	3	9
4216701276	29.47920	-95.16245	Galveston	Yes	Yes	No	--	--	7	20	--	--	--	--

Appendix A: Geophysical Log Information Including location, Placement on Cross Sections, updated Picks for Stratigraphy and Picks for Base of Salinity Zone

API	Lat (NAD 83)	Long (NAD 83)	County	Study Area	Sand Picks	Strat. Update	Dip Cross Section				Strike Cross Section			
							Fig. D-1 to D-6		Fig. 4.12 - 4.17		Fig. D-7 to D-9		Fig. 4.18 - 4.20	
							Sec.	Pos.	Sec.	Pos.	Sec.	Pos.	Sec.	Pos.
4216701336	29.30265	-95.06685	Galveston	Yes	Yes	Yes	7	20	7	24	3	8	3	8
4216701387	29.35707	-95.02440	Galveston	Yes	No	Yes	--	--	--	--	3	9	--	--
4216701448	29.33472	-95.08216	Galveston	Yes	No	Yes	7	19	--	--	--	--	--	--
4216701453	29.37105	-95.11151	Galveston	Yes	No	Yes	7	18	--	--	--	--	--	--
4216701481	29.41867	-95.05158	Galveston	Yes	Yes	No	--	--	--	--	--	--	--	--
4216701846	29.24293	-94.89318	Galveston	Yes	Yes	No	--	--	--	--	--	--	--	--
4216701876	29.40416	-95.16287	Galveston	Yes	Yes	Yes	7	17	7	22	--	--	--	--
4216701916	29.20780	-94.94156	Galveston	Yes	Yes	Yes	7	22	--	--	--	--	--	--
4216702012	29.36710	-94.77076	Galveston	Yes	Yes	No	--	--	--	--	--	--	--	--
4216730039	29.25170	-95.04785	Galveston	Yes	No	Yes	7	21	--	--	--	--	--	--
4216730091	29.29577	-94.82015	Galveston	Yes	Yes	Yes	6	19	6	21	--	--	--	--
4216730283	29.38392	-94.88556	Galveston	Yes	Yes	No	--	--	6	20	--	--	--	--
4216730702	29.26724	-95.04948	Galveston	Yes	Yes	No	--	--	7	25	--	--	--	--
4216730792	29.43365	-95.16296	Galveston	Yes	Yes	No	--	--	7	21	--	--	--	--
4216731114	29.35271	-95.08974	Galveston	Yes	Yes	No	--	--	7	23	--	--	--	--
4218500034	30.50365	-95.99538	Grimes	No	Yes	Yes	7	2	--	--	--	--	--	--
4218500061	30.59206	-96.02513	Grimes	No	No	Yes	7	1	--	--	--	--	--	--
4218500150	30.36425	-95.89584	Grimes	No	No	Yes	7	3	--	--	--	--	--	--
4218530009	30.26691	-95.85650	Grimes	Yes	Yes	Yes	7	4	7	1	--	--	--	--
4218530399	30.27003	-95.92869	Grimes	Yes	Yes	No	--	--	--	--	--	--	--	--
4220100048	30.08224	-95.69085	Harris	Yes	No	Yes	7	8	--	--	--	--	--	--
4220100104	30.06644	-95.67935	Harris	Yes	Yes	Yes	7	9	7	7	--	--	--	--
4220100465	30.02059	-95.68081	Harris	Yes	Yes	No	--	--	7	8	--	--	--	--
4220100709	30.02742	-95.61554	Harris	Yes	Yes	No	--	--	7	9	--	--	--	--
4220100760	30.13798	-95.54763	Harris	Yes	Yes	No	--	--	--	--	--	--	--	--
4220100875	30.04228	-95.54727	Harris	Yes	Yes	No	--	--	--	--	--	--	--	--
4220100882	30.01008	-95.54043	Harris	Yes	Yes	No	--	--	--	--	--	--	--	--
4220100883	30.11643	-95.49470	Harris	Yes	Yes	No	--	--	--	--	--	--	--	--
4220100911	30.08162	-95.46378	Harris	Yes	Yes	No	--	--	--	--	--	--	--	--
4220100991	30.04842	-95.46086	Harris	Yes	Yes	No	--	--	--	--	--	--	--	--
4220101017	30.00336	-95.31803	Harris	Yes	Yes	No	--	--	--	--	--	--	--	--
4220101024	30.07382	-95.13717	Harris	Yes	Yes	No	--	--	--	--	--	--	--	--
4220101065	30.02814	-95.08917	Harris	Yes	Yes	No	--	--	--	--	--	--	--	--
4220102604	29.78346	-94.93975	Harris	Yes	Yes	No	--	--	--	--	--	--	--	--
4220102658	29.96399	-95.08266	Harris	Yes	Yes	No	--	--	--	--	--	--	--	--

Appendix A: Geophysical Log Information Including location, Placement on Cross Sections, updated Picks for Stratigraphy and Picks for Base of Salinity Zone

API	Lat (NAD 83)	Long (NAD 83)	County	Study Area	Sand Picks	Strat. Update	Dip Cross Section				Strike Cross Section			
							Fig. D-1 to D-6		Fig. 4.12 - 4.17		Fig. D-7 to D-9		Fig. 4.18 - 4.20	
							Sec.	Pos.	Sec.	Pos.	Sec.	Pos.	Sec.	Pos.
4220102672	29.96133	-95.11604	Harris	Yes	Yes	No	--	--	--	--	--	--	--	--
4220102680	29.91314	-95.04022	Harris	Yes	Yes	No	--	--	--	--	--	--	--	--
4220102698	29.96340	-95.19029	Harris	Yes	Yes	No	--	--	6	11	--	--	--	--
4220102722	29.95490	-95.18246	Harris	Yes	Yes	Yes	6	12	6	12	--	--	--	--
4220102773	29.86436	-95.08507	Harris	Yes	Yes	No	--	--	--	--	--	--	--	--
4220102801	29.81214	-95.12207	Harris	Yes	No	Yes	6	14	--	--	--	--	--	--
4220102936	29.78157	-95.25046	Harris	Yes	Yes	No	--	--	--	--	--	--	--	--
4220102971	29.94824	-95.25655	Harris	Yes	Yes	No	--	--	6	10	--	--	--	--
4220102972	29.96136	-95.35923	Harris	Yes	Yes	Yes	--	--	--	--	1	12	1	10
4220103152	29.87576	-95.32810	Harris	Yes	Yes	No	--	--	--	--	--	--	--	--
4220103224	29.98358	-95.45573	Harris	Yes	Yes	No	--	--	--	--	--	--	--	--
4220103252	29.94422	-95.40321	Harris	Yes	No	Yes	--	--	--	--	1	11	--	--
4220103319	29.93270	-95.45754	Harris	Yes	Yes	No	--	--	--	--	--	--	--	--
4220103343	29.91684	-95.45053	Harris	Yes	Yes	No	--	--	--	--	--	--	--	--
4220103384	29.88391	-95.45815	Harris	Yes	Yes	No	--	--	--	--	--	--	--	--
4220103495	29.78383	-95.41839	Harris	Yes	Yes	No	--	--	7	15	--	--	--	--
4220103510	29.78674	-95.45036	Harris	Yes	Yes	Yes	7	11	7	14	--	--	--	--
4220103533	29.95970	-95.51608	Harris	Yes	Yes	No	--	--	--	--	--	--	--	--
4220103544	29.96825	-95.57475	Harris	Yes	Yes	No	--	--	7	10	--	--	--	--
4220103568	29.90920	-95.55277	Harris	Yes	Yes	No	--	--	7	11	--	--	--	--
4220103587	29.90895	-95.51904	Harris	Yes	Yes	No	--	--	7	12	--	--	--	--
4220103956	29.88568	-95.65989	Harris	Yes	Yes	No	--	--	--	--	--	--	--	--
4220103982	29.88091	-95.6953	Harris	Yes	No	Yes	--	--	--	--	--	--	--	--
4220104062	29.80041	-95.55888	Harris	Yes	Yes	No	--	--	--	--	--	--	1	8
4220104068	29.75720	-95.57470	Harris	Yes	Yes	Yes	--	--	--	--	--	--	1	7
4220104089	29.82667	-95.63211	Harris	Yes	Yes	No	--	--	--	--	--	--	--	--
4220104100	29.80558	-95.70608	Harris	Yes	Yes	No	--	--	--	--	--	--	--	--
4220104215	29.85341	-95.76386	Harris	Yes	Yes	No	--	--	--	--	--	--	--	--
4220104275	29.80827	-95.78348	Harris	Yes	Yes	No	--	--	--	--	--	--	--	--
4220104295	29.99124	-95.85084	Harris	Yes	Yes	No	--	--	--	--	--	--	--	--
4220104328	29.75423	-95.70266	Harris	Yes	Yes	No	--	--	--	--	--	--	--	--
4220104395	29.74225	-95.67512	Harris	Yes	Yes	Yes	--	--	--	--	1	8	1	6
4220104424	29.70156	-95.60764	Harris	Yes	Yes	No	--	--	--	--	--	--	--	--
4220104871	29.67083	-95.40139	Harris	Yes	No	Yes	7	12	--	--	--	--	--	--
4220105058	29.65538	-95.39857	Harris	Yes	Yes	No	--	--	7	16	--	--	--	--
4220105409	29.67356	-95.49495	Harris	Yes	Yes	No	--	--	--	--	--	--	--	--

Appendix A: Geophysical Log Information Including location, Placement on
Cross Sections, updated Picks for Stratigraphy and Picks for Base of Salinity Zone

API	Lat (NAD 83)	Long (NAD 83)	County	Study Area	Sand Picks	Strat. Update	Dip Cross Section				Strike Cross Section			
							Fig. D-1 to D-6		Fig. 4.12 - 4.17		Fig. D-7 to D-9		Fig. 4.18 - 4.20	
							Sec.	Pos.	Sec.	Pos.	Sec.	Pos.	Sec.	Pos.
4220105413	29.62963	-95.47949	Harris	Yes	Yes	No	--	--	--	--	--	--	--	--
4220105568	29.62669	-95.30101	Harris	Yes	No	Yes	7	13	--	--	--	--	--	--
4220105675	29.56647	-95.07659	Harris	Yes	Yes	No	--	--	--	--	--	--	--	--
4220105710	29.53896	-95.14014	Harris	Yes	Yes	No	--	--	--	--	--	--	--	--
4220106044	29.63260	-95.04834	Harris	Yes	Yes	Yes	6	16	6	17	2	9	2	11
4220106075	29.65259	-95.06985	Harris	Yes	Yes	No	--	--	6	16	--	--	--	--
4220106114	29.56826	-95.24174	Harris	Yes	No	Yes	7	14	--	--	2	7	--	--
4220106223	29.72639	-94.99219	Harris	Yes	Yes	No	--	--	--	--	--	--	--	--
4220107603	30.03134	-95.22552	Harris	Yes	Yes	Yes	6	11	6	9	1	13	1	11
4220107836	29.81209	-95.24807	Harris	Yes	Yes	No	--	--	--	--	--	--	--	--
4220107892	30.07902	-95.88521	Harris	Yes	Yes	Yes	--	--	--	--	--	--	--	--
4220107904	29.85059	-95.53120	Harris	Yes	Yes	No	--	--	7	13	--	--	1	9
4220108007	29.80805	-95.60449	Harris	Yes	No	Yes	--	--	--	--	1	9	--	--
4220130016	29.66755	-95.24691	Harris	Yes	Yes	No	--	--	--	--	--	--	--	--
4220130089	30.08828	-95.87547	Harris	Yes	Yes	No	--	--	--	--	--	--	--	--
4220130129	29.89334	-95.26756	Harris	Yes	Yes	No	--	--	--	--	--	--	--	--
4220130958	30.06437	-95.13697	Harris	Yes	Yes	Yes	--	--	--	--	1	14	1	12
4220131057	29.85857	-95.77147	Harris	Yes	Yes	No	--	--	--	--	--	--	--	--
4220131129	29.96923	-95.7416	Harris	Yes	No	Yes	--	--	--	--	--	--	--	--
4220131287	29.90594	-95.79511	Harris	Yes	Yes	No	--	--	--	--	--	--	--	--
4220131368	29.59665	-95.16944	Harris	Yes	No	Yes	--	--	--	--	2	8	--	--
4220131506	30.02493	-95.90927	Harris	Yes	Yes	No	--	--	--	--	--	--	--	--
4220131544	29.58752	-95.20278	Harris	Yes	Yes	No	--	--	--	--	--	--	2	10
4220131622	29.89459	-95.50895	Harris	Yes	No	Yes	7	10	--	--	1	10	--	--
4220132038	29.89659	-95.16463	Harris	Yes	Yes	Yes	6	13	6	13	--	--	--	--
4220132062	29.88481	-95.25567	Harris	Yes	Yes	No	--	--	--	--	--	--	--	--
4220132187	30.08653	-95.51857	Harris	Yes	Yes	No	--	--	--	--	--	--	--	--
4220132368	29.94353	-95.85086	Harris	Yes	Yes	No	--	--	--	--	--	--	--	--
4220132375	29.96773	-95.68572	Harris	Yes	Yes	No	--	--	--	--	--	--	--	--
4220132613	29.74388	-95.15617	Harris	Yes	No	Yes	6	15	--	--	--	--	--	--
4220132669	29.99235	-95.83180	Harris	Yes	Yes	No	--	--	--	--	--	--	--	--
4220132705	29.82291	-95.40224	Harris	Yes	No	No	--	--	--	--	--	--	--	--
4220132756	29.80478	-95.04264	Harris	Yes	No	No	--	--	--	--	--	--	--	--
4220138000	29.62939	-95.27963	Harris	Yes	Yes	No	--	--	--	--	--	--	--	--
4229100086	30.30699	-95.06035	Liberty	Yes	Yes	Yes	5	8	5	1	--	--	--	--
4229100300	30.25239	-94.98135	Liberty	Yes	Yes	No	--	--	5	3	--	--	--	--
4229102426	30.13162	-94.88650	Liberty	Yes	Yes	No	--	--	5	8	--	--	--	--

Appendix A: Geophysical Log Information Including location, Placement on
Cross Sections A, updated Picks for Stratigraphy and Picks for Base of Salinity Zone

API	Lat (NAD 83)	Long (NAD 83)	County	Study Area	Sand Picks	Strat. Update	Dip Cross Section				Strike Cross Section			
							Fig. D-1 to D-6		Fig. 4.12 - 4.17		Fig. D-7 to D-9		Fig. 4.18 - 4.20	
							Sec.	Pos.	Sec.	Pos.	Sec.	Pos.	Sec.	Pos.
4229102431	30.22577	-94.96396	Liberty	Yes	Yes	No	--	--	5	4	--	--	--	--
4229102866	30.07037	-94.89543	Liberty	Yes	Yes	No	--	--	5	9	--	--	--	--
4229103880	30.08064	-95.02643	Liberty	Yes	Yes	Yes	5	11	5	7	--	--	1	13
4229104384	29.94111	-94.89399	Liberty	Yes	Yes	No	--	--	5	11	--	--	--	--
4229105018	30.25893	-95.04544	Liberty	Yes	Yes	Yes	5	9	5	2	--	--	--	--
4229105450	30.13964	-94.93018	Liberty	Yes	Yes	No	--	--	5	6	--	--	--	--
4229105498	30.02917	-95.03296	Liberty	Yes	No	Yes	--	--	--	--	1	15	--	--
4229131549	30.20729	-95.06474	Liberty	Yes	No	Yes	5	10	--	--	--	--	--	--
4229131788	29.91132	-94.87198	Liberty	Yes	Yes	Yes	5	13	5	12	--	--	--	--
4229132099	30.04505	-94.92759	Liberty	Yes	No	Yes	5	12	--	--	1	16	--	--
4229132153	30.01809	-94.82781	Liberty	Yes	Yes	No	--	--	5	10	--	--	--	--
4229132387	30.11111	-95.01127	Liberty	Yes	Yes	No	--	--	5	5	--	--	1	14
4232100341	29.10364	-95.90529	Matagorda	Yes	Yes	Yes	10	16	10	9	--	--	--	--
4232100435	29.05512	-95.95864	Matagorda	Yes	Yes	No	--	--	--	--	--	--	--	--
4232100553	29.088005	-95.854509	Matagorda	Yes	No	Yes	10	17	--	--	--	--	--	--
4232100670	29.06437	-95.78445	Matagorda	Yes	Yes	Yes	10	18	10	10	--	--	--	--
4232100824	28.81413	-95.69096	Matagorda	Yes	Yes	Yes	10	21	10	14	--	--	--	--
4232100836	28.94991	-95.77687	Matagorda	Yes	Yes	Yes	10	19	10	11	3	1	3	1
4232101026	28.98472	-95.94899	Matagorda	Yes	Yes	No	--	--	--	--	--	--	--	--
4232101064	28.87536	-95.83220	Matagorda	Yes	Yes	No	--	--	--	--	--	--	--	--
4232130497	28.89045	-95.69538	Matagorda	Yes	Yes	No	--	--	10	13	--	--	--	--
4232130952	29.15321	-95.92332	Matagorda	Yes	Yes	No	--	--	10	8	--	--	2	3
4232131008	28.87463	-95.74167	Matagorda	Yes	No	Yes	10	20	--	--	--	--	--	--
4232131364	28.87683	-95.78901	Matagorda	Yes	Yes	No	--	--	10	12	--	--	--	--
4232131592	28.769217	-95.631683	Matagorda	Yes	No	Yes	10	22	--	--	--	--	--	--
4233900086	30.36450	-95.45155	Montgomery	No	Yes	Yes	6	7	--	--	--	--	--	--
4233900104	30.32929	-95.48821	Montgomery	Yes	Yes	No	--	--	6	2	--	--	--	--
4233900202	30.28734	-95.45105	Montgomery	Yes	Yes	Yes	6	8	6	4	--	--	--	--
4233900868	30.44750	-95.51212	Montgomery	No	Yes	Yes	6	5	--	--	--	--	--	--
4233900901	30.39554	-95.50585	Montgomery	No	Yes	Yes	6	6	--	--	--	--	--	--
4233900910	30.35380	-95.52549	Montgomery	Yes	Yes	No	--	--	6	1	--	--	--	--
4233900926	30.35040	-95.43460	Montgomery	Yes	Yes	No	--	--	6	3	--	--	--	--
4233900934	30.28519	-95.54005	Montgomery	Yes	Yes	No	--	--	--	--	--	--	--	--
4233901014	30.13186	-95.75087	Montgomery	Yes	Yes	Yes	7	6	7	5	--	--	--	--
4233901039	30.21397	-95.63763	Montgomery	Yes	Yes	No	--	--	--	--	--	--	--	--
4233901102	30.13868	-95.62143	Montgomery	Yes	Yes	No	--	--	--	--	--	--	--	--
4233901109	30.22290	-95.54650	Montgomery	Yes	Yes	No	--	--	--	--	--	--	--	--

Appendix A: Geophysical Log Information Including location, Placement on
Cross Sections, updated Picks for Stratigraphy and Picks for Base of Salinity Zone

API	Lat (NAD 83)	Long (NAD 83)	County	Study Area	Sand Picks	Strat. Update	Dip Cross Section				Strike Cross Section			
							Fig. D-1 to D-6		Fig. 4.12 - 4.17		Fig. D-7 to D-9		Fig. 4.18 - 4.20	
							Sec.	Pos.	Sec.	Pos.	Sec.	Pos.	Sec.	Pos.
4233901142	30.12703	-95.65832	Montgomery	Yes	Yes	No	--	--	7	6	--	--	--	--
4233901387	30.17304	-95.45694	Montgomery	Yes	Yes	No	--	--	--	--	--	--	--	--
4233901420	30.12727	-95.44840	Montgomery	Yes	Yes	No	--	--	--	--	--	--	--	--
4233901423	30.15415	-95.45890	Montgomery	Yes	Yes	No	--	--	--	--	--	--	--	--
4233901604	30.24098	-95.28118	Montgomery	Yes	Yes	No	--	--	--	--	--	--	--	--
4233901718	30.14716	-95.29188	Montgomery	Yes	Yes	Yes	6	10	6	7	--	--	--	--
4233901732	30.05907	-95.29636	Montgomery	Yes	Yes	No	--	--	6	8	--	--	--	--
4233901734	30.10333	-95.38417	Montgomery	Yes	Yes	No	--	--	--	--	--	--	--	--
4233901737	30.11438	-95.40618	Montgomery	Yes	Yes	No	--	--	--	--	--	--	--	--
4233901846	30.18295	-95.19491	Montgomery	Yes	Yes	No	--	--	--	--	--	--	--	--
4233901872	30.31614	-95.29677	Montgomery	Yes	Yes	No	--	--	--	--	--	--	--	--
4233901879	30.18368	-95.49519	Montgomery	Yes	Yes	No	--	--	--	--	--	--	--	--
4233901881	30.17530	-95.73288	Montgomery	Yes	Yes	No	--	--	7	4	--	--	--	--
4233901887	30.32821	-95.62037	Montgomery	Yes	Yes	No	--	--	--	--	--	--	--	--
4233930072	30.29016	-95.78422	Montgomery	Yes	Yes	No	--	--	7	2	--	--	--	--
4233930478	30.27581	-95.70225	Montgomery	Yes	Yes	No	--	--	--	--	--	--	--	--
4233930704	30.24257	-95.17203	Montgomery	Yes	Yes	No	--	--	--	--	--	--	--	--
4233930737	30.13779	-95.33871	Montgomery	Yes	Yes	Yes	--	--	--	--	--	--	--	--
4233930820	30.22918	-95.37157	Montgomery	Yes	Yes	Yes	6	9	6	5	--	--	--	--
4233930849	30.15412	-95.14774	Montgomery	Yes	Yes	No	--	--	--	--	--	--	--	--
4233930852	30.10874	-95.70379	Montgomery	Yes	No	Yes	7	7	--	--	--	--	--	--
4240700127	30.71482	-95.27895	San Jacinto	No	Yes	Yes	5	3	--	--	--	--	--	--
4240700156	30.45655	-95.17475	San Jacinto	No	Yes	Yes	5	6	--	--	--	--	--	--
4240700214	30.39270	-95.14436	San Jacinto	No	Yes	Yes	5	7	--	--	--	--	--	--
4240730033	30.62752	-95.25246	San Jacinto	No	Yes	Yes	5	4	--	--	--	--	--	--
4240730078	30.54623	-95.16280	San Jacinto	No	No	Yes	5	5	--	--	--	--	--	--
4247100097	30.84169	-95.35547	Walker	No	No	Yes	5	2	--	--	--	--	--	--
4247100148	30.69914	-95.73971	Walker	No	Yes	Yes	6	2	--	--	--	--	--	--
4247100180	30.64676	-95.63448	Walker	No	Yes	Yes	6	3	--	--	--	--	--	--
4247100189	30.56486	-95.57381	Walker	No	Yes	Yes	6	4	--	--	--	--	--	--
4247100199	31.04624	-95.43941	Walker	No	No	Yes	5	1	--	--	--	--	--	--
4247130022	30.76020	-95.76494	Walker	No	Yes	Yes	6	1	--	--	--	--	--	--
4247300014	30.09753	-96.05243	Waller	Yes	Yes	No	--	--	--	--	--	--	--	--
4247300031	30.18388	-95.99388	Waller	Yes	Yes	No	--	--	--	--	--	--	--	--
4247300037	30.19784	-95.88016	Waller	Yes	Yes	No	--	--	--	--	--	--	--	--
4247300049	29.93838	-95.97511	Waller	Yes	Yes	Yes	8	8	8	3	--	--	--	--
4247300108	29.85491	-95.85487	Waller	Yes	Yes	No	--	--	--	--	--	--	--	--

Appendix A: Geophysical Log Information Including location, Placement on
Cross Sections A, updated Picks for Stratigraphy and Picks for Base of Salinity Zone

API	Lat (NAD 83)	Long (NAD 83)	County	Study Area	Sand Picks	Strat. Update	Dip Cross Section				Strike Cross Section			
							Fig. D-1 to D-6		Fig. 4.12 - 4.17		Fig. D-7 to D-9		Fig. 4.18 - 4.20	
							Sec.	Pos.	Sec.	Pos.	Sec.	Pos.	Sec.	Pos.
4247300178	29.85645	-95.89902	Waller	Yes	Yes	No	--	--	8	5	--	--	--	--
4247300199	29.81914	-95.93566	Waller	Yes	No	Yes	8	10	--	--	--	--	--	--
4247300243	29.97985	-96.09310	Waller	Yes	Yes	Yes	8	7	8	2	--	--	--	--
4247300274	29.91633	-96.10084	Waller	Yes	Yes	No	--	--	--	--	--	--	--	--
4247300278	29.82801	-96.08030	Waller	Yes	Yes	No	--	--	--	--	--	--	--	--
4247300288	29.79902	-96.03348	Waller	Yes	Yes	No	--	--	--	--	--	--	--	--
4247300318	29.90571	-95.93164	Waller	Yes	Yes	Yes	8	9	8	4	--	--	--	--
4247330027	29.91293	-95.88852	Waller	Yes	Yes	No	--	--	--	--	--	--	--	--
4247330043	29.79428	-95.89030	Waller	Yes	No	Yes	8	11	--	--	--	--	--	--
4247330066	30.21495	-95.81109	Waller	Yes	Yes	Yes	7	5	7	3	--	--	--	--
4247330401	29.79163	-95.87384	Waller	Yes	Yes	No	--	--	8	6	--	--	--	--
4247330432	30.17914	-96.01476	Waller	Yes	Yes	No	--	--	--	--	--	--	--	--
4247700239	30.26028	-96.40298	Washington	No	No	Yes	8	2	--	--	--	--	--	--
4247700272	30.17959	-96.25459	Washington	No	No	Yes	8	3	--	--	--	--	--	--
4247700294	30.09501	-96.27081	Washington	No	No	Yes	8	4	--	--	--	--	--	--
4247700366	30.13317	-96.58739	Washington	No	No	Yes	9	1	--	--	--	--	--	--
4247730625	30.32995	-96.39442	Washington	No	Yes	Yes	8	1	--	--	--	--	--	--
4248100671	29.25823	-95.89117	Wharton	Yes	Yes	No	--	--	--	--	--	--	2	4
4248100696	29.29294	-95.97534	Wharton	Yes	Yes	No	--	--	--	--	--	--	--	--
4248100824	29.26967	-95.94209	Wharton	Yes	Yes	No	--	--	--	--	--	--	--	--
4248100943	29.44330	-96.13765	Wharton	Yes	Yes	No	--	--	10	3	--	--	--	--
4248100997	29.42608	-95.99932	Wharton	Yes	No	Yes	--	--	--	--	1	3	--	--
4248101038	29.26036	-96.06995	Wharton	Yes	No	Yes	10	13	--	--	--	--	--	--
4248101205	29.47412	-96.19234	Wharton	Yes	Yes	Yes	10	9	10	2	--	--	--	--
4248101218	29.47471	-96.28022	Wharton	No	Yes	Yes	10	8	--	--	--	--	--	--
4248102562	29.15600	-96.01043	Wharton	Yes	Yes	Yes	10	15	10	7	--	--	2	1
4248130832	29.54556	-96.07528	Wharton	Yes	Yes	No	--	--	--	--	--	--	--	--
4248131622	29.49655	-96.03637	Wharton	Yes	Yes	No	--	--	--	--	--	--	--	--
4248132039	29.31225	-96.15098	Wharton	Yes	No	Yes	10	11	--	--	--	--	--	--
4248132944	29.23562	-96.01585	Wharton	Yes	Yes	Yes	10	14	10	6	2	1	2	2
4248133370	29.33491	-96.06911	Wharton	Yes	Yes	No	--	--	10	5	--	--	--	--
4248133410	29.38637	-96.06225	Wharton	Yes	Yes	Yes	--	--	--	--	1	2	1	2
4248133442	29.36820	-96.15147	Wharton	Yes	Yes	Yes	10	12	10	4	1	1	1	1
4248133720	29.59158	-96.14145	Wharton	Yes	Yes	No	--	--	--	--	--	--	--	--
4248134033	29.28588	-96.16281	Wharton	No	No	Yes	10	10	--	--	--	--	--	--
4248134100	29.57053	-96.07629	Wharton	Yes	No	Yes	9	8	--	--	--	--	--	--
4248134117	29.53142	-96.13721	Wharton	Yes	Yes	No	--	--	--	--	--	--	--	--

Appendix A: Geophysical Log Information Including location, Placement on Cross Sections, updated Picks for Stratigraphy and Picks for Base of Salinity Zone

API	Lat (NAD 83)	Long (NAD 83)	County	Study Area	Sand Picks	Strat. Update	Dip Cross Section				Strike Cross Section			
							Fig. D-1 to D-6		Fig. 4.12 - 4.17		Fig. D-7 to D-9		Fig. 4.18 - 4.20	
							Sec.	Pos.	Sec.	Pos.	Sec.	Pos.	Sec.	Pos.
4270400070	28.36853	-95.39958	Gulf	No	Yes	Yes	10	26	--	--	--	--	--	--
4270400071	28.54754	-95.48637	Gulf	No	No	Yes	10	24	--	--	--	--	--	--
4270430005	28.44307	-95.50108	Gulf	No	Yes	Yes	10	25	--	--	--	--	--	--
4270430073	28.71593	-95.54282	Gulf	No	No	Yes	10	23	--	--	--	--	--	--
4270440026	28.36353	-95.35498	Gulf	No	No	Yes	10	27	--	--	--	--	--	--
4270600022	28.90946	-95.18475	Gulf	No	Yes	Yes	8	25	--	--	--	--	--	--
4270600027	28.99588	-94.86635	Gulf	No	No	Yes	7	25	--	--	--	--	--	--
4270600071	28.69533	-95.24333	Gulf	No	No	Yes	9	24	--	--	--	--	--	--
4270600086	29.06912	-94.91740	Gulf	No	No	Yes	7	23	--	--	--	--	--	--
4270600088	28.9865407	-95.1078837	Gulf	N	No	Yes	--	--	--	--	--	--	--	--
4270600124	28.85188	-94.72446	Gulf	No	No	Yes	7	28	--	--	--	--	--	--
4270600141	29.02960	-94.65775	Gulf	No	No	Yes	6	22	--	--	--	--	--	--
4270630042	29.24878	-94.64197	Gulf	No	No	Yes	5	21	--	--	--	--	--	--
4270640020	28.65543	-95.17908	Gulf	No	No	Yes	9	25	--	--	--	--	--	--
4270640031	29.20613	-94.59445	Gulf	No	No	Yes	5	22	--	--	--	--	--	--
4270640054	29.12361	-94.69842	Gulf	No	No	Yes	6	20	--	--	--	--	--	--
4270640090	28.97555	-94.64252	Gulf	No	Yes	Yes	6	23	--	--	--	--	--	--
4270640097	28.76600	-94.64170	Gulf	No	No	Yes	7	30	--	--	--	--	--	--
4270640110	28.92988	-94.85612	Gulf	No	No	Yes	7	26	--	--	--	--	--	--
4270640212	28.72427	-94.95706	Gulf	No	No	Yes	8	28	--	--	--	--	--	--
4270640251	28.89294	-94.56990	Gulf	No	No	Yes	6	24	--	--	--	--	--	--
4270640256	28.77404	-95.24395	Gulf	No	No	Yes	9	23	--	--	--	--	--	--
4270640267	28.81686	-94.69554	Gulf	No	No	No	7	29	--	--	--	--	--	--
4270640276	28.99703	-94.90419	Gulf	No	No	Yes	7	24	--	--	--	--	--	--
4270640355	28.85602	-95.08657	Gulf	No	No	Yes	8	26	--	--	--	--	--	--
4270640360	28.58504	-95.10559	Gulf	No	No	Yes	9	26	--	--	--	--	--	--
4270640376	28.87283	-94.76575	Gulf	No	No	Yes	7	27	--	--	--	--	--	--
4270640380	29.12580	-94.66660	Gulf	No	Yes	Yes	6	21	--	--	--	--	--	--
4270640434	28.78240	-95.00300	Gulf	No	No	Yes	8	27	--	--	--	--	--	--
4270640446	28.88543	-94.56456	Gulf	No	No	Yes	6	25	--	--	--	--	--	--
4270800022	29.4993243	-94.3832358	Gulf	No	No	Yes	--	--	--	--	--	--	--	--
4270840145	29.12953	-94.46689	Gulf	No	No	Yes	5	23	--	--	--	--	--	--
4270840166	28.82041	-94.43761	Gulf	No	No	Yes	5	26	--	--	--	--	--	--
4270840170	28.80109	-94.50881	Gulf	No	No	Yes	6	26	--	--	--	--	--	--
4270840174	28.88410	-94.47392	Gulf	No	No	Yes	5	25	--	--	--	--	--	--
4270840279	28.80600	-94.44850	Gulf	No	Yes	Yes	6	27	--	--	--	--	--	--

Appendix A: Geophysical Log Information Including location, Placement on Cross Sections, updated Picks for Stratigraphy and Picks for Base of Salinity Zone

API	Lat (NAD 83)	Long (NAD 83)	County	Study Area	Sand Picks	Strat. Update	Dip Cross Section				Strike Cross Section			
							Fig. D-1 to D-6		Fig. 4.12 - 4.17		Fig. D-7 to D-9		Fig. 4.18 - 4.20	
							Sec.	Pos.	Sec.	Pos.	Sec.	Pos.	Sec.	Pos.
4270840289	28.99360	-94.50867	Gulf	No	No	Yes	5	24	--	--	--	--	--	--
6047404000	30.29310	-95.21420	Montgomery	Yes	Yes	No	--	--	--	--	--	--	--	--
9942201180	29.93077	-95.73363	Harris	Yes	Yes	No	--	--	--	--	--	--	--	--
9942201360	29.66024	-95.38508	Harris	Yes	Yes	No	--	--	7	17	--	--	--	--
9965000000	29.72423	-95.74811	Fort Bend	Yes	Yes	No	--	--	--	--	--	--	--	--
9965000039	30.17333	-95.58361	Montgomery	Yes	Yes	No	--	--	--	--	--	--	--	--
9965035010	29.95722	-95.68278	Harris	Yes	Yes	No	--	--	34	7	--	--	--	--
9965144020	29.82583	-95.33528	Harris	Yes	Yes	No	--	--	--	--	--	--	--	--
9965144030	29.81944	-95.33445	Harris	Yes	Yes	No	--	--	--	--	--	--	--	--
9965223010	29.70917	-95.26278	Harris	Yes	Yes	No	--	--	--	--	--	--	--	--

Table A-2 List of geophysical logs with manually picked elevations for base of fresh water, slightly saline, moderately saline, very saline, and brine salinity zones

API	Lat (NAD 83)	Long (NAD 83)	Ground Elevation (ft, msl)	Base Elevation (ft, msl)			
				1,000 TDS	3,000 TDS	10,000 TDS	35,000 TDS
4201500230	30.01004	-96.12960	177	-1200	--	-2633	--
4201500255	29.82370	-96.16398	170	-1580	--	--	--
4201500262	29.76085	-96.20192	198	-883	--	-2934	--
4201500530	29.76093	-96.05938	150	--	--	--	--
4201500683	29.63866	-96.11890	135	-812	-2973	-3277	--
4201530401	29.62376	-96.10735	119	-791	-2416	-2777	--
4201530524	29.72345	-96.11853	147	-1053	--	--	--
4203900064	29.52766	-95.34807	56	-1757	-2433	-2757	--
4203900965	29.32989	-95.23858	25	--	-1477	-1647	--
4203900984	29.31907	-95.24332	24	-1285	-1463	-1546	--
4203901023	29.30276	-95.18275	20	--	-1360	-1455	--
4203901186	29.39741	-95.31406	36	-1290	-1441	-1683	--
4203901326	29.48489	-95.36393	54	-1087	-1484	-1740	-4324
4203901420	29.36516	-95.37812	39	-1276	-1441	-1608	-2274
4203901452	29.31662	-95.47059	40	-1181	-1381	-1557	-2320
4203901711	29.26269	-95.34805	25	--	-1209	-1350	-2044
4203901814	29.40642	-95.51047	50	--	-1572	-1974	-2909
4203901910	29.25873	-95.53747	38	-1094	-1356	-1581	--
4203902772	29.14260	-95.79624	45	-817	-1046	-1325	--
4203902865	29.18654	-95.70782	41	--	--	-1120	--

Appendix A: Geophysical Log Information Including location, Placement on Cross Sections, updated Picks for Stratigraphy and Picks for Base of Salinity Zone

API	Lat (NAD 83)	Long (NAD 83)	Ground Elevation (ft, msl)	Base Elevation (ft, msl)			
				1,000 TDS	3,000 TDS	10,000 TDS	35,000 TDS
4203902872	29.15849	-95.68163	35	-843	-1048	-1272	--
4203903798	29.20112	-95.51932	33	--	--	--	-2403
4203903898	29.07845	-95.60827	29	--	-861	-1042	-1512
4203903927	29.09236	-95.71755	34	-850	-1088	-1230	-1733
4203904069	29.01443	-95.70175	27	-100	-1184	-1348	-2508
4203904203	29.19267	-95.42010	30	-975	--	-1363	-2089
4203904224	29.23591	-95.41423	32	-851	-1161	-1285	-2075
4203904263	29.24091	-95.32256	14	-450	-1028	-1292	-1932
4203904277	29.12977	-95.30537	2	-250	-977	-1396	-2002
4203904291	29.02418	-95.29214	5	-300	-1129	--	-1536
4203904467	29.10806	-95.45512	20	-832	-1207	-1326	-1993
4203904481	29.23450	-95.15266	6	-886	-1070	-1398	-2101
4203904519	28.99697	-95.29577	5	-300	--	-1159	--
4203930006	29.27032	-95.70345	61	-982	--	--	--
4203930024	29.33660	-95.28892	20	-1356	-1470	--	--
4203930263	28.97223	-95.38366	8	-247	-1066	-1285	-1638
4203930519	29.00958	-95.51241	13	--	-930	-1204	--
4203930677	28.99216	-95.57003	13	--	-929	-1153	--
4203932063	29.39083	-95.22450	39	--	--	--	-2679
4203932152	29.42036	-95.44757	54	-1246	--	--	-3128
4203932309	29.46407	-95.27716	45	--	--	-1686	-3229
4203932561	29.17237	-95.60713	31	-753	-1018	-1232	-1812
4207100226	29.86306	-94.90034	57	-910	--	--	--
4207100699	29.83352	-94.89755	33	-1397	-1551	-1736	-2893
4207100832	29.75639	-94.88572	29	-1231	-1592	--	-2388
4207100972	29.75410	-94.82718	3	-672	-1231	-1423	-2331
4207101074	29.85802	-94.87344	38	--	--	--	-4627
4207102466	29.59869	-94.71389	5	--	-1141	-1390	-2158
4207102740	29.64089	-94.75510	0	-119	-1166	-1569	-1956
4207102853	29.58255	-94.87603	0	--	-1324	-1721	-2717
4207102880	29.53176	-94.83537	0	-804	-1285	-1552	-2517
4207102975	29.52433	-94.87682	0	-776	-1393	-1639	-2571
4207103062	29.65318	-94.94776	-1	--	-1377	-1795	-2817
4207103096	29.55808	-94.96872	0	-1161	-1313	-1626	-2609
4207130898	29.83206	-94.84599	30	-1004	-1257	-1717	-2650
4207131458	29.81320	-94.82988	27	-953	-1195	-1713	-2274
4207132442	29.84842	-94.92916	31	-1659	--	--	--
4208900110	29.63676	-96.22707	160	-1363	--	--	--

Appendix A: Geophysical Log Information Including location, Placement on Cross Sections, updated Picks for Stratigraphy and Picks for Base of Salinity Zone

API	Lat (NAD 83)	Long (NAD 83)	Ground Elevation (ft, msl)	Base Elevation (ft, msl)			
				1,000 TDS	3,000 TDS	10,000 TDS	35,000 TDS
4208900127	29.58919	-96.24502	159	-610	--	--	--
4215700001	29.75413	-95.87074	146	-1092	-2217	-3350	--
4215700016	29.75654	-95.82512	131	-1110	-2123	-3410	--
4215700030	29.76072	-95.78042	123	-941	-2537	-3265	--
4215700781	29.53282	-95.57280	63	-1430	-2051	-3215	--
4215700893	29.64777	-95.59879	82	-1661	-2245	-3305	--
4215700894	29.58563	-95.67306	75	--	-2581	-3725	-4067
4215700902	29.55937	-95.73802	75	-1717	--	--	--
4215700919	29.65109	-95.66632	80	-1787	-2299	-3294	--
4215700940	29.69697	-95.72363	93	-1602	-2629	-3158	--
4215701026	29.67017	-95.84968	106	-1131	--	-3020	-4126
4215701031	29.69888	-95.83201	130	-1125	--	--	--
4215701074	29.61114	-95.84268	91	-1335	-2026	--	--
4215701104	29.53039	-95.84398	97	--	-2449	--	--
4215701137	29.57139	-95.99014	121	-1294	-2239	--	--
4215701300	29.59016	-95.92637	113	-1270	-2089	-3300	--
4215701329	29.71781	-95.90895	147	-958	--	--	--
4215701374	29.43381	-96.00990	74	-1165	-2350	-3301	--
4215701396	29.42846	-95.97101	90	-1519	-2233	-3097	--
4215701643	29.34681	-95.83019	78	-1206	-1676	-1891	-4512
4215701674	29.32147	-95.84903	69	-800	-1353	-1694	-2152
4215701698	29.39774	-95.84973	90	-1515	-2397	-3584	--
4215701729	29.40504	-95.79294	84	-1710	-2804	-4084	--
4215701965	29.44748	-95.70168	71	-1830	-2494	-3921	--
4215702129	29.36717	-95.72522	75	-1214	--	--	-4695
4215702136	29.35776	-95.64327	64	-1343	-1517	-1947	--
4215702217	29.35251	-95.59361	49	-1067	-1418	-1893	-2673
4215702459	29.45705	-95.61153	62	-1301	-1912	-2447	--
4215702773	29.49275	-95.51455	64	-1723	--	--	--
4215702830	29.38279	-95.89987	85	-1628	-2487	-3345	--
4215702848	29.31141	-95.65810	54	-1074	--	--	-2382
4215730311	29.67987	-95.97702	115	--	-1747	--	--
4215730373	29.48631	-95.77068	77	--	--	-3910	--
4215730386	29.61766	-95.70489	85	--	--	-3444	--
4215730396	29.61462	-95.70276	81	--	--	-3482	--
4215730949	29.32824	-95.75624	69	-1006	-1378	-1519	-1730
4215730998	29.68074	-95.91694	107	-1318	-1918	--	--
4215731087	29.65869	-95.78842	93	-1415	-2013	--	--

Appendix A: Geophysical Log Information Including location, Placement on Cross Sections, updated Picks for Stratigraphy and Picks for Base of Salinity Zone

API	Lat (NAD 83)	Long (NAD 83)	Ground Elevation (ft, msl)	Base Elevation (ft, msl)			
				1,000 TDS	3,000 TDS	10,000 TDS	35,000 TDS
4215731152	29.46506	-95.46982	60	-1775	-2122	-2611	--
4215731161	29.51379	-95.69240	78	-1957	--	-3257	-3997
4215731513	29.57228	-95.46688	67	--	--	-3034	--
4215731695	29.62787	-95.97879	116	-1427	-2093	-3354	--
4215731805	29.46308	-95.95219	99	-1583	-2453	-3144	--
4215731983	29.59861	-95.81901	91	--	-1972	-3210	--
4215732782	29.58525	-95.48677	70	--	--	-3056	--
4216700035	29.52209	-95.21560	30	-745	-1450	-1950	--
4216700056	29.52552	-95.02596	13	-705	-1469	-1692	-2817
4216700956	29.46414	-94.72671	0	--	-1109	-1260	-1985
4216700958	29.46813	-94.60553	9	--	-908	-1260	-1909
4216700959	29.44504	-94.67590	1	--	-1052	-1311	-2028
4216700961	29.46041	-94.81207	0	-804	-1187	-1425	-2041
4216700966	29.43604	-94.91272	7	-963	-1243	-1412	-3055
4216701072	29.26650	-94.88302	6	--	-991	-1261	-2015
4216701075	29.33070	-94.94054	5	--	-1036	-1301	-2147
4216701080	29.31860	-94.96662	5	-913	-1141	-1319	-1876
4216701132	29.34500	-94.96830	6	-1067	-1200	-1433	-2086
4216701142	29.36454	-94.96317	15	-500	-1197	-1360	--
4216701276	29.47920	-95.16245	29	-940	-1472	-1709	--
4216701336	29.30265	-95.06685	17	-906	-1072	-1314	-1830
4216701481	29.41867	-95.05158	25	--	-1222	-1574	-2108
4216701846	29.24293	-94.89318	1	-27	-969	-1211	-1828
4216701876	29.40416	-95.16287	31	-711	-1124	-1445	-2305
4216701916	29.20780	-94.94156	5	-18	-913	-1254	-1790
4216702012	29.36710	-94.77076	5	--	-1187	-1447	-1790
4216730091	29.29577	-94.82015	6	-500	-1351	-1443	-2846
4216730283	29.38392	-94.88556	0	-500	-1296	-1479	-2952
4216730702	29.26724	-95.04948	4	-9	-1028	-1220	-1723
4216730792	29.43365	-95.16296	21	--	--	-1572	-2692
4216731114	29.35271	-95.08974	25	-750	-1232	-1547	-1931
4218530009	30.26691	-95.85650	333	-941	-1427	-2563	--
4218530399	30.27003	-95.92869	342	-720	-1651	-2600	--
4220100104	30.06644	-95.67935	174	-972	-1621	-2689	--
4220100465	30.02059	-95.68081	158	-1548	-1800	--	--
4220100709	30.02742	-95.61554	158	-1728	-1970	-3100	--
4220100760	30.13798	-95.54763	168	-1454	-1970	--	--
4220100875	30.04228	-95.54727	149	-1693	-2213	--	--

Appendix A: Geophysical Log Information Including location, Placement on Cross Sections, updated Picks for Stratigraphy and Picks for Base of Salinity Zone

API	Lat (NAD 83)	Long (NAD 83)	Ground Elevation (ft, msl)	Base Elevation (ft, msl)			
				1,000 TDS	3,000 TDS	10,000 TDS	35,000 TDS
4220100882	30.01008	-95.54043	124	-1570	-2401	-2600	--
4220100883	30.11643	-95.49470	110	-1696	--	-2450	--
4220100911	30.08162	-95.46378	133	-1799	-2041	-2626	--
4220100991	30.04842	-95.46086	110	-2000	-2470	--	--
4220101017	30.00336	-95.31803	88	-1398	-2349	-2934	--
4220101024	30.07382	-95.13717	67	-1598	-2502	-2977	--
4220101065	30.02814	-95.08917	70	-1740	-2685	-3224	--
4220102604	29.78346	-94.93975	23	-1228	-2050	-2434	--
4220102658	29.96399	-95.08266	54	-1822	-2799	-3224	--
4220102672	29.96133	-95.11604	64	-1790	-2731	-3196	--
4220102680	29.91314	-95.04022	53	-1667	-3027	-3498	--
4220102698	29.96340	-95.19029	66	--	-2733	-3264	--
4220102722	29.95490	-95.18246	59	-1785	-2774	-3185	--
4220102773	29.86436	-95.08507	3	-1790	-3132	-3849	--
4220102936	29.78157	-95.25046	53	-2139	-2715	-3592	--
4220102971	29.94824	-95.25655	65	-1664	-2748	-3270	--
4220102972	29.96136	-95.35923	81	--	-2321	--	--
4220103152	29.87576	-95.32810	60	-1199	-2826	-3260	--
4220103224	29.98358	-95.45573	104	-2042	-2787	-3065	--
4220103319	29.93270	-95.45754	98	--	--	-2974	--
4220103343	29.91684	-95.45053	90	-1587	-2642	-3144	--
4220103384	29.88391	-95.45815	84	-1450	-2715	-3195	--
4220103495	29.78383	-95.41839	53	-1977	-2827	--	--
4220103510	29.78674	-95.45036	65	-1627	-2549	-3137	-3912
4220103533	29.95970	-95.51608	122	--	-2619	-2921	-4144
4220103544	29.96825	-95.57475	130	-1669	-2222	--	--
4220103568	29.90920	-95.55277	112	-1332	-2447	-3037	--
4220103587	29.90895	-95.51904	108	-1324	-2508	-2892	--
4220103956	29.88568	-95.65989	128	-1232	-2172	--	--
4220104062	29.80041	-95.55888	90	-1663	-2759	-3129	--
4220104068	29.75720	-95.57470	73	-1450	-2916	-3285	--
4220104089	29.82667	-95.63211	94	-1489	-2475	-3123	--
4220104100	29.80558	-95.70608	112	-1386	--	--	--
4220104215	29.85341	-95.76386	144	--	-2263	--	--
4220104275	29.80827	-95.78348	137	-1040	-2177	--	--
4220104295	29.99124	-95.85084	204	-901	-1883	--	--
4220104328	29.75423	-95.70266	90	-1492	-2634	-3209	--
4220104395	29.74225	-95.67512	90	-1600	-2737	-3267	--

Appendix A: Geophysical Log Information Including location, Placement on Cross Sections, updated Picks for Stratigraphy and Picks for Base of Salinity Zone

API	Lat (NAD 83)	Long (NAD 83)	Ground Elevation (ft, msl)	Base Elevation (ft, msl)			
				1,000 TDS	3,000 TDS	10,000 TDS	35,000 TDS
4220104424	29.70156	-95.60764	81	-1731	-2471	--	--
4220105058	29.65538	-95.39857	54	-1941	-2531	-3290	-4556
4220105409	29.67356	-95.49495	55	-1757	-3245	-3515	--
4220105413	29.62963	-95.47949	60	-1845	-2890	-3653	--
4220105675	29.56647	-95.07659	13	-682	-1358	-1600	-2912
4220105710	29.53896	-95.14014	27	-733	-1295	-1801	-3025
4220106044	29.63260	-95.04834	18	-1047	-1342	-1649	-2915
4220106075	29.65259	-95.06985	19	-1538	-1739	-2247	-2915
4220106223	29.72639	-94.99219	20	--	-1619	-2434	-4061
4220107603	30.03134	-95.22552	75	-1464	-2402	-3518	-4666
4220107836	29.81209	-95.24807	37	-1996	-2920	-3628	--
4220107892	30.07902	-95.88521	284	-708	-2114	-2723	--
4220107904	29.85059	-95.53120	91	-1448	-2686	-2889	--
4220130016	29.66755	-95.24691	31	-2216	-2572	-3293	--
4220130089	30.08828	-95.87547	261	-801	--	--	--
4220130129	29.89334	-95.26756	58	-1743	-3119	-3407	--
4220130958	30.06437	-95.13697	57	-1533	-2661	-3210	--
4220131057	29.85857	-95.77147	145	-1111	-2079	--	--
4220131287	29.90594	-95.79511	161	-1030	-1975	--	--
4220131506	30.02493	-95.90927	245	-760	-1799	-3016	-4303
4220131544	29.58752	-95.20278	31	-1057	-1490	-2011	--
4220132038	29.89659	-95.16463	51	--	--	-3193	--
4220132062	29.88481	-95.25567	53	-1781	-2923	-3531	--
4220132187	30.08653	-95.51857	142	-1632	--	-2559	-3902
4220132368	29.94353	-95.85086	171	--	-1872	--	--
4220132375	29.96773	-95.68572	148	-867	-2005	--	--
4220132669	29.99235	-95.83180	197	-975	--	--	--
4229100086	30.30699	-95.06035	143	-1500	-2150	-2600	-3590
4229100300	30.25239	-94.98135	121	--	-2131	-2809	--
4229102426	30.13162	-94.88650	91	--	-2575	--	--
4229102431	30.22577	-94.96396	116	--	-1938	--	--
4229102866	30.07037	-94.89543	74	-1799	-2846	-3340	--
4229103880	30.08064	-95.02643	78	-1414	-2490	-3268	-4350
4229104384	29.94111	-94.89399	47	--	-2211	-3373	-4901
4229105018	30.25893	-95.04544	105	-1422	-2115	-2785	--
4229105450	30.13964	-94.93018	97	-1856	-2841	-3250	--
4229131788	29.91132	-94.87198	48	-1418	-1983	-2964	-4797
4229132387	30.11111	-95.01127	81	-1596	-2451	-3600	--

Appendix A: Geophysical Log Information Including location, Placement on Cross Sections, updated Picks for Stratigraphy and Picks for Base of Salinity Zone

API	Lat (NAD 83)	Long (NAD 83)	Ground Elevation (ft, msl)	Base Elevation (ft, msl)			
				1,000 TDS	3,000 TDS	10,000 TDS	35,000 TDS
4232100341	29.10364	-95.90529	55	--	--	-1427	-1760
4232100435	29.05512	-95.95864	56	-1204	-1264	-1387	--
4232100670	29.06437	-95.78445	35	-709	-1121	-1177	-2053
4232100824	28.81413	-95.69096	8	-550	-1119	-1261	--
4232100836	28.94991	-95.77687	26	-770	-1111	-1189	-1822
4232101026	28.98472	-95.94899	49	-1152	--	-1307	--
4232101064	28.87536	-95.83220	22	-409	-876	-1100	--
4232130497	28.89045	-95.69538	13	-432	-832	-1130	--
4232130952	29.15321	-95.92332	65	-1188	-1389	-1459	-2294
4232131364	28.87683	-95.78901	15	-498	-1017	-1086	--
4233900104	30.32929	-95.48821	187	-950	--	--	--
4233900202	30.28734	-95.45105	174	-1252	-1998	-2745	-4006
4233900910	30.35380	-95.52549	282	-768	--	--	--
4233900926	30.35040	-95.43460	238	-913	--	--	--
4233900934	30.28519	-95.54005	172	-1171	-1367	--	--
4233901014	30.13186	-95.75087	228	-595	-1596	-2443	--
4233901039	30.21397	-95.63763	215	-1438	-2431	--	--
4233901102	30.13868	-95.62143	151	-1373	-2109	-2198	--
4233901109	30.22290	-95.54650	198	-1220	-1633	--	--
4233901142	30.12703	-95.65832	173	-710	--	--	--
4233901387	30.17304	-95.45694	145	-1653	-2060	-2400	--
4233901420	30.12727	-95.44840	124	--	-2049	--	--
4233901423	30.15415	-95.45890	146	-1727	--	-2500	--
4233901604	30.24098	-95.28118	133	-1434	-1721	--	--
4233901718	30.14716	-95.29188	115	-1782	-2436	--	--
4233901732	30.05907	-95.29636	81	--	-2352	-3185	--
4233901734	30.10333	-95.38417	101	-1658	-2083	-2750	--
4233901737	30.11438	-95.40618	103	-1566	-2068	--	--
4233901846	30.18295	-95.19491	106	--	-1991	-2936	--
4233901872	30.31614	-95.29677	195	-1137	-1758	-3041	--
4233901879	30.18368	-95.49519	159	-1552	-1949	--	--
4233901881	30.17530	-95.73288	264	-648	--	--	--
4233930072	30.29016	-95.78422	311	-1322	--	--	--
4233930478	30.27581	-95.70225	178	-999	-2099	-2698	--
4233930704	30.24257	-95.17203	102	--	-1658	--	--
4233930820	30.22918	-95.37157	155	--	-1857	-3323	--
4233930849	30.15412	-95.14774	101	--	-1906	-2841	-4168
4247300014	30.09753	-96.05243	200	-1062	--	--	--

Appendix A: Geophysical Log Information Including location, Placement on Cross Sections, updated Picks for Stratigraphy and Picks for Base of Salinity Zone

API	Lat (NAD 83)	Long (NAD 83)	Ground Elevation (ft, msl)	Base Elevation (ft, msl)			
				1,000 TDS	3,000 TDS	10,000 TDS	35,000 TDS
4247300031	30.18388	-95.99388	287	-1170	--	--	--
4247300037	30.19784	-95.88016	286	-1083	-1800	--	--
4247300049	29.93838	-95.97511	215	-636	-2298	-2946	--
4247300108	29.85491	-95.85487	166	--	--	-3278	--
4247300243	29.97985	-96.09310	135	-1110	--	-2493	--
4247300274	29.91633	-96.10084	135	-1391	-1917	--	--
4247300278	29.82801	-96.08030	143	-718	-1726	--	--
4247300288	29.79902	-96.03348	125	--	--	-3376	--
4247300318	29.90571	-95.93164	193	-636	-2281	-3249	--
4247330027	29.91293	-95.88852	174	-823	-1892	--	--
4247330066	30.21495	-95.81109	250	-1124	-1663	-2518	-3278
4247330401	29.79163	-95.87384	156	-874	-2283	--	--
4247330432	30.17914	-96.01476	290	-960	--	-2790	--
4248100671	29.25823	-95.89117	63	-700	-1370	-1444	--
4248100696	29.29294	-95.97534	84	-1556	-2531	-3446	--
4248100824	29.26967	-95.94209	83	-700	-1589	--	--
4248100943	29.44330	-96.13765	105	-1220	-2758	-3165	--
4248101205	29.47412	-96.19234	137	-1017	--	--	--
4248102562	29.15600	-96.01043	73	-1232	-1683	-1843	-4300
4248130832	29.54556	-96.07528	124	-1114	-3186	--	--
4248132944	29.23562	-96.01585	87	-1583	-1792	--	--
4248133370	29.33491	-96.06911	91	-1545	-2478	--	--
4248133410	29.38637	-96.06225	93	-1537	-2177	-2932	--
4248133442	29.36820	-96.15147	106	-1279	-2148	-2967	--
4248133720	29.59158	-96.14145	135	-1053	--	--	--
4248134117	29.53142	-96.13721	127	-1607	--	--	--
9942201180	29.93077	-95.73363	152	-1225	-1969	--	--
9942201360	29.66024	-95.38508	48	-1897	-2678	-3300	--
9965000000	29.72423	-95.74811	98	-1599	--	--	--
9965000039	30.17333	-95.58361	162	-1476	--	--	--
9965035010	29.95722	-95.68278	136	-920	-2002	--	--
9965144020	29.82583	-95.33528	64	-1500	--	--	--
9965144030	29.81944	-95.33445	51	-1600	--	--	--
9965223010	29.70917	-95.26278	0	-2489	--	--	--

Appendix A: Geophysical Log Information Including location, Placement on
Cross Sections, updated Picks for Stratigraphy and Picks for Base of Salinity Zone

Table A-3 List of geophysical logs with formation picks that update the stratigraphic surfaces developed by Young and others (2012)

API	Dip		Strike		Datum	Base Beaumont	Base Lissie	Base Willis	Upper Goliad	Lower Goliad	Upper Lagarto	Base Lagarto	Lower Lagarto	Oakville	Base Catahoula
	Sec.	Pos.	Sec.	Pos.											
4247100199	D-5	1	--	--	298	--	--	--	--	--	--	--	--	--	--
4247100097	D-5	2	--	--	218	--	--	--	--	--	--	--	--	--	-227
4240700127	D-5	3	--	--	329	--	--	319	--	--	--	73	--	-341	-1117
4240730033	D-5	4	--	--	315	--	--	239	--	--	125	-435	--	-885	-2165
4240730078	D-5	5	--	--	240	--	--	134	--	47	-440	-891	--	-1400	-2840
4240700156	D-5	6	--	--	253	--	253	-112	--	-307	-753	-1167	-1395	-1667	-3142
4240700214	D-5	7	--	--	149	--	149	-261	--	-536	-931	-1491	-1736	-2056	-3614
4229100086	D-5	8	--	--	140	--	-70	-410	--	-1045	-1425	-2005	-2291	-2630	-4140
4229105018	D-5	9	--	--	144	--	-66	-488	--	-1092	-1500	-2116	-2433	-2786	-4401
4229131549	D-5	10	--	--	114	--	-178	-639	--	-1211	-1739	-2381	-2795	-3094	-4855
4229103880	D-5	11	--	--	90	-37	-855	-1410	-1694	-2306	-2894	-3962	-4376	-5064	-7855
4229132099	D-5	12	S-1	16	94	--	-923	-1509	--	-1896	-2390	-3334	-3747	-4321	-6492
4229131788	D-5	13	--	--	73	-263	-915	-1401	-1502	-2557	-3234	-4178	-4670	-5280	-7533
4207131458	D-5	14	--	--	29	-251	-876	-1429	-1911	-3171	-3779	-4746	-5112	-5871	-8240
4207100972	D-5	15	S-2	11	3	-415	-917	-1402	-2062	-3422	-4112	-5147	-5462	-6272	-8617
4207102696	D-5	16	--	--	18	-417	-967	-1482	-2462	-4019	-4647	-5475	-5972	-6954	-9232
4207102740	D-5	17	--	--	20	-430	-1030	-1530	-2421	-3985	-4790	-5660	-6146	-7092	-9614
4207102432	D-5	18	--	--	9	-521	-1131	-1566	-2646	-4451	-5157	-6004	-6509	-7966	--
4216700956	D-5	19	--	--	16	-564	-1154	-1799	-2709	-4579	-5339	-5989	-6814	-9535	--
4216700959	D-5	20	S-3	11	17	-578	-1233	-1853	-2753	-4663	-5552	-6553	-7805	--	--
4270630042	D-5	21	--	--	75	-705	-1295	-2065	-3915	-5735	-7110	-8125	-9712	--	--
4270640031	D-5	22	--	--	90	-755	-1310	-1993	-4086	-6336	-7753	-9183	--	--	--
4270840145	D-5	23	--	--	100	-990	-1708	-2469	-4699	-7123	--	--	--	--	--
4270840289	D-5	24	--	--	95	-1457	-2418	-3405	-8863	--	--	--	--	--	--

Appendix A: Geophysical Log Information Including location, Placement on Cross Sections, updated Picks for Stratigraphy and Picks for Base of Salinity Zone

API	Dip		Strike		Datum	Base Beaumont	Base Lissie	Base Willis	Upper Goliad	Lower Goliad	Upper Lagarto	Base Lagarto	Lower Lagarto	Oakville	Base Catahoula
	Sec.	Pos.	Sec.	Pos.											
4270840174	D-5	25	--	--	101	-1546	-2746	-4110	-8615	--	--	--	--	--	--
4270840166	D-5	26	--	--	85	-1620	-3295	-4481	-11409	--	--	--	--	--	--
4247130022	D-6	1	--	--	405	--	--	--	--	--	--	--	--	--	385?
4247100148	D-6	2	--	--	272	--	--	--	--	--	--	--	--	--	-323
4247100180	D-6	3	--	--	363	--	--	--	--	--	--	--	--	45	-1267
4247100189	D-6	4	--	--	308	--	--	--	--	--	148	-127	--	-452	-1780
4233900868	D-6	5	--	--	270	--	--	--	--	-90	-370	-695	--	-1135	-2670
4233900901	D-6	6	--	--	344	--	--	132	--	-233	-762	-1086	--	-1511	-3033
4233900086	D-6	7	--	--	249	--	--	40	--	-693	-1061	-1391	--	-1811	-3381
4233900202	D-6	8	--	--	184	--	--	-96	--	-531	-1026	-1446	--	-1911	-3531
4233930820	D-6	9	--	--	172	--	89	-218	--	-528	--	-1433	--	-1738	-3323
4233901718	D-6	10	--	--	127	--	-118	-428	--	-1063	-1789	-2293	-2628	-2993	-4523
4220107603	D-6	11	S-1	13	91	--	-459	-884	-884	-1810	-2294	-2849	-3081	-3442	-5089
4220102722	D-6	12	--	--	78	-102	-562	-1037	-1119	-2052	-2567	-3152	-3399	-3832	-5742
4220132038	D-6	13	--	--	65	--	--	--	--	--	-2790	-3360	-3670	-4117	-5995
4220102801	D-6	14	--	--	58	--	--	--	--	--	--	-4007	-4392	-4764	-7012
4220132613	D-6	15	--	--	42	-273	-838	-1458	-1740	-2668	-3383	-4118	-4468	-4878	-7229
4220106044	D-6	16	S-2	9	34	-356	-964	-1360	-1801	-3202	-4132	-4888	-5226	-6061	-9156
4207103096	D-6	17	--	--	20	-400	-850	-1660	-2460	-4110	-4965	-5830	-6340	-7162	N
4216700966	D-6	18	S-3	10	22	-448	-998	-1841	-2853	-4763	-5303	-5998	-6726	-8393	N
4216730091	D-6	19	--	--	15	-790	-1352	-2317	-4765	-7155	-8535	-9550	-9925	N	--
4270640054	D-6	20	--	--	99	-693	-1194	-1863	-3909	-5807	-7420	-8303	-10443	--	--
4270640380	D-6	21	--	--	140	-620	-1099	-1753	-3825	-5733	-7164	-8009	-10144	--	--
4270600141	D-6	22	--	--	65	-669	-1254	-2191	-5446	-8744	--	--	--	--	--
4270640090	D-6	23	--	--	67	-932	-1542	-2533	-6083	-8082	--	--	--	--	--
4270640251	D-6	24	--	--	92	-1131	-1858	-2907	-7966	--	--	--	--	--	--

Appendix A: Geophysical Log Information Including location, Placement on Cross Sections, updated Picks for Stratigraphy and Picks for Base of Salinity Zone

API	Dip		Strike		Datum	Base Beaumont	Base Lissie	Base Willis	Upper Goliad	Lower Goliad	Upper Lagarto	Base Lagarto	Lower Lagarto	Oakville	Base Catahoula
	Sec.	Pos.	Sec.	Pos.											
4270640446	D-6	25	--	--	97	-1162	-1943	-2993	-7706	--	--	--	--	--	--
4270840170	D-6	26	--	--	93	-1253	-2290	-3377	-10344	--	--	--	--	--	--
4270840279	D-6	27	--	--	81	-1234	-2379	-3496	--	--	--	--	--	--	--
4218500061	D-7	1	--	--	263	--	--	--	--	--	--	--	--	--	--
4218500034	D-7	2	--	--	377	--	--	--	--	--	--	--	--	310	-609
4218500150	D-7	3	--	--	378	--	--	--	--	--	78	-57	--	-472	-1994
4218530009	D-7	4	--	--	331	--	--	206	--	-209	-555	-854	--	-1219	-2849
4247330066	D-7	5	--	--	292	--	--	70	--	-500	-925	-1253	--	-1663	-3034
4233901014	D-7	6	--	--	249	--	--	-141	--	-875	-1293	-1651	--	-2121	-3896
4233930852	D-7	7	--	--	210	--	--	-190	--	-905	-1320	-1668	--	-2182	-3970
4220100048	D-7	8	--	--	221	--	159	-189	--	-901	-1279	-1589	--	-2169	-3929
4220100104	D-7	9	--	--	183	--	183	-237	--	-966	-1387	-1697	-2026	-2263	-3907
4220131622	D-7	10	S-1	10	122	--	-208	-780	--	-1675	-2098	-2603	-2818	-3178	-4804
4220103510	D-7	11	--	--	88	28	-238	-812	--	-1812	-2252	-2862	-3366	-3816	-5640
4220104871	D-7	12	--	--	61	-84	-591	-1116	-1253	-2441	-2876	-3421	-3639	-4254	-6584
4220105568	D-7	13	--	--	62	-215	-804	-1204	-1334	-2548	-3172	-3763	-4110	-4793	-6888
4220106114	D-7	14	S-2	7	58	-284	-582	-1214	-1520	-2832	-3652	-4437	-4815	-5682	-8269
4216700035	D-7	15	--	--	49	-341	-641	-1279	-1841	-3201	-3924	-4661	-4931	-5841	-9821
4203900847	D-7	16	--	--	53	-422	-749	-1417	-1847	-3397	-4167	-4817	-5259	-6149	-9978
4216701876	D-7	17	--	--	49	-571	-903	-1591	-2229	-4051	-4961	-5671	-6227	-7426	-10753
4216701453	D-7	18	--	--	45	-570	-1009	-1611	-2387	-4266	-5150	-5970	-6621	-7790	N
4216701448	D-7	19	--	--	38	-577	-1024	-1652	-2457	-4368	-5168	-6052	-6553	-7927	N
4216701336	D-7	20	S-3	8	34	-586	-1072	-1704	-2374	-4348	-5094	-6024	-6501	-8091	--
4216730039	D-7	21	--	--	26	-674	-1084	-1784	-2654	-4584	-5474	-6514	-7243	-8724	--
4216701916	D-7	22	--	--	26	-806	-1254	-1844	-3057	-5214	-6174	-7329	--	-10219	--
4270600086	D-7	23	--	--	52	-678	-1135	-1708	-3422	-6013	-7308	N	--	--	--

Appendix A: Geophysical Log Information Including location, Placement on
Cross Sections, updated Picks for Stratigraphy and Picks for Base of Salinity Zone

API	Dip		Strike		Datum	Base Beaumont	Base Lissie	Base Willis	Upper Goliad	Lower Goliad	Upper Lagarto	Base Lagarto	Lower Lagarto	Oakville	Base Catahoula
	Sec.	Pos.	Sec.	Pos.											
4270640276	D-7	24	--	--	87	--	--	-1789	-4041	-6390	--	--	--	--	--
4270600027	D-7	25	--	--	67	-823	-1255	-1975	-4553	-7604	-8813	-11141	--	--	--
4270640110	D-7	26	--	--	83	--	--	-2060	-6088	--	--	--	--	--	--
4270640376	D-7	27	--	--	89	--	--	-2567	-6410	--	--	--	--	--	--
4270600124	D-7	28	--	--	85	--	--	-2506	-6743	--	--	--	--	--	--
4270640097	D-7	30	--	--	90	--	-2440	--	--	--	--	--	--	--	--
4247730625	D-8	1	--	--	276	--	--	--	--	--	--	--	--	--	276
4247700239	D-8	2	--	--	362	--	--	--	--	--	--	--	--	287	-593
4247700272	D-8	3	--	--	299	--	--	--	--	--	--	--	--	-803	-2081
4247700294	D-8	4	--	--	287	--	--	--	--	-263	-548	-778	--	-1158	-2353
4201530138	D-8	5	--	--	267	--	--	127	1	-435	-736	-1008	--	-1368	-2703
4201500230	D-8	6	--	--	160	--	154	-20	-188	-633	-850	-1185	--	-1535	-2740
4247300243	D-8	7	--	--	152	--	128	-128	-249	-726	-951	-1308	--	-1523	-2702
4247300049	D-8	8	--	--	224	--	--	-226	-1121	-1926	-2104	-2513	--	-2834	-4300
4247300318	D-8	9	--	--	211	--	-19	-259	-968	-1771	-2173	-3024	--	-3024	-4634
4247300199	D-8	10	--	--	186	--	-182	-422	-707	-1401	-1860	-2415	--	-2902	-4773
4247330043	D-8	11	--	--	175	--	-129	-346	-711	-1395	-1802	-2268	--	-2787	-4528
4215700001	D-8	12	--	--	155	--	-193	-425	-785	-1515	-1955	-2405	--	-2945	-4645
4215701026	D-8	13	--	--	122	--	-366	-663	-898	-1893	-2328	-2868	-3137	-3472	-5253
4215731983	D-8	14	S-1	6	102	24	-405	-693	-938	-1888	-2428	-3138	-3348	-3778	-5700
4215700894	D-8	15	--	--	89	-186	-501	-778	-1419	-2481	-2983	-3718	-4071	-4556	-6712
4215701974	D-8	16	--	--	72	-210	-747	-1140	-1730	-2788	-3242	-4048	-4454	-5128	N
4215702459	D-8	17	S-2	4	73	-217	-752	-1179	-1656	-2747	-3235	-4082	-4477	-5177	-7237
4215702320	D-8	18	--	--	40	-357	-885	-1232	-1367	-2442	-3089	-3896	-4282	-4960	N
4203901815	D-8	19	--	--	62	-362	-846	-1165	-1769	-2913	-3623	-4443	-4863	-5727	-8172
4203904823	D-8	20	--	--	57	-355	-829	-1136	-2224	-3622	-4252	-5128	-5642	-6620	N

Appendix A: Geophysical Log Information Including location, Placement on
Cross Sections, updated Picks for Stratigraphy and Picks for Base of Salinity Zone

API	Dip		Strike		Datum	Base Beaumont	Base Lissie	Base Willis	Upper Goliad	Lower Goliad	Upper Lagarto	Base Lagarto	Lower Lagarto	Oakville	Base Catahoula
	Sec.	Pos.	Sec.	Pos.											
4203901452	D-8	21	--	--	54	-364	-868	-1166	-2196	-3714	-4299	-5118	-5609	-6686	N
4203904224	D-8	22	S-3	5	45	-415	-950	-1275	-2210	-3645	-4412	-5338	-6345	-7985	N
4203904277	D-8	23	--	--	22	-561	-1158	-1468	-2471	-4385	-4958	-6008	-7318	-8857	N
4203904291	D-8	24	--	--	14	-646	-1171	-1506	-2971	-4665	-6325	-7401	N	--	--
4270600022	D-8	25	--	--	25	-830	-1370	-1724	-3715	-6195	-7555	-8975	N	--	--
4270640355	D-8	26	--	--	93	--	--	--	-4364	-6913	--	-11058	--	--	--
4270640434	D-8	27	--	--	95	--	--	--	-6454	-8755	--	-11790	--	--	--
4270640212	D-8	28	--	--	89	--	--	--	-6371	--	--	--	--	--	--
4247700366	D-9	1	--	--	438	--	--	--	--	--	--	--	--	340	-417
4201500017	D-9	2	--	--	335	--	--	--	--	--	--	-296	--	-697	-1665
4201530539	D-9	3	--	--	314	--	--	--	--	150	--	-513	--	-956	-2041
4201500663	D-9	4	--	--	263	--	--	23	--	-607	-869	-1297	--	-1737	-3052
4201500262	D-9	5	--	--	212	--	108	-98	--	-883	-1141	-1537	--	-1969	-3503
4201530601	D-9	6	--	--	161	--	-76	-208	-968	-1815	-2215	-2636	-2829	-3058	-4755
4201500683	D-9	7	--	--	152	--	-85	-342	-470	-1463	-1753	-2167	-2392	-2725	-4689
4248134100	D-9	8	--	--	137	71	-181	-384	-522	-1567	-1857	-2342	-2656	-3013	-5167
4215731752	D-9	9	--	--	141	-12	-259	-489	-859	-1907	-2301	-2819	-3205	-3622	-5636
4215731805	D-9	10	S-1	4	120	-85	-270	-632	-960	-2110	-2470	-3110	-3483	-3946	-5845
4215701392	D-9	11	--	--	108	-111	-350	-684	-1152	-2397	-2782	-3434	-3852	-4285	-6285
4215730122	D-9	12	--	--	98	-195	-511	-813	-1441	-2801	-3265	-3929	-4304	-4847	-6998
4215701674	D-9	13	--	--	77	-223	-583	-923	-1548	-2945	-3423	-4073	-4513	-5087	--
4215731815	D-9	14	S-2	2	92	-175	-601	-963	-1772	-3114	-3660	-4363	-4790	-5376	-7753
4203902752	D-9	15	--	--	66	-278	-597	-1009	-1820	-3342	-3834	-4521	-5107	-6021	N
4203902865	D-9	16	--	--	57	-479	-881	-1325	-1903	-3619	-4215	-4923	-5678	-6626	N
4203903754	D-9	17	--	--	47	-564	-917	-1358	-2275	-3294	-4104	-4912	-5618	-6990	N
4203903878	D-9	18	--	--	21	-669	-1008	-1431	-2363	-3426	-4325	-5143	-5856	-7811	N

Appendix A: Geophysical Log Information Including location, Placement on
Cross Sections, updated Picks for Stratigraphy and Picks for Base of Salinity Zone

API	Dip		Strike		Datum	Base Beaumont	Base Lissie	Base Willis	Upper Goliad	Lower Goliad	Upper Lagarto	Base Lagarto	Lower Lagarto	Oakville	Base Catahoula
	Sec.	Pos.	Sec.	Pos.											
4203903898	D-9	19	--	--	48	-682	-1042	-1512	-2273	-3466	-4322	-5252	-6079	-7947	N
4203930350	D-9	20	S-3	2	34	-684	-1296	-1643	-2416	-4066	-4691	-5726	-7001	-9059	N
4203932110	D-9	21	--	--	30	-790	-1262	-1815	-2983	-4672	-5160	-6755	N	--	--
4203904811	D-9	22	--	--	23	-777	-1302	-1597	-3112	-4887	-6027	-7989	N	--	--
4270640256	D-9	23	--	--	99	--	--	-1761	-3987	-5846	--	--	--	--	--
4270600071	D-9	24	--	--	47	--	--	-1803	-4491	-7701	--	--	--	--	--
4270640020	D-9	25	--	--	84	--	--	-1945	-4851	-9473	--	--	--	--	--
4270640360	D-9	26	--	--	100	--	--	-2723	-6233	N	--	--	--	--	--
4214932088	D-10	1	--	--	388	--	--	--	--	--	--	--	--	--	-2
4214931329	D-10	2	--	--	417	--	--	--	--	--	--	282	--	-59	-663
4208931531	D-10	3	--	--	293	--	--	184	--	-249	-348	-609	--	-1037	-1900
4208900057	D-10	4	--	--	250	--	--	131	--	-386	-538	-822	--	-1197	-2065
4208900090	D-10	5	--	--	331	--	--	16	-130	-709	-922	-1219	--	-1616	-2569
4208931246	D-10	6	--	--	232	--	104	-93	-423	-1110	-1348	-1688	--	-2234	-3333
4208900270	D-10	7	--	--	179	--	-131	-428	-867	-1559	-1837	-2288	--	-2883	-4379
4248101218	D-10	8	--	--	176	--	-47	-330	-781	-1664	-1892	-2377	--	-3006	-4617
4248101205	D-10	9	--	--	137	--	-113	-370	-991	-1473	-2033	-2553	-2928	-3245	-4861
4248134033	D-10	10	--	--	137	69	-163	-518	-998	-1923	-2313	-2738	-3157	-3580	-5333
4248132039	D-10	11	--	--	114	--	-184	-495	-1333	-2200	-2673	-3065	-3415	-3866	-5761
4248133442	D-10	12	S-1	1	125	1	-197	-463	-1266	-2240	-2605	-3061	-3381	-3918	-5742
4248101038	D-10	13	--	--	102	--	--	-562	-1497	-2581	-3047	-3584	-3938	-4487	-6339
4248132944	D-10	14	S-2	1	121	-112	-384	-677	-1613	-2802	-3549	-4351	-4652	-5257	-7117
4248102562	D-10	15	--	--	92	-200	-463	-748	-1338	-2448	-3138	-3779	-4288	-5158	N
4232100341	D-10	16	--	--	69	-352	-694	-1098	-1664	-3240	-4115	-4801	-5466	-6361	N
4232100553	D-10	17	--	--	67	--	--	-1142	-1577	-3275	-4208	-4894	-5695	-6880	N
4232100670	D-10	18	--	--	56	-461	-944	-1256	-1792	-3614	-4400	-5334	-6255	-7604	N

Appendix A: Geophysical Log Information Including location, Placement on
Cross Sections, updated Picks for Stratigraphy and Picks for Base of Salinity Zone

API	Dip		Strike		Datum	Base Beaumont	Base Lissie	Base Willis	Upper Goliad	Lower Goliad	Upper Lagarto	Base Lagarto	Lower Lagarto	Oakville	Base Catahoula
	Sec.	Pos.	Sec.	Pos.											
4232100836	D-10	19	S-3	1	46	-388	-923	-1218	-1828	-3825	-4404	-5823	-6949	-8783	N
4232131008	D-10	20	--	--	49	-556	-973	-1242	-2097	-4016	-4626	-6195	--	-8555	--
4232100824	D-10	21	--	--	29	-631	-1104	-1353	-2593	-4585	-5239	-7790	--	-13371	N
4232131592	D-10	22	--	--	17	-693	-1205	-1496	-2742	-4834	-5366	--	--	--	--
4270430073	D-10	23	--	--	71	-759	-1257	-1507	-2954	-5265	-6587	--	--	--	--
4270400071	D-10	24	--	--	79	-891	-1349	-1631	-4361	-7059	N	--	--	--	--
4270430005	D-10	25	--	--	55	--	-1547	-1800	-5785	--	--	--	--	--	--
4270400070	D-10	26	--	--	77	-1048	-1778	-2083	-7088	--	--	--	--	--	--
4270440026	D-10	27	--	--	82	--	--	-2137	-7299	--	--	--	--	--	--
4220107892	--	--	--	--	294	--	--	-107	--	1218	--	-1984	--	-2478	-4052
4220131129	--	--	--	--	164	--	99	-290	--	-1326	-1753	-2147	-2452	-2744	-4466
4220103982	--	--	--	--	157	--	-166	-450	-499	-1557	--	-2314	-2837	-3121	-4673
4220108007	--	--	--	--	116	6	-391	-763	-883	-2104	-2449	-2864	-3109	-3429	-5079
4220104068	--	--	--	--	86	-33	-601	-1017	-1123	-2429	--	-3161	-3360	-3753	-5496
4215731513	--	--	--	--	84	-200	-728	-1125	-1727	-3192	-3599	-3998	-4323	-5006	-7234
4203900015	--	--	--	--	58	-303	-929	-1428	-2059	-3526	-3806	-4395	-4723	-5496	-7978
4203930346	--	--	S-2	6	68	-390	-885	-1448	-1748	-3254	-3561	-4177	-4573	-5305	-7809
4203901203	--	--	--	--	59	-371	-914	-1414	-2104	-3610	-4018	-4583	-4896	-5768	-8357
4203901526	--	--	-	-	45	-396	-988	-1414	-2363	-3603	-4327	-5177	-5642	-6859	NP
4203900984	--	--	--	--	45	-479	-936	-1482	-2158	-3918	-4700	-5637	-6295	-7845	NP
4203901032	--	--	--	--	40	-494	-1025	-1433	-2396	-4189	-4975	-5559	-6365	-8134	NP
4203904481	--	--	S-3	7	28	-552	-1071	-1428	-2196	-3718	-4616	-5308	-5954	-7644	NP
4203930506	--	--	--	--	22	-547	-998	-1436	-2221	-3758	-4369	-5461	-6376	-8418	NP
4203904518	--	--	--	--	12	-615	-1013	-1498	-2914	-4866	-5613	-7232	NP	--	--
4270600088	--	--	--	--	80	-710	-1188	-1691	-3484	-5817	-7220	-8602	NP	--	--
4215701350	--	--	--	--	128	--	-16	-373	-880	-1797	--	-2621	-2953	-3220	-5237

Appendix A: Geophysical Log Information Including location, Placement on
Cross Sections, updated Picks for Stratigraphy and Picks for Base of Salinity Zone

API	Dip		Strike		Datum	Base Beaumont	Base Lissie	Base Willis	Upper Goliad	Lower Goliad	Upper Lagarto	Base Lagarto	Lower Lagarto	Oakville	Base Catahoula
	Sec.	Pos.	Sec.	Pos.											
4215731695	--	--	--	--	151	--	-230	-483	-905	-1915	--	-2750	-3052	-3411	-6251
4215731108	--	--	S-1	5	120	--	-387	-651	-901	-2073	-2484	-3110	-3434	-3843	-5804
4215702819	--	--	--	--	121	--	-451	-652	-812	-2052	-2474	-3060	-3463	-3872	-5793
4215701752	--	--	--	--	89	-227	-528	-900	-1021	-2392	-2752	-3409	-3807	-4292	-5625
4215701729	--	--	--	--	92	-97	-533	-870	-1326	-2755	-3133	-3902	-4330	-4938	NP
4215731388	--	--	--	--	86	-144	-516	-887	-1278	-2652	-3068	-3798	-4207	-4787	NP
4215730976	--	--	S-2	3	84	-249	-621	-998	-1430	-2863	-3441	-4151	-4580	-5192	-7345
4215702199	--	--	--	--	64	-298	-721	-1040	-2033	-3411	-4015	-4664	-5130	-5900	NP
4203901916	--	--	--	--	59	-450	-817	-1115	-1838	-3158	-3903	-4494	-5075	-6235	NP
4203931761	--	--	--	--	49	-474	-947	-1353	-2008	-3487	-4078	-4773	-5392	NP	--
4203904181	--	--	S-3	4	40	-557	-1096	-1477	-2461	-3827	-4515	-5360	-6333	-8097	NP
4203904467	--	--	--	--	35	-567	-1091	-1477	-2957	-4360	-5252	-6262	-7258	-9162	NP
4203904402	--	--	--	--	18	--	-1140	-1461	-3357	-4943	-6073	-6995	NP	--	--
4203932225	--	--	--	--	21	--	-1159	-1439	-2862	-4483	-5851	NP	--	--	--
4248133410	--	--	S-1	2	106	--	-316	-653	-994	-2089	-2490	-2940	-3327	-3753	-5588
4248100997	--	--	S-1	3	88	--	-257	-658	-986	-1983	-2435	-2988	-3384	-3851	-5626
4215700940	--	--	S-1	7	107	--	-597	-748	-929	-2137	-2581	-3043	-3366	-3714	-5388
4220104395	--	--	S-1	8	91	--	-514	-766	-891	-2044	-2492	-2934	-3205	-3607	-5289
4220108007	--	--	S-1	9	116	6	-391	-763	-883	-2104	-2449	-2864	-3109	-3429	-5079
4220103252	--	--	S-1	11	87	--	-413	-948	--	-1655	-2118	-2723	-2929	-3333	-4938
4220102972	--	--	S-1	12	83	--	-509	-915	-1004	-1786	-2180	-2820	-3026	-3415	-4997
4220130958	--	--	S-1	14	109	-18	-446	-871	-1041	-1921	-2471	-3051	-3444	-3903	-5802
4229105498	--	--	S-1	15	85	--	--	-1204	-1443	-2415	-2963	-3610	-3914	-4279	-6507
4215731152	--	--	S-2	5	96	-293	-743	-1213	-1832	-3093	-3688	-4552	-4883	-5696	-8241
4220131368	--	--	S-2	8	41	-374	-1122	-1472	-1899	-3317	-4139	-4844	-5262	-5958	-8609
4207103062	--	--	S-2	10	18	-425	-934	-1370	-1781	-3228	-4054	-4936	-5264	-6029	N

Appendix A: Geophysical Log Information Including location, Placement on Cross Sections, updated Picks for Stratigraphy and Picks for Base of Salinity Zone

API	Dip		Strike		Datum	Base Beaumont	Base Lissie	Base Willis	Upper Goliad	Lower Goliad	Upper Lagarto	Base Lagarto	Lower Lagarto	Oakville	Base Catahoula
	Sec.	Pos.	Sec.	Pos.											
4203903888	--	--	S-3	3	36	-518	-1071	-1624	-2264	-3396	-4447	-5141	-6293	-8180	N
4203904271	--	--	S-3	6	30	-489	-1003	-1433	-2633	-4049	-5034	-5928	-6869	-8692	N
4216701387	--	--	S-3	9	33	-536	-978	-1762	-2327	-4183	-4737	-5296	-6058	-7815	N
4270800022	--	--	S-3	12	40	-710	-1356	-1717	-3820	-5495	-6235	-7405	-8036	N	--
4233930737	--	--	--	--	97	--	--	--	--	--	--	--	--	-2738	--
4201530738	--	--	--	--	129	--	-68	-428	-678	-1348	-1818	-2100	-2698	-3211	--
4203902715	--	--	--	--	61	-188	-403	-738	-1168	-1868	-2328	-3018	-4168	-5053	--

Appendix A: Geophysical Log Information Including location, Placement on
Cross Sections, updated Picks for Stratigraphy and Picks for Base of Salinity Zone

This page is intentionally left blank.

Appendix B

**Maps of Percent Sand and Clay, Total Sand and Clay Thickness,
and Maximum Sand and Clay Interval for Geological Formations**

This page is intentionally left blank.

Appendix B: Maps of Percent Sands, Total Sand Thickness, and
Maximum Sand Interval for Geological Formations

LIST OF FIGURES

Figure B-1	Maps of log coverage, sand percentage, total sand thickness and maximum sand interval for the Beamount Formation in the Chicot Aquifer. Log coverage is the percentage of the formation intersected by the portion of the geophysical log analyzed for the presence of sand beds.....	B-1
Figure B-2	Maps of log coverage, sand percentage, total sand thickness and maximum sand interval for the Lisse Formation in the Chicot Aquifer. Log coverage is the percentage of the formation intersected by the portion of the geophysical log analyzed for the presence of sand beds.....	B-2
Figure B-3	Maps of log coverage, sand percentage, total sand thickness and maximum sand interval for the Willis Formation in the Chicot Aquifer. Log coverage is the percentage of the formation intersected by the portion of the geophysical log analyzed for the presence of sand beds.....	B-3
Figure B-4	Maps of log coverage, sand percentage, total sand thickness and maximum sand interval for the Upper Goliad Formation in the Evangeline Aquifer. Log coverage is the percentage of the formation intersected by the portion of the geophysical log analyzed for the presence of sand beds.....	B-4
Figure B-5	Maps of log coverage, sand percentage, total sand thickness and maximum sand interval for the Lower Goliad Formation in the Evangeline Aquifer. Log coverage is the percentage of the formation intersected by the portion of the geophysical log analyzed for the presence of sand beds.....	B-5
Figure B-6	Maps of log coverage, sand percentage, total sand thickness and maximum sand interval for the Upper Lagarto Formation in the Evangeline Aquifer. Log coverage is the percentage of the formation intersected by the portion of the geophysical log analyzed for the presence of sand beds.....	B-6
Figure B-7	Maps of log coverage, sand percentage, total sand thickness and maximum sand interval for the Middle Lagarto Formation in the Burkeville Confining Unit. Log coverage is the percentage of the formation intersected by the portion of the geophysical log analyzed for the presence of sand beds.....	B-7
Figure B-8	Maps of log coverage, sand percentage, total sand thickness and maximum sand interval for the Lower Lagarto Formation in the Jasper Aquifer. Log coverage is the percentage of the formation intersected by the portion of the geophysical log analyzed for the presence of sand beds.	B-8
Figure B-9	Maps of log coverage, sand percentage, total sand thickness and maximum sand interval for the Oakville Formation in the Jasper Aquifer. Log coverage is the percentage of the formation intersected by the portion of the geophysical log analyzed for the presence of sand beds.....	B-9
Figure B-10	Maps of log coverage, clay percentage, and total clay thickness for the Beamount Formation in the Chicot Aquifer. Log coverage is the percentage of the formation intersected by the portion of the geophysical log analyzed for the presence of clay beds.....	B-10
Figure B-11	Maps of log coverage, clay percentage, and total clay thickness for the Lissie Formation in the Chicot Aquifer. Log coverage is the percentage of the formation intersected by the portion of the geophysical log analyzed for the presence of clay beds.....	B-11

Appendix B: Maps of Percent Sands, Total Sand Thickness, and
Maximum Sand Interval for Geological Formations

Figure B-12	Maps of log coverage, clay percentage, and total clay thickness for the Willis Formation in the Chicot Aquifer. Log coverage is the percentage of the formation intersected by the portion of the geophysical log analyzed for the presence of clay beds.....	B-12
Figure B-13	Maps of log coverage, clay percentage, and total clay thickness for the Upper Goliad Formation in the Evangeline Aquifer. Log coverage is the percentage of the formation intersected by the portion of the geophysical log analyzed for the presence of clay beds.	B-13
Figure B-14	Maps of log coverage, clay percentage, and total clay thickness for the Lower Goliad Formation in the Evangeline Aquifer. Log coverage is the percentage of the formation intersected by the portion of the geophysical log analyzed for the presence of clay beds.	B-14
Figure B-15	Maps of log coverage, clay percentage, and total clay thickness for the Upper Lagarto Formation in the Evangeline Aquifer. Log coverage is the percentage of the formation intersected by the portion of the geophysical log analyzed for the presence of clay beds.	B-15
Figure B-16	Maps of log coverage, clay percentage, and total clay thickness for the Middle Lagarto Formation in the Burkeville Confining Unit. Log coverage is the percentage of the formation intersected by the portion of the geophysical log analyzed for the presence of clay beds.	B-16
Figure B-17	Maps of log coverage, clay percentage, and total clay thickness for the Lower Lagarto Formation in the Jasper Aquifer. Log coverage is the percentage of the formation intersected by the portion of the geophysical log analyzed for the presence of clay beds.	B-17
Figure B-18	Maps of log coverage, clay percentage, and total clay thickness for the Oakville Formation in the Jasper Aquifer. Log coverage is the percentage of the formation intersected by the portion of the geophysical log analyzed for the presence of clay beds.....	B-18

Appendix B: Maps of Percent Sands, Total Sand Thickness, and Maximum Sand Interval for Geological Formations

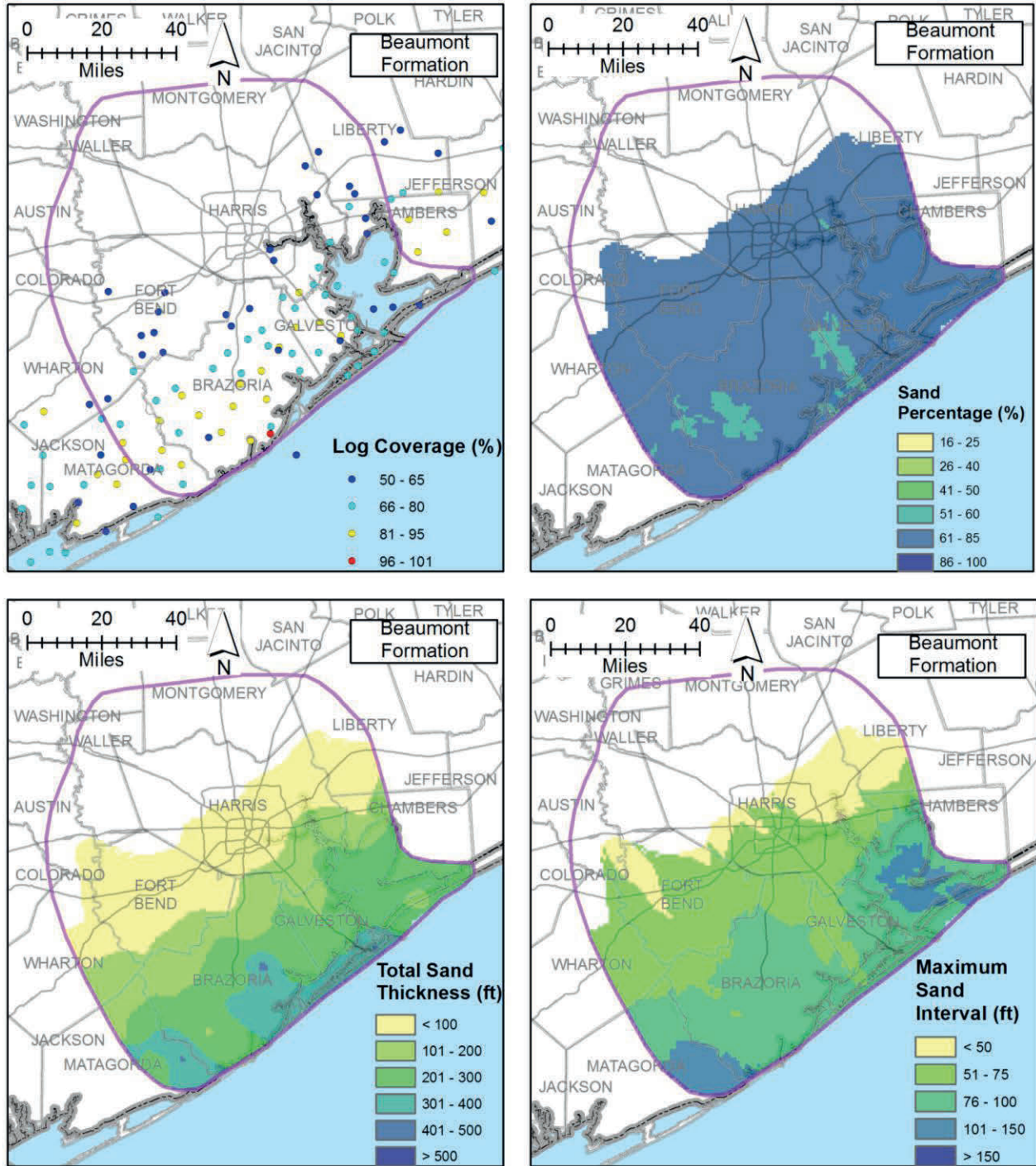


Figure B-1 Maps of log coverage, sand percentage, total sand thickness and maximum sand interval for the Beaumont Formation in the Chicot Aquifer. Log coverage is the percentage of the formation intersected by the portion of the geophysical log analyzed for the presence of sand beds.

Appendix B: Maps of Percent Sands, Total Sand Thickness, and Maximum Sand Interval for Geological Formations

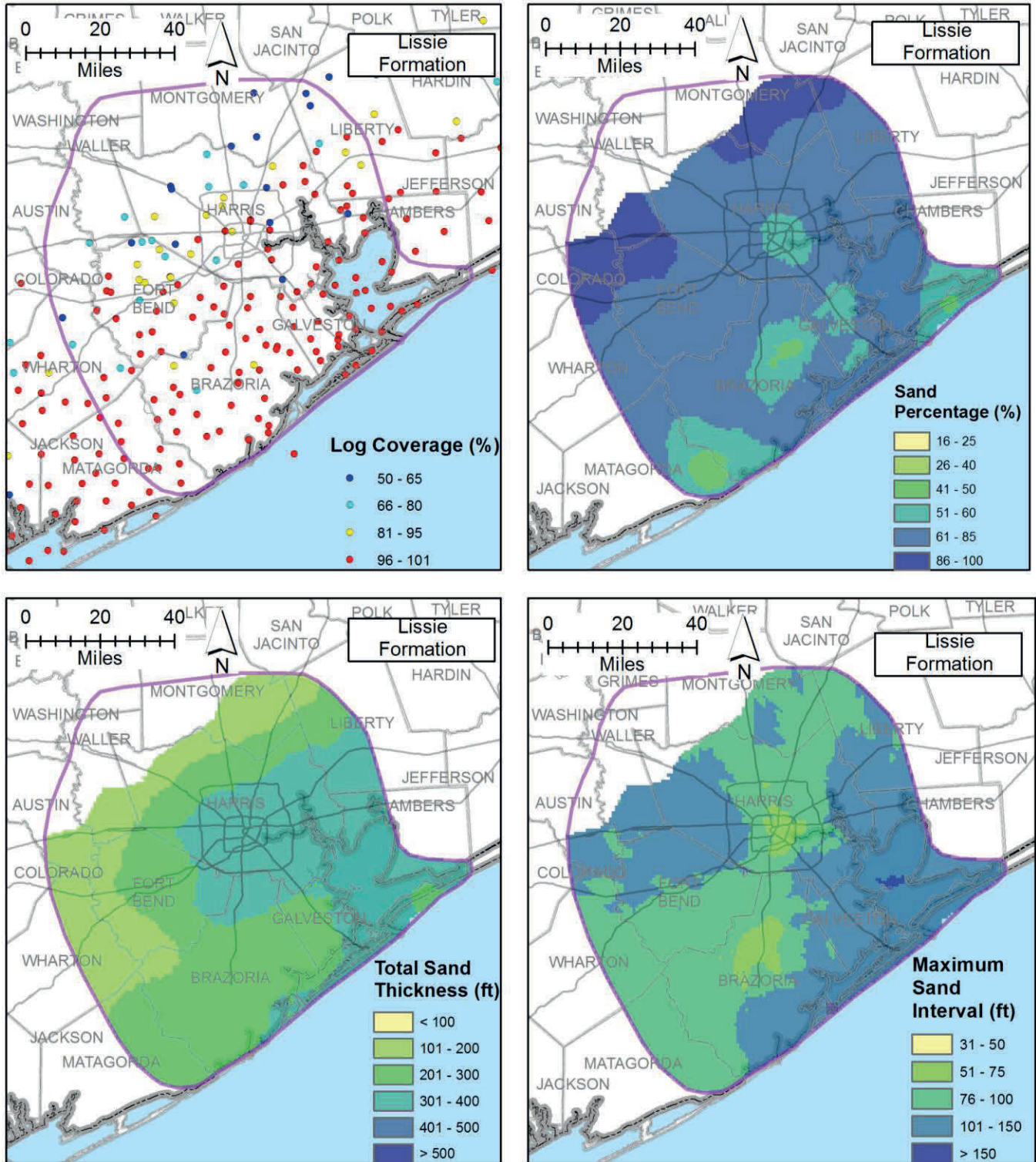


Figure B-2 Maps of log coverage, sand percentage, total sand thickness and maximum sand interval for the Lissie Formation in the Chicot Aquifer. Log coverage is the percentage of the formation intersected by the portion of the geophysical log analyzed for the presence of sand beds.

Appendix B: Maps of Percent Sands, Total Sand Thickness, and Maximum Sand Interval for Geological Formations

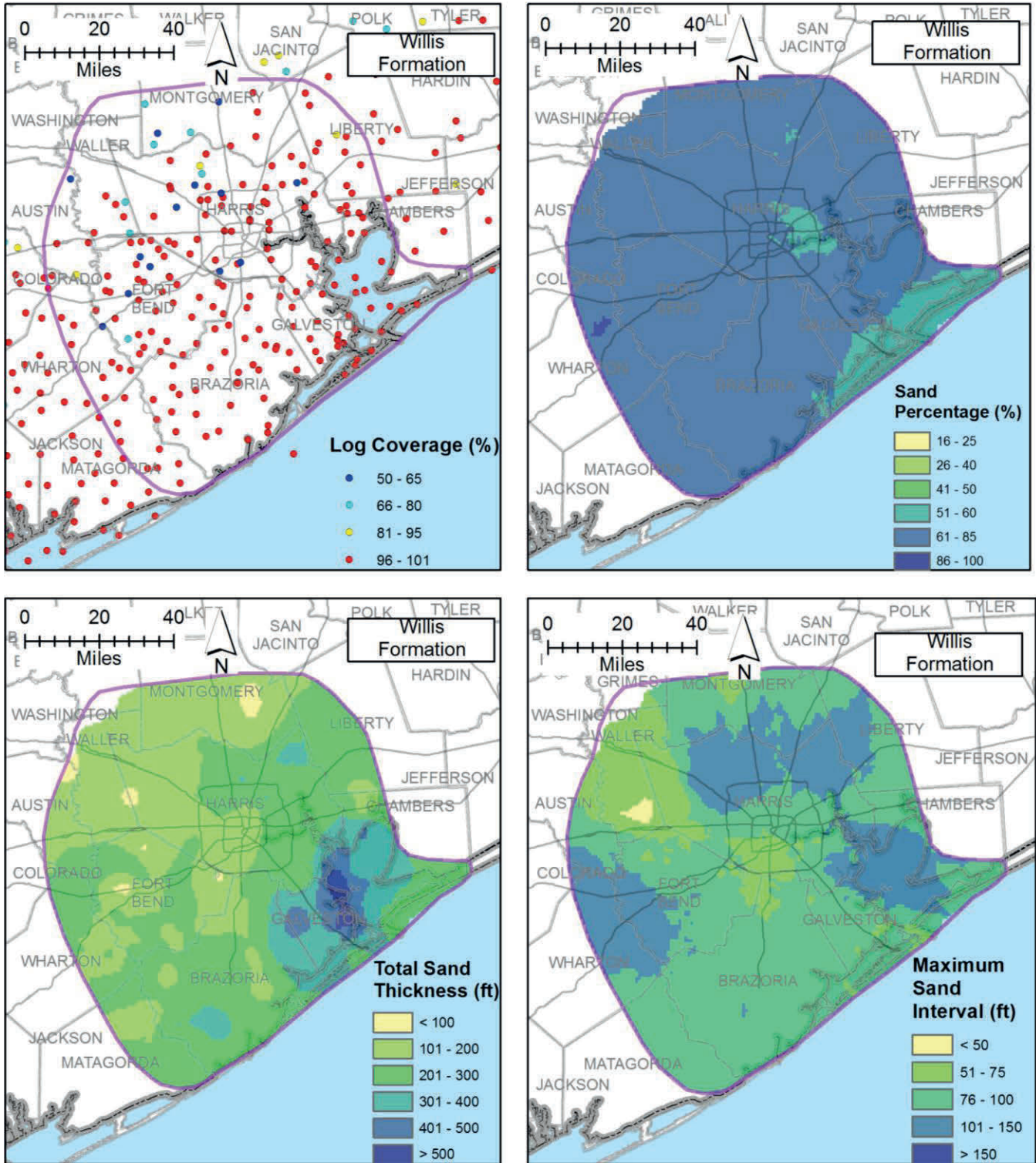


Figure B-3 Maps of log coverage, sand percentage, total sand thickness and maximum sand interval for the Willis Formation in the Chicot Aquifer. Log coverage is the percentage of the formation intersected by the portion of the geophysical log analyzed for the presence of sand beds.

Appendix B: Maps of Percent Sands, Total Sand Thickness, and Maximum Sand Interval for Geological Formations

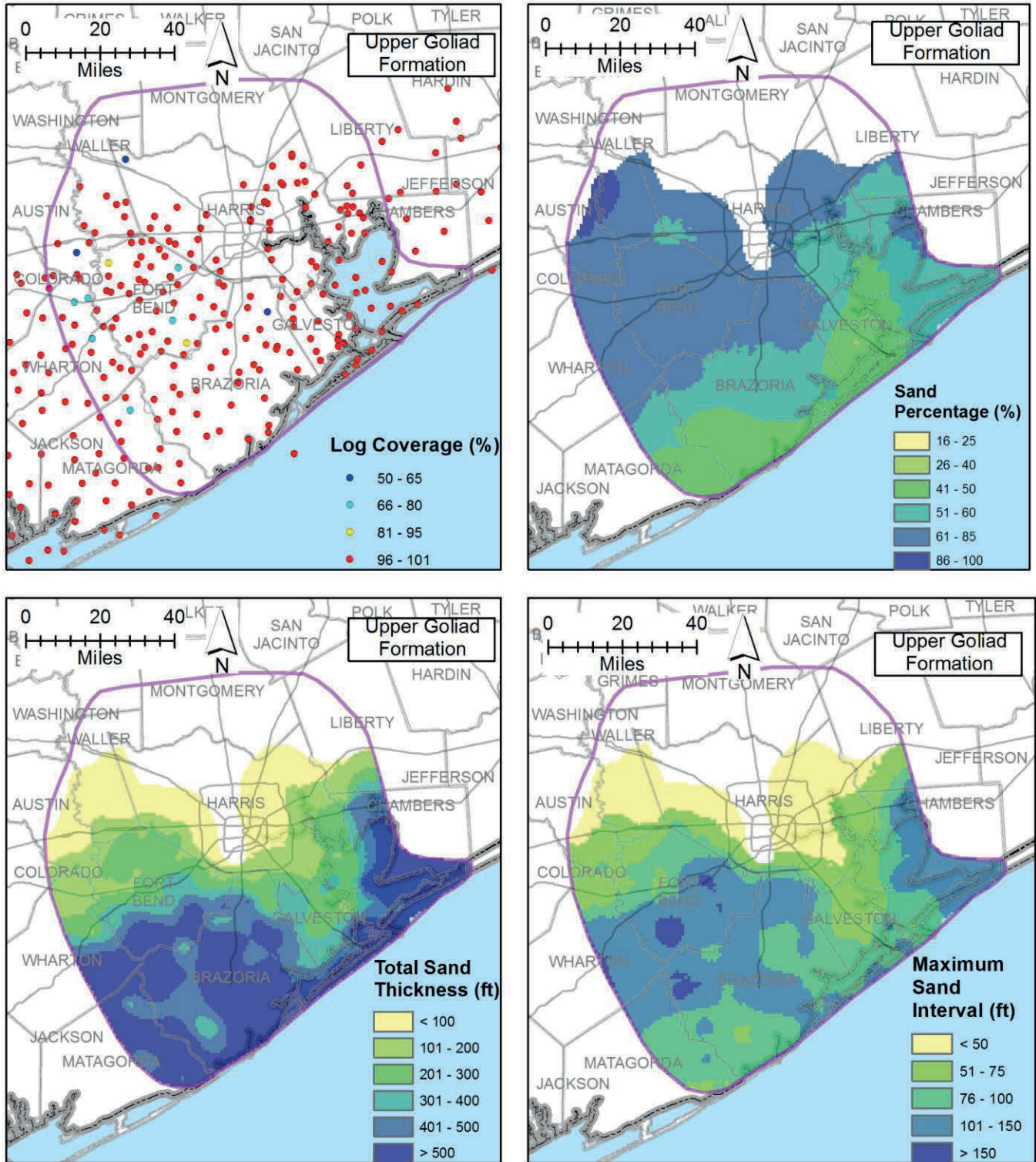


Figure B-4 Maps of log coverage, sand percentage, total sand thickness and maximum sand interval for the Upper Goliad Formation in the Evangeline Aquifer. Log coverage is the percentage of the formation intersected by the portion of the geophysical log analyzed for the presence of sand beds.

Appendix B: Maps of Percent Sands, Total Sand Thickness, and Maximum Sand Interval for Geological Formations

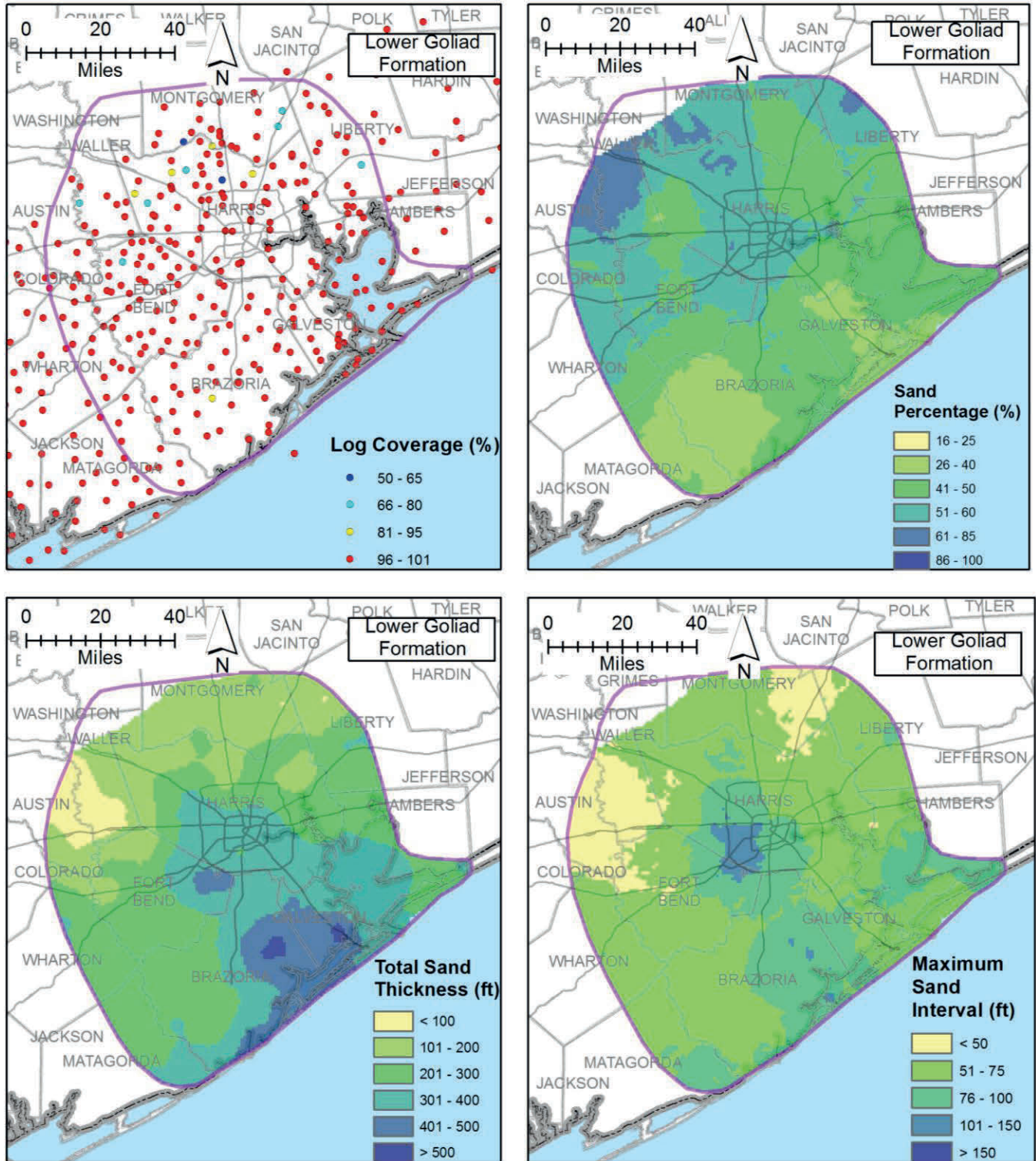


Figure B-5 Maps of log coverage, sand percentage, total sand thickness and maximum sand interval for the Lower Goliad Formation in the Evangeline Aquifer. Log coverage is the percentage of the formation intersected by the portion of the geophysical log analyzed for the presence of sand beds.

Appendix B: Maps of Percent Sands, Total Sand Thickness, and Maximum Sand Interval for Geological Formations

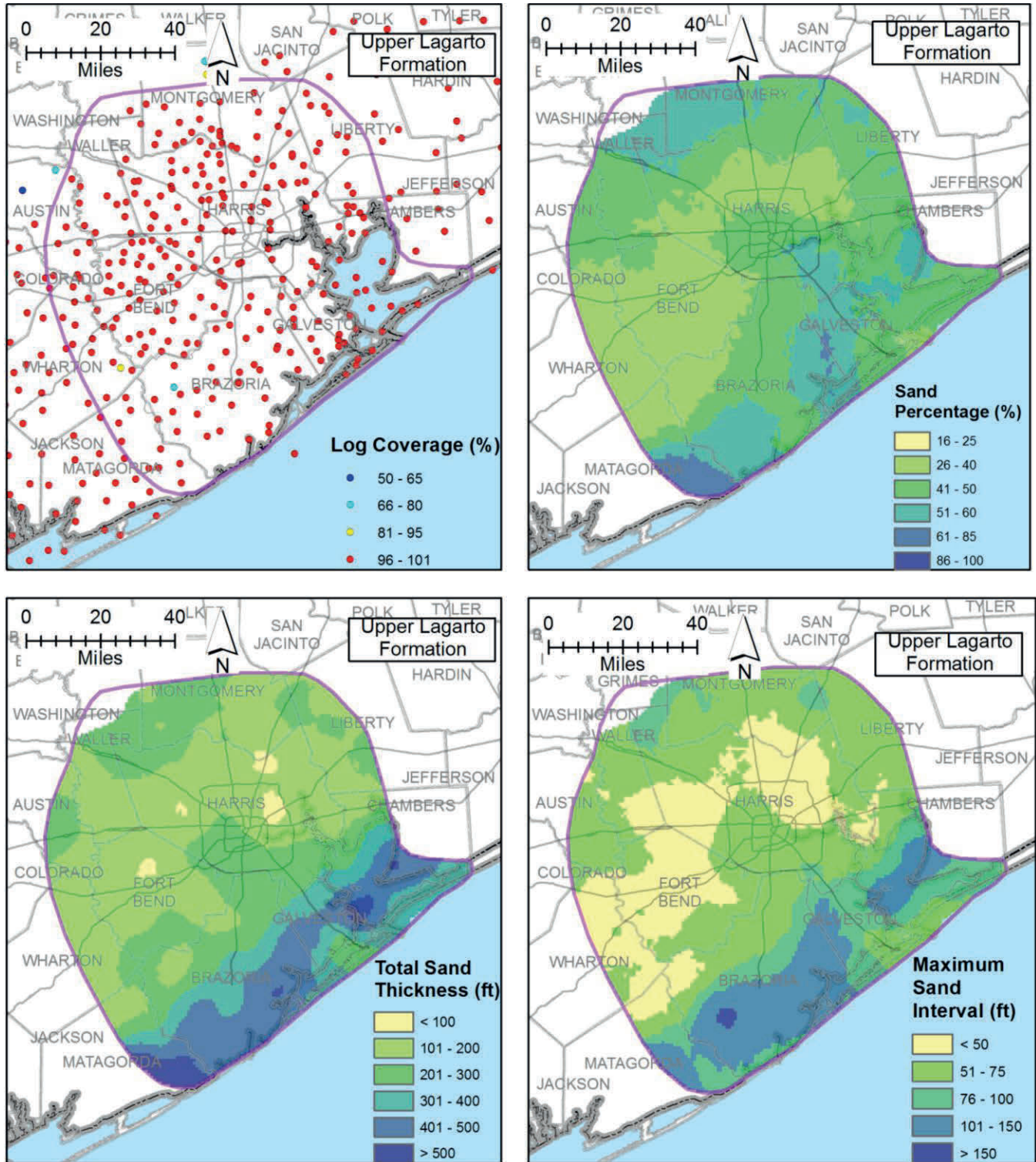


Figure B-6 Maps of log coverage, sand percentage, total sand thickness and maximum sand interval for the Upper Lagarto Formation in the Evangeline Aquifer. Log coverage is the percentage of the formation intersected by the portion of the geophysical log analyzed for the presence of sand beds.

Appendix B: Maps of Percent Sands, Total Sand Thickness, and Maximum Sand Interval for Geological Formations

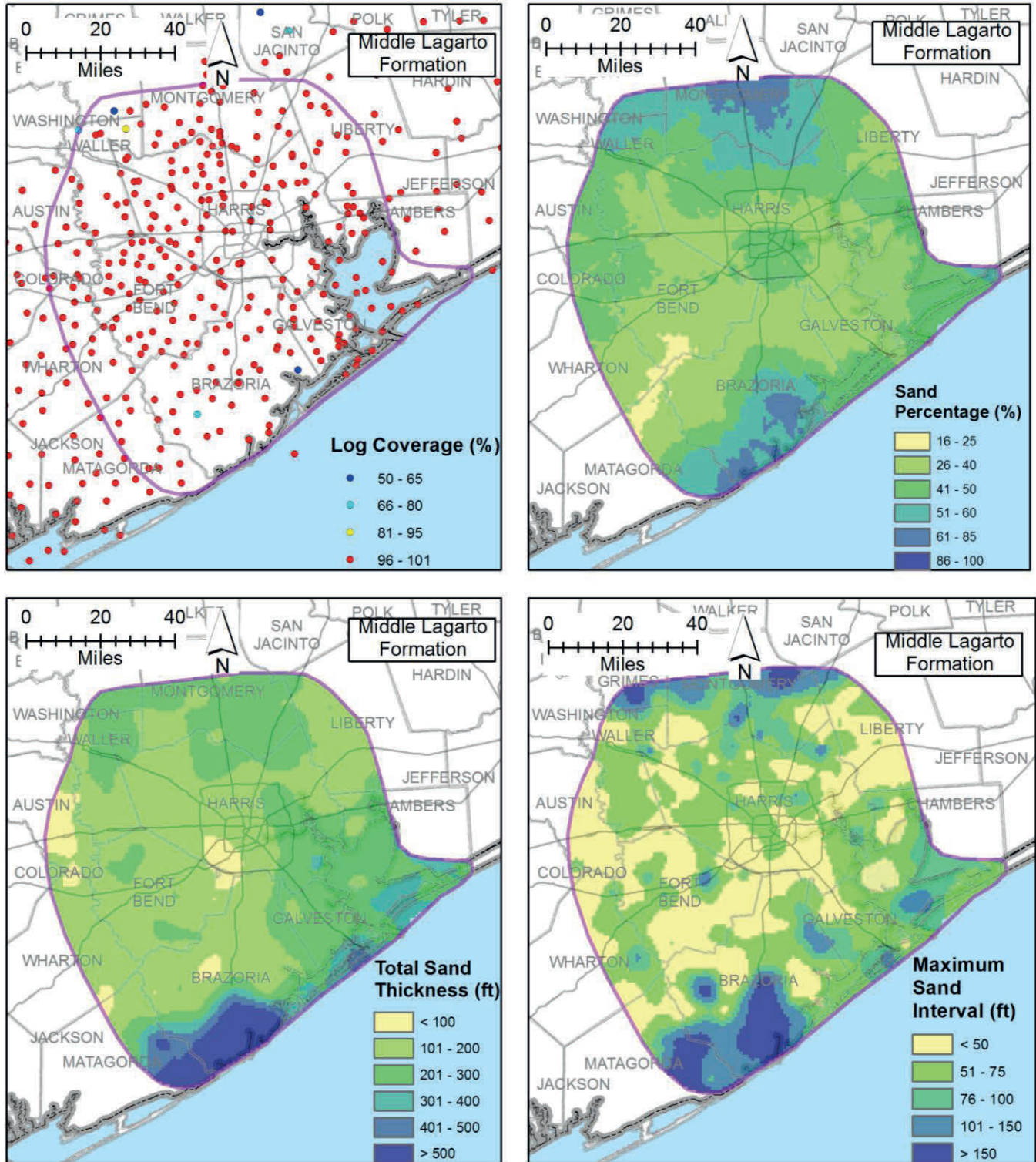


Figure B-7 Maps of log coverage, sand percentage, total sand thickness and maximum sand interval for the Middle Lagarto Formation in the Burkeville Confining Unit. Log coverage is the percentage of the formation intersected by the portion of the geophysical log analyzed for the presence of sand beds.

Appendix B: Maps of Percent Sands, Total Sand Thickness, and Maximum Sand Interval for Geological Formations

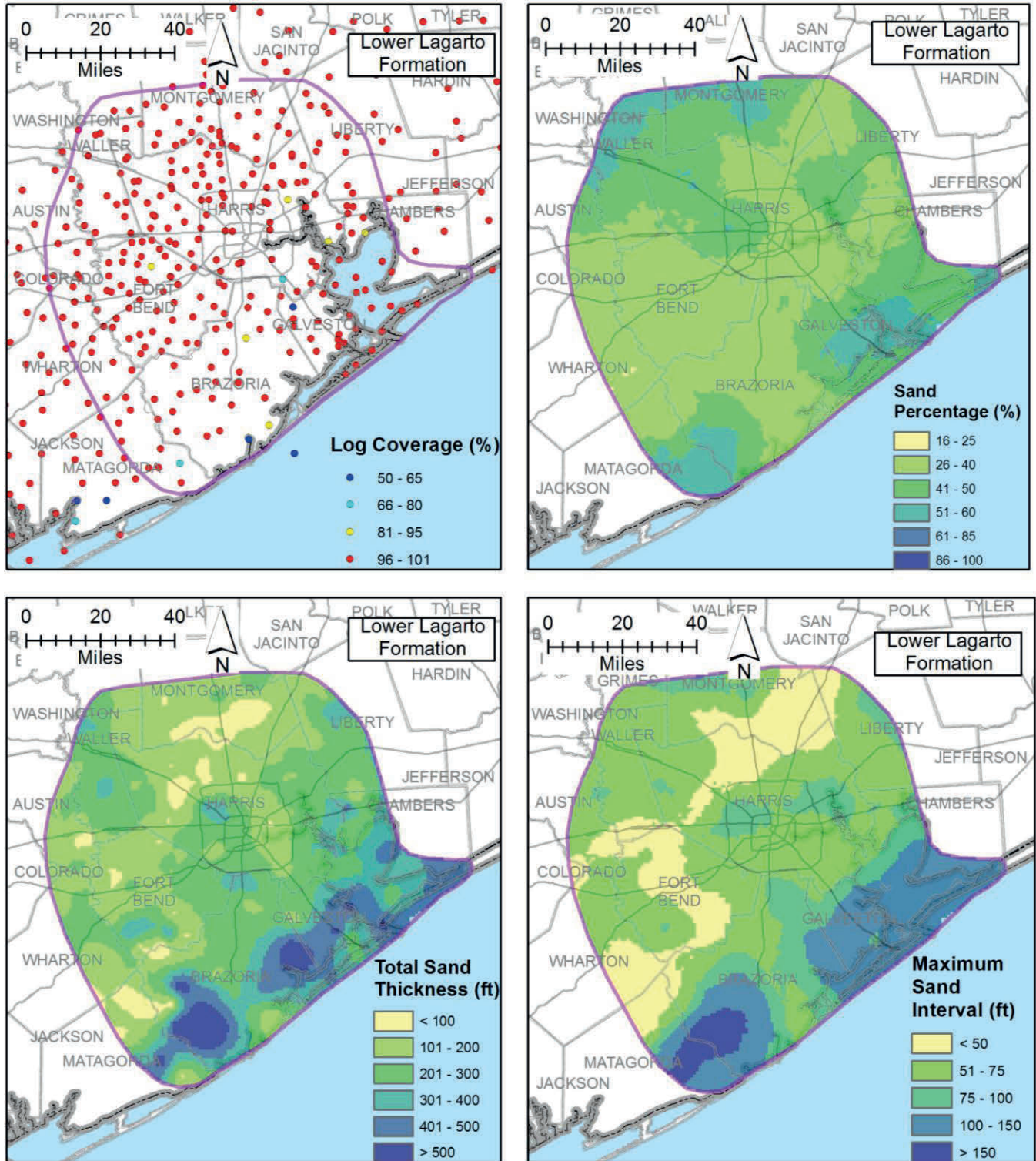


Figure B-8 Maps of log coverage, sand percentage, total sand thickness and maximum sand interval for the Lower Lagarto Formation in the Jasper Aquifer. Log coverage is the percentage of the formation intersected by the portion of the geophysical log analyzed for the presence of sand beds.

Appendix B: Maps of Percent Sands, Total Sand Thickness, and Maximum Sand Interval for Geological Formations

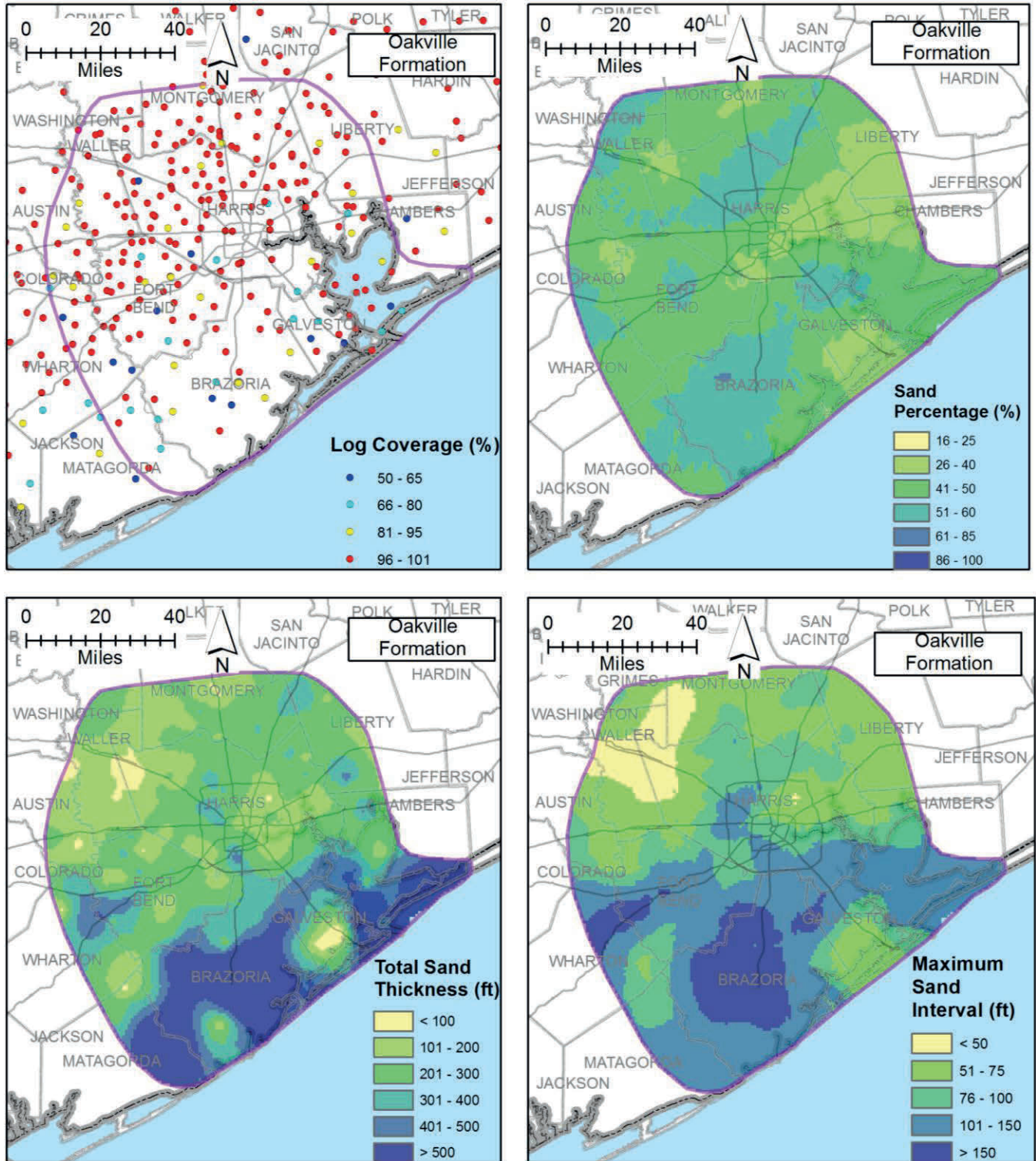


Figure B-9 Maps of log coverage, sand percentage, total sand thickness and maximum sand interval for the Oakville Formation in the Jasper Aquifer. Log coverage is the percentage of the formation intersected by the portion of the geophysical log analyzed for the presence of sand beds.

Appendix B: Maps of Percent Sands, Total Sand Thickness, and Maximum Sand Interval for Geological Formations

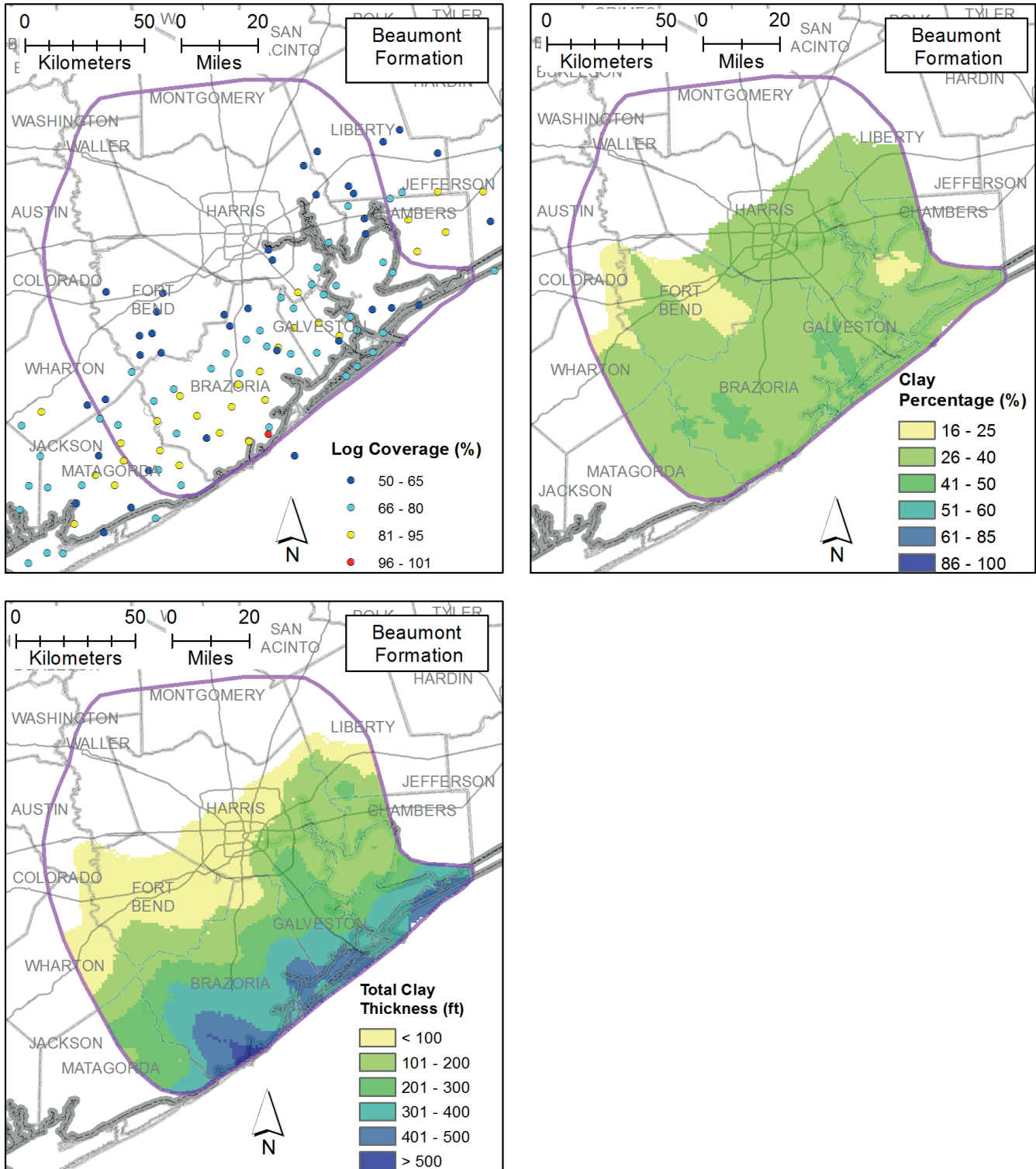


Figure B-10 Maps of log coverage, clay percentage, and total clay thickness for the Beaumont Formation in the Chicot Aquifer. Log coverage is the percentage of the formation intersected by the portion of the geophysical log analyzed for the presence of clay beds.

Appendix B: Maps of Percent Sands, Total Sand Thickness, and Maximum Sand Interval for Geological Formations

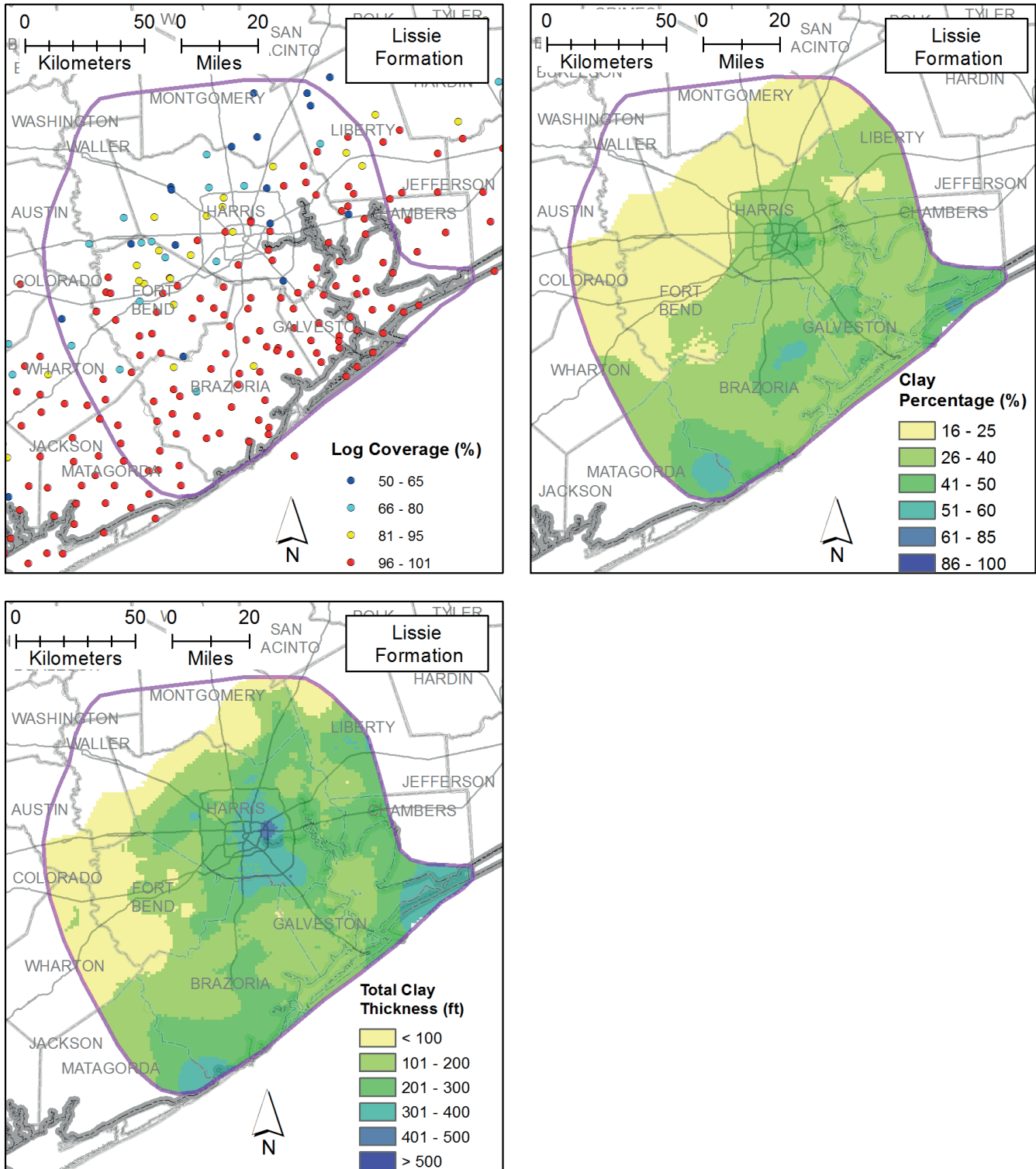


Figure B-11 Maps of log coverage, clay percentage, and total clay thickness for the Lissie Formation in the Chicot Aquifer. Log coverage is the percentage of the formation intersected by the portion of the geophysical log analyzed for the presence of clay beds.

Appendix B: Maps of Percent Sands, Total Sand Thickness, and Maximum Sand Interval for Geological Formations

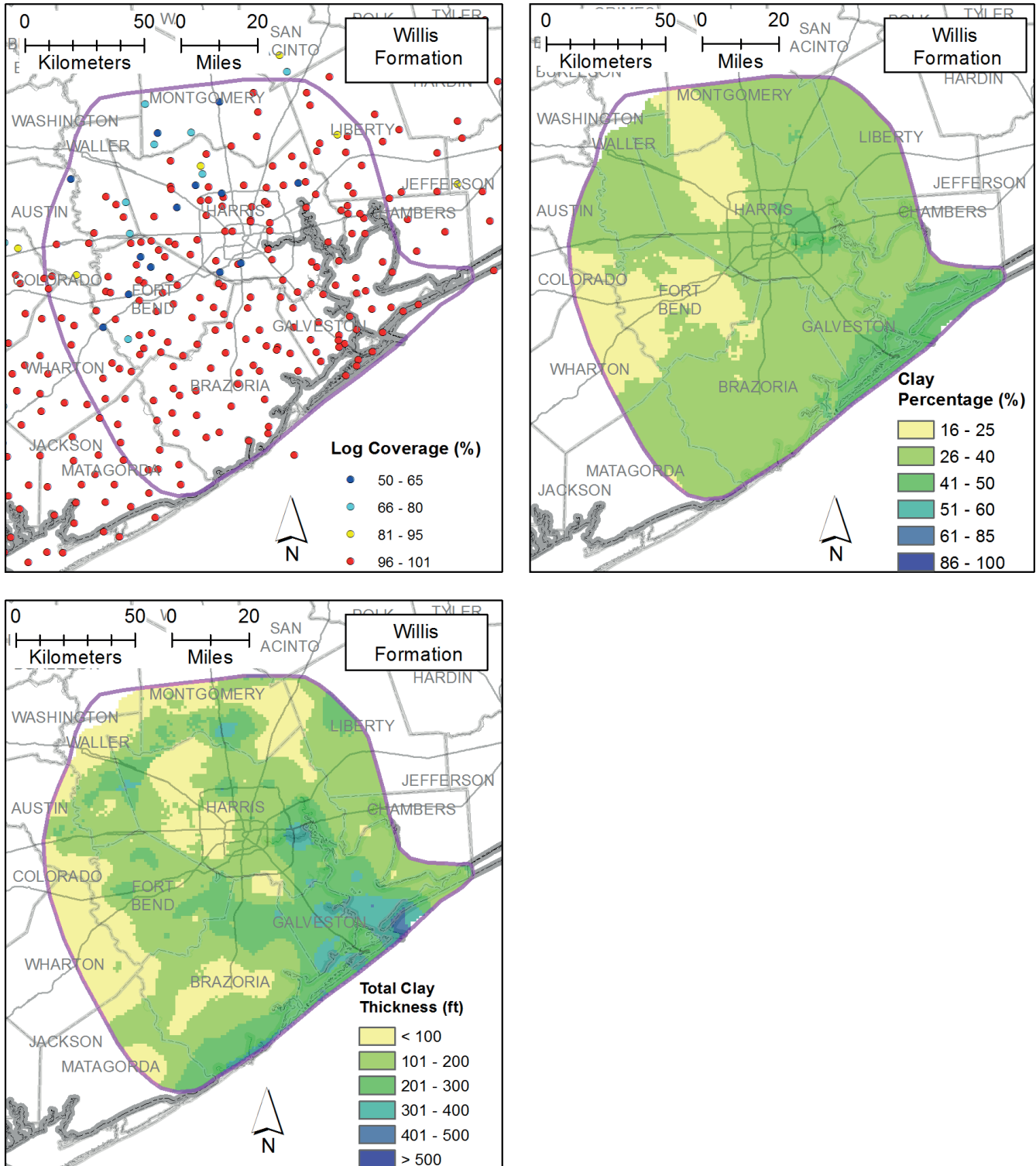


Figure B-12 Maps of log coverage, clay percentage, and total clay thickness for the Willis Formation in the Chicot Aquifer. Log coverage is the percentage of the formation intersected by the portion of the geophysical log analyzed for the presence of clay beds.

Appendix B: Maps of Percent Sands, Total Sand Thickness, and Maximum Sand Interval for Geological Formations

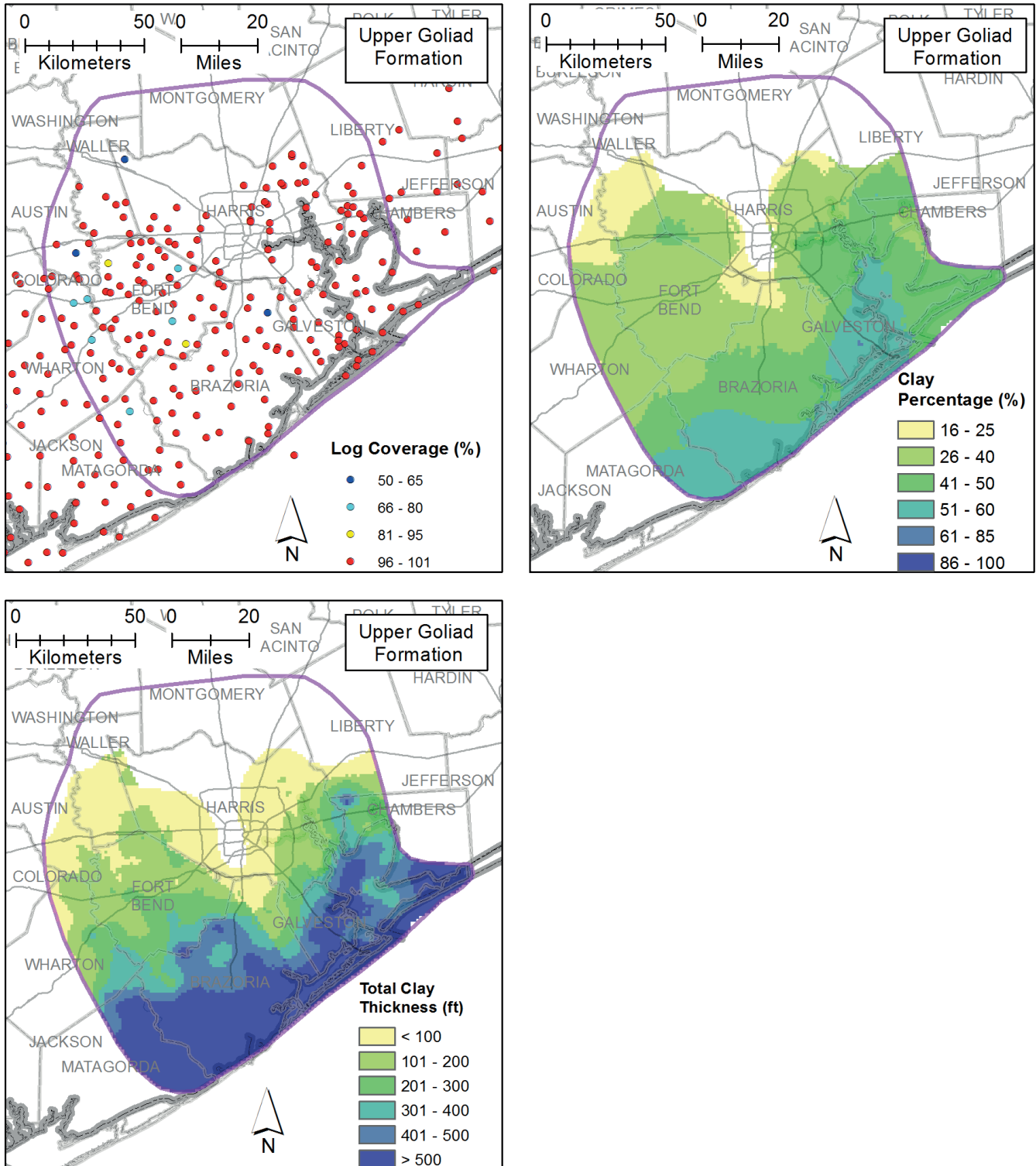


Figure B-13 Maps of log coverage, clay percentage, and total clay thickness for the Upper Goliad Formation in the Evangeline Aquifer. Log coverage is the percentage of the formation intersected by the portion of the geophysical log analyzed for the presence of clay beds.

Appendix B: Maps of Percent Sands, Total Sand Thickness, and Maximum Sand Interval for Geological Formations

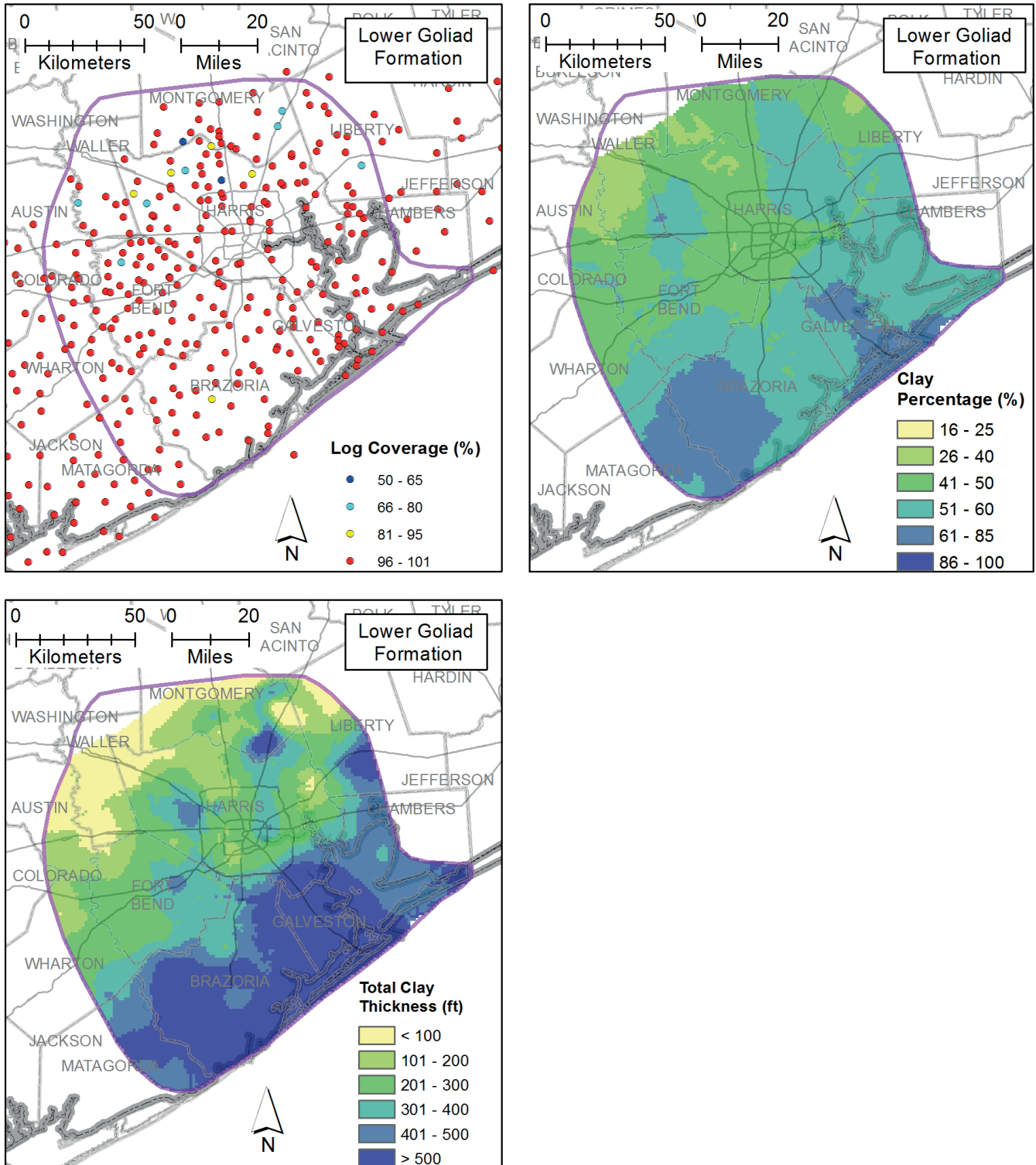


Figure B-14 Maps of log coverage, clay percentage, and total clay thickness for the Lower Goliad Formation in the Evangeline Aquifer. Log coverage is the percentage of the formation intersected by the portion of the geophysical log analyzed for the presence of clay beds.

Appendix B: Maps of Percent Sands, Total Sand Thickness, and Maximum Sand Interval for Geological Formations

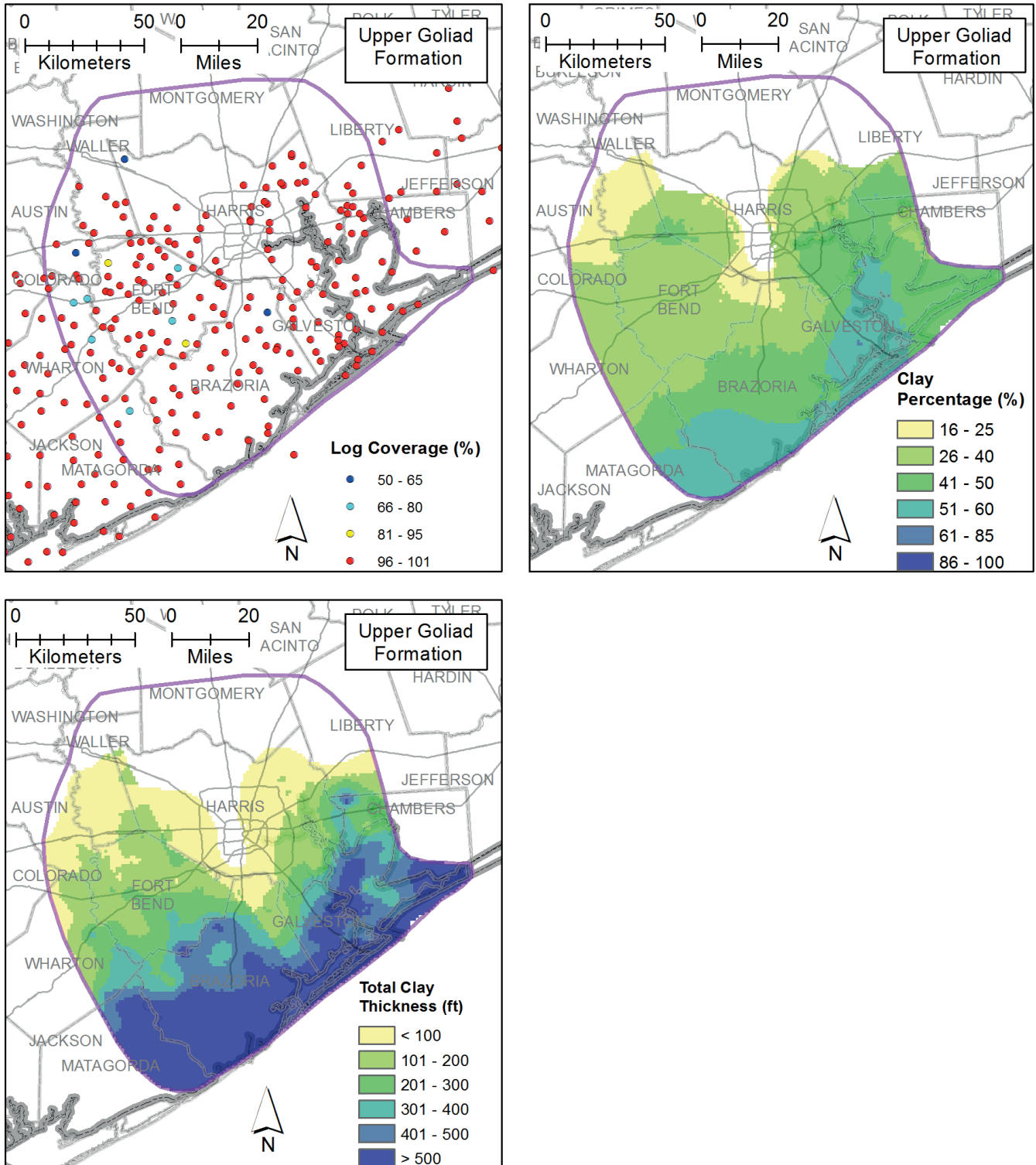


Figure B-15 Maps of log coverage, clay percentage, and total clay thickness for the Upper Lagarto Formation in the Evangeline Aquifer. Log coverage is the percentage of the formation intersected by the portion of the geophysical log analyzed for the presence of clay beds.

Appendix B: Maps of Percent Sands, Total Sand Thickness, and Maximum Sand Interval for Geological Formations

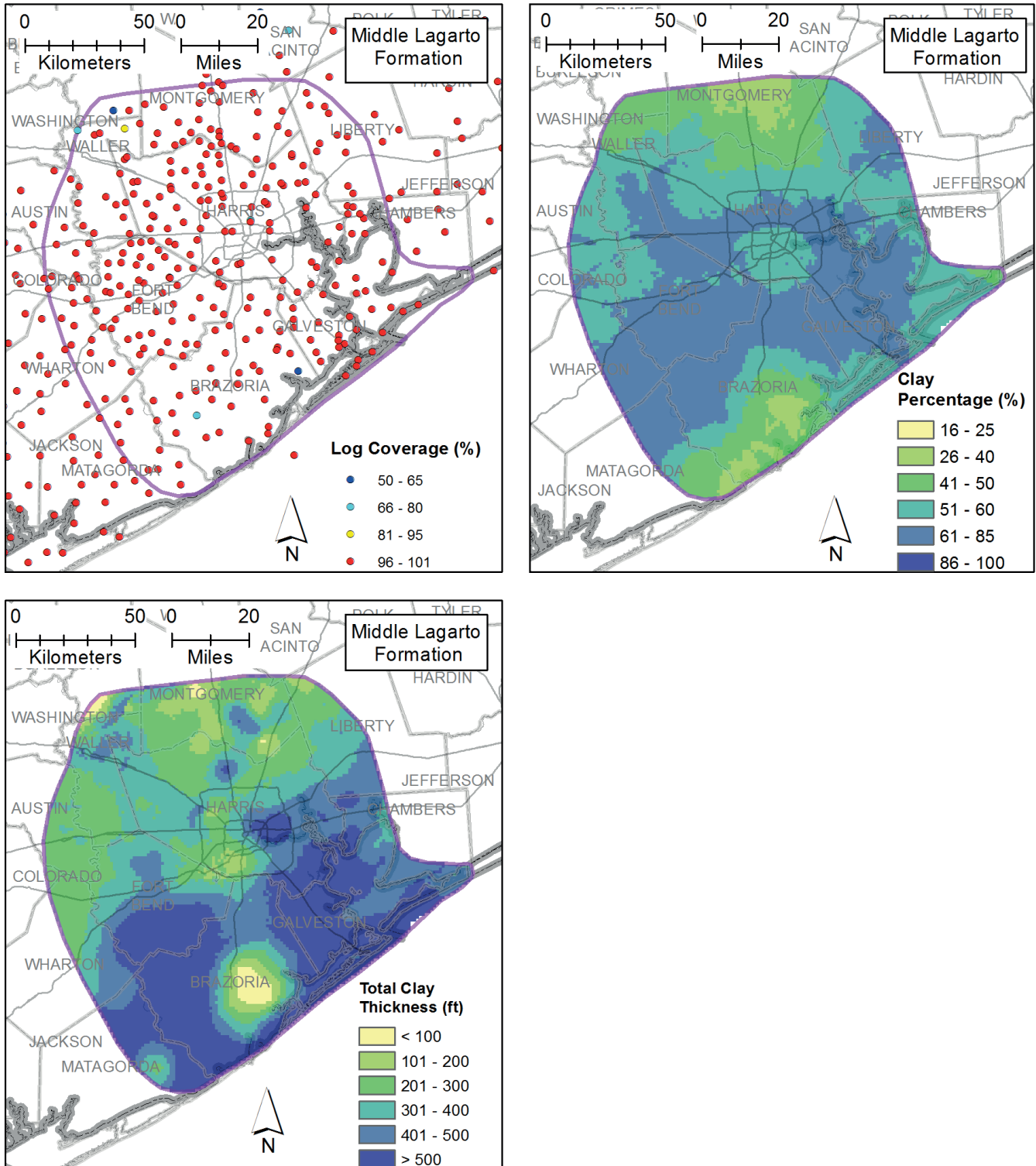


Figure B-16 Maps of log coverage, clay percentage, and total clay thickness for the Middle Lagarto Formation in the Burkeville Confining Unit. Log coverage is the percentage of the formation intersected by the portion of the geophysical log analyzed for the presence of clay beds.

Appendix B: Maps of Percent Sands, Total Sand Thickness, and Maximum Sand Interval for Geological Formations

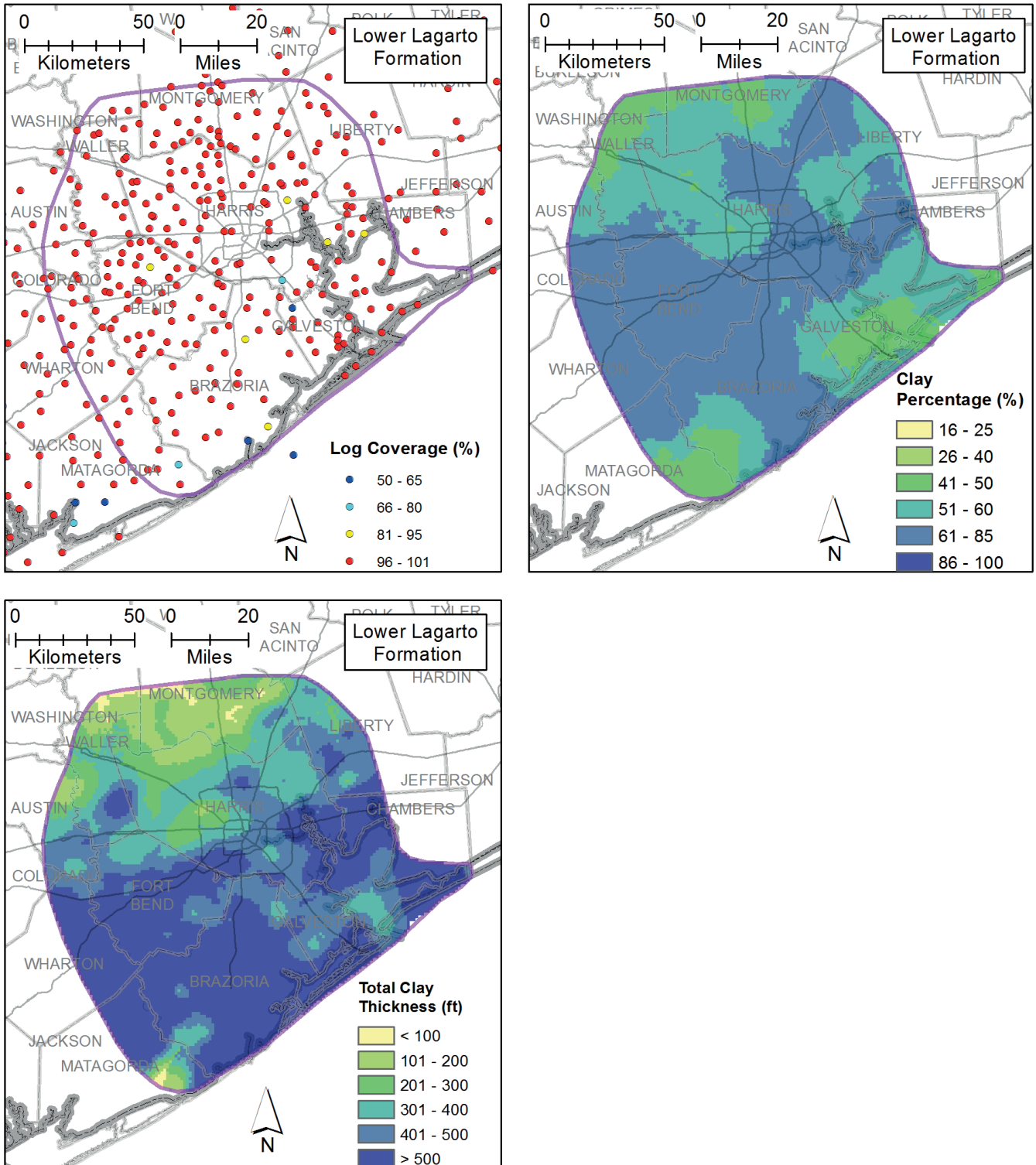


Figure B-17 Maps of log coverage, clay percentage, and total clay thickness for the Lower Lagarto Formation in the Jasper Aquifer. Log coverage is the percentage of the formation intersected by the portion of the geophysical log analyzed for the presence of clay beds.

Appendix B: Maps of Percent Sands, Total Sand Thickness, and Maximum Sand Interval for Geological Formations

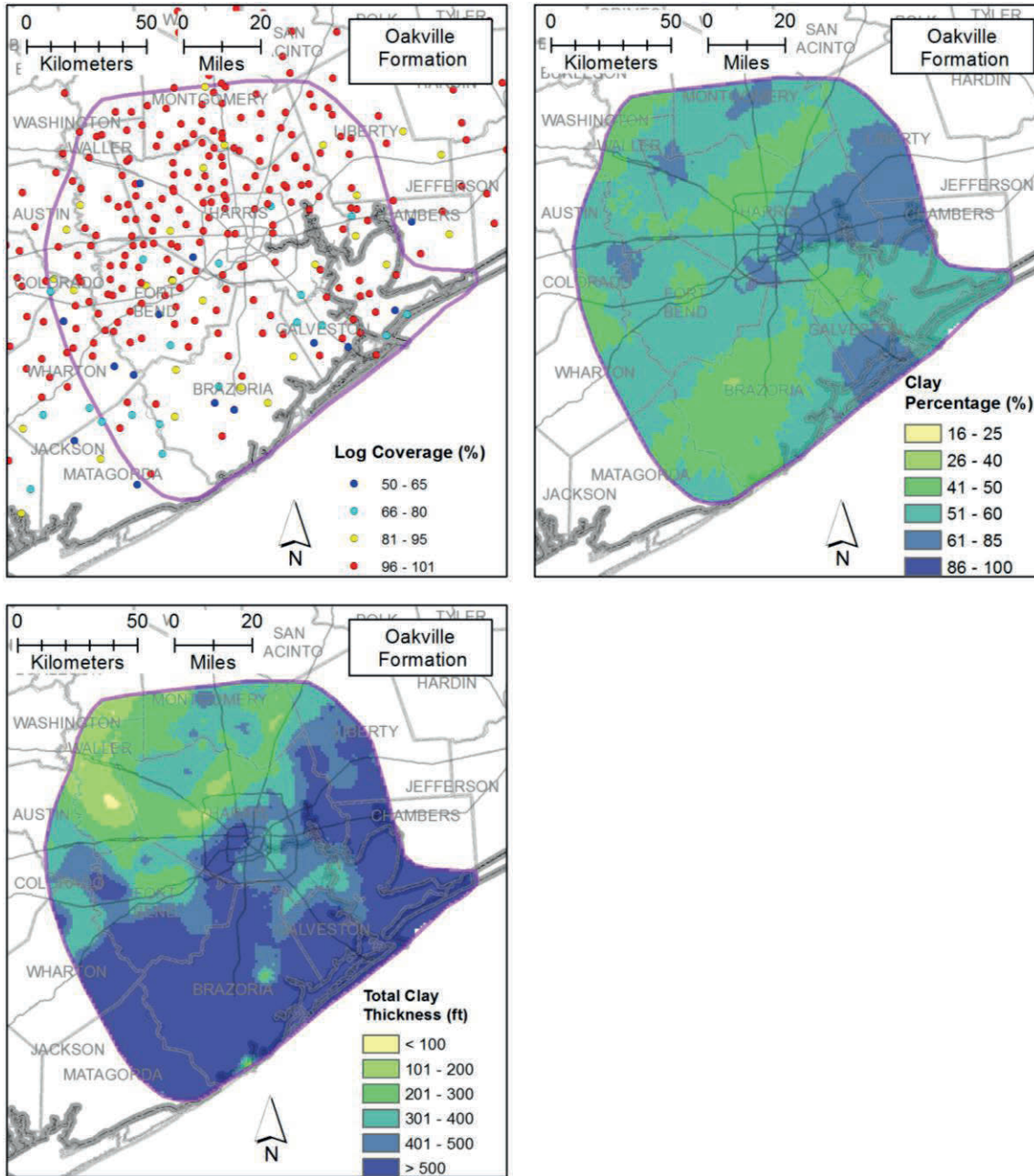


Figure B-18 Maps of log coverage, clay percentage, and total clay thickness for the Oakville Formation in the Jasper Aquifer. Log coverage is the percentage of the formation intersected by the portion of the geophysical log analyzed for the presence of clay beds.

Appendix C

Maps of the Geophysical Logs that are Used to Construct Dip Cross-Sections D-5, D-6, D-7, D-8, D-9, and D-10 and Strike Cross-Sections S-1, S-2, and S-3

This page is intentionally left blank.

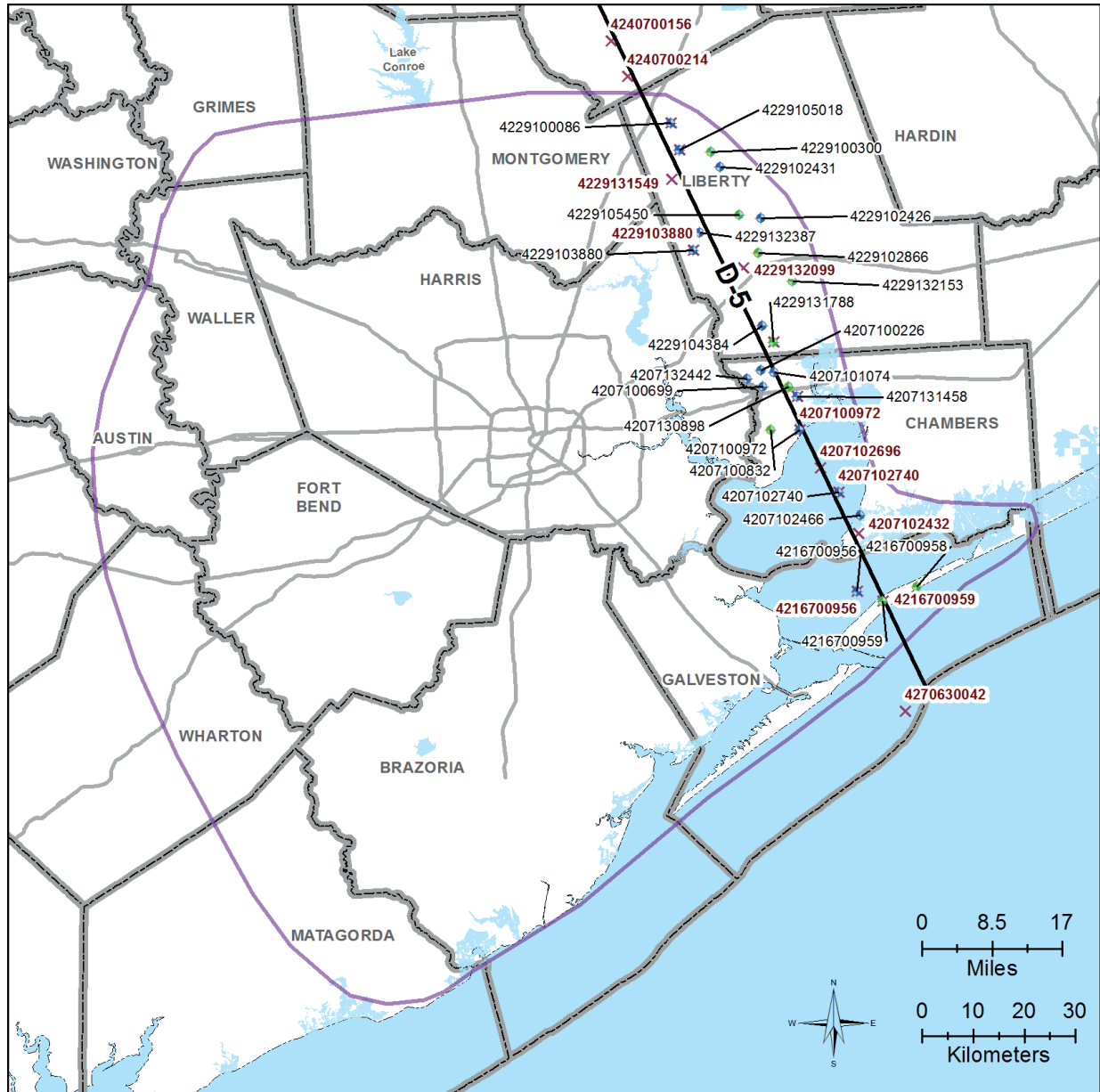
LIST OF FIGURES

Figure C-1	Location of the geophysical logs the comprise Cross-Section D-5.....	C-1
Figure C-2	Location of the geophysical logs the comprise Cross-Section D-6.....	C-2
Figure C-3	Location of the geophysical logs the comprise Cross-Section D-7.....	C-3
Figure C-4	Location of the geophysical logs the comprise Cross-Section D-8.....	C-4
Figure C-5	Location of the geophysical logs the comprise Cross-Section D-9.....	C-5
Figure C-6	Location of the geophysical logs the comprise Cross-Section D-10.....	C-6
Figure C-7	Location of the geophysical logs the comprise Cross-Section S-1.....	C-7
Figure C-8	Location of the geophysical logs the comprise Cross-Section S-2.....	C-8
Figure C-9	Location of the geophysical logs the comprise Cross-Section S-3.....	C-9

Appendix C: Maps of the Geophysical Logs that are Used to Construct
Dip Cross-Sections D-5, D-6, D-7, D-8, D-9, and D-10 and Strike Cross-Sections S-1, S-2, and S-3

This page is intentionally left blank.

Appendix C: Maps of the Geophysical Logs that are Used to Construct Dip Cross-Sections D-5, D-6, D-7, D-8, D-9, and D-10 and Strike Cross-Sections S-1, S-2, and S-3



Logs Used for Cross-Section D-5

Legend

- Study Area
- County Lines
- Major Highways
- Municipalities

- Cross-Section Line
- Logs with Updated Stratigraphic Picks
- Digitized Log with Sand Picks**
 - From TWDB Study
 - From This Study



Prepared for:



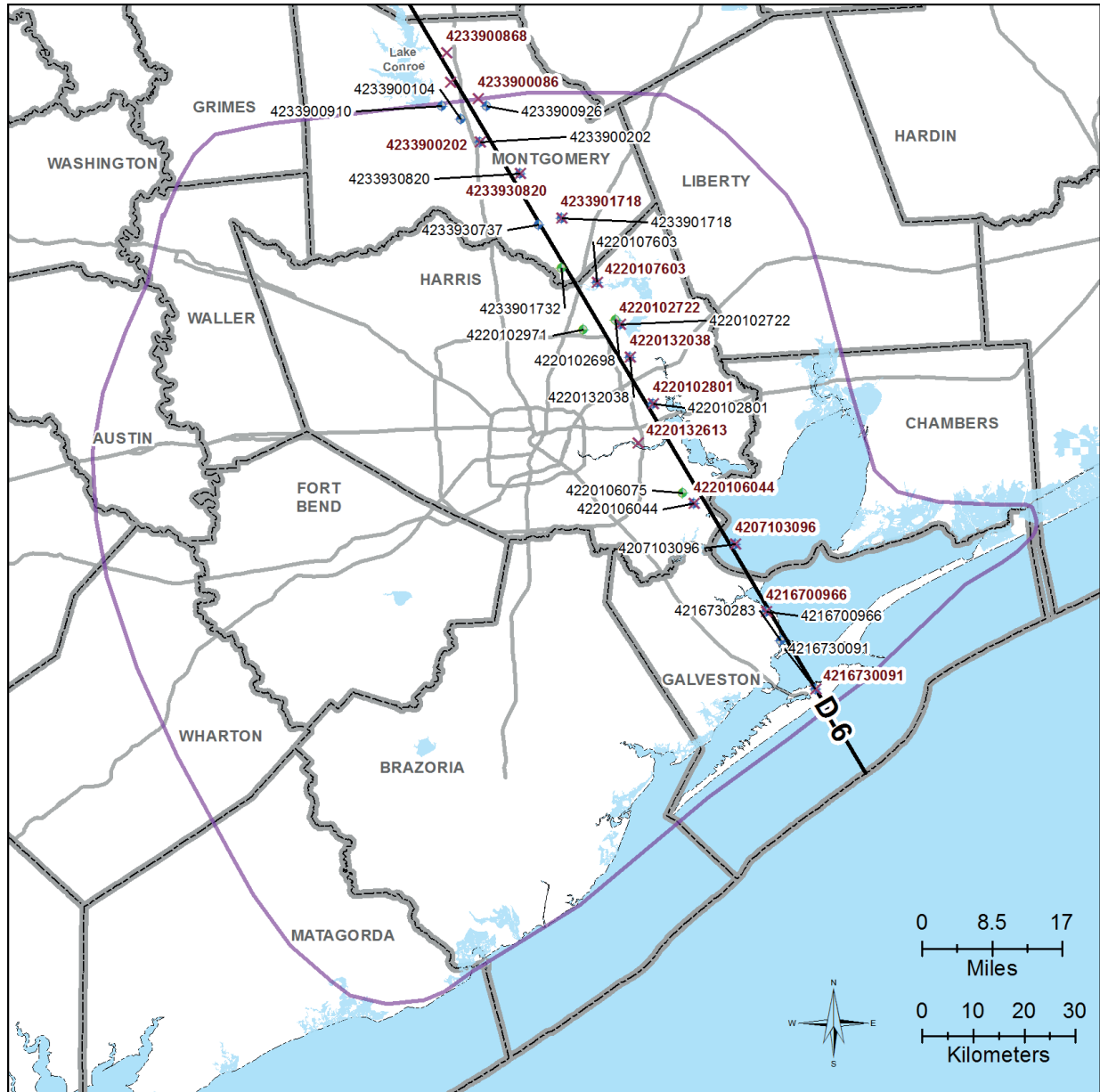
Prepared by:



S:\AUS\HGSDM.M001.SUBS\GIS\mxd_report\Arc10.2_Transect_5.mxd

Figure C-1 Location of the geophysical logs that comprise Cross-Section D-5

Appendix C: Maps of the Geophysical Logs that are Used to Construct Dip Cross-Sections D-5, D-6, D-7, D-8, D-9, and D-10 and Strike Cross-Sections S-1, S-2, and S-3



Logs Used for Cross-Section D-6

Legend

- Study Area
- County Lines
- Major Highways
- Municipalities

- Cross-Section Line
- Logs with Updated Stratigraphic Picks
- Digitized Log with Sand Picks**
- From TWDB Study
- From This Study



Prepared for:



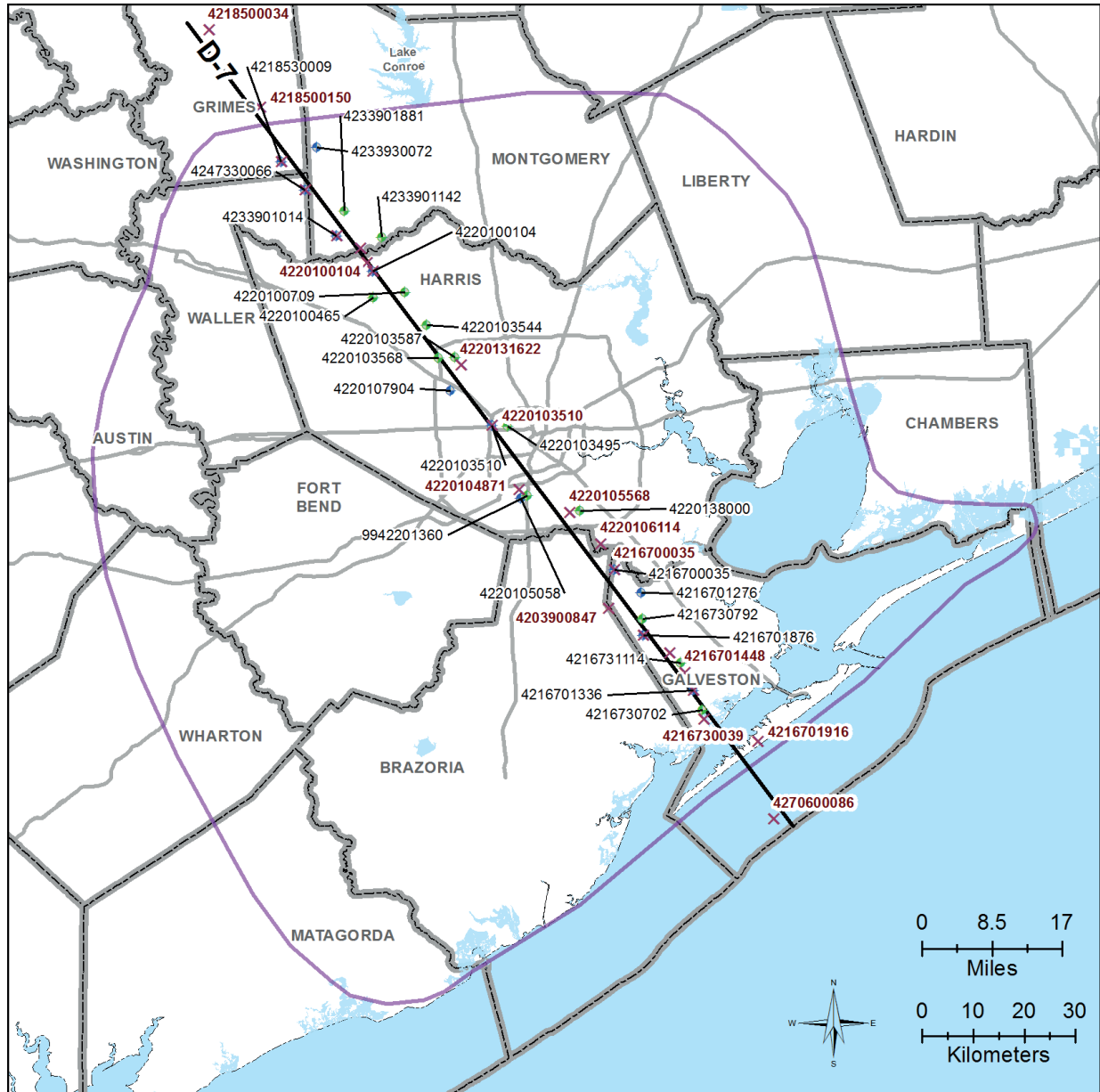
Prepared by:



S:\AUS\HGSDM.M001.SUBS\GIS\mxd_report\Arc10.2_Transect_6.mxd

Figure C-2 Location of the geophysical logs that comprise Cross-Section D-6

Appendix C: Maps of the Geophysical Logs that are Used to Construct Dip Cross-Sections D-5, D-6, D-7, D-8, D-9, and D-10 and Strike Cross-Sections S-1, S-2, and S-3

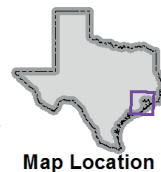


Logs Used for Cross-Section D-7

Legend

- Study Area
- County Lines
- Major Highways
- Municipalities

- Cross-Section Line
- Logs with Updated Stratigraphic Picks
- Digitized Log with Sand Picks**
 - From TWDB Study
 - From This Study



Prepared for:



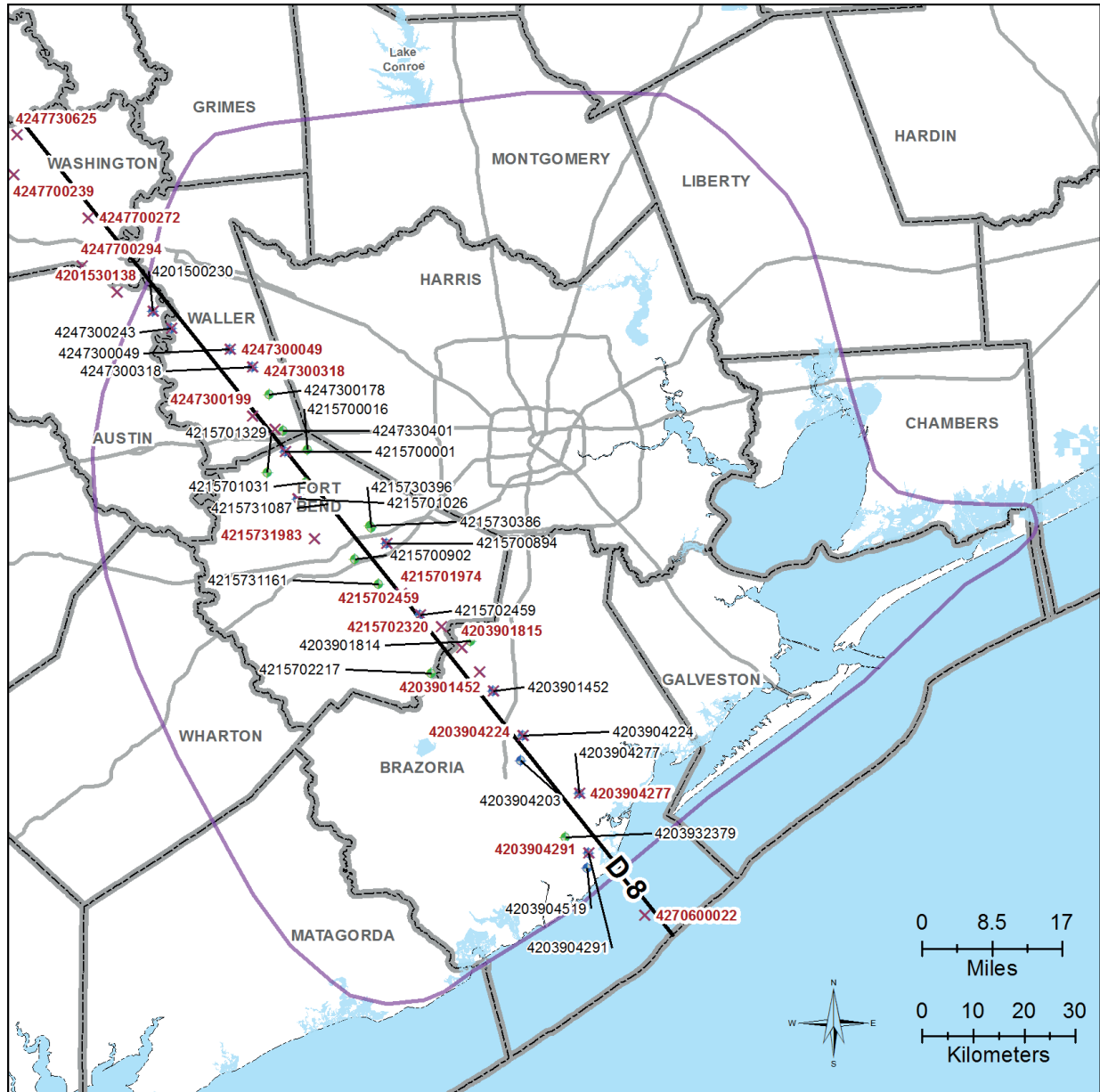
Prepared by:



S:\AUS\HGSDM.M001.SUBS\GIS\mxd_report\Arc10.2_Transect_7.mxd

Figure C-3 Location of the geophysical logs that comprise Cross-Section D-7

Appendix C: Maps of the Geophysical Logs that are Used to Construct Dip Cross-Sections D-5, D-6, D-7, D-8, D-9, and D-10 and Strike Cross-Sections S-1, S-2, and S-3



Logs Used for Cross-Section D-8

Legend

- Study Area
- County Lines
- Major Highways
- Municipalities

- Cross-Section Line
- Logs with Updated Stratigraphic Picks
- Digitized Log with Sand Picks**
- From TWDB Study
- From This Study



Prepared for:



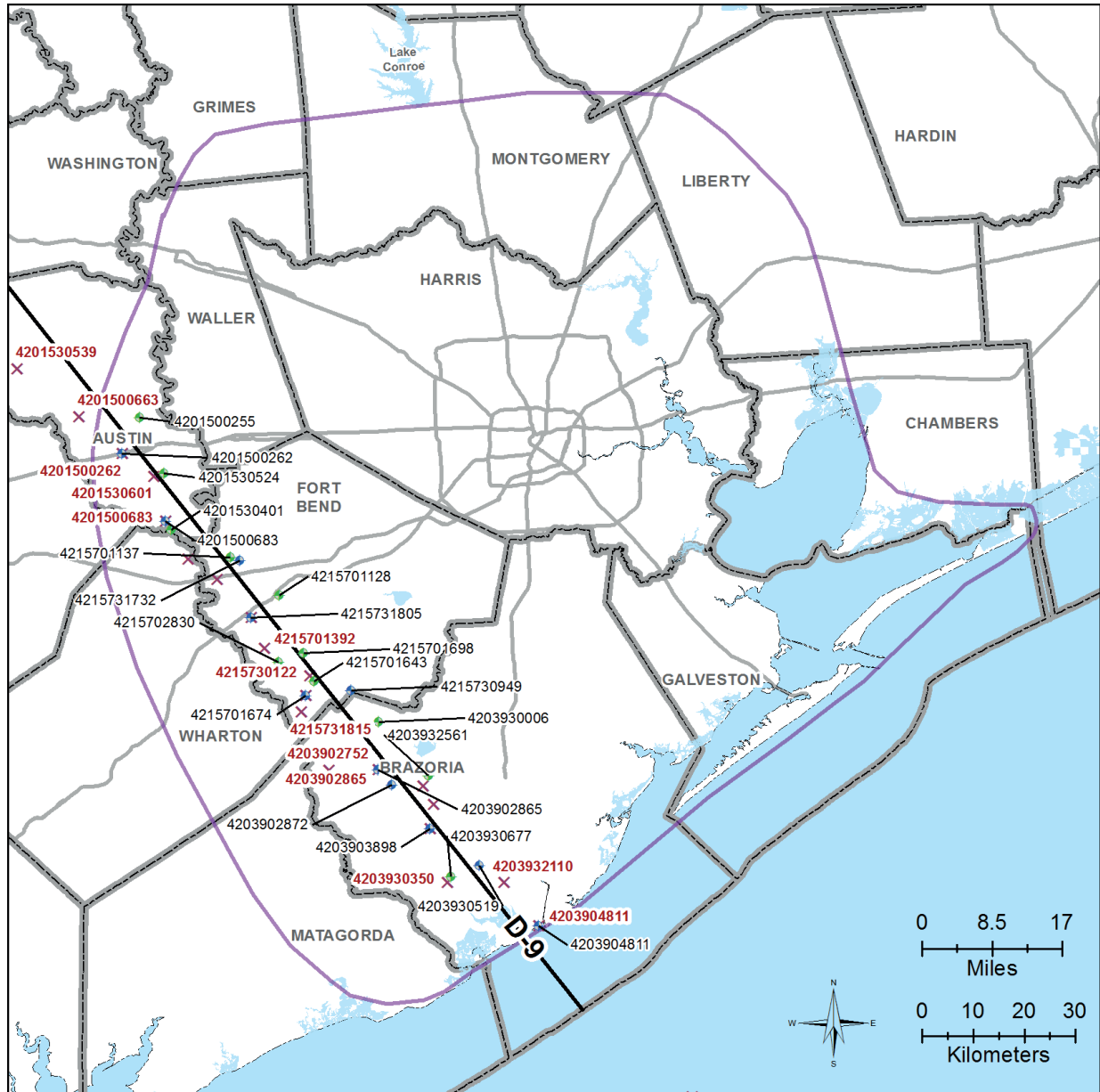
Prepared by:



S:\AUS\HGSDM.M001.SUBS\GIS\mxd_report\Arc10.2_Transect_8.mxd

Figure C-4 Location of the geophysical logs that comprise Cross-Section D-8

Appendix C: Maps of the Geophysical Logs that are Used to Construct Dip Cross-Sections D-5, D-6, D-7, D-8, D-9, and D-10 and Strike Cross-Sections S-1, S-2, and S-3



Wells Used for Cross-Section D-9

Legend

- Study Area
- County Lines
- Major Highways
- Municipalities
- Cross-Section Line
- Logs with Updated Stratigraphic Picks
- Digitized Log with Sand Picks**
 - From TWDB Study
 - From This Study



Prepared for:



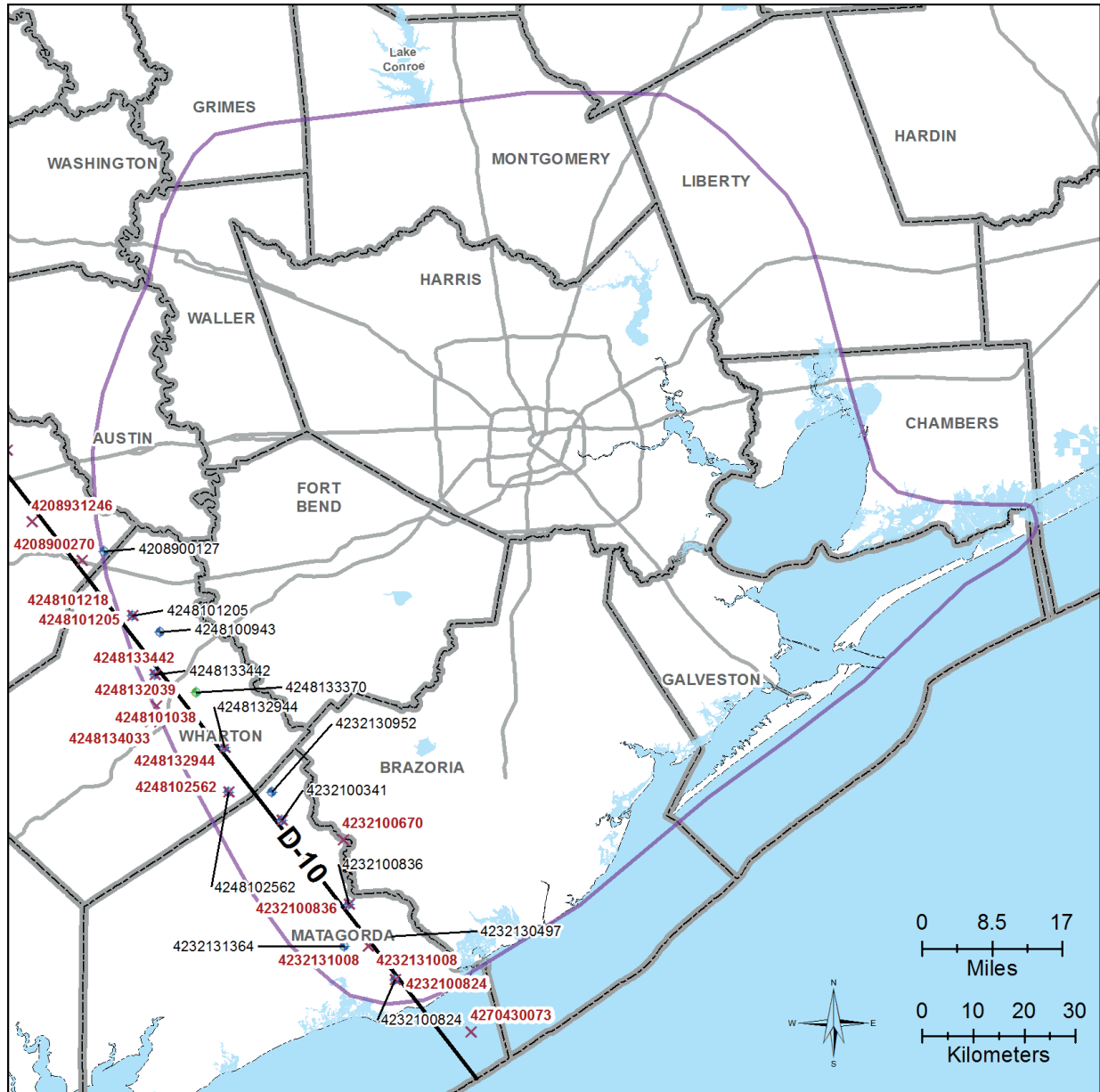
Prepared by:



S:\AUS\HGSDM.M001.SUBS\GIS\mxd_report\Arc10.2_Transect_9.mxd

Figure C-5 Location of the geophysical logs that comprise Cross-Section D-9

Appendix C: Maps of the Geophysical Logs that are Used to Construct Dip Cross-Sections D-5, D-6, D-7, D-8, D-9, and D-10 and Strike Cross-Sections S-1, S-2, and S-3



Wells Used for Cross-Section D-10

Legend

- Study Area
- County Lines
- Major Highways
- Municipalities

Cross-Section Line

- Logs with Updated Stratigraphic Picks
- Digitized Log with Sand Picks**
 - From TWDB Study
 - From This Study



Prepared for:



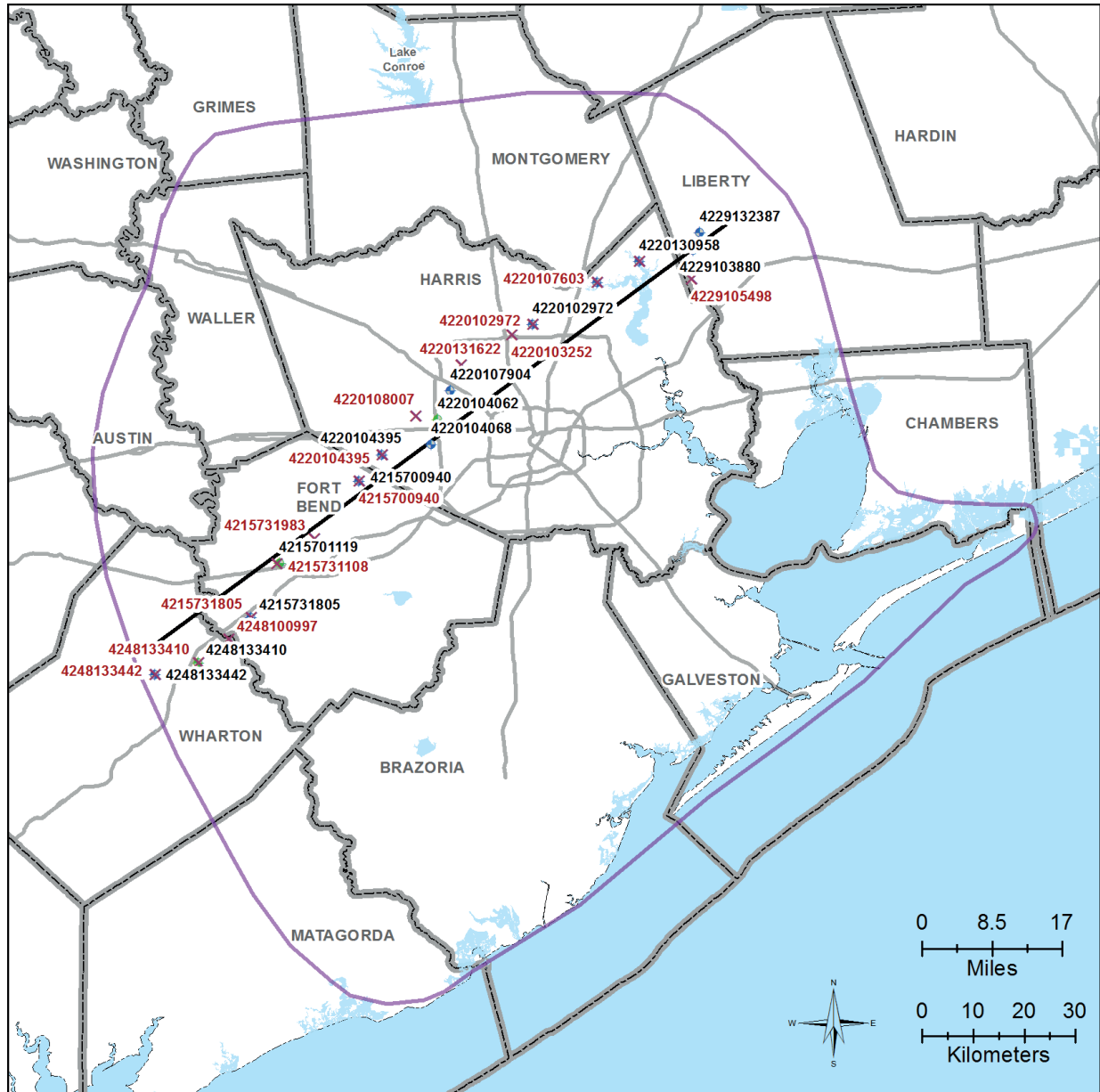
Prepared by:



S:\AUS\HGSDM.M001.SUBS\GIS\mxd_report\Arc10.2_Transect_10.mxd

Figure C-6 Location of the geophysical logs that comprise Cross-Section D-10

Appendix C: Maps of the Geophysical Logs that are Used to Construct Dip Cross-Sections D-5, D-6, D-7, D-8, D-9, and D-10 and Strike Cross-Sections S-1, S-2, and S-3



Logs Used for Cross-Section S-1

Legend

- Study Area
- County Lines
- Major Highways
- Municipalities

- Cross-Section Line
- Logs with Updated Stratigraphic Picks

Digitized Log with Sand Picks

- From TWDB Study
- From This Study



Prepared for:



Prepared by:



S:\AUS\HGSDM.M001.SUBS\GIS\mxd_report\Arc10.2_Strike_1.mxd

Figure C-7 Location of the geophysical logs that comprise Cross-Section S-1

Appendix C: Maps of the Geophysical Logs that are Used to Construct Dip Cross-Sections D-5, D-6, D-7, D-8, D-9, and D-10 and Strike Cross-Sections S-1, S-2, and S-3



Logs Used for Cross-Section S-2

Legend

- Study Area
- County Lines
- Major Highways
- Municipalities

- Cross-Section Line
- Logs with Updated Stratigraphic Picks

Digitized Log with Sand Picks

- From TWDB Study
- From This Study



Prepared for:



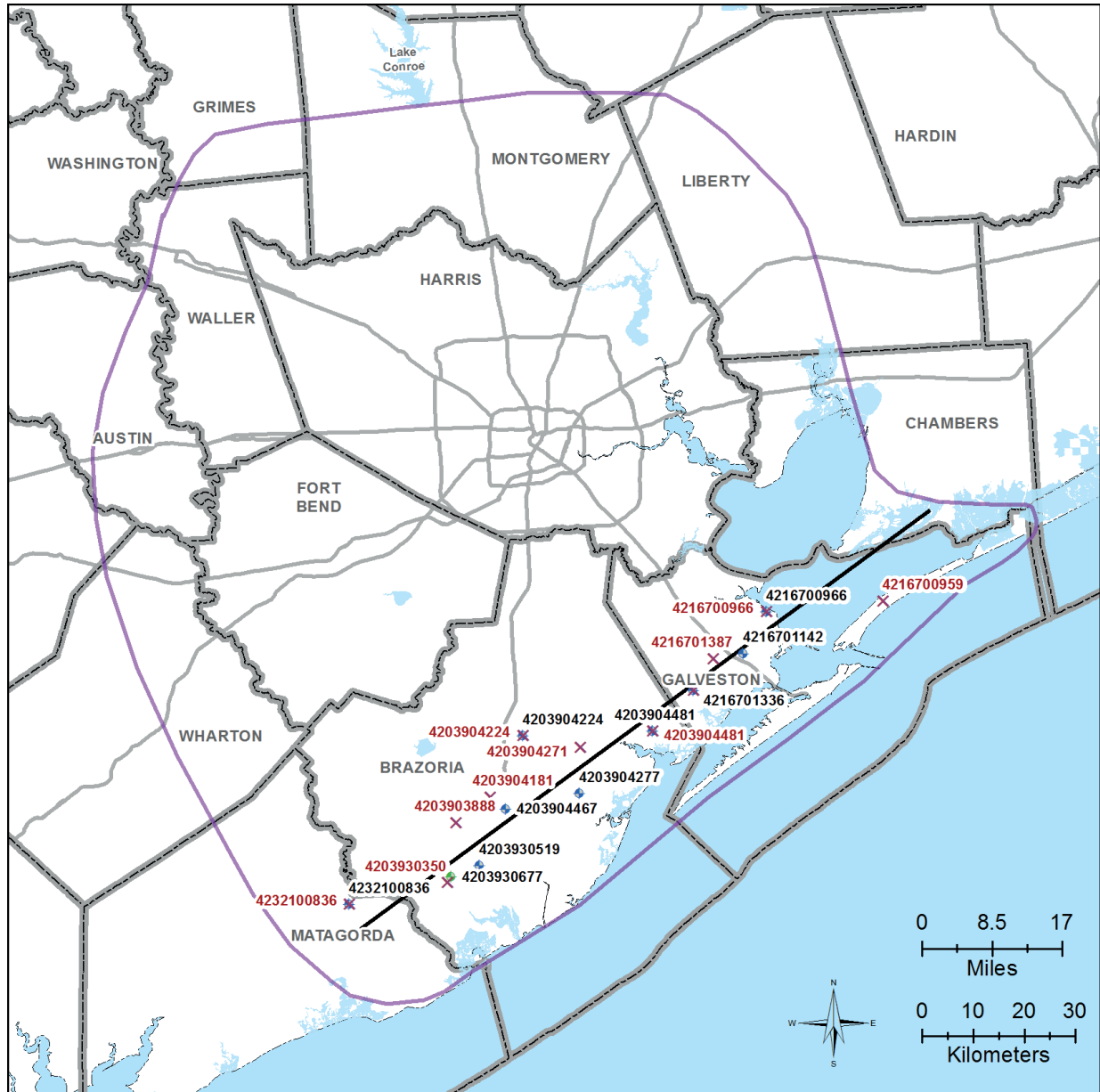
Prepared by:



S:\AUS\HGSDM.M001.SUBS\GIS\mxd_report\Arc10.2_Strike_2.mxd

Figure C-8 Location of the geophysical logs that comprise Cross-Section S-2

Appendix C: Maps of the Geophysical Logs that are Used to Construct Dip Cross-Sections D-5, D-6, D-7, D-8, D-9, and D-10 and Strike Cross-Sections S-1, S-2, and S-3



Logs Used for Cross-Section S-3

Legend

- Study Area
- County Lines
- Major Highways
- Municipalities

- Cross-Section Line
- Logs with Updated Stratigraphic Picks

Digitized Log with Sand Picks

- From TWDB Study
- From This Study



Prepared for:



Prepared by:



S:\AUS\HGSDM.M001.SUBS\GIS\mxd_report\Arc10.2_Strike_3.mxd

Figure C-9 Location of the geophysical logs that comprise Cross-Section S-3

Appendix C: Maps of the Geophysical Logs that are Used to Construct
Dip Cross-Sections D-5, D-6, D-7, D-8, D-9, and D-10 and Strike Cross-Sections S-1, S-2, and S-3

This page is intentionally left blank.

Appendix D
**Cross Sections Showing Sand and Clay Sequences,
Stratigraphy, and Fault Zones**

This page is intentionally left blank.

TABLE OF CONTENTS

D.1	Cross Sections Showing Sand and Clay Sequences, Stratigraphy and Fault Zones	D-1
D.1.1	Mapping of Marine Shale Wedges	D-1
D.1.2	Mapping of Major Sandstone-Rich Packages (Fairways).....	D-1
D.1.3	Mapping of Clay-Rich Zones	D-2
D.1.4	Mapping of Fault Zones	D-3
D.1.5	General Observations	D-3

LIST OF FIGURES

Figure D-1	Sand and clay sequences, stratigraphy, and fault zones mapped along Cross-Section D-5 in Figure 3-3.....	D-7
Figure D-2	Sand and clay sequences, stratigraphy, and fault zones mapped along Cross-Section D-6 in Figure 3-3.....	D-8
Figure D-3	Sand and clay sequences, stratigraphy, and fault zones mapped along Cross-Section D-7 in Figure 3-3.....	D-9
Figure D-4	Sand and clay sequences, stratigraphy, and fault zones mapped along Cross-Section D-8 in Figure 3-3.....	D-10
Figure D-5	Sand and clay sequences, stratigraphy, and fault zones mapped along Cross-Section D-9 in Figure 3-3.....	D-11
Figure D-6	Sand and clay sequences, stratigraphy, and fault zones mapped along Cross-Section D-10 in Figure 3-3.....	D-12
Figure D-7	Sand and clay sequences, stratigraphy, and fault zones mapped along Cross-Section S-1 in Figure 3-3.....	D-13
Figure D-8	Sand and clay sequences, stratigraphy, and fault zones mapped along Cross-Section S-2 in Figure 3-3.....	D-14
Figure D-9	Sand and clay sequences, stratigraphy, and fault zones mapped along Cross-Section S-3 in Figure 3-3.....	D-15

Appendix D: Cross-Sections Showing Sand and Clay Sequences,
Stratigraphy, and Fault Zones

This page is intentionally left blank.

D.1 Cross Sections Showing Sand and Clay Sequences, Stratigraphy and Fault Zones

Gulf Coast Aquifer formations were studied for the occurrence of significant sand and clay sequences using six dip cross sections (D-5, D-6, D-7, D-8, D-9, and D-10) and three strike cross sections (S-1, S-2, and S-3) shown in Figure 3-3. The analysis included adding and replacing logs to provide a more complete cross section through the Texas Gulf Coast Aquifer System as compared to earlier work by Young and others (2012). The nine geologic cross sections use the TWDB structure as their basis for defining formation boundaries. Because additional logs were made available with this study, the TWDB structure (Young and others, 2012) was reviewed and in some cases modified on these sections. Any edits on these sections were performed by Dr. Thomas Ewing, who also served in the same technical role for the TWDB North Gulf Coast Aquifer stratigraphy study.

D.1.1 Mapping of Marine Shale Wedges

The methods of Galloway and others (1982, 1986) were followed in connecting marine shale wedges to their landward, non-marine formation boundaries. The marine shale wedges were identified by correlating their top and base, as well as a surface of maximum transgression. These three surfaces come to a landward common point in most cases, corresponding to the beginning of the landward unit boundary. The wedge boundaries are approximate in their seaward reaches, as the overlying and underlying sand-bearing units pass into deltaic, shoreline and shelf/slope facies. In these areas, marine shale could be identified through most of the succession; however, as these areas are of limited interest for brackish water resources, all lesser marine shales in these areas have not been identified.

The dip cross sections in Figures D-1 through D-6 show six major marine shale wedges that are based upon the chronostratigraphy documented by Brown and Loucks (2009). These shale wedges represent continuous and coherent clays that serve as effective aquitards. Three of the wedges are named for the foraminifera (i.e., fossil) that exists at the time shale wedges were formed and thereby serves as a paleomarker for that shale. The six major marine shale wedges are named as follows:

- Jackson Shale – serves as the lower boundary of the Catahoula Formation;
- Anahuac Shale – serves as the lower boundary for the Oakville Formation and therefore the Jasper Aquifer and the upper boundary for the Catahoula Formation;
- Marg A Shale – serves as the lower boundary for the Lagarto Formation and the upper boundary for the Oakville Formation. Named for the foraminifera called *Marginulina A*;
- Amph B Shale - serves as the lower boundary for the Goliad Formation and the upper boundary for the Lagarto Formation. Named for the foraminifera called *Amphistegina B*;
- Tex W Shale - serves as the boundary that divides the Goliad Formation into a lower and upper unit. The shale is associated with the foraminifera *Textularia W stapperi*; and
- Pliocene Shale - serves as the lower boundary for the Willis Formation and the upper boundary for the Goliad Formation. The shale is associated with the Pliocene-aged foraminifera called *Bigenerian A floridana* and *Buliminella*.

D.1.2 Mapping of Major Sandstone-Rich Packages (Fairways)

The first step was to identify sandstone-rich packages of potential interest for brackish groundwater resources. These sand-stone rich packages potentially are more conductive to groundwater flow and many have major

Appendix D: Cross Sections Showing Sand and Clay Sequences, Stratigraphy, and Fault Zones

shale or mudstone confining units. There are three varieties of sandstone-rich packages that were visible on the geophysical logs:

- Aggradational Sandstones - Thick high net-sandstone aggradational packages (marked in green on the sections) are commonly found above and sometimes below the marine wedges, and also down dip within the units in a marginal-marine environment. These marginal-marine packages are the result of stacked shoreline deposition. They form targets of high continuity in a strike direction and substantial continuity in a dip direction.
- Thick Sandstone Packages - Packages of sandstones containing closely-spaced 20-feet or thicker sandstone bodies are the principal fairway type in the non-marine sections, and are present on all sections (marked in pink). These zones appear to represent a variety of depositional environments. Most are smaller, complex channel systems and their associated crevasse splays; these are generally dip-elongate but have some strike continuity. Others of undetermined origin appear to be more strike-elongate, perhaps representing sand-poor shoreline or washover systems.
- Large Individual channel sandstones – Individual channel sandstones that are more than 50 feet thick are identified (in red) on several of the dip sections throughout the study area. These channel sandstones are likely to be somewhat continuous in a dip direction, and discontinuous in a strike direction.

D.1.3 Mapping of Clay-Rich Zones

After the major fairways were identified, the units of purer mudstone or shale were identified. Shale units were divided into two varieties: thinner units with low resistivity that could form excellent seals even when relatively thin (dark gray); and thicker zones that are free from significant siltstone or thin sandstone (light gray). The remainder of the sections (uncolored) consist of mud-rich sequences with thin siltstone or sandstone beds, which are probably aquitards but are not thought to provide as good a seal to vertical groundwater flow as the gray zones.

The mud-rich zones were formed in floodplain environments up dip and lagoonal environments down dip. Lagoon-formed mudstone may also contain thin carbonate units (oyster reefs). In down dip regions, marine shales are also colored gray where they are interbedded with marginal-marine (deltaic or shoreline) sands. These clay-rich sections form the sealing units between sandstone aquifer fairways. The relationship between seal thickness and seal efficiency is not well determined; even a thin (foot-thick) but plastic, clay-rich shale can form an effective seal for hydrocarbons and water. Vertical conductivity of these units may be governed by the presence of faulting: either reactivated faults that formed during shelf-margin progradation at earlier times, or faults related to salt domes and other salt-tectonic features. That said, a thicker shale unit may help to limit leakiness on these features.

For all dip cross sections, the clay-rich zones associated with the Burkeville Confining Unit described by Baker (1979) and represented as an individual model layer in the Houston Area Groundwater Model (Kasmarek, 2013) is associated with the Lagarto Formation but its exact placement is not specifically shown.

D.1.4 Mapping of Fault Zones

Within the study area, faulting and related folding are due primarily to differential loading of sediment and gravity-driven subsidence and seaward movement. In areas with a thick, mobile salt layer, the result is a wide variety of salt-related features, particularly piercement salt domes, salt pillows, and areas of enhanced subsidence called salt-withdrawal basins. Over pressured shales (identified in cross sections) at depths below the Catahoula also form mobile substrates that allow fault systems to develop.

Delta systems and related shorelines have prograded the shelf margin throughout the Cenozoic, from a line that connects the cities of Freer-Cuero-Sealy-Conroe-Jasper 55 million years ago, to the present shoreline by 30 million years ago, to the present shelf margin up to 150 miles from shore (Ewing, 1991). As sediments are deposited into deep water at the margin, they are massively unstable and develop large normal faults, often with thousands of feet of displacement. These faults expand the shelf-margin section (sometimes as much as ten-fold) and are, therefore, known as growth faults. The major faults may occur as single faults, but more often a complex zone of faulting is formed, that takes its name from the shelf-margin unit with which it is associated.

Once the shelf margin has moved seaward past a given location, and fault activity decreases, that area forms part of the continental shelf. However, some (but not all) faults are reactivated during this depositional period and affect younger units. These reactivated faults may still have displacements up to a few hundred feet and may also generate broad anticlines on their downthrown side. Some faults reach the surface and form gentle fault scarps; others die out somewhere in the subsurface. The shelf-margin section is generally located deeper than 8,000 feet below sea level; shallower units are in the subsiding continental shelf section.

Figure 2-3 shows the major growth fault zones in the study area after Ewing (1991). These are, from northwest to southeast, the Wilcox fault zone; the Yegua fault zone; the Frio fault zone; and the Fleming fault zone (Lower Miocene). The last continues offshore and is succeeded by a Goliad fault zone (Corsair fault zone, middle Miocene) and faulting related to Plio-Pleistocene progradation and salt movement (High Island, South and East).

The faults zones shown on Figure 2-3 are identified on each of the six dip cross sections as dark black sub-vertical lines originating at the bottom of the cross section. In the vicinity of each fault zone, we looked for evidence of offsets in the dip between logs to determine if noticeable offset occurred between the well logs. Despite our increasing the number of logs per cross section, the spacing distance between the logs was not sufficient to accurately pinpoint the fault zone locations. As a result, the location of major faults is largely diagrammatic and based upon Ewing (1991). The height of the line reflects the upper extent of where there is a likelihood that the fault zone may have been reactivated and affected stratigraphic offset. The analysis herein suggests that, if such reactivation had occurred, the offset along the black lines would be between 100 and 400 feet.

D.1.5 General Observations

The study area is located in the Houston Salt Basin. The southwestern dip line, Cross-Section D-10, is transitional to Central Texas stratigraphy. In the area of Cross-Section D-10, the Catahoula Formation is sand-rich and includes up-dip fluvial and down-dip deltaic environments. Aggradational shore zone sandstones (green sands in the cross sections) are well developed above and below the Anahuac marine shale; they become better defined westward on dip Cross-Sections D-8 and D-10. Lagoonal and mud-rich floodplain environments begin to appear in the upper Oakville and persist into the Lower Goliad, giving a diffused "Burkeville confining zone." This

Appendix D: Cross Sections Showing Sand and Clay Sequences, Stratigraphy, and Fault Zones

mud-rich zone is thicker and better expressed in the western part of the area but indistinct to the east, as illustrated in the Strike Cross-Sections S-1, S-2, and S-3. The up-dip end of the Anahuac-related shore zone sandstone in the Oakville and other fluvial sandstones, just northwest of the up-dip strike Cross-Section S-1, may contain waters with TDS as low as 10,000 mg/L in areas. All marine shale intervals are well developed, but (except for the Jackson) pinch out before intersecting brackish groundwater zones. Throughout the study area, the Chicot deposits are very sand-rich with few muddy breaks. Listed below are notable observations in the twelve cross sections.

Dip Cross-Section D-5

- The Goliad is truncated by Willis Formation as part of a regional Late Miocene erosional event (Ewing, 2016).
- There is a lower sand percentage area in the upper Catahoula, Oakville and Lagarto zones, mostly occurring in the brackish-water zone; but its borders are not clearly defined, and substantial sandy intervals occur within the low-sand zone.
- A salt withdrawal basin is evident at Log 11, near the North Dayton salt dome. A withdrawal basin is associated with extensional faulting associated with salt withdrawal or movement.

Dip Cross-Section D-6

- The sub-Willis truncation of the Goliad is present but less pronounced than in Dip Section D-5.
- Low sand percentages are mostly up dip in Catahoula through Lagarto units. Thicker channel sandstones occur in the Lower Catahoula (logs 5 and 6) and in the Lagarto (log 12).
- Burkeville Unit generally consists of diffused clays across much of its extent.
- Some relatively thick sand bodies with brackish water are noted at logs 12 and 7.

Dip Cross-Section D-7

- Note the thick, high-quality “Alta Loma sand” within the Lissie in the fresh-water zone logs 14 to 20.
- Burkeville Unit is generally present but consists of diffused clays across much of its extent.
- The Lagarto appears to be quite sandy up dip.
- Nearshore sandstones in the Oakville at logs 7, 8, and 9 may contain slightly saline water resources.

Dip Cross-Section D-8

- The Willis Formation unconformity above the Goliad Formation is nearly absent.
- A salt withdrawal basin is evident at Logs 8 and 9, near the Hockley salt dome. A withdrawal basin is associated with extensional faulting associated with salt withdrawal or movement.
- There is a larger area of low sand percentage in Lagarto and Lower Goliad units in the brackish-water zone.
- A well-defined Burkeville Unit consists of thick and continuous mud at logs 10 through 18.
- Nearshore sandstones in the Oakville occur in the slightly to moderately saline zones.

Dip Cross-Section D-9

- A salt withdrawal basin is evident at Logs 5 and 6, near the Brookshire salt dome. A withdrawal basin is associated with extensional faulting associated with salt withdrawal or movement.
- Some of the Goliad Formation is truncated in the up-dip areas.
- A well-defined Burkeville mud-rich zone occurs in the Lagarto and lower Goliad from up dip to down dip locations at logs 4 through 16.
- Sands with brackish water occur below this confining layer in areas at logs 10 to 12.

Appendix D: Cross Sections Showing Sand and Clay Sequences, Stratigraphy, and Fault Zones

Dip Cross-Section D-10

- An extensive sand-poor belt in the Lagarto and adjacent units in up dip and mid-dip areas at logs 5-15.
- Some Oakville nearshore sandstones exist in the brackish groundwater zone at logs 7 and 8.
- Notable channel sandstones occur in Lower Goliad at logs 12 to 15.

Strike Cross-Section S-1

- There is a good expression of Burkeville Unit in the west. The Burkeville Unit becomes diffused and irregular to the east.
- Oakville nearshore sandstones in the moderately saline to slightly saline zones on this line.
- The sub-Willis unconformity is evident in eastern Harris County.

Strike Cross-Section S-2

- The Burkeville Unit is thick in the west, but it diffuses to east.
- Brackish-water occurs mostly in Upper Goliad.
- Slightly saline is prevalent in the Lower Goliad Formation.

Strike Cross-Section S-3

- There is no expression of a consistent Burkeville Unit.
- Brackish water resources occur in sand-rich Willis and Lissie.
- Prevalent fresh-water occurs "Alta Loma" sand in logs 7 through 9.

References:

- Brown, L.F., Jr. and R.G. Loucks. 2009. Chronostratigraphy of Cenozoic Depositional Sequences and System Tracts: A Wheeler Chart of the Northwest Margin of the Gulf of Mexico Basin, Report of Investigations No. 273: The University of Texas at Austin, Bureau of Economic Geology.
- Ewing, T.E. 1990. Tectonic map of Texas: University of Texas at Austin, Bureau of Economic Geology, scale 1:750,000, 4 sheets.

Appendix D: Cross Sections Showing Sand and Clay Sequences,
Stratigraphy, and Fault Zones

This page is intentionally left blank.

Appendix D: Cross Sections Showing Sand and Clay Sequences, Stratigraphy, and Fault Zones

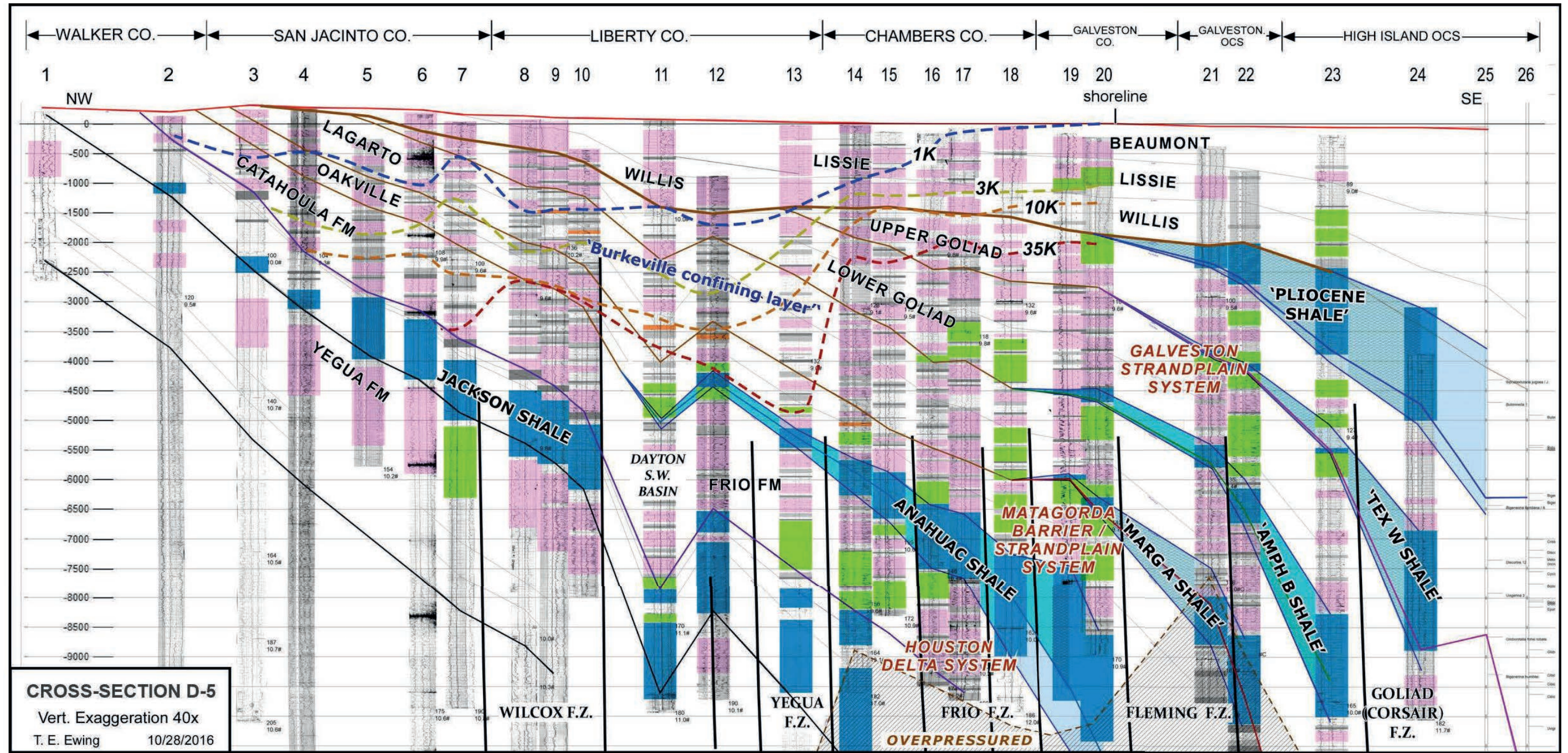


Figure D-1 Sand and clay sequences, stratigraphy, and fault zones mapped along Cross-Section D-5 in Figure 3-3

Appendix D: Cross Sections Showing Sand and Clay Sequences, Stratigraphy, and Fault Zones

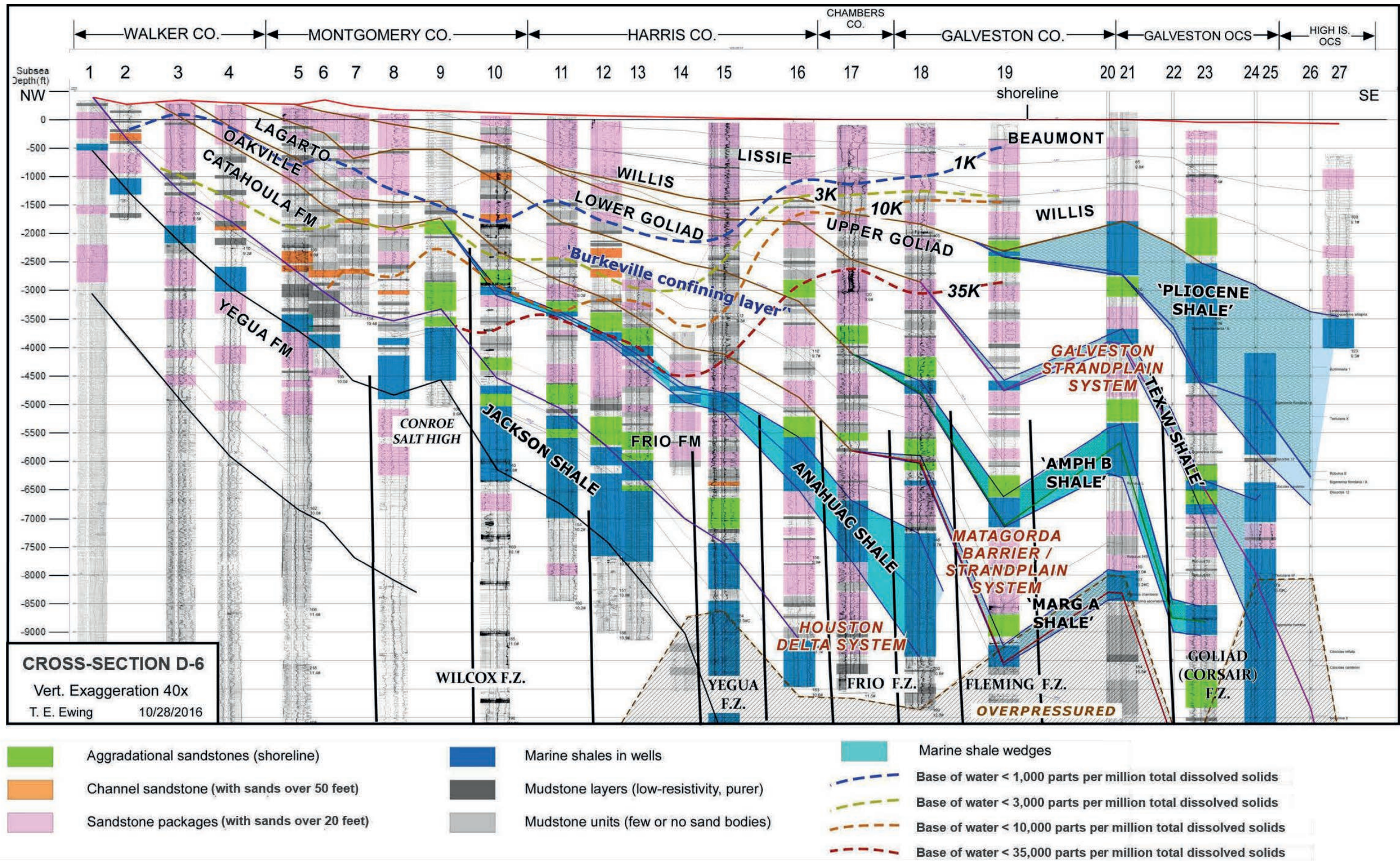


Figure D-2 Sand and clay sequences, stratigraphy, and fault zones mapped along Cross-Section D-6 in Figure 3-3

Appendix D: Cross Sections Showing Sand and Clay Sequences,
Stratigraphy, and Fault Zones

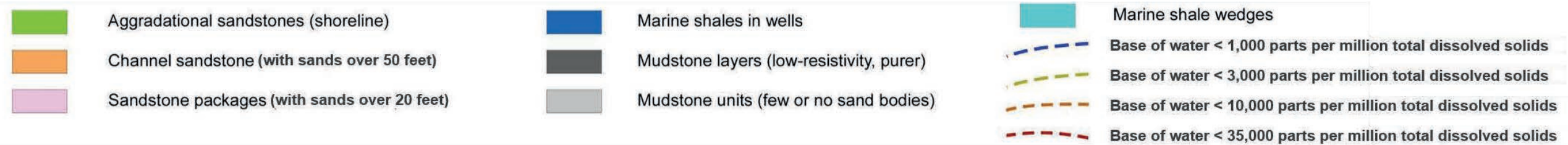
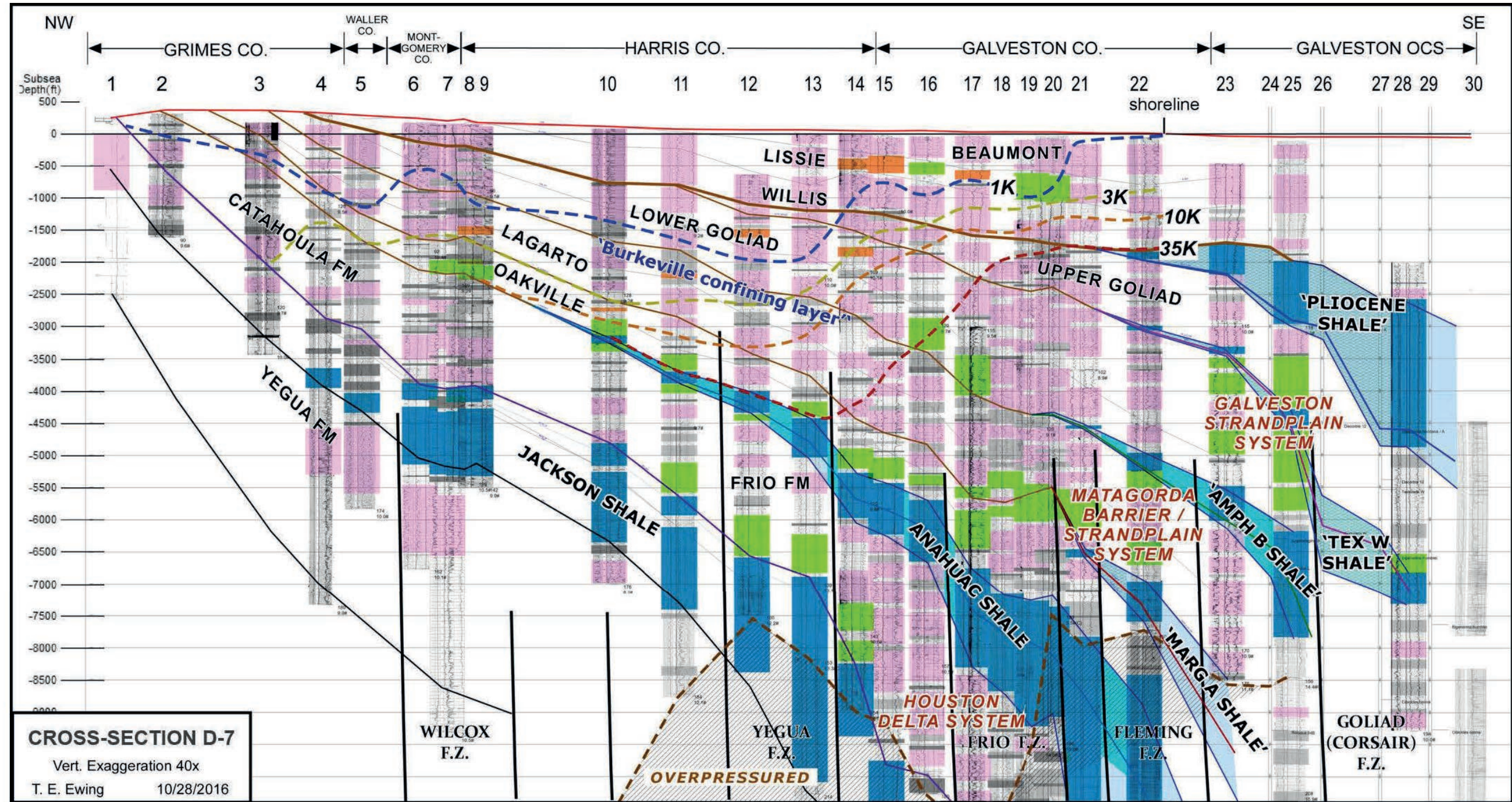


Figure D-3 Sand and clay sequences, stratigraphy, and fault zones mapped along Cross-Section D-7 in Figure 3-3

Appendix D: Cross Sections Showing Sand and Clay Sequences,
Stratigraphy, and Fault Zones

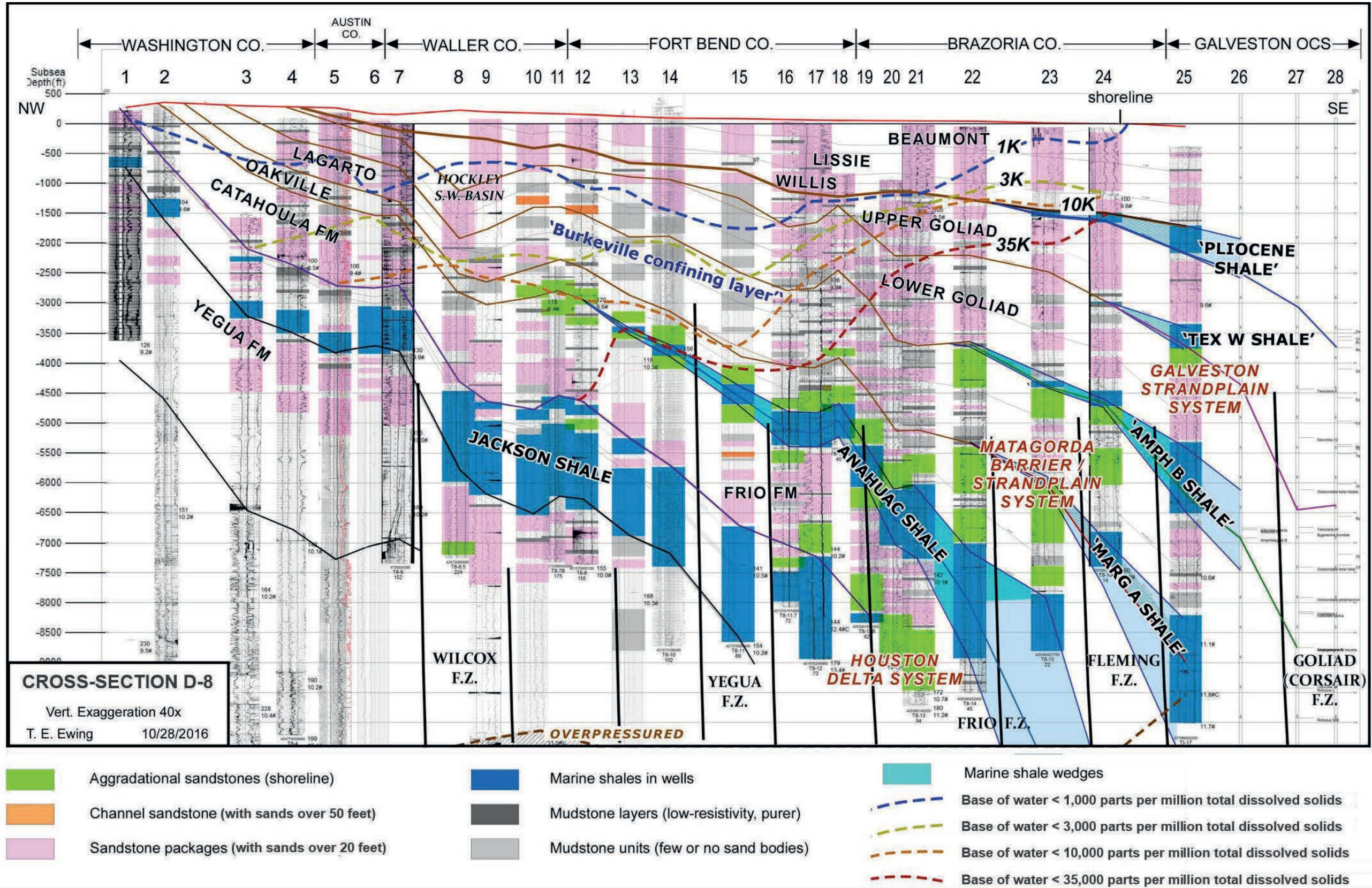


Figure D-4 Sand and clay sequences, stratigraphy, and fault zones mapped along Cross-Section D-8 in Figure 3-3

Appendix D: Cross Sections Showing Sand and Clay Sequences, Stratigraphy, and Fault Zones

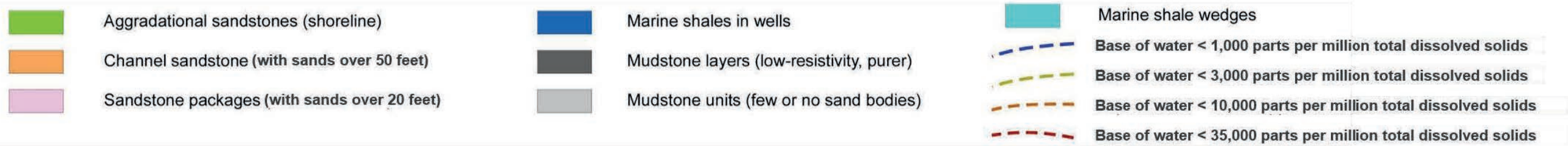
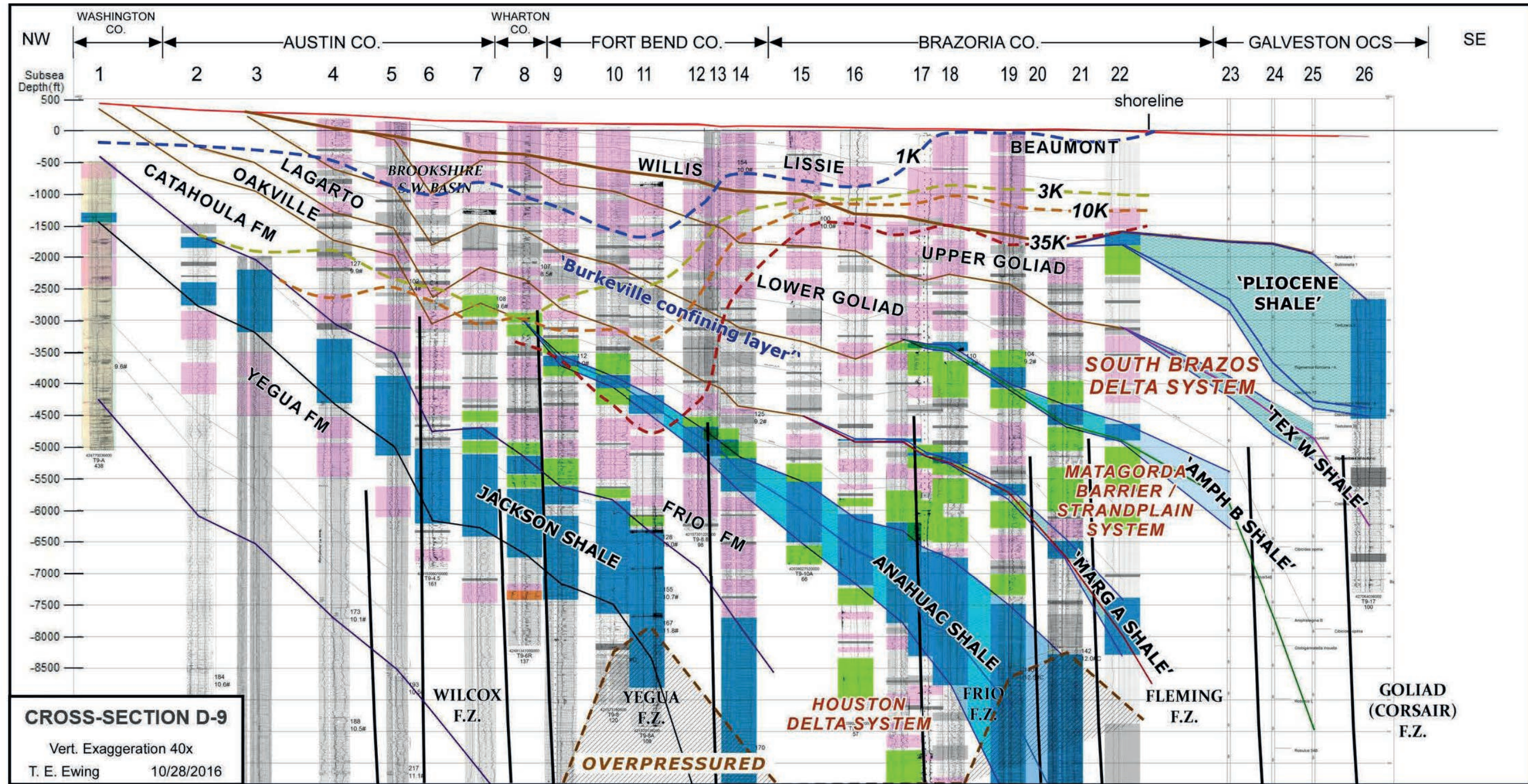


Figure D-5 Sand and clay sequences, stratigraphy, and fault zones mapped along Cross-Section D-9 in Figure 3-3

Appendix D: Cross Sections Showing Sand and Clay Sequences, Stratigraphy, and Fault Zones

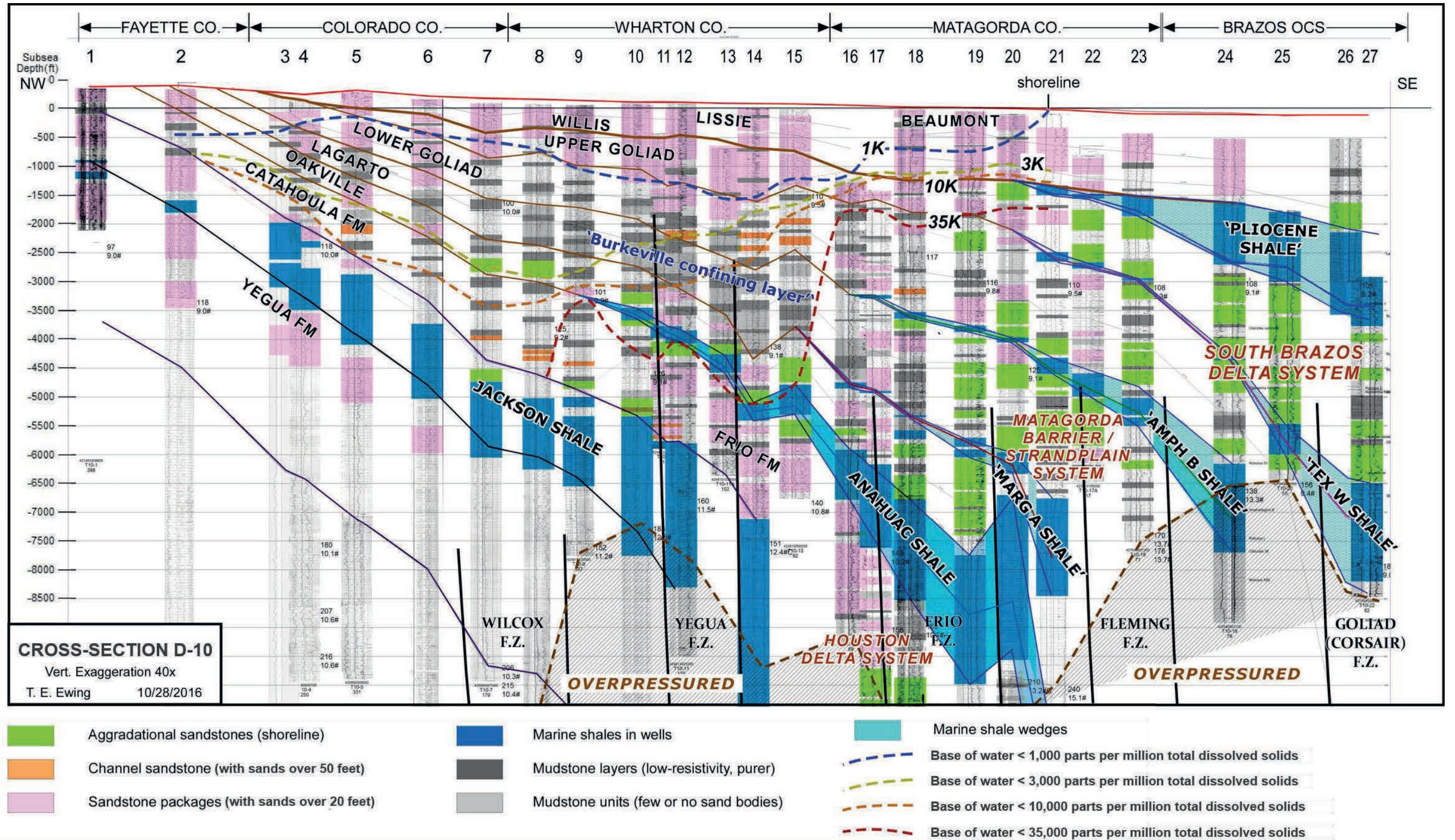
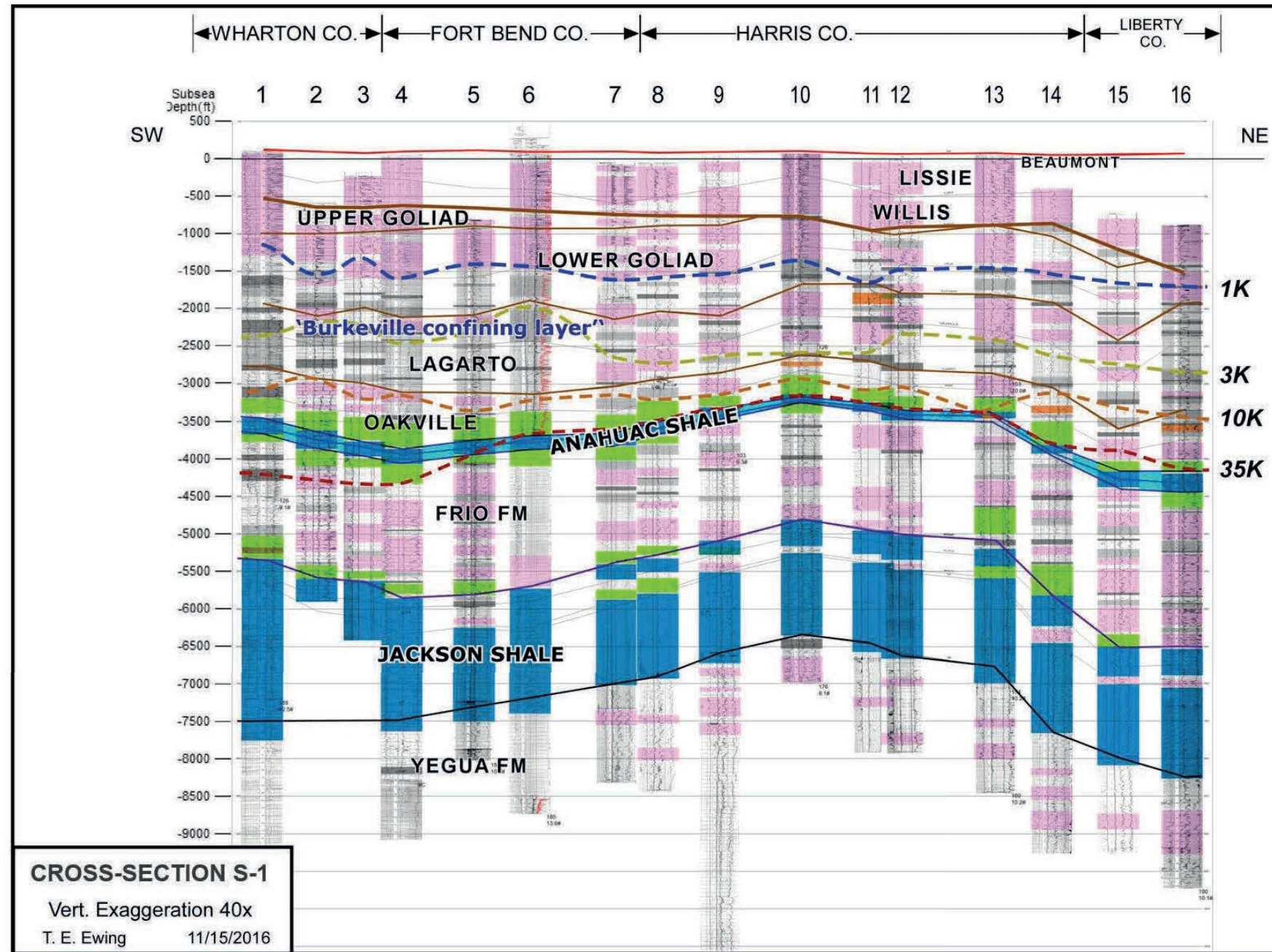


Figure D-6 Sand and clay sequences, stratigraphy, and fault zones mapped along Cross-Section D-10 in Figure 3-3

Appendix D: Cross Sections Showing Sand and Clay Sequences,
Stratigraphy, and Fault Zones






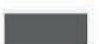

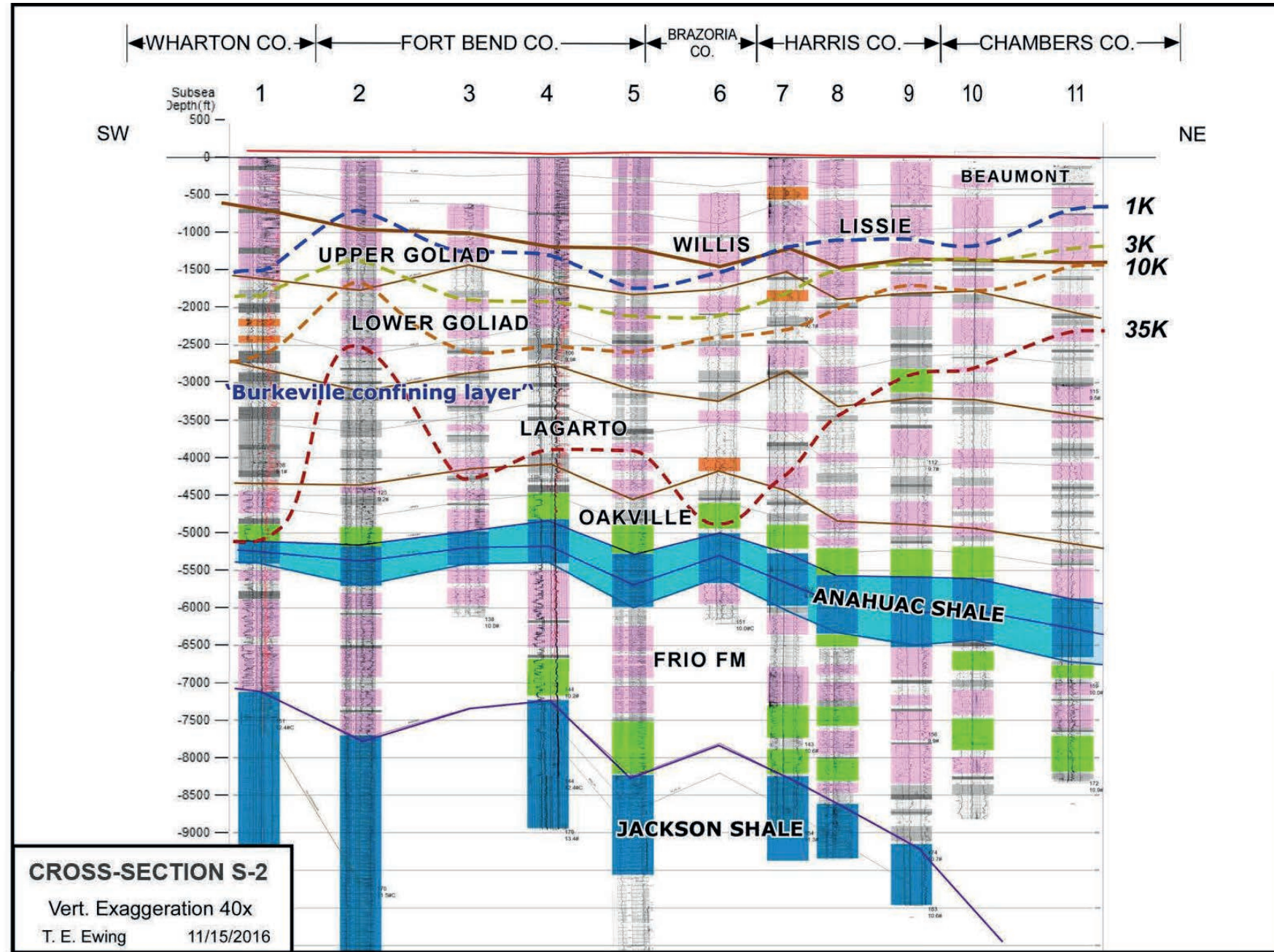
- | | | | | | |
|---|--|---|--|---|---|
|  | Aggradational sandstones (shoreline) |  | Marine shales in wells |  | Marine shale wedges |
|  | Channel sandstone (with sands over 50 feet) |  | Mudstone layers (low-resistivity, purer) |  | Base of water < 1,000 parts per million total dissolved solids |
|  | Sandstone packages (with sands over 20 feet) |  | Mudstone units (few or no sand bodies) |  | Base of water < 3,000 parts per million total dissolved solids |
| | | | |  | Base of water < 10,000 parts per million total dissolved solids |
| | | | |  | Base of water < 35,000 parts per million total dissolved solids |

Figure D-7 Sand and clay sequences, stratigraphy, and fault zones mapped along Cross-Section S-1 in Figure 3-3

Appendix D: Cross Sections Showing Sand and Clay Sequences, Stratigraphy, and Fault Zones







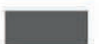


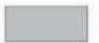



- | | | | | | |
|---|--|---|--|---|---|
|  | Aggradational sandstones (shoreline) |  | Marine shales in wells |  | Marine shale wedges |
|  | Channel sandstone (with sands over 50 feet) |  | Mudstone layers (low-resistivity, purer) |  | Base of water < 1,000 parts per million total dissolved solids |
|  | Sandstone packages (with sands over 20 feet) |  | Mudstone units (few or no sand bodies) |  | Base of water < 3,000 parts per million total dissolved solids |
| | | | |  | Base of water < 10,000 parts per million total dissolved solids |
| | | | |  | Base of water < 35,000 parts per million total dissolved solids |

Figure D-8 Sand and clay sequences, stratigraphy, and fault zones mapped along Cross-Section S-2 in Figure 3-3

Appendix D: Cross Sections Showing Sand and Clay Sequences, Stratigraphy, and Fault Zones

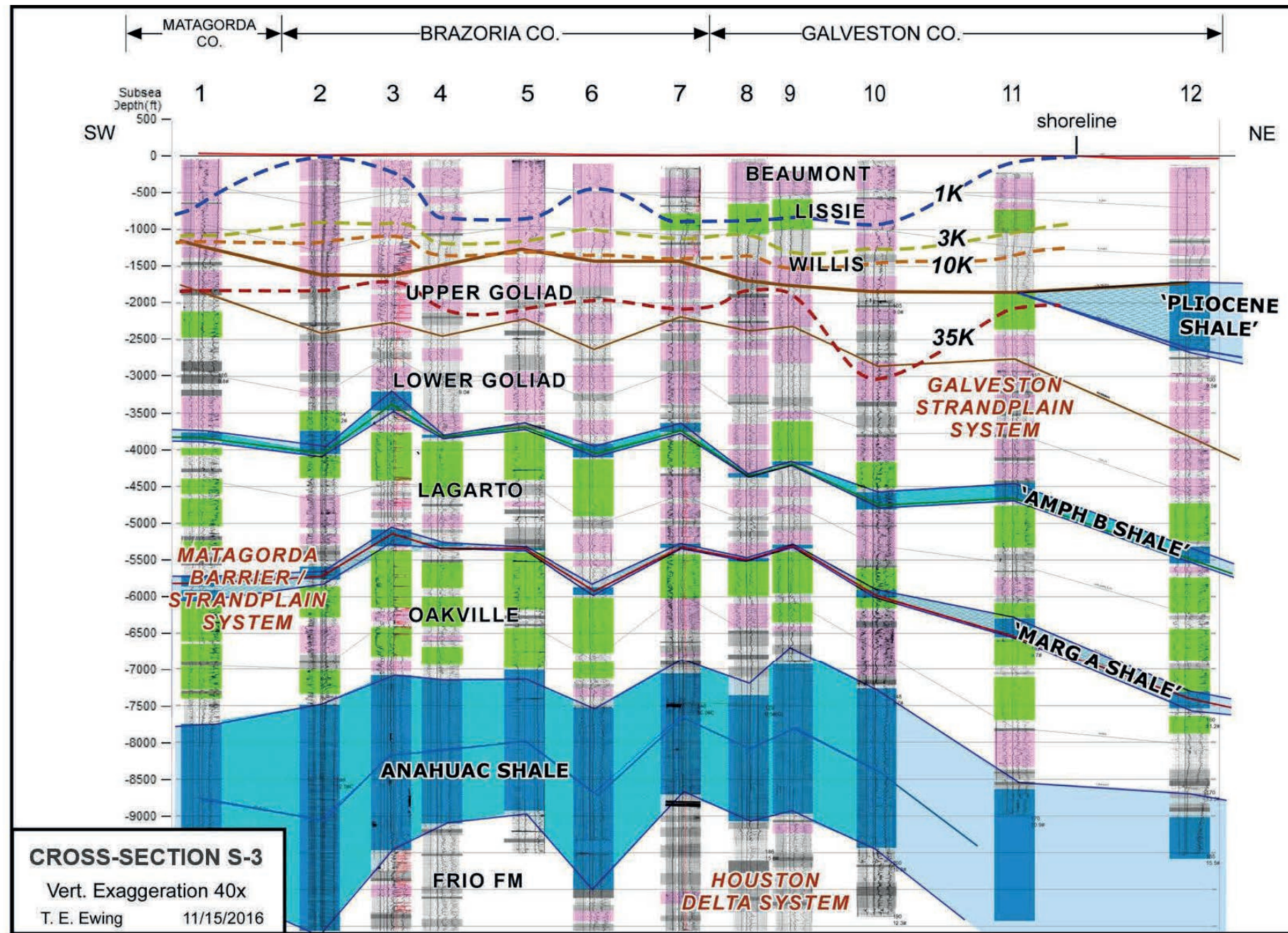


Figure D-9 Sand and clay sequences, stratigraphy, and fault zones mapped along Cross-Section S-3 in Figure 3-3

Appendix D: Cross Sections Showing Sand and Clay Sequences,
Stratigraphy, and Fault Zones

This page is intentionally left blank.

Appendix E

Location of Geophysical Logs Used to Estimate Porosity

This page is intentionally left blank.

Appendix E: Location of Geophysical Logs
Used to Estimate Porosity

LIST OF TABLES

Table E-1 Location of geophysical logs used to estimate porosity E-1

Appendix E: Location of Geophysical Logs
Used to Estimate Porosity

This page is intentionally left blank.

Appendix E: Location of Geophysical Logs
Used to Estimate Porosity

Table E-1 Location of geophysical logs used to estimate porosity

Map_ID	API_10	County	Latitude (NAD 83)	Longitude (NAD 83)
P-11	4201530673	Austin	29.78594919	-96.30172079
P-12	4201530717	Austin	29.67415196	-96.21570296
P-13	4203932634	Matagorda	29.29366621	-95.7284297
P-14	4203932751	Matagorda	28.93558884	-95.38769861
P-17	4207132057	Chambers	29.86715429	-94.88229454
P-20	4218530399	Grimes	30.27003078	-95.92868655
P-22	4220131351	Harris	30.08595624	-95.63451607
P-23	4220132735	Harris	29.61329542	-95.20593278
P-28	4233930837	Montgomery	30.25268493	-95.36448826
P-33	4248133500	Wharton	29.52834216	-96.2438476
P-35	4216730792	Galveston	29.43364928	-95.16295605
P-36	4215732782	Fort Bend	29.5852544	-95.4867687
P-37	4220131057	Harris	29.85856536	-95.77147401
P-38	9965000000	Fort Bend	29.72423	-95.74811

Appendix E: Location of Geophysical Logs
Used to Estimate Porosity

This page is intentionally left blank.

Appendix F

Estimating TDS Concentrations From Geophysical Logs

This page is intentionally left blank.

TABLE OF CONTENTS

F.1	Definition and Measurement of TDS Concentrations	F-1
F.2.1	Mean Ro Method.....	F-2
F.2.2	Rwa Minimum Method.....	F-6

LIST OF FIGURES

Figure F-1	Calculated TDS concentration versus measured TDS concentration for groundwater samples from the Texas Gulf Coast Aquifer System grouped into class intervals based on their equivalents of bicarbonate.....	F-8
Figure F-2	Location of wells with screen information and with calculated or measured TDS concentrations in the TWDB groundwater database.....	F-9
Figure F-3	R _o -TDS graph for the Chicot Aquifer Group (including the Beaumont, Lissie, and Willis formations) generated from the TWDB Gulf Coast BRACs study . The blue line is the formation resistivity value for a 1,000 mg/L TDS concentration and the red line is the formation resistivity value for 3,000 mg/L TDS concentration.	F-10
Figure F-4	R _o -TDS graph for the Evangeline Aquifer Group (including the Upper Goliad, Lower Goliad, Upper Lagarto, and Middle Lagarto formations) generated from the TWDB Gulf Coast BRACs study . The blue line is the formation resistivity value for a 1,000 mg/L TDS concentration and the red line is the formation resistivity value for 3,000 mg/L TDS concentration.	F-11
Figure F-5	R _o -TDS graph for the Jasper Aquifer Group (including the Lower Lagarto, Oakville, Upper Lagarto, and Middle Lagarto formations) generated from the TWDB Gulf Coast BRACs study. The blue line is the formation resistivity value for a 1,000 mg/L TDS concentration and the red line is the formation resistivity value for 3,000 mg/L TDS concentration.	F-12
Figure F-6	Additional pairs of geophysical log(s) and a water wells that were used to evaluate to determine the relationship between R _o and TDS Concentrations (mg/L) for the (a) Chicot Aquifer; (b) the Evangeline Aquifer, and the (c) Jasper Aquifer	F-13

LIST OF TABLES

Table F-1	Comparison between measured and calculated TDS concentrations for 575 wells in the study area that have well screen information	F-2
Table F-2	Comparison of the TDS concentrations associated with well pairs created from this study and the well pairs used by Young and others (2016) to generate Ro-TDS graphs for the Chicot, Evangeline, and Jasper Aquifers.....	F-3
Table F-3	Comparison of the maximum and minimum TDS concentrations associated with well pairs created from this study and the well pairs used by Young and others (2016) to generate Ro-TDS graphs for the Chicot, Evangeline, and Jasper Aquifers	F-3
Table F-4	Results of the Kolmogorov-Smirnov test of the residuals from the Young and Others (2016) samples versus the samples newly acquired for the current study area.....	F-4
Table F-5	Predicted TDS concentrations for different formation resistivity using the regression equations developed from the Ro-TDS data associated the Chicot Aquifer Group, Evangeline Aquifer Group, and Jasper/Catahoula Aquifer Group from Young and others (2016)	F-5

Appendix F: Estimating TDS Concentrations
From Geophysical Logs

This page is intentionally left blank.

F.1 Definition and Measurement of TDS Concentrations

TDS concentrations are generally understood to include all the inorganic salts and small amounts of organic matter that are dissolved in water (World Health Organization, 2016; Government of Canada, 2016). However, because of the difficulty associated with measuring all the substances dissolved in water, several approaches are used to measure TDS concentrations. Three of the commonly used approaches for measuring TDS are:

1. Filterable Residue Approach: Filter the water sample, and then evaporate it at 180 degrees Celsius (°C) in a pre-weighed dish until the weight of the dish no longer changes. The increase in weight of the dish represents the TDS concentration, and it is reported in mg/L.
2. Conductivity Approach: The electrical conductivity of the water sample is measured, and the TDS concentration is estimated based on a linear correlation equation relating TDS concentration and specific conductivity.
3. Ion Summation Approach: Laboratory measurements are used to measure individual ions and compounds, and their masses are summed to represent TDS concentration.

For this study, the measured TDS concentrations were obtained from the TWDB Groundwater Database and most were determined using the filterable residue approach. For convenience and for consistency with how the TWDB reports its water quality data, the filterable residue approach will be associated with “measured” TDS concentration values, and the ion summation approach will be associated with “calculated” TDS concentration values. The “calculated” TDS concentration values were determined using **Equation F-1**.

$$\text{TDS} = \text{major ions} + \text{SiO}_2 \quad (\text{Equation F-1})$$

where

TDS	=	total dissolved solid concentrations (mg/L)
Major ions	=	concentration of sodium, calcium, magnesium, nitrate, potassium, strontium, fluoride, sulfate, chloride, bicarbonate, and iron (mg/L)
SiO ₂	=	concentration of silica oxide in solution (mg/L)

Figure F-1 shows the difference between measured (filterable residue approach) and calculated (ion summation approach) TDS concentrations using data obtained from 9,200 water wells shown in **Figure F-2**. The data also show that the calculated TDS concentrations are consistently greater than the measured TDS concentrations. For several well samples, the calculated TDS concentrations are as much as 50% greater than the measured TDS concentrations. By color-coding the data points based on percentage of the milliequivalents comprised by the bicarbonate ion, one can see that the differences between the measured and calculated values increase with increases in the percentage of bicarbonate ions. This relationship exists because a limitation of the filterable residue approach as some of the bicarbonate mass is lost during the evaporation of the water when the bicarbonate ion is converted to carbon trioxide, carbon dioxide, and water. According to Collier (1993), 50.8% of the bicarbonate ion is driven off as carbon dioxide and water vapor during the evaporation process and 49.2% of the bicarbonate ion remains as carbon trioxide.

As discussed by Young and others (2013, 2016), the relative amount of bicarbonate in groundwater in the Texas Gulf Coast Aquifer generally decreases with increased magnitude in the concentration of TDS concentration. To illustrate this relationship, **Table F-1** provides the ratio of measured to calculated TDS concentrations for different concentration ranges of TDS in the study area. The data from 575 water wells show that the ratio of

Appendix F: Estimating TDS Concentrations
From Geophysical Logs

measured to calculated values increases from 0.75 for concentration values below 500 mg/L to 0.96 for concentration values above 3,000 mg/L.

Table F-1 Comparison between measured and calculated TDS concentrations for 575 wells in the study area that have well screen information

Range of Measured TDS Concentrations (mg/L)	Number of Samples	Average TDS Concentrations (mg/L)		
		Measured	Calculated	Measured/Calculated
> 0	575	467	598	0.78
0 to 500	416	325	432	0.75
500 to 1,000	129	680	873	0.78
1,000 to 2,000	26	1,263	1,443	0.87
2,000 to 3,000	2	2,878	3,045	0.94
3,000 to 4,000	2	3,710	3,873	0.96

F.2.1 Mean Ro Method

The primary purpose of this section is to explain the underlying assumptions and data associated with both the Mean R_o Method and the R_{wa} Minimum Method.

Figure F-3, **Figure F-4**, and **Figure F-5** show the R_o -TDS graphs generated by Young and others (2016) for well-log pairs in the Chicot Aquifer (Beaumont, Lissie, and Willis formations), the Evangeline Aquifer (Upper Goliad, Lower Goliad, Upper Lagarto, and Middle Lagarto formations), and the Jasper/Catahoula Aquifer Group (Lower Lagarto, Oakville, and Catahoula formations), respectively. For each R_o -TDS graph, the TDS concentrations used in the correlation was calculated based on the ion summation approach. Each figure includes up to three types of data and a line as part of the R_o -TDS graph. The line represents the equation that predicts TDS concentration based on the formation resistivity and was developed from a regression analysis (Davis, 1986).

In Figures F-3, F-4, and F-5, the data used by Young and others (2016) are divided into red and blue points. The red points are from well-log pairs located outside of the current study area and the blue points are from well-log pairs located inside of the current study area. The green points are from the well-log pairs collected as part of this study and are also located inside the study area. The green points were not used to produce the regression line. **Figure F-6** shows the location of the well pairs in the current study area that are associated with the green and blue data points.

The green points in Figures F-3 through F-6 are from the well-log pairs collected in this study in the study area. They represent 175 geophysical logs additional to those available in TWDB HB-30 study (Young and others, 2016). A summary of the number of TDS values in the TWDB study compared to the number collected for this study is presented in **Table F-2** and **Table F-3**. The comparison shows that both the new data set (green points) as well as the collective data set (green and blue points) for the study area provides a significantly smaller range and number of TDS concentration values for analysis as compared to the TWDB HB-30 data (red and blue points). This is true for all three aquifers. Because of the low range of the TDS concentration data collected for this analysis and the relatively smaller number of samples, R_o -TDS regressions were poor.

Appendix F: Estimating TDS Concentrations
From Geophysical Logs

Table F-2 Comparison of the TDS concentrations associated with well pairs created from this study and the well pairs used by Young and others (2016) to generate R_o-TDS graphs for the Chicot, Evangeline, and Jasper Aquifers

Aquifer	Gulf Coast Study by Young and others (2016)								This Study			
	Outside the Study Area				Inside the Study Area				Inside the Study Area			
	Well Pairs	Number of TDS Values (mg/L)			Well Pairs	Number of TDS Values (mg/L)			Well Pairs	Number of TDS Values (mg/L)		
		<300	> 250 & < 1,000	> 1,000		<300	> 250 & < 1,000	> 1,000		<300	> 250 & < 1,000	> 1,000
Chicot	140	6	83	51	27	2	19	6	42	0	38	4
Evangeline	295	3	122	170	13	0	12	1	20	0	20	0
Jasper	116	0	17	99	0	0	0	0	2	0	1	1

Table F-3 Comparison of the maximum and minimum TDS concentrations associated with well pairs created from this study and the well pairs used by Young and others (2016) to generate R_o-TDS graphs for the Chicot, Evangeline, and Jasper Aquifers

Aquifer	Gulf Coast Study by Young and others (2016)						This Study			
	Outside the Study Area			Inside the Study Area			Inside the Study Area			
	Well Pairs	TDS Values (mg/L)		Well Pairs	TDS Values (mg/L)		Well Pairs	TDS Values (mg/L)		
		Min	Max		Min	Max		Min	Max	
Chicot	140	102	8,075	27	148	1,810	42	348	3,606	
Evangeline	295	255	5,252	13	344	1,095	20	363	752	
Jasper	116	513	6,989	0	NA	NA	2	512	1,179	

Because of the lack of success in deriving R_o-TDS relationships using only well-pair data from the current study area, we evaluated whether the Young and others (2016) relationships could be shown to be applicable to the current study. Because some data from the current study area, not all, were used in deriving the Young and others (2016) R_o-TDS relationships, we would expect those relationships generally to remain valid. However, new TDS and resistivity data have been added in the current study, so we statistically tested the new data for their consistency with the Young and others (2016) data in the study area.

The Kolmogorov–Smirnov (KS) test is a nonparametric test of the equality of continuous, one-dimensional probability distributions (Conover, 1980). The KS test can be used to compare two sample populations for their similarity. In our case, we were interested in comparing the data in the study area used by Young and others (2016) to derive the R_o-TDS relationships to the new data collected in the study area in the current work. To normalize the datasets for comparison, we first calculated the residuals in log-transformed space (compared to the regression lines derived for each formation in Young and others [2016]) and compared the residual sample populations.

Appendix F: Estimating TDS Concentrations
From Geophysical Logs

Statistical tests such as the KS test propose a “null hypothesis,” and then test the plausibility of that hypothesis being true. Our null hypothesis is that the two sample populations are statistically the same. The measure of that plausibility is called the “p-value.” A typical cutoff for rejecting the null hypothesis is a p-value of less than 0.05. **Table F-4** shows the results of the KS testing by aquifer. For the Chicot and Evangeline aquifers, the p-value is greater than 0.05, and we accept the hypothesis that the two samples are statistically the same. This provides statistical evidence that the R_o -TDS relationships derived in Young and others (2016) are applicable for the current study. For the Jasper Aquifer and Catahoula Formation, no new samples were available for the current study, so the KS test cannot be applied. Given the lack of new data for the Jasper and Catahoula, the most appropriate path forward is to use the previously derived R_o -TDS relationship.

Table F-4 Results of the Kolmogorov-Smirnov test of the residuals from the Young and Others (2016) samples versus the samples newly acquired for the current study area

Aquifer	n1*	n2	p-value
Chicot	27	42	0.88
Evangeline	13	20	0.89
Jasper and Catahoula	0	2	n/a

*n1 is the number of samples in the study area for the Young and Others (2016) study, while n2 is the number of samples in the study area acquired for the current study

Equation F-2, Equation F-3, and Equation F-4 provide the empirical equations developed by Young and others (2016) for sands to predict the TDS concentration in groundwater for the Chicot, Evangeline, and Jasper aquifers, respectively. These equations were used to generate **Table F-5**, which shows TDS concentration as a function of formation resistivity.

$$TDS = e^{(-0.95 * \ln(R_o) + 9.4)} \quad \text{(Equation F-2)}$$

$$TDS = e^{(-1.03 * \ln(R_o) + 9.66)} \quad \text{(Equation F-3)}$$

$$TDS = e^{(-0.95 * \ln(R_o) + 9.49)} \quad \text{(Equation F-4)}$$

where

TDS = calculated using the ion summation approach (mg/L)

R_o = Formation resistivity (ohm-m)

Appendix F: Estimating TDS Concentrations
From Geophysical Logs

Table F-5 Predicted TDS concentrations for different formation resistivity using the regression equations developed from the R_o -TDS data associated the Chicot Aquifer Group, Evangeline Aquifer Group, and Jasper/Catahoula Aquifer Group from Young and others (2016)

Formation Resistivity	Predicted TDS Concentrations (mg/L)		
	Chicot Aquifer	Evangeline Aquifer	Jasper/ Catahoula Aquifer
30	474	477	524
25	564	575	623
20	697	723	770
18	771	806	851
16	862	910	952
14	979	1,044	1,081
12	1,133	1,223	1,251
10	1,348	1,475	1,488
8	1,666	1,855	1,839
6	2,191	2,494	2,417
4	3,222	3,785	3,553

Note: TDS=total dissolved solids determined by the ion summation approach

The groundwater TDS values used to develop Equations F-2, F-3, and F-4 used the ionic summation approach to calculate TDS. For the purpose of determining TDS concentrations for classifying water quality in Texas, the TDS concentration needs to be based on a measured filterable residue approach. In order to use the equation to calculate a TDS concentration based on a filterable residual approach a conversion factor is required. These conversion factors were calculated for the Chicot, Evangeline and Jasper aquifers in the northern region of the Texas Gulf Coast Aquifer System by Young and others (2016) and are presented in **Table F-6**. These conversion factors will be used to apply the Mean R_o -TDS Method for determining whether groundwater associated with a sand layer identified on a geophysical log will be assigned the category of fresh water or slightly saline water. An example application of the conversion factors in Table F-6 is that a TDS concentration of 1,000 mg/L in the Chicot Aquifer based on the ion summation approach is converted to a TDS concentration of 820 mg/L based on the filterable residue approach by a conversion factor of 0.82.

Table F-6 TDS concentration range-specific factors for converting TDS concentrations based on the ion summation approach to the filterable residue approach

Aquifer	Factors by Range of TDS Concentration	
	700 to 1,400 mg/L	2,800 to 3,300 mg/L
Chicot	0.82	0.93
Evangeline	0.86	0.95
Jasper	0.82	0.95

Note: TDS=total dissolved solids determined by the ion summation approach

Appendix F: Estimating TDS Concentrations
From Geophysical Logs

F.2.2 R_{wa} Minimum Method

The development of the R_{wa} Minimum method follows the formulas provided by Estep (1988) and Meyer and others (2014). For TDS concentrations above 5,000 mg/L, we used the R_{wa} Minimum method to predict TDS concentrations. We implemented the R_{wa} Minimum method using **Equation F-5**.

$$R_{we77} = \Phi^m \times R_{o77} \quad \text{(Equation F-5)}$$

where

- R_{we77} = resistivity of water equivalent (ohm-meters) at 77 °F
- Φ = porosity
- m = the cementation exponent
- R_{o77} = the formation resistivity of a 100% water saturated formation (ohm-meters) at 77 °F

After applying Equation F-4, we applied **Equation F-6** to convert resistivity to specific conductance and then we applied **Equation F-7** to convert specific conductance to TDS.

$$C_{w77} = 10,000 / R_{we77} \quad \text{(Equation F-6)}$$

$$\text{TDS} = ct * C_{w77} \quad \text{(Equation F-7)}$$

where

- C_{w77} = specific conductance ($\mu\text{mhos/cm}$ at 77 °F)
- ct = specific conductivity-total dissolved solids concentration conversion factor
- TDS = TDS concentrations (mg/L) that is measured using the filterable residue approach

The application of Equations F-4, F-5, and F-6 requires that three variables be defined. These variables are porosity or Φ , the cementation exponent, m , and ct, the conversion factor from specific conductivity to TDS. The value for porosity is defined using **Equation F-8**. Equation F-8 defines porosity as a parameter that is depth dependent. The values for ct and m are set as constants at 0.57 and 1.3, respectively. These values for ct and m are values used by Young and others (2016).

$$\Phi = 36.6 - 0.001 * d \quad \text{(Equation F-8)}$$

where

- Φ = porosity
- d = depth (feet)

Estep (1998) provides two ranges for the cementation exponent that are relevant to the Texas Gulf Coast Aquifer System. For fine to medium loose sandstone, Estep (1998) provides a range of 1.3 to 1.4 for the cementation exponent. For slightly cemented sandstone, Estep (1998) provides a range of 1.4 to 1.5 for the cementation exponent. Because the Texas Gulf Coast Aquifer System is largely an unconsolidated deposit, the exponent of 1.3 was selected by Young and others (2016).

For a groundwater solution that is fully dominated by sodium chloride, the value of ct is 0.56. (Schlumberger, 2009). In their Figure 13-9, Young and others (2016) calculate a value of ct of 0.57 as the conversion factor from specific conductance and measured TDS concentration based on the filterable residue approach.

A potential use for R_{wa} Minimum method is to classify groundwater in the sand units based on the formation resistivity of the sand where the TDS concentrations are greater than or equal to 5,000 mg/L. **Table F-7** provides

Appendix F: Estimating TDS Concentrations
From Geophysical Logs

the formation resistivity for which the R_{wa} Minimum method predicts TDS concentrations of 10,000 mg/L, which is the transition between moderately saline and very saline groundwater, and of 35,000 mg/L, which is the transition between very saline water and brine.

Table F-7 Formation resistivity cutoff values for the R_{wa} Minimum Method that produces measured TDS concentration values of 10,000 and 35,000 mg/L using a ct conversion factor of 0.57 and a porosity range from 0.36 to 0.27

Porosity	Formation Resistivity (at 77°F)	Measured TDS Concentrations (mg/L)
0.36	2.15	10,000
	0.71	35,000
0.33	2.40	10,000
	0.80	35,000
0.3	2.70	10,000
	0.91	35,000
0.27	3.10	10,000
	1.04	35,000

Appendix F: Estimating TDS Concentrations
From Geophysical Logs

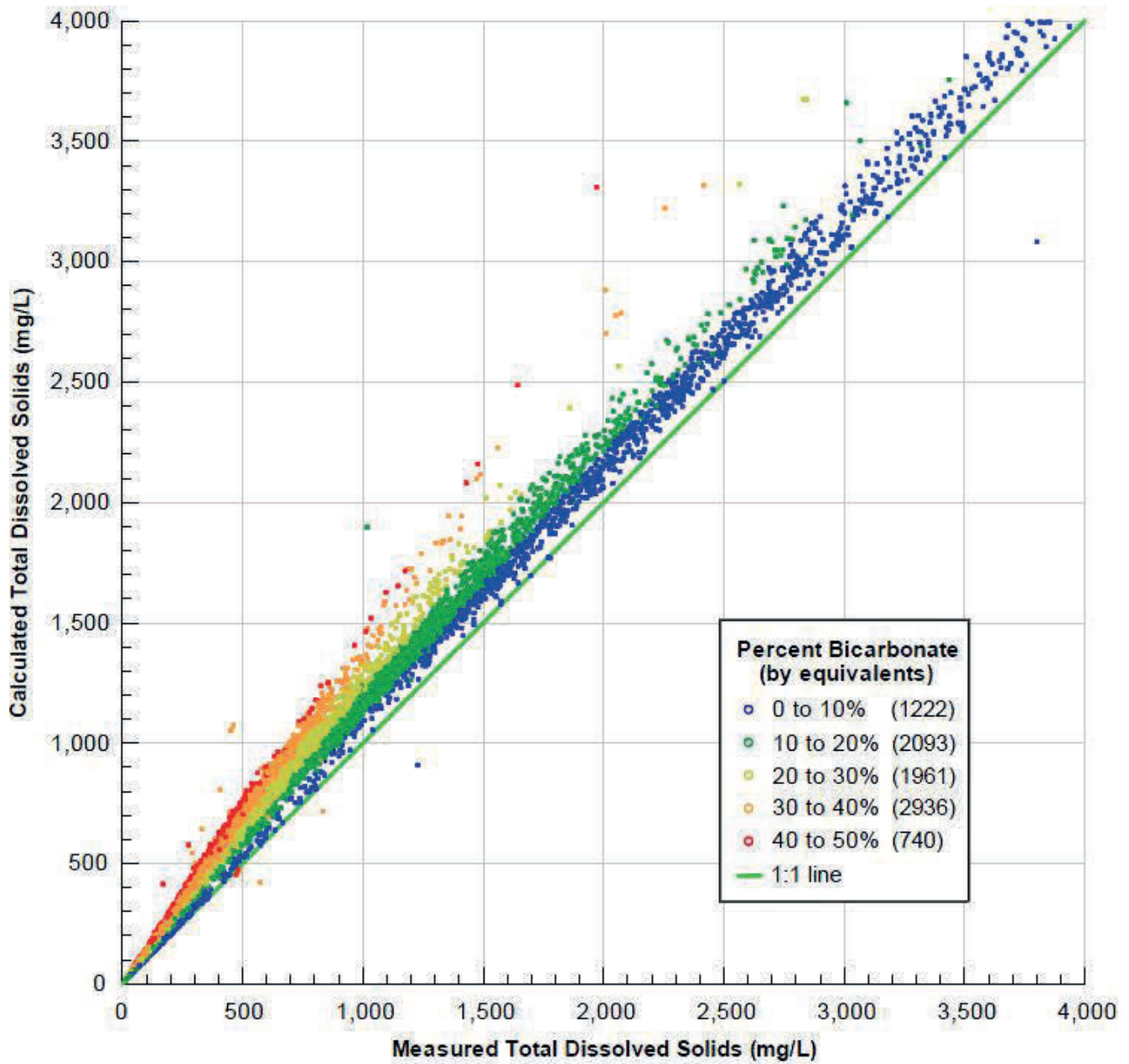
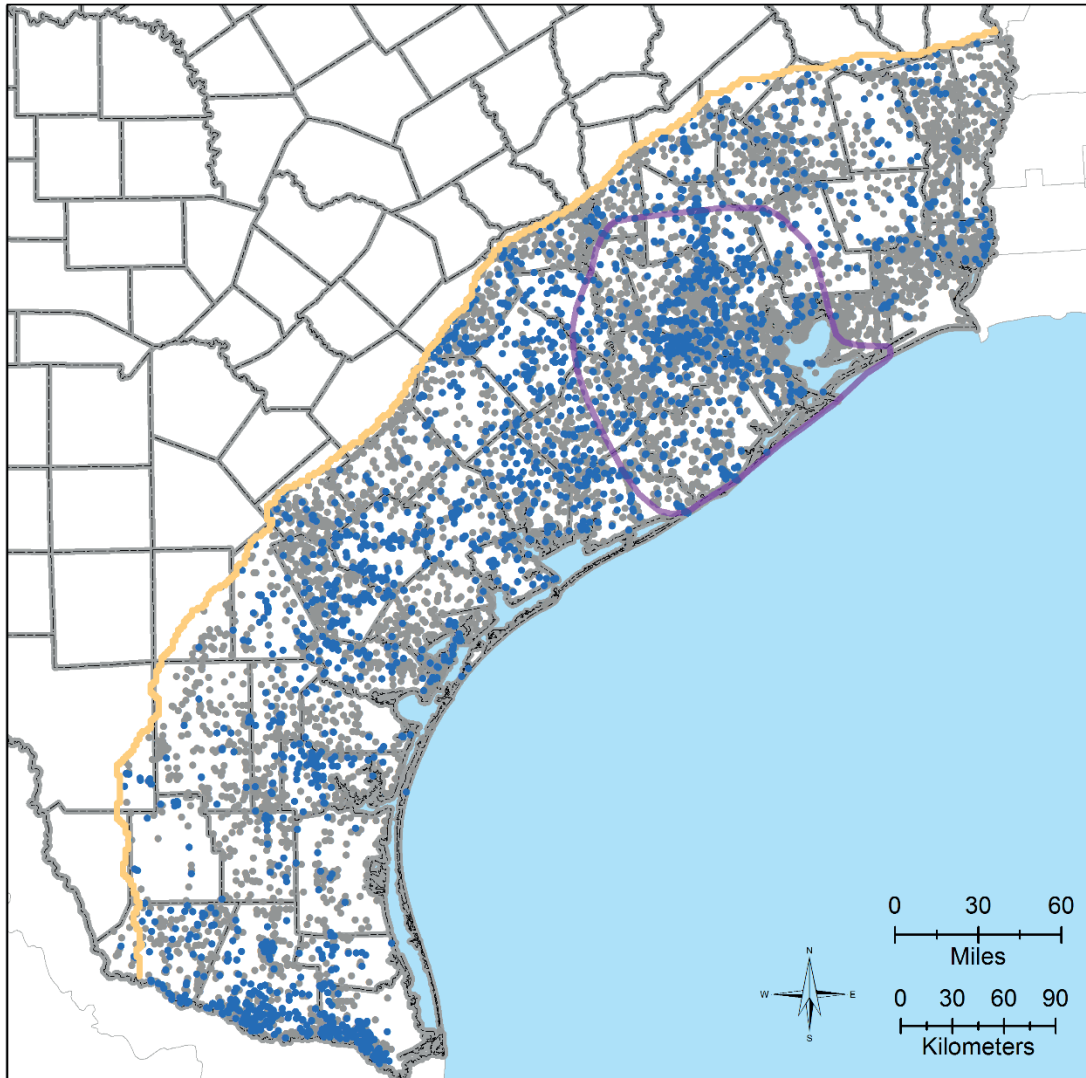


Figure F-1 Calculated TDS concentration versus measured TDS concentration for groundwater samples from the Texas Gulf Coast Aquifer System grouped into class intervals based on their equivalents of bicarbonate

Appendix F: Estimating TDS Concentrations
From Geophysical Logs



**Wells with a Measured Total Dissolved Solids
Concentration Measurement**

Legend

- Has Screen Depth Info
- No Screen Depth Info
- Catahoula Updip Extent
- ▭ Study Area
- ▭ Counties



Map Location

Prepared for:



Prepared by:



Figure F-2

Location of wells with screen information and with calculated or measured TDS concentrations in the TWDB groundwater database

Appendix F: Estimating TDS Concentrations
From Geophysical Logs

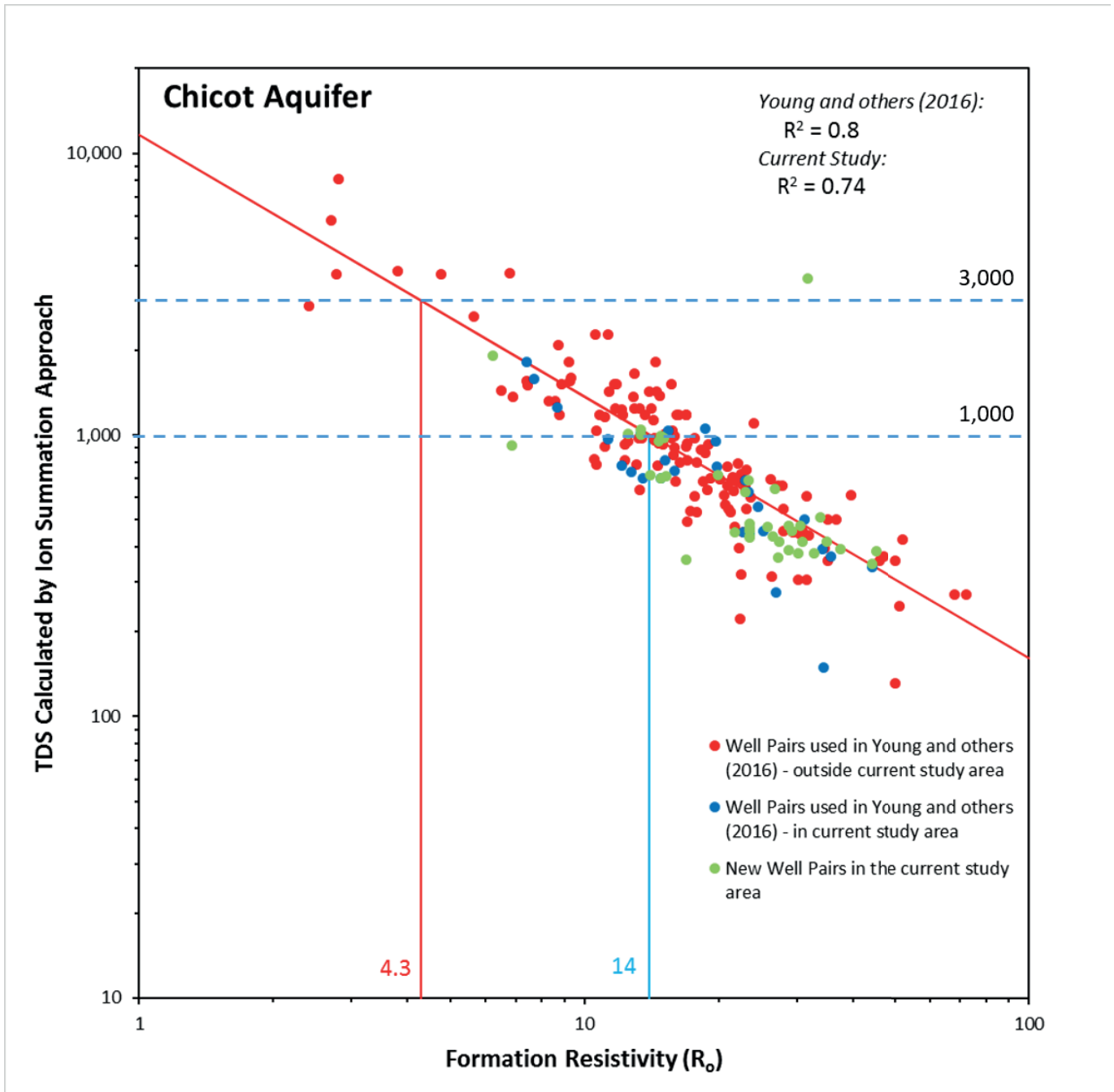


Figure F-3 R_o -TDS graph for the Chicot Aquifer Group (including the Beaumont, Lissie, and Willis formations) generated from the TWDB Gulf Coast BRACs study. The blue line is the formation resistivity value for a 1,000 mg/L TDS concentration and the red line is the formation resistivity value for 3,000 mg/L TDS concentration.

Appendix F: Estimating TDS Concentrations
From Geophysical Logs

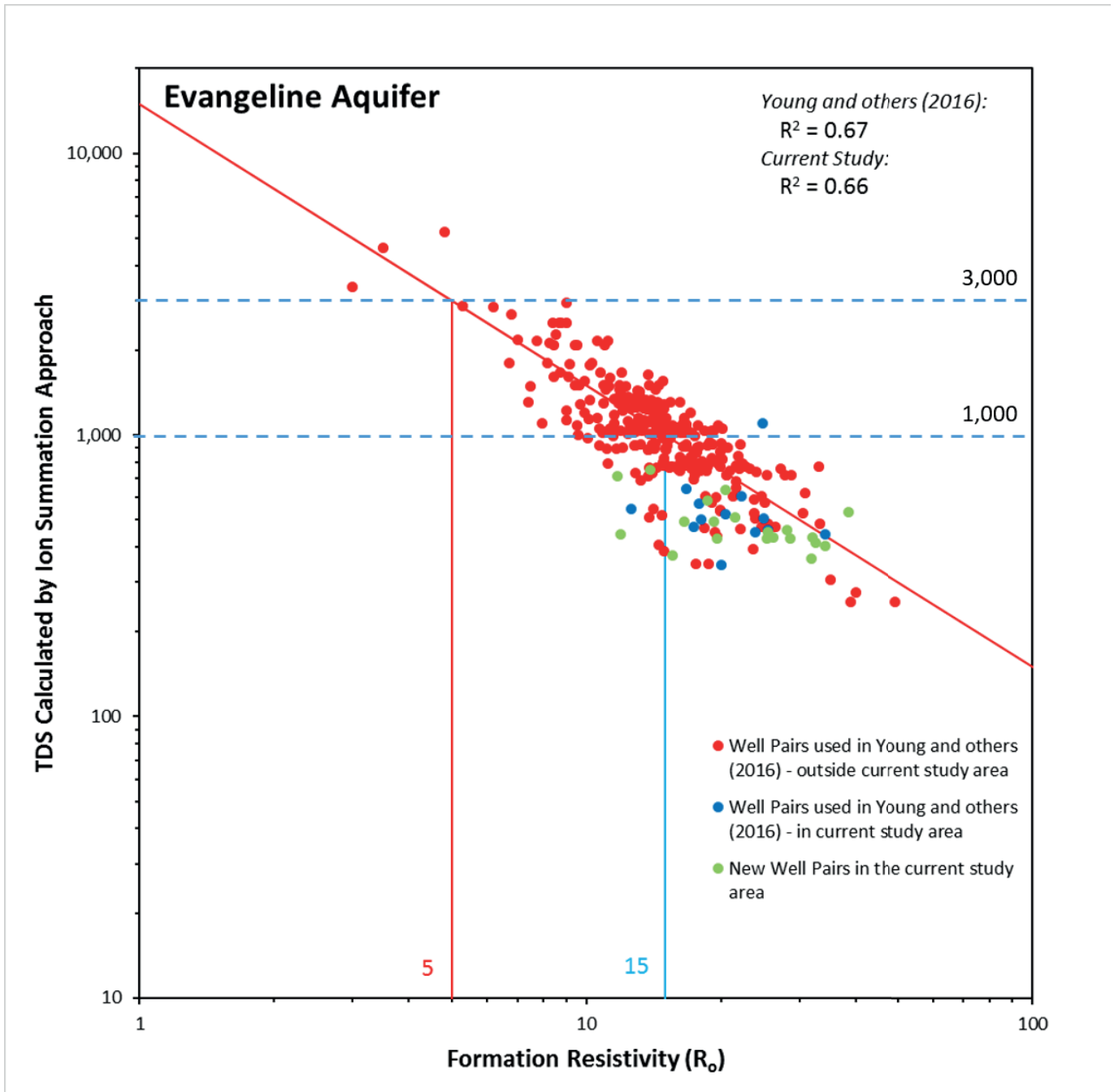


Figure F-4 R_0 -TDS graph for the Evangeline Aquifer Group (including the Upper Goliad, Lower Goliad, Upper Lagarto, and Middle Lagarto formations) generated from the TWDB Gulf Coast BRACs study. The blue line is the formation resistivity value for a 1,000 mg/L TDS concentration and the red line is the formation resistivity value for 3,000 mg/L TDS concentration.

Appendix F: Estimating TDS Concentrations
From Geophysical Logs

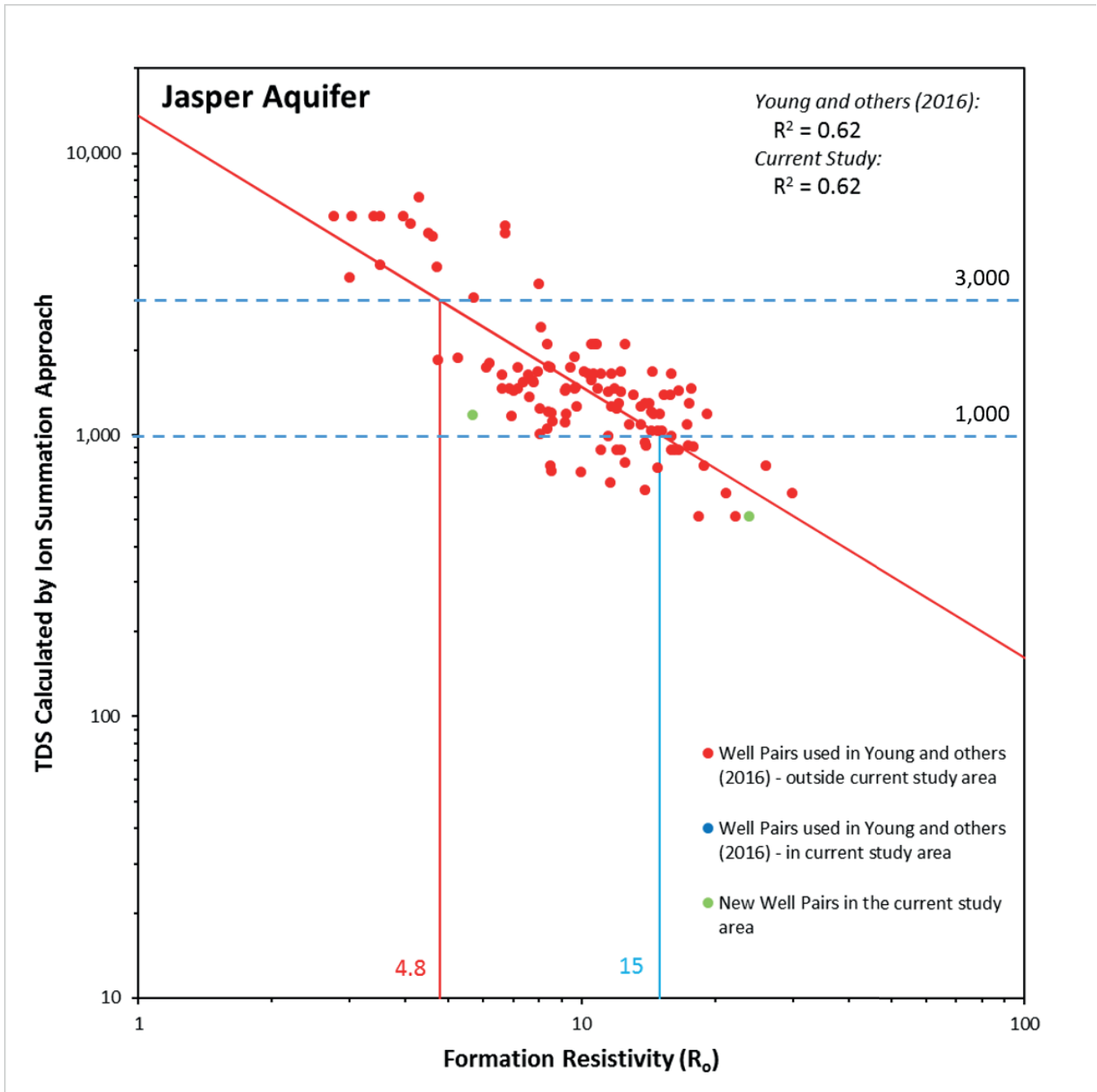
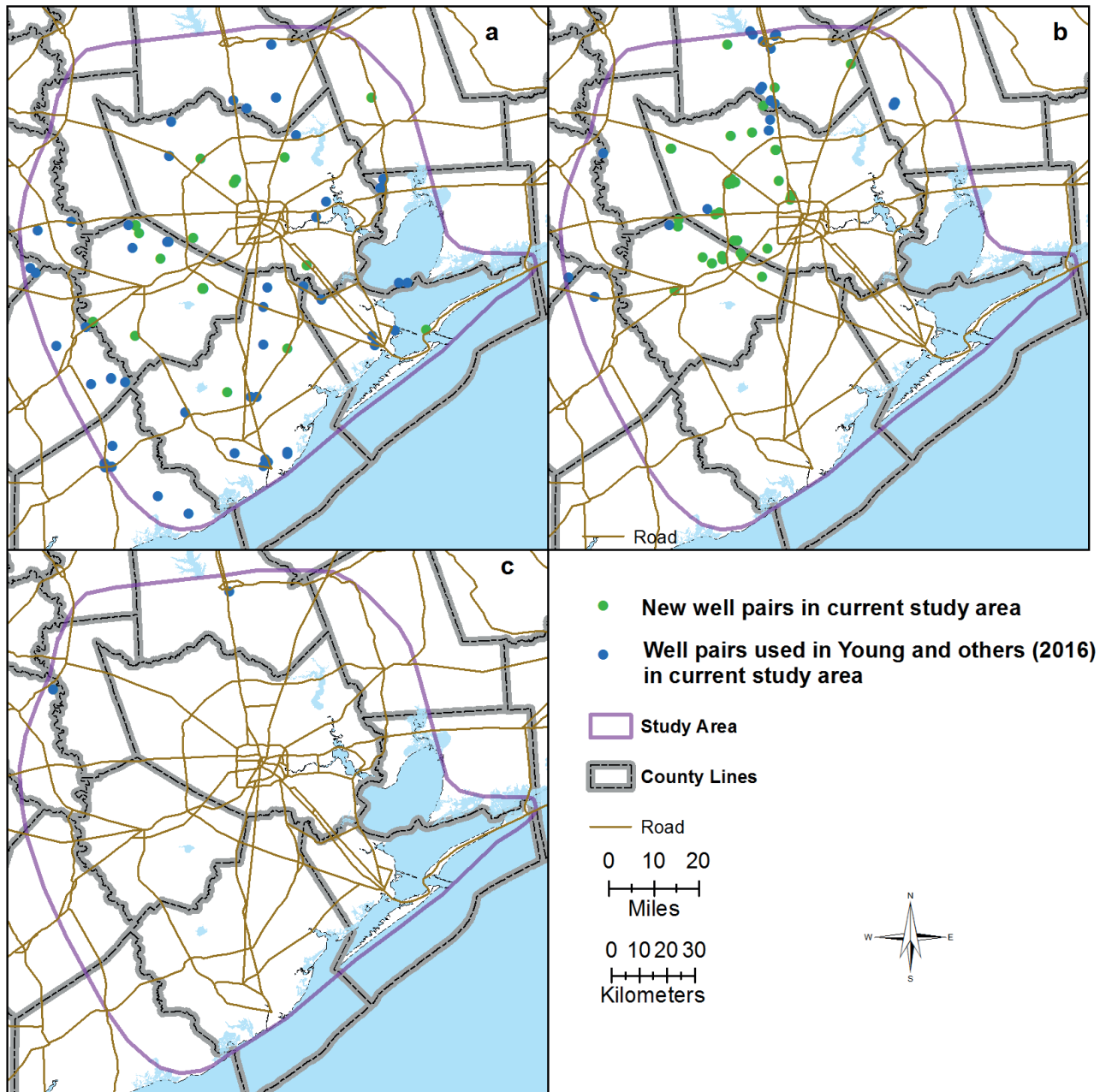


Figure F-5 R_0 -TDS graph for the Jasper Aquifer Group (including the Lower Lagarto, Oakville, Upper Lagarto, and Middle Lagarto formations) generated from the TWDB Gulf Coast BRACs study. The blue line is the formation resistivity value for a 1,000 mg/L TDS concentration and the red line is the formation resistivity value for 3,000 mg/L TDS concentration.

Appendix F: Estimating TDS Concentrations
From Geophysical Logs



S:\AUS\HGSDM.M001.SUBS\GIS\mxd_report\Arc10.2_Figure_5_2_RoTDS_pairs_by_Aq_tyan.mxd

Figure F-6 Additional pairs of geophysical log(s) and a water wells that were used to evaluate to determine the relationship between R_o and TDS Concentrations (mg/L) for the (a) Chicot Aquifer; (b) the Evangeline Aquifer, and the (c) Jasper Aquifer

Appendix F: Estimating TDS Concentrations
From Geophysical Logs

This page is intentionally left blank